Document Title:	**DNA Analysis and the Postmortem Submersion Interval from the Microbiome of Waterlogged Skeletal Remains**
Author(s):	**Claire Cartozzo, Ph.D.**
Document Number:	**306480**
Date Received:	**April 2023**
Award Number:	**2018-R2-CX-0016**

Graduate Research Fellowship in Science, Technology, Engineering, and Mathematics (NIJ-2018-13638)

Applied Research Proposal

Award NIJ 2018-R2-CX-0016

DNA Analysis and the Postmortem Submersion Interval from the Microbiome of Waterlogged Skeletal Remains

Claire Cartozzo, PhD
Integrative Life Sciences
Virginia Commonwealth University
cartozzocm@vcu.edu

Fnal Progress Report
Submission Date: 7/16/20

DUNS:
EIN:

Virginia Commonwealth University
P.O. Box 980568
800 East Leigh Street, Suite 3200
Richmond, VA 23298-0568

VCU FP No. FP00008144
VCU Index No. 510704

Project/Grant Period: 1/1/19 – 12/31/19 (Extension 7/31/20)

DocuSigned by:
Andrea J. Publow
B0782CE1A50C44F...

Signature of Submitting Official

7/16/2020

Date

I. Goals and Objectives

Part I: *To examine the effects of a freshwater lake and river on DNA recovery from skeletal remains in aquatic environments*

Objectives:

- To determine which extraction method, organic phenol-chloroform or solid-phase, and bone type, rib or scapula, is better for DNA recovery from skeletal remains in freshwater
- Identify variance of DNA recovery in different bones and bodies of water (e.g. freshwater river and lake)

Part II: *To determine the extent of microbial colonization and pattern of succession that are involved in the aquatic decomposition of skeletal remains*

Objectives:

- To use microbes to estimate post-mortem submersion interval (PMSI)
- Identify variance in microbial succession and potential indicator species in different bone types and bodies of water

Scholarly Products:
Manuscripts in Preparation
Development of quantitative PCR (qPCR) based method for studying temporal DNA degradation in waterlogged bone
Thornton, I., **Cartozzo, C.**, Mays, D., Singh, B. and Simmons, T.

II. Accomplishments and Scholarly Products

Part I: *To examine the effects of a freshwater lake and river on DNA recovery from skeletal remains in aquatic environments*
Progress: Complete

We have concluded the field collection portion of the project and begun laboratory analyses. All samples (~400) have undergone DNA extraction, using ChargeSwitch® gDNA Plant Kit and traditional organic extraction. If samples did not successfully amplify, then they were purified via DNeasy Powerclean Pro Cleanup Kit. After purification, samples were quantified using porcine specific primers (SW240) and SYBR green technology.

While it was initially proposed that we would purchase the AnimalType (pig) Kit to generate short tandem repeat profiles (STR profies), difficulty in product ordering resulting in the creation of a porcine specific STR kit (4 loci and amelogenin), using genomic pig DNA. The kit was utilized to analyze a subset of the initially proposed samples and has yet to be validated. Resulting profiles were assessed and compared by both bone types, extraction methods, locations and collection period (accumulated degree days) by examining peak presence or absence and the percent of complete profiles.

Part II: *To determine the extent of microbial colonization and pattern of succession that are involved in the aquatic decomposition of skeletal remains*
Progress: Complete

As reported in Part I, we have concluded the field portion along with DNA extraction (ChargeSwitch® gDNA Plant Kit) and purification (DNeasy Powerclean Pro Cleanup Kit). Additionally, library preparation and sequencing via Illumina MiSeq FGx has been completed for both field sites (Henley Lake and James River at the Rice Rivers Center). In addition to surveying the microbial composition (16S rDNA) of waterlogged bone, we were also able to process the same samples for eukaryotic communities (18S rDNA)

The resulting sequences were analyzed using a new workflow and framework, which included a mixture of mothur and R software. The new method was used to evaluate environmental parameters, sample types, field locations, 16S rDNA/18S rDNA and model development. While we hoped to assess and quantify the differences in microbial communities obtained from different sampling methods, such as bone powder and swabs, we were unable to order the necessary supplies, as a result of the COVID19 shutdown. Therefore, we encourage future studies to explore different sampling methods before implementation into forensic casework.

Scholarly Products:
Manuscripts in Preparation

Postmortem Submersion Interval (PMSI) Estimation for the Microbiome of *Sus scrofa* Bone in a Freshwater Lake. (Submitted to Environmental Microbiology)
Cartozzo, C., Simmons, T., Swall, J. and Singh, B.

Postmortem Submersion Interval (PMSI) Estimation for the Microbiome of *Sus scrofa* Bone in a Freshwater River. (Submitted to Forensic Science International)
Cartozzo, C., Singh. B., Swall, J. and Simmons, T.

The Microbiome Associated with *Sus scrofa* Bone from Lacustrine and Riverine Environments in Virginia
Cartozzo, C., Simmons, T., Swall, J. and Singh, B.

The Impact of Submersion in Aquatic Environments on STR Profile Development from *Sus scrofa* Skeletal Elements
Cartozzo, C., Singh. B., Swall, J. and Simmons, T.

Prediction of Minimum Postmortem Submersion Interval Based on Eukaryotic Community Succession on Skeletal Remains Recovered from a Lentic Environment
Randall, S., **Cartozzo, C.**, Simmons, T., Swall, J. and Singh, B.

Prediction of Minimum Postmortem Submersion Interval Based on Eukaryotic Community Succession on Skeletal Remains Recovered from a Lotic Environment
Randall, S., **Cartozzo, C.**, Simmons, T., Swall, J. and Singh, B.

Conference Presentations

2020 American Academy of Forensic Sciences, *Anaheim, CA* (Poster)

- Modeling Postmortem Submersion Interval (PMSI) Estimation From the Microbiome of Bone in a Fresh Water Lake, E46, p 586
  Claire Cartozzo M.S*, Baneshwar Singh Ph.D, Jenise Swall Ph.D and Tal Simmons Ph.D
- Postmortem Submersion Interval (PMSI) Estimation from the Microbiome of Bone in a Freshwater River, A132, p 176
  Claire Cartozzo M.S*, Baneshwar Singh Ph.D, Jenise Swall Ph.D and Tal Simmons Ph.D
- Creating a Quantitative Polymerase Chain Reaction (qPCR) Based Method for Studying Temporal DNA Degradation in Waterlogged Bone, H69, p 812
  Isis Thornton*, **Claire Cartozzo M.S**, D'Arcy Mays Ph.D, Baneshwar Singh Ph.D, and Tal Simmons Ph.D

2020 American Academy of Forensic Sciences, *Anaheim, CA* (Oral)

- Estimating the Postmortem Submersion Interval (PMSI) from the Microbiome of Bone from Lacustrine and Riverine Environments in Virginia, H159, p 902
  Claire Cartozzo M.S*, Baneshwar Singh Ph.D, Jenise Swall Ph.D and Tal Simmons Ph.D
- Prediction of Minimum Postmortem Submersion Interval (PMSImin) Based on Eukaryotic Community Succession on Skeletal Remains Recovered From an Aquatic Environment, A97, p 140
  Sala Randall*, **Claire Cartozzo M.S**, Tal Simmons Ph.D, Jenise Swall Ph.D and Baneshwar Singh Ph.D

2019 American Academy of Forensic Sciences, *Baltimore, MD* (Poster)

- Postmortem Submersion Interval (PMSI) Estimation from the Microbiome of Bone in a Freshwater Lake Across 4,750 Accumulated Degree Days, H30, p 251
  Claire Cartozzo M.S*, Tal Simmons Ph.D and Baneshwar Singh Ph.D

2018 American Academy of Forensic Sciences, *Seattle, WA* (Oral)

- Predicting the Postmortem Submersion Interval from the Microbiome of Bone in a Freshwater Lake, A87, p 127
  Claire Cartozzo M.S.*, Baneshwar Singh Ph.D, and Tal Simmons Ph.D

III. Training and Professional Development

Training and professional development of the PI, Claire Cartozzo, continued through laboratory analyses (i.e primer design, porcine-specific STR kit design) and by increasing her professional network. Specifically, she attended the microbiome shareholders meeting at the 2019 American Academy of Forensic Sciences annual

conference. Regarding laboratory skills, she has gained further experience with the Illumina MiSeq, has been exposed to primer selection for the ABI 7500 Real-Time instrument and learned how to design reactions for capillary electrophoresis fragment analysis. Finally, she had the opportunity to mentor both undergraduate and graduate students in the VCU FRSC Molecular Biology Lab.

VCU Graduate School

Electronic Thesis/Dissertation (ETD) Approval Form

Student name Claire Cartozzo **Vnumber:** 00717307

Document type: Master's thesis x Doctoral dissertation

Department: Integrative Life Sciences

Thesis/dissertation title: DNA Analysis and the Postmortem Submersion Interval from the Microbiome of Waterlogged Sus scrofa Skeletal Remains

Approval numbers:

IRB (Institutional Review Board)

IACUC (Institutional Animal Care and Use Committee)

Exempt

x Not applicable

Thesis/dissertation and final oral defense

Date: 04/17/2020

Graduate Advisory Committee (type name and sign)

		Not Approved	Approved
DocuSigned by: Tal Simmons	tlsimmons@vcu.edu		x
DocuSigned by:	bsingh@vcu.edu		x
DocuSigned by:	jswall@vcu.edu		x
DocuSigned by:	rbfranklin@vcu.edu		x
DocuSigned by: Jamie Fredericks	jamie.fredericks@eku.edu		x
DocuSigned by: Tal Simmons 42DAE0B8F1444F2...	tlsimmons@vcu.edu		x

Graduate program director/department chair: DocuSigned by: Robert M. Tombes 513F5C52423B425... rtombes@vcu.edu **Date:** 4/21/2020

School/college dean: DocuSigned by: Robert M. Tombes 513F5C52423B425... rtombes@vcu.edu **Date:** 4/21/2020

Release options and final approval

Student name Claire Cartozzo **V number:** 00717307

Check one of the following options:

Release the thesis/dissertation as soon as it is approved by the Graduate School.

Release the thesis/dissertation after a period of one year.

x Release the thesis/dissertation after a period of five years.

Do not release the thesis/dissertation until the copyright expires, with the exception of releasing the work to my advisor(s), my department(s), and scholars who are physically present in the VCU Libraries (typically for creative works). **Attach justification; limit one page.**

Electronic theses and dissertations (ETD) make VCU student research and creativity available online as full-text documents and multimedia presentations for use by the university community and others involved in research. In some cases, a student and their advisor can choose to delay the public online release of the ETD. Typical reasons for selecting a delayed release of the ETD include proprietary work and future publishing rights. Based on the justification provided, the Graduate School reserves the right not to accept the release terms. The citation and abstract will appear publicly online for the duration of any restrictions placed on the work.

Rights and obligations

I hereby certify that, if appropriate, I have obtained and attached hereto a written permission statement from the owner(s) of each third party copyrighted matter to be included in my thesis, dissertation, or project report (hereafter "my work"), allowing distribution as specified above. I certify that the version I am submitting is the same as that approved by my advisory committee. I hereby grant to Virginia Commonwealth University or its agents the non-exclusive license to copy, archive, and make accessible, under the conditions specified above, my work in whole or in part in all forms of media, now or hereafter known. I retain all other ownership rights to the copyright of my work. As such, I retain the right to use all or part of my work in future works, such as articles or books.

Student agreement: DocuSigned by: Claire Cartozzo 5DFC3FFE485C47B... cartozzocm@vcu.edu **Date:** 4/13/2020

Major adviser approval: DocuSigned by: Tal Simmons 42DAE0B8F1444F2... tlsimmons@vcu.edu **Date:** 4/21/2020

Graduate School dean: DocuSigned by: F.D.Boudinot/Sarah E. A. Steele 8C03B6703D194B9... graduatedc@vcu.edu **Date:** 6/12/2020

This resource was prepared by the author(s) using Federal funds provided by the U.S. Department of Justice. Opinions or points of view expressed are those of the author(s) and do not necessarily reflect the official position or policies of the U.S. Department of Justice.

This resource was prepared by the author(s) using Federal funds provided by the U.S. Department of Justice. Opinions or points of view expressed are those of the author(s) and do not necessarily reflect the official position or policies of the U.S. Department of Justice.

DNA Analysis and the Postmortem Submersion Interval from the Microbiome of Waterlogged *Sus scrofa* Skeletal Remains

A dissertation submitted in partial fulfillment of the requirements for the degree of Doctor of Philosophy at Virginia Commonwealth University.

by

Claire Cartozzo

B.S. Biological Sciences, 2014
Louisiana State University

M.S. Forensic Science (Biology), 2016
Virginia Commonwealth University

Director: Dr. Tal Simmons,
Professor, Department of Forensic Science

Virginia Commonwealth University
Richmond, VA
May, 2020

This resource was prepared by the author(s) using Federal funds provided by the U.S. Department of Justice. Opinions or points of view expressed are those of the author(s) and do not necessarily reflect the official position or policies of the U.S. Department of Justice.

Acknowledgements

First, I would like to thank my advisors Dr. Tal Simmons and Dr. Baneshwar Singh for their support throughout my time at VCU. About six years ago, Tal agreed to mentor me from across an ocean; since then, she has provided invaluable insight to forensic anthropology casework and research. Meanwhile, Dr. Singh opened his lab to me without hesitation and has provided endless encouragement. I would also like to extend a thank you to my committee members Dr. Jenise Swall, Dr. Rima Franklin and Dr. Jamie Fredericks for their contributions and willingness to answer any and all of my questions. Without a program and funding, I would not have been able to continue my research at VCU, so I would also like to thank the VCU Life Sciences Program and Dr. Verrelli.

To all of those that have contributed to this project, a special thank you, as I know decomposition studies do not always smell pleasant: Kailey Babcock, Matt Alvarez, Tyler Kennedy, Alaina Albino, Chastyn Smith, Jordan Frantz, Sala Randall, Jordan Cox and Isis Thornton. I also want to extend my appreciation to members of the Singh Lab that have come and gone. Without the laughter and comradery this experience would have been less enjoyable. I would be remiss if I failed to mention Denise and Brittany. For helping with field setup, collections, brainstorming, the craziness of mothur and struggles of graduate school, I cannot thank Denise enough and I will always cherish our time working together, especially our conference travels. For answering all of my questions, brainstorming, providing a wonderful excel sheet and introducing me to strange planet, which helped me survive my last semester, many thanks, Brittany.

To those outside of my academic life, you have been extremely understanding as I have worked to pursue my dreams. First, none of this would have been possible without the sacrifices my parents made to ensure I could receive a good education. For everything that you have done, I love you and offer my deepest thanks. Growing up without your love and support would have been unimaginable, so thank you Sam for being my younger brother. To the Henley family, without your support and encouragement this project would not have been possible, especially as part of the study was performed in Henley Lake. Finally, I would like to thank John Henley who has been there for it all and has a solid argument for a honorary masters and doctoral degrees. I am who I am today because of my relationships with each of you and I love y'all.

Abstract

Following water-related deaths, soft tissue on victims' remains may be entirely absent after a temperature dependent period of time. Due to their physical and chemical components, which protect them from environmental deterioration and biological attack, bones preserve DNA for longer periods of time. Therefore, the ability to both identify an individual and estimate the postmortem submersion interval (PMSI) may depend on DNA obtained from skeletal remains. The goals of the dissertation were to examine differences in both the degradation of skeletal DNA and the microbiome inhabiting bone in freshwater aquatic environments (e.g., Henley Lake and the James River). At each location, five porcine ribs and scapulae were placed in 10'' x 10'' cages and submerged. Every ca. 250 accumulated degree days (ADD), one cage was collected for a total of nineteen collections at the lake (November 2016 to June 2018) and twenty-four collections at the river (November 2017 to November 2018). In concurrence with bone samples, water samples were also collected from the level of submersion.

To evaluate microbial changes, all samples underwent 16S rDNA variable region 4 (V4) library preparation and Illumina MiSeq sequencing. Site-specific analyses indicated significant differences among water, rib and scapula samples. Overall, alpha-diversity increased with time at both sites, but was higher at the James River. Furthermore, beta-diversity within each site ordinated chronologically along one axis and separated according to location along the second axis. Relative abundances were used to both identify taxa that differed between samples and to generate random forest models for estimating PMSI. Models fit using 34 scapula family-level taxa provided a tighter prediction of PMSI with root mean square error of 333.8 ADD (~37 days) at Henley Lake when compared to ribs; meanwhile, ribs outperformed scapulae at the James River, predicting PMSI with root mean square error of within 472.31 ADD (~27 days).

To evaluate how bone DNA was impacted by prolonged submersion, a subset of samples, including those collected every ca. 1000 ADD from both sites, underwent extraction using both organic phenol-chloroform and ChargeSwitch® gDNA Plant Kit before being amplified and separated via the ABI 7500 and Prism® 3130 genetic analyzer, respectively. Findings suggest that peak presence and percent complete profiles were significantly different among ADD and between bone types. Likelihood of obtaining successful STR

profile decreases with ADD and target fragment size of a STR locus. Results suggest that, regardless of extraction method and submersion site, ribs should be prioritized as they preserve recoverable DNA for longer periods of time and generate more complete STR profile in aquatic environment . Overall, this dissertation confirms that bacterial succession on skeletal remains can be used to predict long-term PMSI in both freshwater lakes and rivers. Along with microorganisms, temperature and water have been reported to fragment or damage DNA, which was observed with submersion time, as bone type and ADD impacted STR profile development.

Table of Contents

Chapter 1: Prediction of the Postmortem Interval from the Microbiome

Introduction

In this chapter we explore the role of the necromicrobiome in postmortem interval (PMI) estimation. Due primarily to advances in technology, studies of the microbiome are just now moving from the recognition of their utility, to the rigorous experimental studies of sufficient sample size and geographic diversity needed to provide data, to the application stage, where it is hoped that statistical analyses may be able to provide appropriate confidence interval-based PMI estimations. Both prokaryotes (bacteria and cyanobacteria) and eukaryotes (protists, fungi, plants and animals) are included when discussing the microbiome, and although the majority of studies have focused on prokaryotic communities due to the availability of a better documented reference database, eukaryotic communities should not be ignored. Because of the many ways in which the microbiome can be characterized, PMI estimation can be achieved through a variety of both single and combined techniques.

Although Vass (2001) first proposed nearly two decades ago that the microbiome could be used to determine PMI, bacterial culturing of decomposition by products produced too many organisms to classify. Only in recent years, with the advent of next generation sequencing (NGS), has it become possible to fully explore the potential of microbial succession and the presence of indicator taxa to inform the chronology of the decomposition process. Both bacterial and eukaryotic organisms have symbiotic relationships with human hosts, and, at the death of the host, these organisms undergo changes in their community structure which continue until the host, as substrate (nutrient source) is exhausted. As an integral part of this process, microorganisms already present in the depositional environment (terrestrial or aqueous) may also establish a relationship with the host, and still others may be brought to the body by the necrophagous insects they inhabit as well. Thus, a study of the necromicrobiome is first and foremost a study in community ecology, where the dominance of particular taxa may appear and disappear, wax and wane, as the inherent characteristics of the decaying host morph from one stage to the next. The microbiome community in, e.g. the soil under a decaying host, continues to undergo changes long after the visible nutrients (the corpse) have become skeletonized or even been removed from the area of deposition. Thus, based on the constituents of the microbial community, the microbiome has the potential to both help

investigators identify the place of deposition as well as inform investigators about time since death.

The necromicrobiome community can be described in terms of succession, diversity, relative abundance, and the presence of indicator taxa. The community associated with the corpse (and its depositional environment) changes at various points along the decomposition sequence, and correlates to numerous markers of already well-defined visible decomposition stages. The microbiome diversity may indicate that a particular stage of decomposition (e.g. Megyesi, et al. 2005) has been reached because the diversity increases (e.g. with the arrival of necrophagous insects who carry their own microbiome) or decreases (e.g. at the end of the active decomposition stage). The diversity of the microbiome (number of different taxa present) may also change over time, rising or declining in correlation to the decomposition stages; they may even indicate other stages not defined by current scoring systems, as whilst invisible, they may be defined by the corpse reaching a particular accumulated degree days (ADD) marker. The advent or disappearance of various organisms, otherwise known as succession, may also be used to identify trends in the relative abundance (proportion) of organisms present at any given time. Lastly, indicator taxa are those which may appear and be associated with only one stage of decomposition or ADD interval. Thus techniques usually associated with ecology and paleontology may be applied to PMI estimation via a study of the necromicrobiome.

This chapter will discuss the current state of the field of microbiome studies of decomposition as related to the estimation of PMI, with relation to the analysis of the microbiome presenting available techniques, a review of metagenomics, an overview of the microbiology of decomposition, as well as current techniques available for PMI estimation using the microbiome community.

Microbiome Analysis (Metagenomics)

The advancements in next-generation sequencing within the last decade have allowed for the identification and characterization of microorganisms previously unknown. While sequencing is no longer a limiting factor, managing the sequences generated by the sequencing platforms has created new challenges. The methods for sequencing and analyzing microorganisms include marker gene analysis, metagenomics,

metatranscriptomics, metaproteomics and metametabolomics. This section will focus on marker gene analysis (Figure 1.1). Additional methods may be explored in Singh et al. (2017).

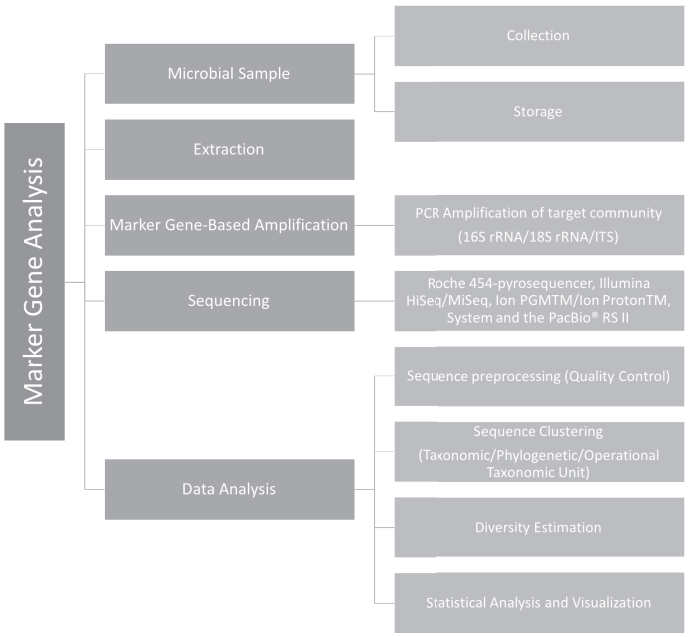

Figure 1.1. Diagram demonstrating the workflow of marker gene-based analyses

Marker gene analysis begins with sample collection and storage, which should be performed using the appropriate protective equipment and sterile collection methods. Once samples are collected, they should be stored in a manner that minimizes bacterial community change before DNA extraction. Extracted samples are then used for polymerase chain reaction (PCR) amplification, where bacteria, eukaryotes or fungi can be targeted using marker genes. The amplified products are then sequenced on a platform of choice (see Table 1.1 for comparison) and the resulting sequence data can be analyzed in software programs, or customizable pipelines, to classify sequences, estimate diversity and statistically test differences.

Collection and Storage

The final sequences obtained from a sample can be impacted by several factors through the collection and storage processes. These factors may include: the collection conditions, technique or method, location, quantity, transportation and storage conditions, length of time until microbial DNA extraction, and the method used for extraction (Grice et al. 2008; Hart et al. 2015; Lauber et al. 2010; Wesolowska-Andersen et al. 2014). Generally,

samples should be collected aseptically by individuals wearing the appropriate personal protective equipment (PPE) (i.e. lab coat, aprons, safety glasses or goggles, surgical masks, booties, gloves, hair covers, etc.) and using collection equipment that has been sterilized (e.g. a flame and 95% ethanol or autoclaved) (Singh and Crippen 2015; Singh et al. 2017). With the appropriate PPE and collection tools, samples can be obtained via swabs, punch biopsies or scrapings, as they have been reported to produce approximately identical microbial profiles (Grice et al. 2008); however, the period or duration of sampling by swabbing or scraping should be standardized (e.g. 30 seconds or 1 minute) and samples should be replicated (i.e. duplicates or triplicates) to ensure the collected DNA is sufficient for analysis (Singh and Crippen 2015). Microorganisms collected from the gastrointestinal (GI) tract, oral cavity, vagina and skin provide optimal information (Wilson 2009); these should therefore be locations to consider when sampling for carrion-based decomposition studies as well as for forensic investigations (Singh and Crippen 2015). As soon as the samples are collected, they should be stored on ice or in liquid nitrogen for transportation to the lab. While it is preferred for samples to be processed within 2 hours of collection (Rochelle et al. 1994), it is not always practical. Studies have reported that samples can be stored at 4 °C for up to 10 days (Insam and Goberna 2004), -20 °C for up to two weeks (Lauber et al. 2010) and -80 °C for up to 6 months (Kakirde et al. 2010; Carroll et al. 2012) without significant changes in the microbial community. If the sample is frozen, it should remain frozen until microbial DNA extraction can be performed, as repeated freeze-thaw cycles result in DNA fragmentation, which significantly alters microbial diversity analysis (Cardona et al. 2012).

Extraction

Due to unknown microbial diversity and inhibitors, microbial DNA sample extractions have unique challenges inherent to their environment, relating to their physiological, biological and chemical properties (Kakride et al. 2010). Since extraction is the first step, any variations should be minimized to ensure the success of downstream metagenomic analyses. Specifically, the selection of a DNA extraction method, one of the most crucial steps in sample processing (Inceoglu et al. 2010), can change functional results and/or microbial structure interpretation (Henderson et al. 2013; Wagner Mackenzie et al. 2015; Wesolowska-Andersen et al. 2014). In addition, different extraction methods may promote

lysis of gram-negative bacteria over gram-positive (Mahalanabis et al. 2009), resulting in skewed profiles.

Microbial DNA extractions can be performed directly (Ogram et al. 1987) or indirectly (Holben et al. 1988; Jacobsen and Rasmussen 1992). Briefly, indirect extraction methods use a density gradient to separate prokaryotic cells before lysis, making it only applicable for bacteria and archaea, while direct methods use the entire sample for extraction (i.e. prokaryotes and eukaryotes). Of the two, direct methods are faster, require less input and produce higher yields of DNA (Singh and Crippen 2015); the drawback, however, is that these direct methods also co-extract PCR inhibitors, such as humic acid, polyphenols and polysaccharides (Miller et al. 1999; Roh et al. 2006; Kakirde et al. 2010). Despite their differences, both direct and indirect methods produce similar DNA diversities (Delmont et al. 2011). Both direct and indirect microbial DNA extraction methods may be separated into two steps (i.e. lysis and isolation) and the processes in each step may vary based on the DNA extraction method used.

In general, lysis begins with the breakdown of microbial cell walls by physical, chemical and/or enzymatic methods (Kuczynski et al. 2012). The most common physical disruption techniques used are freeze-thawing and bead-mill homogenization (Miller et al. 1999). Once the cell wall is broken down, nucleic acids are purified and separated from the remaining cell debris, humic acids and other contaminants (Kakirde et al. 2010). The resulting DNA extract can then be used for downstream analyses. For a more detailed explanation of various extraction methods, readers are encouraged to review Singh and Crippen (2015).

Marker Gene-based Metagenomic Analysis

Microbial DNA extracts can be used for marker gene-based amplification and/or for whole genome sequencing, or WGS (Tringe and Rubin 2005). Currently, the most common microbial detection and characterization method is marker gene-based amplification (e.g. 16S rDNA for bacteria and archaea, 18S rDNA for eukaryotes and internal transcribed spacer or ITS for fungi), as it provides better taxonomic coverage (i.e. microbial community structure) compared to WGS, which infers microbial community function (Kuczynski et al. 2012). Specifically, marker gene analysis amplifies short **hypervariable regions** (see

Glossary) from a gene in the targeted community, resulting in **amplicons** that are tagged with unique barcodes for identification. The amplified products are then sequenced on next-generation sequencing (NGS) platforms (discussed below). The amplification success depends on several factors including, but not limited to primer design and target region (De la Cuesta-Zuluaga and Escobar 2013).

First, marker gene-based amplification relies on the ubiquity of **ribosomal RNA (rRNA) molecules** whose sequences can be used to infer evolutionary relationships because they contain both conserved and variable regions. Generally, **universal primers** used for **polymerase chain reaction (PCR)** amplification are designed to anneal to the conserved regions that flank the target or variable region, which is used for taxonomic identification (de la Cuesta-Zuluaga and Escobar 2013; Head et al. 1998). Secondly, the targeted community (i.e. bacteria or archaea, eukaryotes, and fungi) will dictate which universal primers can be used.

All bacteria and archaea have a **small ribosomal subunit (SSU)** that is encoded by the 16S rRNA gene. The entire 16S rRNA gene is approximately 1541 bp long (*Escherichia coli*) and consists of 9 hypervariable regions (V1-V9) with nine highly conserved regions interspersed (Mankin et al. 1986). Additionally, there are several reference databases available for the identification of the tagged products: Ribosomal Database Project (RDP) (Cole et al. 2009), Greengenes (DeSantis et al. 2006), Silva (Quast et al. 2013), GenBank (Benson et al. 2005).

Eukaryotes are identified by the 18S ribosomal small subunit rRNA gene (SSU), a homolog of the 16S rRNA gene, that is 1798 bp long (*Saccharomyces cerevisiae*) (Mankin et al. 1986). While the 18S rRNA gene and 16S rRNA gene can both be amplified from partially degraded samples, as they are present in multiple copies (Mankin et al. 1986), the 18S rRNA gene lacks the variability of the 16S rRNA gene, making lower level taxonomic classification difficult (Schoch et al. 2012). Fortunately, the increasing number of 18S rRNA sequences being input into the database (e.g. SILVA) has exposed polymorphisms in primer target regions, indicating that diversity may be evading detection (Wang et al. 2014). Within eukaryotes, the second largest kingdom, fungi, can be targeted using the internal transcribed spacer (ITS) within the **ribosomal cistron** (Schoch et al. 2012). The cistron, which contains 18S, 5.8S and 28S rRNA genes, is transcribed by RNA

polymerase I. Once the resulting transcribed unit is split, the two internal transcribed spaces are removed. The resulting spacers (including the 5.8S gene) are considered the ITS region. Like the 18S and 16S rRNA genes, the ITS region is easy to amplify even when present in small amounts as there are multiple copies present throughout the region.

Even though the aforementioned gene sequences can be used for phylogenetic analysis, limited sequencing technology results in studies utilizing partial sequences for marker gene-based analyses (e.g V4 or V4/V3) (Yang et al. 2016). The partial sequence or target region selected depends on the experimental questions and design, available databases and studies used to compare results, as no specific region has been shown to be ideal for all samples (Chakravorty et al. 2007; Kumar et al. 2011). Studies have evaluated various primers to determine which combination is best suited for specific target communities (Klindworth et al. 2013; Caporaso et al. 2012). Additional information regarding primer design and selection can be found in Walters et al. (2016), Singh and Crippen (2015), and Smith and Peay (2014).

Glossary
Hypervariable regions: Regions of DNA that evolve at faster than normal rates
Amplicons: product of PCR amplification
Ribosomal RNA (rRNA): RNA portion of the ribosome that contains complementary sequences to messenger RNA (mRNA); three molecules in prokaryotes (5S, 16S and 23S) and four in eukaryotes (5S, 5.8S, 18S and 28S)
Universal primers: primers designed to anneal to highly conserved regions (result of slow evolution rates) across different species
PCR: molecular biology technique used to amplify DNA segments; three steps (1) denaturation, (2) annealing and (3) extension
small ribosomal subunit (SSU): 30S subunit; part of the 70S ribosome located in prokaryotes; binds and reads mRNA during translation
Ribosomal cistron: sequences of genetic material that are required to make RNA molecules or polypeptides

Sequencing

The tagged PCR products, resulting from marker gene-based amplification, can then be sequenced via NGS platforms; commonly used platforms include: the Roche 454-pyrosequencer (Roche Diagnostic Corp., Indianapolis, IN, USA), Illumina HiSeq/MiSeq® sequencer (Illumina Inc.), Ion PGM™/Ion Proton™ System (Thermo Fisher Scientific Inc.), PacBio® RS II sequencing system (Pacific Biosciences of California, Inc., Menlo Park, CA, USA), and MinION (Oxford Nanopore Technologies, Oxford, UK) (Singh and Crippen

2015; Mitsuhashi et al. 2017). When selecting a NGS platform, it is important to consider the research question, cost, time, read length, error rate and coverage. Recently, Illumina's HiSeq® and MiSeq® sequencers have become the platform of choice (Salipante et al. 2014), as they generate total reads lengths of 600 bp (paired-end sequencing) or 500 bp (paired-end sequencing), respectively. Additionally, Illumina's sequencers are easy to operate, have low cost per sample, and produce lower error rates and higher sequence depth, when compared to other platforms (Table 1.1). Of the two platforms, the Illumina MiSeq® is preferred for marker gene-based analysis, as it generates longer reads with data sufficient for small projects (Singh et al. 2017).

Table 1.1 A comparison of the most common next-generation sequencing platforms (modified from Singh and Crippen 2015).

Platforms	Technologies							Comments
	Emulsion PCR	Pyrosequencing	Semiconductor Sequencing	Bridge Amplification	Reversible dye terminator sequencing	Single molecule real-time sequencing	Nanopore-based single molecule sequencing	
Roche 454	✓	✓						• Longer reads (700 bp) • High cost/Mb • High error rate (compared to MiSeq®/HiSeq®) • Marker gene-based sequencing
Ion PGM™	✓		✓					• Faster sequencing • Longer reads (400 bp) but lower throughput compared to theMiSeq®/HiSeq® • High error rate • Excessive hands-on time • Size selection is an issue for marker gene-based analysis
Ion Proton™	✓		✓					• Higher throughput compared to Ion PGM • Lower throughput compared to the HiSeq® • Generally shorter reads (200 bp)
Illumina MiSeq®				✓	✓			• High throughput • Low error rate • Comparable read length (300 + 300 bp) • Preferred for marker gene-based analysis
Illumina HiSeq® 2500				✓	✓			• Similar to MiSeq® • Higher throughput • Slightly shorter read length (250 + 250 bp) • Preferred for shotgun sequencing
PacBio® RS II						✓		• No amplification step • Longest reads (8500 bp) • Low throughput • High error rate • Beneficial DNA template that are difficult to sequence
MinION							✓	• Real-time analysis • Simple sample preparation • Portable • Read length depends on sequence method (e.g. Rapid 1D – 15 min) • Nanopore technology can sequence multiple molecules simultaneously

Data Analysis

With the magnitude of data being generated by sequencing platforms, manufacturer software programs and external data analysis pipelines have risen to the forefront of the

field. The manufacturer-provided software programs, such as IonReporter™ or MiSeq® Reporter Software, are sufficient for generating taxonomic profiles, although they omit preprocessing and quality control steps. External data analysis pipelines (e.g mothur [Schloss et al. 2009], QIIME [Caporaso et al. 2010], RDPipeline [Cole et al. 2009], and CloVR [Angiuoli et al. 2011]) are customizable, allowing for preprocessing steps to be incorporated into the analysis. As there are several external pipelines available for analyzing marker gene-based metagenomic data, selection should be based on the user's bioinformatics skill and the size of the dataset. The RDPipeline (Cole et al. 2009) is user friendly, suited for small datasets and is web-based; mothur (Schloss et al. 2009) and QIIME (Caporaso et al. 2010) are the two most commonly used external pipelines, as both handle large datasets, may be customized, are compatible with multiple sequencing platforms, and yield similar results.

Using the aforementioned software programs or pipelines, the raw sequences undergo quality control processing to (1) remove low quality sequences, including sequences with **ambiguous base calls** and long/short reads, and (2) minimize errors, such as **insertions**, **deletions** and/or **homopolymers** (Huse et al. 2007; Schloss et al. 2011). Depending on the sequencing platform used (e.g Ion PGM and Roche 454), noise correction software is recommended to reduce noise from **flowgrams** and improve sequence quality (Singh et al. 2017). The next quality control step includes identifying and removing chimeric sequences, which account for 5 – 45% of raw sequences (Haas et al. 2011; Schloss et al. 2011). The removal of **chimeras** is important, as they artificially inflate diversity estimations; this can be performed using several software packages (e.g ChimeraSlayer [Haas et al. 2011], Decipher [Wright et al. 2012], Perseus [Quince et a. 2011] and Uchime [Edgar et al. 2011]).

After the preprocessing and quality control steps are complete, the remaining sequences are clustered via taxonomy, phylogeny or operational taxonomic unit (OTU) methods. Taxonomy-based clustering relies on grouping sequences into taxonomic groups based on their similarity to sequences in a known database, such as RDP (http://rdp.cme.msu.edu), Greengenes (DeSantis et al. 2006) (http://www.arb-silva.de/), and National Center for Biotechnology Information (NCBI) taxonomy database (http://ncbi.nlm.nih.gov/taxonomy). Sequences can also be clustered based on phylogenetic relationships among DNA sequences. Phylogenetic-based clustering

approaches deduce relationships using either *de novo* alignments and tree building tools or reference databases (e.g SILVA [Quast et al. 2013] or Greengenes [DeSantis et al. 2006]). Finally, using OTU sequence similarity thresholds of $\geq$ 97%, $\geq$ 95%, $\geq$ 90% and $\geq$ 85%, which hypothetically represent species, genus, family and order, respectively, sequences are clustered *de novo* (Cressman et al. 2010). The clustered sequences can then be normalized and used for alpha (α) and beta (β) diversity estimation (Achtman and Wagner 2008). The normalization step is imperative to ensure that all samples have equal number of sequences, as NGS libraries vary among samples, and unequal sampling can introduce prejudice into estimations of bias (Gihring et al. 2012).

Estimating diversity can be performed in most bioinformatics pipelines (e.g. mothur and QIIME). Alpha (α) -diversity, the diversity within samples, can be calculated for OTU or taxonomy clustered sequences using Shannon Index and/or Inverse-Simpson Index; β-diversity, between sample diversity, can be determined using Jaccard similarity coefficient, Yue and Clayton θ similarity coefficient or Bray-Curtis similarity coefficient. The resulting β-diversities can be visualized using principal coordinate analysis (PCoA) or nonmetric multidimensional scaling (NMDS) in R (R Development Core Team 2011) using the Vegan package (Oksanen et al. 2012). Similarly, α- and β-diversity can be calculated from phylogenetically clustered sequences using phylogenetic diversity and UniFrac (Lozupone and Knight 2005), respectively. Specifically, β-diversity can be calculated using either weighted UniFrac (quantitative) or unweighted UniFrac (qualitative) distances, which can be used for community clustering with 'unweighted pair group method with arithmetic mean' (UPGMA) or for multivariate analysis (i.e. PCoA and NMDS).

While PCoA and NMDS are beneficial for visualizing how samples group in 2D or 3D output, they cannot determine if the separation between groups is significant; therefore, analysis of molecular variance (AMOVA) or multi-response permutation procedures (MRPP) can be used to test for statistical significance. If groups are significantly different, then either indicator species analysis (ISA) (Dufrene and Legendre 1997) or random forest (Breiman 2001) modeling can identify indicator or predictor taxa, which may aid in developing generalized additive models (GAMs) and generalized linear models (GLMs) (Metcalf et al. 2013; Pechal et al. 2013).

Glossary
Ambiguous base calls: bases used when the true base is unknown; the most popular is "N" that represents any possible nucleotide
Insertions: addition of at least one base into a DNA sequence
Deletions: removal of at least one base from a DNA sequence
Homopolymers: portion of DNA that has the same base tandemly repeated
Flowgrams: fractional intensity of the pairs of nucleotides in a sequence
Chimeric sequences (chimeras): a combination of two or more parent sequences; an artifact of PCR amplification

Microbiology of Taphonomy

Taphonomy, a term originally coined by Efremov (1940), is most succinctly defined as the events and/or processes impacting the preservation (or decomposition) and recovery of remains (Christensen et al. 2014). Generally, the decomposition process, while continuous, can be divided into broad categories (i.e. fresh, early decomposition, advanced decomposition and skeletonization) (Megysei et al. 2005; Moffatt et al. 2016) that roughly coincide amongst researchers past and present (Adlam and Simmons 2007). These stages can be associated with microbial and arthropod activity. Briefly, fresh decay involves the digestion of tissues by internal bacteria (Janaway et al. 2009); specifically, putrefaction is characterized by gaseous buildup (i.e. bloat) from internal bacteria undergoing anaerobic respiration (Vass 2001; Janaway et al. 2009). Marbling, or the darkening of the circulatory systems vessels resulting from an increase in digestive system bacteria, is also associated with putrefaction (Knight 2002). The decrease in gas and release of fluids post bloat marks the shift from early to advanced decomposition, where body cavities (i.e. the trunk) become exposed to the environment, and it is this point that the rate of decomposition increases due to fly larvae, ultimately resulting in skeletonization (Hyde et al. 2013). Overall, the aforementioned processes are dependent on both biotic (i.e. insects, scavengers, microorganisms, etc.) and abiotic (i.e. temperature, pH, moisture, etc.) factors. Body individuality, deposition location, season, postmortem trauma and topography are all factors that may also influence decomposition (Hyde et al. 2017).

Understanding decomposition and its associated factors is imperative to aid investigators in estimating the postmortem interval (PMI) on land (Metcal et al. 2016; Pechal et al. 2014; Cobaugh et al. 2015; Hauther et al. 2015; Metcalf et al. 2013; Hyde et al. 2015) or, if remains are deposited in water, the postmortem submersion interval (PMSI) (Benbow et al. 2015; Dickson et al. 2011; Heaton, et al. 2010) and identifying or locating clandestine

graves (Finley et al. 2016). The National Research Council of the National Academies released a report aimed at strengthening science as applied to the criminal justice system (2009), and subsequently "the use of metagenomics to produce investigative leads" was highlighted as pertinent to Forensic Pathology and Medicolegal Death Investigations (TWG 2016). In response, researchers in the field of forensic science have developed microbiome tools and technologies to aid and improve investigations, which will be addressed in the following sections. In order to perform the following studies, human and nonhuman models, such as swine and rats, are used. While it is acknowledged that using animal models in decomposition studies presents some challenges concerning their acceptance in court and direct applicability to human cases, they provide the opportunity for proof of concept studies, large volume experiments, replication, validation, and easy to compare results, which is often not possible using human remains.

Terrestrial Environments

An attempt to record bacteria involved in terrestrial human decomposition was first made and then abandoned by Vass (2001); however, earlier studies by Melvin et al. (1984) and Micozzi (1986) were successful in identifying some microbial changes in animal models. Specifically, Melvin et al. (1984) analyzed the transmigration of intestinal bacteria in mice over a three-day period at varying temperatures (4, 25 and 37 ^{o}C). Using scanning electron microscopy, initial signs of transmigration were observed within 2-3 hours at 37 ^{o}C, 5-6 hours at 25 ^{o}C and 72 hours at 4 ^{o}C. Meanwhile, microbiological cultures revealed a succession-like pattern. Initially, Staphylococcal species were noted followed by coliform-type organisms and *candida* species, while the last group of bacteria were a mixture of anaerobic species. Ultimately, it was proposed that transmigration of microorganisms is both time- and temperature-dependent. Although earlier studies (i.e. Melvin et al. 1984) yielded preliminary information regarding microbial succession during decomposition, NGS sequencing technologies and data analysis pipelines/software have allowed for the identification of microbial communities associated with decomposition stages and body locations for both animal and human models (Metcalf et al. 2013; Pechal et al. 2013; Pechal et al. 2014; Hyde et al. 2013). Additionally, PMI estimation models have been developed using the identified microorganisms.

Using mice models on gravesoil (soil associated with decomposition) in a controlled laboratory setting, Metcalf et al. (2013) identified microbial (bacteria and eukaryotes) community changes in soil, skin (head and torso) and abdominal samples for eight time points spanning 48 days (see Soil Environments). Both 16S rRNA and 18S rRNA genes were sequenced using the Illumina HiSeq and analyzed via QIIME (Caporaso et al. 2010). Overall, they reported that bacterial communities varied across sample types (soil and body locations) and differentiated from the starting communities. Briefly, the bloat stage was characterized by an increase in Firmicutes (Family: Lactobacillaceae, Genus: *Lactobacilus*) and Bacteroidetes (Family: Bacteroidaceae, Genus: *Bacteroides*), which are endogenous and facultative anaerobes in the abdominal cavity. However, these taxa decreased after the abdominal cavity was exposed to oxygen, allowing aerobes, such as Rhizobiales (Families: Phyllobacteriaceae, Hyphomicrobiaceae and Brucellaceae), and facultative anaerobes, like Gammaproteobacteria (Family: Enterobacteriaceae), to increase in relative abundance. Additionally, the pH spike (6 to 8.5), due to the release of ammonia-rich and nutrient-filled fluids, resulted in a decrease in Acidobacteria relative abundance and increase in Alphaproteobacteria, specifically Rhizobiales, in soil samples. When comparing sample types, similar taxa became abundant as the organism progressed through the decomposition stages. Specifically, Bacteroidetes (Sphingobacteriaceae), Alphaproteobacteria (Brucellaceae, Phyllobacteriaceae and Hyphomicrobiaceae) and Betaproteobaceteria (Alcaligenaceae) increased in relative abundance in soil and skin samples collected during advanced stages of decomposition, suggesting that skin communities reflect the neighboring environment. Like bacterial communities, microbial eukaryotes changed significantly in all samples, with the exception of the torso. Of these eukaryotes, *O. tipulae* (Family: Rhabditidae), a nematode, became dominant after 20 days. The 'nematode bloom' was likely associated with the increase in bacterial biomass, and the closed system (i.e. laboratory setting) prevented the predation of nematodes by other organisms. While this study was the first to discuss the appearance of nematodes, others have since associated nematodes with the decomposition (Carter *et al.*, 2015; Weiss *et al.*, 2015; Metcalf *et al.*, 2016). As a result of the aforementioned microbial shifts, a model was built to predict PMI within 3 days over a 48-day period (see **Postmortem Interval Estimation via Microorganisms** below**)**.

While mice are easier to work with, smaller and cost less, swine are more similar to humans in terms of size, hair covering, and GI tract bacteria (Schoenly et al. 2006).

Therefore, Pechal et al. (2013) utilized six replicate swine in the spring and six replicates in the summer, in addition to three replicates in autumn and three replicates in winter trials to examine microbial community functional activity over seasons, between years (2010 and 2011) and in the presence or absence of necrophagous insects. 454-pyrosequencing was used to sequence 16S rRNA genes and Biolog EcoPlates™ were used to measure microbial community function. This study showed that there are functional changes at the community-level throughout decomposition, and identified four major phyla that are associated with decomposition: Proteobacteria, Firmicutes, Actinobacteria and Bacteroidetes. Regarding seasonal variation, microbial functional activity overall was highest and most variable during spring. As observed in spring trials, winter samples decreased throughout the early stages of decomposition and increased in later stages. Meanwhile, autumn and summer trials were characterized by a decrease and increase in activity over the decomposition process, respectively. Because no significant difference in normalized microbial metabolic community profiles (MMCPs) between sample locations was found, the samples were pooled and used to test differences between seasons. Using PERMANOVA, significant differences in MMCPs were found among all seasons; therefore, they were separated to examine the differences in early, middle and late stages of decomposition. Overall, significant differences were noted among decomposition stages in the spring and summer trials, but not in the autumn or winter trials. When comparing years, there were annual differences in metabolic profiles, as functional activity on average was significantly higher in 2011 than 2010. This difference was attributed to abiotic and biotic factors. Specifically, ambient temperatures were approximately 18% higher in 2011, which could have increased the available carbon and the activity of microorganisms on the carcass. Additional results discussing the impact on necrophagous insects can be found below (Other Factors: *Insects*).

In another study carried out by Pechal et al. (2014), three swine were placed in a temperate forest habitat in August 2010 and sampled from the buccal cavity and skin on days 0, 1, 3, and 5. According to taxonomic classifications at the phylum and family levels, taxon richness and relative abundances differed throughout decomposition. At the phylum level, Proteobacteria dominated the early stages of decomposition followed by Firmicutes; however, as decomposition progressed Firmicutes became dominant, as Proteobacteria decreased over time. Additionally, there were significant differences in bacterial communities among days sampled, but not within carcass replicates. Using random forest

analyses, five phyla were identified as predictors of time. At the family level, Moraxellaceae was identified as the dominating taxa on the first day; however, it was not present on day three or day five. Meanwhile, both Aerococcaceae and Enterobacteriaceae increased until the third day of decomposition, but were not present on the fifth day. Finally, later stages of decomposition (day 5) were characterized by Clostridiales incertae sedis XI and other Clostridiaceae. Again, there was a significant difference in bacterial community composition among days and no significant differences within replicates; however, there was a significant difference between buccal and skin bacterial communities. Random forest analyses were used to identify ten families useful for estimating time (see below **Postmortem Interval Estimation via Microorganisms)**.

Hyde et al. (2013) published the first marker gene study identifying microbial communities associated with the decomposition of human remains using 454-pyrosequencing of the 16S rRNA gene. Obtaining human cadavers is difficult, as it requires an established facility, special handling, and can be expensive; due to limitations of availability, experimental replication is difficult. Therefore, the study placed two cadavers outdoors at the Southeast Texas Applied Forensic Science (STAFS) facility at two different times: 8-15 September 2011 (STAFS 2011-006) and 2-17 November 2011 (STAFS 2011-016). During this period, samples were collected from the mouth and rectum, using two methods, scraping and swabbing (Table 2). Destructive samples from the colon, body cavity and small intestine were collected post-bloat, at which time sampling ended.

Differences among body sites were revealed by a survey of microbial community richness and analysis of relative abundances. Community richness showed that feces, with an average of 400 OTUs detected, were the richest body site, with stomach, small intestine and mouth samples decreasing in richness, respectively. This suggests that GI tract microbial diversity increases as the digestive tract descends from the mouth to stomach and small intestine, to the colon and finally to the rectum (Hyde et al. 2013). These findings mirror those of the Human Microbiome Project (HMP), whose participant's fecal matter provided the richest microbiome whilst oral cavities had the lowest. Beta diversity (between sample differences) and relative abundances also indicated that the microbial community structure and composition differed among body sites, specifically at the phylum and genus levels. Regarding relative abundances at the phylum level, Firmicutes dominated, while Proteobacteria were present in most samples. Similarly, genera were

significantly different among body sites and among cadavers. For instance, the lower GI tract and body cavity of one cadaver (STAFS 2011-006) shared genera, including *Clostridium, Lactobacillus, Eggerthella,* and *Baceroides*. When comparing cadaver GI tracts, the upper and lower tract differed. The oral microbiome (swab and scrape) of STAFS 2011-016 contained *Streptococcus, Prevotella,* and *Veillonella*, which are typical of healthy participants in the HMP. However, STAFS 2011-016 varied from STAFS 2011-006, where the top ten genera consisted of only *Streptococcus*; despite the variation, these three overall genera were also reported in the top five oral cavity genera in the HMP.

It is commonly reported and accepted that the decomposition environment shifts, post bloat, from aerobic (*Staphylococcus* and Enterobacteriacae) to anaerobic (Clostridia and *Bacteroides*) bacteria (Evans 1963; Janaway et al. 2009; Vass 2001; Melvin et al. 1984). Hyde et al.'s (2013) findings also report the shift from aerobic to anaerobic bacteria; specifically, they found previously documented bacteria (*Clostridium*, *Bifidobacterium* and *Lactobacillus)* and proposed novel bacteria that have not been identified in decomposition studies using culture-based methods. Because the mouth samples were not collected destructively, they could be sampled pre- and post- bloat, allowing for the comparison of taxa relative abundances to determine if and how bacterial communities vary with decomposition stages. In STAFS 2011-006, Firmicutes dominated the pre-bloat swab, while Proteobacteria dominated the pre-bloat scrape; additionally, Firmicutes dominated one end-bloat scrape (Hyde et al. 2013). Meanwhile, the samples collected from STAFS 2011-016 were more similar to each other than to the other cadaver, despite the variation in relative abundance. While the pre-bloat swab and scrape were dominated by Firmicutes and Actinobacteria, respectively, they also contained Bacteroidetes and Actinobacteria. The STAFS 2011-006 end-bloat scrape contained both Firmicutes and Proteobacteria. Although the study did not initially seek to compare collection methods, results suggest that collection methodology appears to impact relative abundance.

Due to the limited sampling time points and body sites in the aforementioned study, a second study was designed by Hyde et al. (2015). The new study placed two cadavers STAFS 2012-021 and STAFS 2012-023 at the STAFS facility in natural conditions and sampled from 15 August to September 8 2012. Samples were collected daily or every other day based on temperature and TBS scores from the mouth, left/right cheeks, left/right bicep region, torso and rectum. Similar to the Hyde et al. (2013) study, sequence

data were obtained through 16S rRNA marker gene amplification and 454-pyrosequencing and were analyzed with QIIME.

Regarding bacterial community richness and diversity, both cadavers STAFS 2012-021 and STAFS 2012-023 were similar for skin and fecal samples collected pre- and post-bloat; conversely, the pre- and post- bloat mouth samples of STAFS 2012-023 were richer and more diverse. Initial unweighted UniFrac-based PCoA clustering indicated that the samples were significantly separated; however, as decomposition progressed, samples clustered together, suggesting that samples from different locations homogenize over time. The phyla level relative abundances underwent similar changes between cadavers, where, for example, the majority of skin samples were initially dominated by Proteobacteria (60-80%). As decomposition progressed, Firmicutes increased along with Actinobacteria in lower abundances (5-10%). Mouth samples also followed the pattern of Proteobacteria dominance followed by an increase in Firmicutes. Meanwhile, fecal samples were characterized initially by Firmicutes (70%) and Bacteroides (20%) with Proteobacteria dominating post-bloat stages until skeletonization, when Firmicutes and Actinobacteria (10-12%) increased. Other locations (left cheek) showed variations, such as Proteobacteria dominating all collections except the last time point when Actinobacteria accounted for 70% of the microbial community.

Just as with body sites, microbial communities present on each cadaver differed, which the authors attributed to individuality (i.e. age, gender, weight) and freezing before placement. It is important to note that STAFS 2012-021 was associated with *Ignatzchineria* (20 - 55%) and *Actinetobacter* (5 - 15%), while, STAFS 2012-023 was dominated by *Clostridium* (10 – 40%) and *Acinetobacter* (5 – 20%), which are genera associated with insect activity. Additionally, *Actinobacter* (Family: Moraxellaceae, Class: Gammaproteobacteria), which was found on both cadavers, is commonly found in soil and has been reported present in animal model studies (Metcalf et al. 2013 and Pechal et al. 2014). Likewise, *Clostridium*, an anaerobic genus, is found in soil as well as feces, freshwater and marine sediments; however, Metcalf et al. (2013) and Pechal et al. (2014) only reported the presence of Clostridiaceae, but not *Clostridium*. The three aforementioned taxonomic groups (*Actinobacter, Ignatzchineria* and *Clostridium*) varied throughout decomposition. Differences in taxa diversity and relative abundance recovered from the left and right sides of the cadavers were also noted. Overall, the results suggest

that bacterial community structure initially varies for body sites, but changes as decomposition progresses. Bacteria associated with necrophagous flies (*Ignatzchineria* and *Wohlfartiimonas*) were identified at early stages of decomposition, while later stages were associated with bacteria commonly found in the soil (*Actinobacter*).

Because previous studies focused on external sampling, Hauther et al. (2015) validated an invasive sampling method, which involved repeated sampling in a small abdominal incision. After daily sample collection, the incision was sealed with tape. The control bodies were sampled once at various PMIs and compared the results to six test bodies. It was concluded that the sampling method did not impact the dominant bacterial populations substantially. Using the established method, a recent study by DeBruyn and Hauther (2017) sought to document postmortem changes in human gut bacterial communities by sampling the caeca of four cadavers placed in natural environments at the University of Tennessee, Knoxville, Anthropology Research Facility (ARF) in the summer of 2011. Initial analysis indicated that one individual had a different starting postmortem gut microbial community compared to the others. This was attributed to the antemortem insertion of a feeding tube (DeBruyn and Hauther 2017). Therefore, the individual was not included in the analyses. Based on the remaining three individuals, taxonomic richness increased and diversity decreased over time. Contrary to the correlation of time since death and the number of OTUs, Simpson's Index (diversity measurement) was found to be inversely correlated to time. Visualization of Bray-Curtis similarities using NMDS showed that microbial communities changed over time and the observed change, while variable, was similar for all three cadavers. Hierarchical clustering revealed a split in communities, which was correlated with decomposition progress (bloat stage) in all three cadavers. In the early stages (prior to the shift), the major phyla identified were characteristic of the human gut microbiome: Firmicutes and Bacteroidetes. Furthermore, the early stage microbial communities were found to be more diverse and similar among the individuals, compared to later stages. Regarding relative abundance, Firmicutes and Bacteroidetes remained the dominant phyla as decomposition progressed.

Generally, it was reported that the gut microbial communities change in a like manner over time, resulting in a common decomposition community that was driven by Clostridiales (*Clostridium* spp. and *Anaerosphaera* spp.) and Gammaproteobacteria (*Ignatzchineria and Wohlfahrtiimonas*). In the end, this study (DeBruyn and Hauther 2017) was able to

identify taxa, such as *Bacteroides* and *Parabacteroides*, that are related inversely to PMI. The use of *Bacteroides* was supported by Hauther et al. (2015), in which *Bacteroides* quantification, via qPCR, demonstrated a quantifiable relationship of increasing PMI with decreasing relative abundance.

Soil Environments

Microorganisms associated with remains and the surrounding environment contribute to decomposition. Specifically, surrounding soil microbial community biomass and activity (Child 1995; Putman 1978; Hopkins et al. 2000; Carter and Tibbett 2006), as well as nematode abundance (Todd et al. 2006; Metcalf et al. 2013), have been reported to: (1) change throughout the decomposition process (Moreno et al. 2011) and across seasons (Carter et al. 2015); (2) become conditioned by previous decomposition events (Carter and Tibbett 2008); and (3) provide decomposition signatures, indicating the presence of remains or clandestine graves (Hopkins et al. 2000; Moreno et al. 2011).

At the University of Tennessee ARF, Moreno et al. (2011) compared soil samples collected in triplicate from underneath nine decomposing remains. Analysis initially indicated that gravesoil was 50% dissimilar on average from itself over time. Damann, et al. (2012) also evaluated moisture content, pH, organic content, total nitrogen content, and biomass by lipid-bound phosphorus at sites throughout the University of Tennessee's ARF, and found significant differences in the soil of the facility compared to similar external environments. Metcalf et al. (2013) examined microbial changes on body sites and in gravesoil samples of mice; the study results, similar to Moreno et al. (2011), suggested that as time progressed the microbial community differentiated from the original microorganisms, while increasing in similarity across sites (Metcalf et al. 2013). Additionally, soil and skin samples were both characterized by families, such as Bacteroidetes, Alphaproteobacteria and Betaproteobacteria, that increased with advanced stages of decay. These findings support the idea that skin communities change to reflect the surrounding environment.

By further analysis using 16S rRNA, 18S rRNA and ITS markers, Metcalf et al. (2016) demonstrated that, once remains are removed, decomposer microbial communities distinct to each soil type (desert, shortgrass prairie and forest) are retained for at least 30

days. These results further support the potential for using microorganisms to determine if decomposing remains were moved or to locate clandestine graves. Similarly, Moreno et al. (2011) reported gravesoil profile uniqueness, which was contributed to microorganisms inherent to the soil and to the decomposing remains; this suggested that it may be possible to test the soil for trace human DNA and/or for indicators that an individual had decomposed there. In decomposition, human materials and fluids are transferred to the soil, which has been supported by Moreno et al. (2011) who found microorganisms commonly associated with the human intestine, mouth and skin in gravesoils. This transfer of microorganisms from the remains to the soil may be inhibited by scavengers and/or insects (Carter et al. 2007). Specifically, insects can consume a cadaver before scavengers arrive and microbes can release repelling toxins, preventing scavengers from consuming all of the remains (only 35 – 75% consumed). When the activity of microbes and insects is decreased (for example, in winter), scavengers can consume almost 100% of the remains, which ultimately impacts the microbial composition of the soil.

Another study by Carter et al. (2015) examined microbial eukaryotic and bacterial communities in control soil and gravesoil, which was collected from below swine carcasses from February and June trials. The authors report that season significantly impacts bacterial communities in carcass-free soils, but it does not impact eukaryotic microbial communities. Meanwhile, both bacterial and microbial eukaryotic gravesoil communities differed significantly between seasons. Specifically, when compared to winter trials, greater relative abundances of the family Chitinophagaceae (Bacteroidetes: Sphingobacteriales) and rhabditid nematodes were identified in summer gravesoils for bacteria and microbial eukaryotes, respectively. Carter et al. (2015) also reported that post-rupture gravesoil bacterial communities differed from their controls in summer and winter; however, the observed change was more drastic in summer samples that were characterized by large abundances of *Sphingobacterium*. Similarly, post-rupture gravesoil eukaryotic communities differed from control soils in the summer but not winter. For example, summer post-rupture gravesoil sample microbial eukaryotes, such as nematode Rhabditidae, slime mold *Fonticula alba*, amoeba Euamoebida, fungus Eurotiomycetes, and fungus Tremellomycetes, were found in significantly high abundances, when compared to winter. Furthermore, Weiss et al. (2016) explored the impact of carcass size on the succession of soil microorganisms. A total of twelve swine carcasses weighing 1, 20, 40 and 50 kg were placed on grassland soil during the summer in Nebraska. Soil

samples were collected after placement and at 24 hour intervals for 1, 2, 4-6, 9 and 15 days postmortem from underneath the carcasses. Overall, the results suggested that carcass decomposition significantly impacted the gravesoil microbial community structure, while carcass size did not.

As previously mentioned, decomposing material (e.g. fluids) are introduced to the soil; therefore, Carter and Tibbett (2008) investigated the impact of repeated burial on soil composition and the decomposition process. To do so, skeletal muscle tissue was mixed and incubated for 70 days in one of three soil types from Great Britain. After 70 days, any remaining tissue was removed and the soils were then placed in microcosms. Half of the samples were then used to rebury skeletal muscle tissue that was incubated for another 42 days. As a result of repeated burial, skeletal muscle tissue underwent more rapid decomposition. The increased decomposition contributed to a change in soil microbial community function and an increase in zymogenous microorganisms, rather than an increase in soil microbial biomass. To further explore the impact of soil on decomposition, Lauber et al. (2014) placed mice on soil that had either been sterilized or left untreated (i.e. with intrinsic microorganisms). Mice that were placed on unaltered soil reached advanced decomposition 2 – 3 times faster than mice on sterile soil. Additionally, microbial communities differed between treatment groups (i.e. sterilized or unaltered soil) for both the skin and gravesoil samples collected during the active and advanced stages of decomposition. For example, microbial eukaryotes, such as Mucoromycotina, were identified in the unaltered group and absent in the sterilized group. Others in this fungi group have been reported to become abundant in the latter stages of plant litter decomposition. Meanwhile, bacterial genera, such as *Morganella* and *Proteus,* were found in high abundances in the later stages of the unaltered group, compared to day 0 and those samples in the sterilized group. Lauber et al. (2014) also proposed that the difference in decay rate may be due to the alpha diversity of microbial communities. For instance, soils with increased microbial diversity also possess a more diverse set of metabolic capabilities, allowing for an increase in decomposition.

Furthermore, plant litter (i.e. leaves, roots, twigs, etc.) in the soil and the environment surrounding the remains may impact decomposition. Specifically, Mant (1950) suggested that plant litter surrounding buried remains increases decomposition, as it aerates the area around the remains and widens the ratio of carbon to nitrogen, increasing microbial activity

(Tibbett and Carter 2008). The plant litter may also introduce decomposer communities that are specifically equipped for decomposition, which could accelerate decomposition. The ability of plant litter to impact decomposition may depend on nutrient content, season and climate, as reported by Bjornlund and Christensen (2005), Mora-gómez et al. (2016) and Duarte et al. (2016).

For more information regarding soil analysis in decomposition studies see Tibbett and Carter (2008) and Hyde et al. (2017).

Aquatic Environments

Human remains deposited in aquatic environments are exposed to conditions that vary from terrestrial environments with regard to water salinity, temperature, depth, tides, currents, pH, aquatic scavengers, floating or sunken debris, oxygenation, etc. Previous studies have utilized salmon and whale carcasses to monitor decomposition in freshwater and marine environments, respectively (Richey et al. 1975; Mathisen et al. 1988; Parmenter and Lamarra 1991; Brickell and Goering 1970; Durbin et al. 1979; Wold and Hershey 1999; Johnston et al. 2004; Goffredie and Orphan 2010; Smith et al. 1989; Allison et al. 1991; Smith et al. 2015; Goffredi et al. 2008; Treude et al. 2009). While these studies provide a foundation for understanding microbial communities in aquatic environments throughout the decomposition process, their applicability to humans is limited due to the fundamental differences between aquatic and terrestrial organisms. As previously discussed and demonstrated, swine are commonly used as models for human decomposition; therefore, two studies (Dickson et al. 2011; Benbow et al. 2015) have utilized swine in studying aquatic decomposition.

First, Dickson et al. (2011) submerged three swine heads in the Otago Harbor, south-eastern New Zealand. The first was deployed for 11 days in autumn, the second for 21 days in early winter and the third for 21 days in late winter. Samples were collected at 2-4 day intervals by raising from cages and swabbing areas of the skin (autumn: cheek, snout and neck wound; winter: cheek). In total, 15 orders, 21 families and 29 genera were identified. Regarding phyla, Proteobacteria, Bacteroidetes, Firmicutes, Fusobacteria and Actinobacteria were dominant. At the genus level, *Flavobacterium, Photobacterium* and *Lutibacter* were identified on the cheek, *Fusobacterium* and Pseudomonadaceae on the

snout, *Vagococcus* on the neck wound. While several genera were indicative of autumn or winter, six genera were shared between seasons: *Arcobacter, Psychrobacter, Pseudoalteromonas, Shewanella, Vibrio,* and *Tenacibaculum*.

Bacterial communities also changed throughout the submersion period in similar patterns (Dickson et al. 2011). For instance, bacterial colonization at the genus level occurred at a single time period in the autumn (69% genera) and winter (79% genera) trials. Some of the early colonizers identified in the first samples, such as *Fusobacterium* and *Nevskia*, were not recovered at later sampling periods. Recurring bacteria were also identified; of the eight genera considered recurring, *Pseudoalteromonas, Psychrobacter* and *Vibrio* were the most frequent and considered poor indicators of the postmortem submersion interval. Meanwhile, other bacterial genera colonized the remains after a specific period of submersion, making them beneficial for PMSI estimation. For autumn carcasses, Bacteroidales *Genus* 8 was detected after 5 days of submersion (80 ADD), *Shewanella* and *Aeromonas* were documented after 7 days or 107 ADD and *Carnobacterium* was documented only on sampling day 7. Regarding winter carcasses, *Polaribacter, Tenacibaculum* and Bacteroidales *Genus 4* were identified after 10 days (60 ADD) of submersion. Overall, the study suggests that colonization of remains submerged in a marine environment occurs in a successional manner, which varies between seasons (autumn and winter), and could be used for estimating the postmortem submersion interval.

A second microbial study focusing on aquatic decomposition was performed by Benbow et al. (2015) in a freshwater stream from 26 June to 17 July 2012 and 9 November to 21 December 2012. During each trial, three stillborn swine carcasses were submerged and sampled from the abdomen/rib cage. Sampling took place weekly in summer and biweekly in winter for a total of four time points. Using 454-pyrosequencing of the 16S rRNA gene amplification products, 17 phyla and 179 genera were identified in the summer trial, which varied slightly with 13 phyla and 202 genera detected. Similar to previous studies, Proteobacteria and Firmicutes were determined to be the dominant phyla in both trials. Over the decomposition process, Proteobacteria decreased from 91.4% to 30.5%, while Firmicutes increased from 2.4% to 58%. Specific succession patterns were identified for both trials. During the summer trial, *Pseudomonas, Psychrobacter* and *Ewingella* dominated Day 0; *Klebsiella, Psychrobacter* and *Citrobacter* dominated Day 7; by Day 14

the community structure shifted to *Zoogloea, Clostridium, Dechloromonas* and *Desulfosporomusa*; finally, Day 21 was dominated by *Clostridium, Enerococcus* and *Lactobacillus.* The winter trial was initially dominated by *Psychrobacter, Pseudomonas* and *Enterococcus*; by Day 14 *Lactococcus* was predominant; *Proteocatella, Clostridium* and *Veillonellaceae* was present on Day 28; and Day 42 was characterized by *Veillonellaceae* and *Clostridium.* Additionally, the observed differences between seasons were significant, and the communities differed between days in the summer trial. Finally, an increase in taxa was observed over the range of decomposition stages; genera increased from 21 to 82 in summer and 38 to 108 in winter.

Other Factors: Freeze-Thaw

As mentioned in the discussion of Terrestrial Environments, Micozzi (1986) was among the first to attempt and succeed in identifying decomposition microbial changes in animal models. He was also one of the first to examine the effects of freeze-thaw on microorganisms. A total of eight female rats of which four were frozen at -7 ^{o}C for four weeks and thawed at room temperature before placing them in the field with the remaining four rats that were killed two hours before placement. One pair of the rats were sampled at baseline, while the remaining three were placed in secure cages in Wissahickon Park, Philadelphia, PA. Sampling involved removing one pair of rats at two days (48 hours), four days (96 hours) and six days (144 hours) for necropsies and bacterial cultures of the heart, lungs, spleen and abdominal viscera. Over the 6-day (144 hour) period, microbial succession from enteric to soil organisms was observed; in addition, the fresh and frozen rats had similar organismal sequences, despite the more rapid procession of enteric microorganism growth in fresh animals. It was also observed that animals exposed to freeze-thaw conditions were more vulnerable to insect and microbial invasion and aerobic external (skin) decay. Conversely, fresh animals experienced putrefaction from within more rapidly, while maintaining resistance to external decay. It was concluded that freeze-thaw exposure disrupted the corpses' tissues, allowing for the introduction of environmental organisms and aerobic decomposition, ultimately decreasing enteric organisms from proliferating.

Since Micozzi's study, Pechal et al. (2017) have revisited the impact of thawing on the postmortem microbiome using two pediatric cases. A pair of half siblings (9-year old male and 13-year old female) were recovered from a chest freezer in the spring of 2015. The

remains were removed from the freezer and placed on clean sheets and covered with a clean damped sheet to prevent drying while thawing before autopsy. Upon removal of the remains from the freezer , microbial samples were collected from the auditory canal, eyes, nares, mouth, umbilicus and rectum, during a period when the remains were partially thawed (24 hours) and fully thawed (48 hours). As the bodies thawed, an increase in OTU richness and diversity was observed. While the buccal samples contained the highest mean number of taxa, the most prevalent increase in diversity was observed in the nares, eyes and rectum. Regarding the number of OTUs, ears, eyes, nares and buccal cavity all experienced an increase from frozen to thawed, while rectal samples decreased and umbilicus samples plateaued after partial thawing (24 hours). Additionally, it was observed that the variability in microorganisms across body sites decreased with thawing. Changes in the community composition included Actinobacteria, Fusobacteria and Gammaproteobacteria increasing, while Firmicutes decreased and Bacteroidetes remained unchanged. At the family level, Corynebacteriaceae, Fusobacteriaceae, Pasteurellaceae, Pseudomonadaceae and Tissierellaceae were found to increase with thawing and Prevotellaceae and Staphylococcaceae were found to decrease. Similar changes or turnovers were observed in genera-level OTUs: *Corynebacterium, Haemophilus, Fusobacterium,* and *Streptococcus* increased; *Staphylococcus* decreased; and *Lactobacillus* was almost undetectable when the remains were partially thawed. Regarding body sites, unique profiles at the genus level were identified throughout the thawing process. As a result, the study showed that microbial communities change during the thawing process, which has important implications when using microorganisms to analyze remains that have been modified after death.

Other Factors: Insects

It has long been accepted by forensic entomologists that necrophagous flies and beetles colonize carrion remains in a successional manner. Although there is hope that the interactions between insects and decomposer microbial communities could determine which insects are attracted to and colonize remains (Jordan and Tomberlin 2017), unfortunately, there is limited understanding of how microbial communities and insects interact throughout decomposition, and researchers are only now beginning to explore these interactions. Some researchers, such as Singh et al. (2015) and Zheng et al. (2013), have begun surveying bacterial diversity on two species of *Lucillia* and black solider flies,

respectively. Meanwhile, others have examined the immediate interaction between insects and the decomposition process.

By collecting insects from salmon-carcass filled freshwater stream, Pechal and Benbow (2016) sought to characterize internal microbial communities of aquatic insects in carcass-free streams and those containing salmon carcasses. Overall, they found a significant difference in mayfly internal microbial communities obtained from carcass-filled and carcass-free streams. For mayflies across all streams, microbial community composition, regarding relative abundance, included five phyla: Actinoacteria, Bacteroidetes, Firmicutes, Proteobacteria and Tenericutes. When comparing one species of mayfly (*A. rusticus*) from different streams, it was observed that Proteobacteria was reduced by 53.8% in streams with salmon carcasses. However, the remaining two species (*Cinygmula* sp. and *Epeorus* sp.) collected from salmon carcasses-filled streams were characterized by an increase in Proteobacteria of 40.3% and 43.9%. Pechal and Benbow (2016) also sought to compare the epinecrotic microbial community of salmon carcasses to terrestrial necrophagous insects, using *Calliphora terranovae* larvae collected from salmon carcasses. Regarding all individuals, three phyla (Bacteroidetes, Firmicutes and Proteobacteria) accounted for more than 90% of the microbial community relative abundance and 20 OTUs were detected in all types of samples. Replicate carcasses and their associated larvae shared only 22.4-26.2% of OTUs, indicating that the larval internal microbiome is partially independent of the food source. Alpha diversity measures were not significantly difference among sample types. However, beta diversity measures (weighted UniFrac) determined that sample type impacted microbial community assembly. Specifically, epinecrotic communities and *C. terranovae* larvae had similar microbial communities, while adults clustered together with minimal overlap between larvae and carcass. Generally, the findings suggest that, while some of the larvae's microbial community may come from the carcass, the majority comes from the main food source. Finally, there was little evidence to suggest that the adult blow fly microbiome is influenced by the carcass.

As discussed in the Terrestrial Environments section, Pechal et al. (2013) used swine carcasses to examine the effects of season, year (2010 and 2011) and insects on microbial community function change throughout decomposition. In the 2010 trial, there was no significant difference between carcasses that were categorized as insect exclusion

(EXC) or insect access (ACC). For ACC carcasses, microbial functional activity increased by 4.2%, while decreasing 35.7% in EXC groups. Variation between EXC and ACC was explained by NMDS ordination and suggested that there was no significant difference in MMCPs between the treatment groups. Unlike the 2010 trial, the mean microbial functional activity of ACC carcasses for the 2011 trial decreased by 46.3% and increased on EXC carcasses by 45.2%. There was no significant difference between groups for carcass MMCPs. Overall, the results were inconsistent regarding the impact of necrophagous insect activity on MMPs.

To further determine how and what insects contribute to the human decomposition microbial community, Metcalf et al. (2016) sampled 79 blow fly tarsi and concluded that blow flies contribute to the decomposition microbial community, even though soil contributes greater quantities of microbial decomposers. Also using human remains, Hyde et al. (2015) identified bacteria associated with myiasis by fly larvae. Specifically, *Ignatzchineria* (Family: Xanthomonadaceae) commonly associated with Sarcophagidae fly larvae was found across all body sites, until skeletonization when the abundance decreased. *Wohlfahrtiimonas* (Family: Xanthomonadaceae), a genera associated with myiasis by Sarchophagidae fly larvae, was also reported to increase on mouse cadavers and in gravesoil by Metcalf et al. (2013). Likewise, Pechal et al. (2014) noted low abundances of Xanthomonadaceae on swine carcasses. This supports that Xanthomonadaceae, regardless of host type, may be contributing to the microbial decomposition community.

Postmortem Interval Estimation via Microorganisms

Universal Signatures

Determining if there is a universal decomposition signature holds important implications to the field of forensic science. First, a universal signature would validate the use of animals as model organisms for human decomposition and allow for the extrapolation of information from animals to humans. Secondly, identifying a universal signature will support the construction of accurate estimation models for PMI and PMSI. Hyde et al. (2017) identified taxa from soil and skin (early and late decomposition stages) from all three models, which can be seen in Table 1.2. It is suggested that family level taxa could be involved universally across animals and humans in terrestrial environments.

Table 1.2. Bacterial taxa present and absent among three models commonly used in decomposition studies: Mouse, Swine and Human (adapted from Hyde et al. 2017)

	Mouse			Swine			Human		
TAXA	Soil	Early Decomposition	Late Decomposition	Soil	Early Decomposition	Late Decomposition	Soil	Early Decomposition	Late Decomposition
Phylum									
Proteobacteria	✓	✓	✓	✓	✓	✓	----------	✓	✓
Firmicutes	✓	✓	✓	✓	✓	✓	----------	✓	✓
Family									
Xanthomonadaceae	✓	✓	✓	✓	✓	✓	----------	✓	✓
Clostridiaceae	✓	✓	✓		✓	✓	----------	✓	✓
Moraxellaceae	×	×	×	✓	✓	✓	----------	✓	✓
Pseudomonadaceae	✓	✓	✓	----------	----------	----------	----------	----------	----------
Sphingomonadaceae	✓	✓	✓	----------	----------	----------	----------	----------	----------
Genus									
Corynebacterium	----------	----------	----------	----------	----------	----------	----------	✓	✓
Clostridium	----------	----------	----------	----------	✓	✓	----------	✓	✓
Ignatzchineria	×	×	×	✓	----------	----------	----------	✓	✓
Pseudomonas	----------	----------	----------	----------	✓	✓	----------	✓	✓

PMI Estimation

Thus far, this chapter has addressed microorganisms associated with terrestrial and aquatic decomposition, soil environments, freeze-thaw cycles, insects and animal models; however, it has not addressed whether it is possible to accurately estimate the PMI. Because microorganisms are always present (regardless of season), can thrive in harsh environments (i.e. hot springs), and respond to changes in a predictable manner, they are a ubiquitous and predictive type of physical evidence. As a result, researchers have used model organisms and human models to capture the microbial community changes. In order to estimate PMI from the documented community changes, models can be developed by regressing the known PMI on the microbial taxa relative abundances. A few studies (Pechal et al. 2014; Metcalf et al. 2013; Metcalf 2016) have used the Random Forest classifier, a machine learning technique, to first create decision trees on a predetermined subset of characters (e.g. relative abundance) and then identify the characters that classify the unknown samples with highest accuracy (Hyde et al. 2017). Another method used for building prediction models relies on identifying taxa that drive

sample separation, which requires using both multi-response permutation and indicator species analysis.

As described in terrestrial environments, Pechal et al. (2014) placed three swine in a temperate forest habitat and collected samples from the buccal cavity and skin four times over a five-day period. To develop PMI estimation models, they used ISA or random forest analysis to select indicator phyla or families. The full random forest model, including five phyla identified, resulted in 84.1% of the variation explained. Of the five phyla identified, Bacteroidetes, Proteobacteria, Actinobacteria and Firmicutes provided the best model (84.4% variation explained). It was observed that the four phyla relative abundances shifted greatly over the decomposition process, suggesting that there are broad patterns in bacterial communities that may be useful for estimating PMI. At the lower taxonomic level, family indicators identified by random forest analysis produced models explaining 62.3 – 92.3% of the variation in physiological time. However, ISA family level indicators, consisting of only 10 taxa (Campylobacteraceae + Enterococcaceae + Prevotellaceae + Moraxellaceae + Hyphomicrobiaceae + Clostridiales Incertae Sedis XI + Porphyromonadaceae + Pasteurellaceae + Bacillales Incertae Sedis XI + Brucellaceae), generated the best model, explaining 94.4% of physiological time variation, which predicted time since placement within 2- 3 hours after death for swine models.

Similarly, Metcalf et al. (2013) used the random forest classifier to build regression models based on bacterial and microbial eukaryotic communities identified on mice models. Overall, they produced models based on 5-10 predictive taxa, which allowed for the estimation of PMI to within ~3 days over a 48-day period. While initial observations suggested that PMI estimation was more informative for early stages of decomposition and that skin and soil sites were preferred over abdominal cavity samples, these trends may be due to the decreased frequency of samples from days 13 – 48 and the variable changes in decomposition stages (e.g. rupture occurring on different days). Intriguingly, neither bacteria nor microbial eukaryotes generated the best PMI estimates, rather a combination of both 16S and 18S rRNA gene datasets insignificantly increased the ability to estimate of PMI. For all sample sites, Rhizobiales (Order) were the most important predictive bacterial taxa; meanwhile, *Oscheius* was the most important microbial eukaryote for skin and abdominal sites and second most for gravesoil. Nevertheless, this study was the first to utilize microbial eukaryotic communities along with bacterial

communities to estimate PMI, and the results suggests that a combination of the two may represent a more accurate prediction method.

In another study by Metcalf et al. (2016), mice models were again used; however, they were placed on three different soil types (mountain pine forest, shortgrass prairie and Moab desert) to decompose. Ultimately, it was concluded that all sample types (skin, abdomen and soil) provided estimates of PMI with an accuracy within 2-3 days over the first 25 days of decomposition, while mouse cecum and gravesoils provided the most accurate estimates. Additionally, when soil type was added to the regression model, the error did not change, suggesting that soil type did not impact accuracy. As a result, gravesoils, an accessible and easily collected piece of evidence, could be beneficial for outdoor crime scenes.

Conclusions

The current literature demonstrates that microbial changes occur in a succession-like pattern throughout the decomposition process in both terrestrial and aquatic environments. These changes can be utilized to estimate PMI or PMSI, especially in scenarios where insects are not present or other methods cannot be applied. In addition, the microbial patterns found in soil have been shown to remain days to years after decomposition and can thus be used to determine if decomposing remains have been moved to a new location and/or to assist in locating clandestine graves. The existence of indicator taxa on various body sites as well as in soil is somewhat less well-documented at the current time at a meaningful taxonomic level, but with larger samples sizes and the employment of random forest modelling may yet prove definitive as a predictor of the PMI.

While the use of microorganisms in forensic science has increased in the last decade, it has not yet been admitted as evidence in a court of law. This serves to highlight the remaining work that needs to be done in order to ensure consistent, valid and reliable results may be applied to legal investigations. Before laboratories address the need to incorporate training and equipment into laboratory workflows, researchers must demonstrate: (1) that microbial communities associated with decomposition are universal across environment, season and geographical location; (2) whether decomposer microorganisms are inherent to the host or the surrounding environment being sampled;

(3) whether metabolic succession is conserved across the physiochemical host phylogeny and context of decay (Metcalf et al. 2016); (4) whether microbial communities do or do not vary based on model organism used; (5) whether scavenger/insect activity ultimately contributes to or alters microbial communities; and (6) that validation strategies and protocols can be conclusively written for implementation into laboratory workflows. Nevertheless, work is ongoing for designing and completing projects that will address current issues, advancing the applicability of microbiome science in forensic investigations.

References

1. Achtman, M. and Wagner, M. (2008) Microbial diversity and the genetic nature of microbial species, *Nature Reviews Microbiology,* 6(6), pp. 431–440.
2. Adlam, R. and Simmons, T. (2007) The effect of repeated physical disturbance on soft tissue decomposition – are taphonomic studies an accurate reflection of decomposition? *Journal of Forensic Sciences,* 52(5), pp. 1007-1014.
3. Angiuoli, S.V., Matalka, M., Gussman, A., galens, K., Vangala, M., Riley, D.R., Arze, C., White, J.R., White, O. and Fricke, W.F. (2011) CloVR: a virtual machine for automated and portable sequence analysis from the desktop using cloud computing, *BMC Bioinformatics*, 12, pp. 356.
4. Benbow, M.E., Pechal, J.L., Lang, J.M., Erb, R. and Wallace, J.R. (2015) The potential of high-throughput metagenomic sequencing of aquatic bacterial communities to estimate the postmortem submersion interval, *Journal of Forensic Sciences*, 60(6), pp. 1500–1510.
5. Benson, D.A., Karsch-Mizrachi, I., Lipman, D.J. and Sayers, E.W. (2005) GenBank. *Nucleic Acids Research*, 33, D34–D38.
6. Bjornlund, L. and Christensen, S. (2005) How does litter quality and site heterogeneity interact on decomposer food webs of a semi-natural forest?, *Soil Biology and Biochemistry*, 37, pp.203–213.
7. Breiman, L. (2001) Random forests. *Machine Learning*, 45, pp. 5–32.
8. Brickell, D.C. and Goering, J.J. (1970) Chemical effects of salmon decomposition on aquatic ecosystems, in Murphy, R.S. (ed.) *Proceedings Symposium on Water Pollution Control in Cold Climates*, U.S. Government Printing Office, Washington, D.C.
9. Caporaso, J.G., Lauber, C.L., Walters, W.A., Berg-Lyons, D., Huntley, J., Fierer, N., Owens, S.M., Betley, J., Fraser, L., Bauer, M., Gormley, N., Gilbert, J.A., Smith, G. and Knight, R. (2012) Ultra-high-throughput microbial community analysis on the Illumina HiSeq and MiSeq platforms, *ISME J,* 6(8), pp. 1621–1624. doi: 10.1038/ismej.2012.8.
10. Cardona, S., Eck, A., Cassellas, M., Gallart, M., Alastrue, C., Dore, J., Azpiroz, F., Roca, J., Guarner, F., and Manichanh, C. (2012) Storage conditions of intestinal microbiota matter in metagenomic analysis, *BMC Microbiology,* 12(158).
11. Carroll, I.M., Ringel-Kulka, T., Siddle, J.P., Klaenhammer, T.R., and Ringel, Y. (2012) Characterization of the fecal microbiota using high-throughput sequencing reveals a stable microbial community during storage, *Plos One,* 7(10): e46953.
12. Carter, D.O. and Tibbett, M. (2006) The decomposition of skeletal muscle tissue (*Ovis aries*) in a sandy loam soil incubated at different temperatures, *Soil Biology and Biochemistry*, 38, pp. 1139–1145.
13. Carter, D.O. and Tibbett, M. (2008) Does repeated burial of skeletal muscle tissue (Ovis aries) in soil affect subsequent decomposition?, *Applied Soil Ecology*, 40(3), pp. 529–535.
14. Carter, D.O., Metcalf, J.L., Bibat, A. and Knight, R. (2015) Seasonal variation of postmortem microbial communities, *Forensic Science, Medicine, and Pathology*, 11, pp. 202–207.
15. Carter, D., Yellowless, D. and Tibbett, M. (2008) Temperature affects microbial

decomposition of cadavers (*Rattus rattus*) in contrasting soils, *Applied Soil Ecology*, 40(1), pp. 129–137.

16. Chakravorty, S., Helb, D., Burday, M., Connell, N. and Alland, D. (2007) A detailed analysis of 16S ribosomal RNA gene segments for the diagnosis of pathogenic bacteria, *Journal of Microbiological Methods*, 69, pp. 330–339.
17. Child, A.M. (1995) Towards an understanding of the microbial decomposition of archaeological bone in the burial environment, *Journal of Archaeological Science*, 22(2), pp. 165–174.
18. Christensen, A, Passalacqua, N, and Bartelink, E. (2014) Forensic Anthropology: Current Methods and Practice. Academic Press, San Diego, CA. pp. 119
19. Cobaugh, K.L., Schaeffer, S.M. and DeBruyn, J.M. (2015) Functional and structural succession of soil microbial communities below decomposing human cadavers, *PLoS One*, 10(6), e0130201.
20. Cole, J.R., Wang, Q., Cardenas, E., Fish, J., Farris, R.J., Kulam-Syed-Mohideen, A.S., McGarrell, D.M., Marsh, T., Garrity, G.M. and Tiedje, J.M. (2009) The Ribosomal Database Project: improved align- ments and new tools for rRNA analysis, *Nucleic Acids Research*, 37, D141–D145.
21. Cressman, M.D., Yu, Z., Nelson, M.C., Moeller, S.J., Lilburn, M.S., and Zerby, H.N. (2010) Interrelations between the microbiotas in the litter and in the intestines of commercial broiler chickens, *Applied and Environmental Microbiology,* 76(19), pp. 6572–6582.
22. Damann FE, Tanittaisong A and Carter DO. (2012) Potential carcass enrichment ofthe University of Tennessee Anthropology Research Facility: a baseline survey of edaphic features. *Forensic Science International*, 222, pp. 4–1
23. DeBruyn J.M. and Hauther K.A. (2017) Postmortem succession of gut microbial communities in deceased human subjects, *PeerJ,* 5, e3437https://doi.org/10.7717/peerj.3437
24. De la Cuesta-Zuluaga, J., and Escobar, J. S. (2016) Considerations for Optimizing Microbiome Analysis Using a Marker Gene, *Frontiers in Nutrition*, *3*, pp. 26. http://doi.org/10.3389/fnut.2016.00026
25. Delmont, T.O., Robe, P., Clark, I., Simonet, P., and Vogel, T.M. (2011) Metagenomic comparison of direct and indirect soil DNA extraction approaches, *Journal of Microbiological Methods,* 86(3), pp. 397–400.
26. DeSantis, T.Z., Hugenholtz, P., Larsen, N., Rojas, M., Brodie, E.L., Keller, K., Huber, T., Dalevi, D., Hu, P. and Anderson, G.L. (2006) Greengenes, a chimera-checked 16S rRNA gene database and workbench compatible with ARB, *Applied and Environmental Microbiology*, 72, pp. 5069–5072.
27. Dickson, G.C., Poulter, R.T.M., Maas, E.W., Probert, P.K. and Kieser, J.A. (2011) Marine bacterial succession as a potential indicator of postmortem submersion interval, *Forensic Science International*, 209**(**1–3), pp. 1–10.
28. Duarte, S., Cássio, F., Ferreira, V., Canhoto, C. and Pascoal, C. (2016) Seasonal variability may affect microbial decom-posers and leaf decomposition more than warming in streams, *Microbial Ecology*, 72, pp. 263–276.
29. Durbin, A.G., Nixon, S.W. and Oviatt, C.A. (1979) Effects of the spawning migration

of the alewife, *Alosa pseudoharengus* on freshwater ecosystems, *Ecology*, 60(1), pp. 8–17.

30. Dufrene, M. and Legendre, P. (1997) Species assemblages and indicator species: the need for a flexible asymmetrical approach, *Ecological Monographs*, 67, pp. 345–366.
31. Edgar, R.C., B.J. Haas, J.C. Clemente, C. Quince, and R. Knight. (2011) UCHIME improves sensitivity and speed of chimera detection, *Bioinformatics,* 27(16), pp. 2194–2200.
32. Efremov, I.A. (1940) Taphonomy: a new branch of paleontology, *Pan American Geologist*, 74, pp. 81-93.
33. Evans, W. (1963) *The Chemistry of Death*, CC Thomas Publishers, Springfield, IL.
34. Finley, S.J., Pechal, J.L., Benbow, M.E., Robertson, B.K. and Javan, G.T. (2016) Microbial Signatures of Cadaver Gravesoil During Decomposition, *Microb Ecol.*, 71(3), pp. 524-529.
35. Gihring, T.M., Green, S.J. and Schadt, C.W. (2012) Massively parallel rRNA gene sequencing exacerbates the potential for biased community diversity comparisons due to variable library sizes, *Environmental Microbiology*, 14, pp. 285–290.
36. Grice, E.A., Kong, H.H., Renaud, G., Young, A.C., NISC Comparative Sequencing Program, Bouffard, G.G., Blakesley, R.W., Wolfsberg, T.G., Turner, M.L. and Segre, J.A. (2008) A diversity profile of the human skin microbiota, *Genome Research*, 18, pp. 1043–1050.
37. Goffredi, S.K. and Orphan, V.J. (2010) Bacterial community shifts in taxa and diversity in response to localized organic loading in the deep sea. *Environmental Microbiology*, 12(2), pp. 344–363.
38. Goffredi, S.K., Wilpiszeski, R., Lee, R. and Orphan, V.J. (2008) Temporal evolution of methane cycling and phylogenetic diversity of archaea in sediments from a deep-sea whale-fall in Monterey Canyon, California, *The ISME Journal*, 2(2), pp. 204–220.
39. Haas, B.J., Gevers, D., Earl, A.M., Feldgarden, M., Ward, D.V., Giannoukos, G., Ciulla, D., Tabbaa, D., Highlander, S.K., Sodergren, E., Methe, B., DeSantis, T.Z., The Human Microbiome Consortium, Petrosino, J.F., Knight, R., and Birren, B.W. (2011) Chimeric 16S rRNA sequence formation and detection in Sanger and 454-pyrosequenced PCR amplicons, *Genome Research,* 21(3), pp. 494–504.
40. Hauther, K.A., Cobaugh, K.L., Jantz, L.M., Sparer, T.E. and DeBruyn, H.M. (2015) Estimating Time Since Death from Postmortem Human Gut Microbial Communities, *Journal of Forensic Sciences,* 60(5), pp. 1234-1240.
41. Head, I.M., Saunders, J.R. and Pickup, R.W. (1998) Microbial evolution, diversity, and ecology: a decade of ribosomal RNA analysis of uncultivated microorganisms, *Microb Ecol*, 35, pp. 1–21.
42. Heaton, V., Lagden, A. Moffatt, C. and Simmons, T. (2010) Predicting the Post-Mortem Submersion Interval for Human Remains Recovered from UK Waterways. *Journal of Forensic Sciences*, 55(2):302-7
43. Henderson, G., Cox, F., Kittelmann, S., Miri, V.H., Zethof, M., Noel, S.J., Waghorn, G.C. and Janssen, P.H. (2013) Effect of DNA extraction methods and sampling

techniques on the apparent structure of cow and sheep rumen microbial communities, *PLoS One*, 8, e74787.

44. Holben, W.E., Jansson, J.K., Chelm, B.K., and Tiedje, J.M. (1988) DNA probe method for the detection of specific microorganisms in the soil bacterial community, *Applied and Environmental Microbiology,* 54(3), pp. 703–711.
45. Hopkins, D.W., Wiltshire, P.E.J. and Turner, B.D. (2000) Microbial characteristics of soils from graves: an investigation at the interface of soil microbiology and forensic science, *Applied Soil Ecology*, 14(3), pp. 283–288.
46. Huse, S.M., Huber, J.A., Morrison, H.G., Sogin, M.L. and Welch, D.M. (2007) Accuracy and quality of massively parallel DNA pyrosequencing, *Genome Biology*, 8, R143.
47. Hyde, E.R., Haarmann, D.P., Lynne, A.M., Bucheli, S.R. and Petrosino, J.F. (2013) The living dead: bacterial community structure of a cadaver at the onset and end of the bloat stage of decomposition, *PLoS One*, 8(10), e77733.
48. Hyde, E.R., Haarmann, D.P., Petrosino, J.F., Lynne, A.M. and Bucheli S.R. (2015) Initial insights into bacterial succession during human decomposition, *International Journal of Legal Medicine*, 129(3), pp. 661–671.
49. Hyde, E.R., Metcalf, J.L., Bucheli, S.R., Lynne, A.M. and Knight, R. (2017) Microbial communities associated with decomposing corpses, in D.O. Carter, J.K Tomberlin, M.Eric Benbow and J.L Metcalf (ed.) *Forensic Microbiology*, John Wiley and Sons Ltd.
50. Inceoglu, O., E.F. Hoogwout, P. Hill, and J.D. van Elsas. 2010. Effect of DNA extraction method on the apparent microbial diversity of soil, *Applied and Environmental Microbiology,* 76(10), pp. 3378–82.
51. Insam, H. and Goberna, M. (2004) *Use of Biolog® for the Community Level Physiological Profiling (CLPP) of Environmental Samples*. Dordrecht, The Netherlands: Kluwer Academic Publishers.
52. Jacobsen, C.S. and Rasmussen, O.F. (1992) Development and application of a new method to extract bacte- rial DNA from soil based on separation of bacteria from soil with cation-exchange resin, *Applied and Environmental Microbiology,* 58(8), pp. 2458–2462.
53. Janaway, R.C., Percival, S.L. and Wilson, A.S. (2009) Decomposition of Human Remains, in Percival, S.L. (ed.) *Microbiology and Aging,* Springer Science+Business Media, LLC, New York, pp. 313–334.
54. Johnston, N.T., MacIsaac, E.A., Tschaplinski, P.J. and Hall, K.J. (2004) Effects of the abundance of spawning sockeye salmon (Oncorhynchus nerka) on nutrients and algal biomass in forested streams, *Canadian Journal of Fisheries and Aquatic Sciences*, 403, pp. 384–403.
55. Jordan and Tomberlin (2017) Abiotic and Biotic Factors Regulating Inter-Kingdom Engagement between Insects and Microbe Activity on Vertebrate Remains, *Insects*, 8(2), pp. 54; doi:10.3390/insects8020054
56. Kakirde, K.S., L.C. Parsley, and Liles, M.R. (2010) Size does matter: Application-driven approaches for soil metagenomics, *Soil Biology and Biochemistry,* 42(11), pp.

1911–1923.
57. Klindworth, A., Pruesse, E., Schweer, T., Peplies, J., Quast, C., Horn, M. and Glockner, F.O. (2013) Evaluation of general 16S ribosomal RNA gene PCR primers for classical and next-generation sequencing-based diversity studies, *Nucleic Acids Research*, 41, e1.
58. Knight, B. (ed.), 2002. The Estimation of the Time Since Death in the Early Postmortem Period. Edward Arnold, London.
59. Kuczynski, J., Lauber, C.L., Walters, W.A., Wegner Parfrey, L., Clemente, J.C., Gevers, D. and Knight, R. (2012) Experimental and analytical tools for studying the human microbiome, *Nature Reviews: Genetics*, 13, pp. 47–58.
60. Kumar, P.S., Brooker, M.R., Dowd, S.E. and Camerlengo, T. (2011) Target region selection is a critical determinant of community fingerprints generated by 16S pyrosequencing, *PLoS One*, 6, e20956.
61. Lauber, C.L., Metcalf, J.L., Keepers, K., Ackermann, G., Carter, D.O. and Knight, R. (2014) Vertebrate decomposition is accelerated by soil microbes, *Applied and Environmental Microbiology*, 80(16), pp. 4920–4929.
62. Lauber, C.L., Zhou, N., Gordon, J.I., Knight, R. and Fierer, N. (2010) Effect of storage conditions on the assessment of bacterial community structure in soil and human-associated samples, *FEMS Microbiology Letters*, 307, pp. 80–86.
63. Lozupone, C. and Knight, R. (2005) UniFrac: a new phylogenetic method for comparing microbial communities, *Applied and Environmental Microbiology*, 71, pp. 8228–8235.
64. Mahalanabis, M., H. Al-Muayad, M.D. Kulinski, D. Altman, and Klapperich, C.M. (2009) Cell lysis and DNA extraction of gram-positive and gram-negative bacteria from whole blood in a disposable microfluidic chip, *Lab Chip,* 9(19), pp. 2811–2817.
65. Mankin, A.S., Skryabin, K.G. and Rubtsov, P.M. (1986) Identification of ten additional nucleotides in the primary structure of yeast 18S rRNA, *Gene*, 44, 143–145.
66. Mant, A.K. (1950) A study in exhumation data. MD thesis, London University.
67. Mathisen, O.A., Parker, P.L., Goering, J.J., Kline, T.C., Poe, P.H. and Scalan, R.S. (1988) Recycling of marine elements transported into freshwater systems by anadromous salmon, *Verhandlungen des Internationalen Verein Limnologie*, 23, pp. 2249–2258.
68. Megyesi, M., Nawrocki, S. and Haskell, N. (2005) Using accumulated degree-days to estimate the postmortem interval from decomposed human remains, *Journal of Forensic Sciences,* 50(3), pp. 618-26.
69. Melvin, J.R., Jr, Cronholm, L.S., Simson, L.R., Jr and Isaacs, A.M. (1984) Bacterial transmigration as an indicator of time of death, *Journal of Forensic Sciences*, 29(2), pp. 412–417.
70. Metcalf, J.L., Wegener Parfrey, L., Gonzalez, A., Lauber, C.L., Knights, D., Ackermann, G., Humphrey, G.C., Gebert, M.J., Van Treuren, W., Berg-Lyons, D., Keepers, K., Guo, Y., Bullard, J, Fierer, N., Carter, D.O., Knight, R. (2013) A microbial clock provides an accurate estimate of the postmortem interval in a mouse model system, *eLife*, 2, doi: 10.7554/eLife.01104

71. Metcalf, J.L., Xu, Z.Z., Weiss, S. *et al.* (2016) Microbial community assembly and metabolic function during mammalian corpse decomposition. *Science*, **351**, 158–162.
72. Micozzi, M.S. (1986) Experimental study of postmortem change under field conditions: effects of freezing, thawing and mechanical injury, *Journal of Forensic Sciences*, 31, pp. 953–961.
73. Miller, D.N., Bryant, J.E., Madsen, E.L. and Ghiorse, W.C. (1999) Evaluation and optimization of DNA extraction and purification procedures for soil and sediment samples, *Applied Environmental Microbiology,* 65(11), pp. 4715–4724.
74. Mitsuhashi, S., Kryukov, K., Nakagawa, S., Yakeuchi, J.S., Shiraishi, Y., Asano, K. and Imanishi, T. (2017) A portable system for rapid bacterial composition analysis using a nanopore-based sequencer and laptop computer, *Scientific Reports,* 7, doi:10.1038/s41598-017-05772-5
75. Moffatt, C., Simmons, T. and Lynch-Aird, J. (2016) An Improved Equation for TBS and ADD: Establishing a Reliable Postmortem Interval Framework for Casework and Experimental Studies, *Journal of Forensic Sciences,* 61(S1), pp. S201-S207
76. Mora-gómez, J., Elosegi, A., Duarte, S., Cassio, F., Pascoal, C. and Romani, A.M. (2016) Differences in the sensitivity of fungi and bacteria to season and invertebrates affect leaf litter decomposition in a Mediterranean stream, *FEMS Microbiology Ecology*, 92, pp. 1–35.
77. Moreno, L.I., Mills, D., Fetscher, J., John-Williams, K., Meadows-Jantz, L. and McCord, B. (2011) The application of amplicon length heterogeneity PCR (LH-PCR) for monitoring the dynamics of soil microbial communities associated with cadaver decomposition, *Journal of Microbiological Methods*, 84(3), pp. 388–393.
78. National Research Council, Committee on Identifying the Needs of the Forensic Sciences Community (2009) *Strengthening Forensic Science in the United States: A Path Forward*, National Academies Press, Washington, DC.
79. Ogram, A., Sayler, G.S., and Barkay, T. (1987) The extraction and purification of microbial DNA from sediments, *Journal of Microbiological Methods,* 7(2–3), pp. 57–66.
80. Oksanen, J., Blanchet, G.F., Kindt, R., Legendre, P., McGlinn, D., Minchin, P.R., O'Hara, R.B., Simpson, G.L., Solymos, P., Stevens, Szoecs, E. and Wagner, H. (2012) Vegan: community ecology package. R package version 2.0-4, https://cran.r-project.org and https://github.com/vegandevs/vegan.
81. Parmenter, R.R. and Lamarra, V.A. (1991) Nutrient cycling in a freshwater marsh: the decomposition of fish and waterfowl carrion, *Limnology and Oceanography*, 36, pp. 976–987.
82. Pechal, J.L. and Benbow, M.E. (2016) Microbial ecology of the salmon necrobiome: evidence salmon carrion decomposition influences aquatic and terrestrial insect microbiomes, *Environmental Microbiology*, 18(5), pp. 1511–1522.
83. Pechal, J.L., Crippen, T.L., Tarone, A.M., Lewis, A.J., Tomberlin, J.K., Benbow, M.E. (2013) Microbial community functional change during vertebrate carrion decomposition, *PLoS One*, 8(11), pp. 1–11.
84. Pechal, J.L., T.L. Crippen, M.E. Benbow, A.M. Tarone, S. Dowd, and J.K. Tomberlin.

(2014) The potential use of bacterial community succession in forensics as described by high throughput metagenomic sequencing, *International Journal of Legal Medicine,* 128, pp. 193–205.

85. Pechal J.L., Schmidt C.J., Jordan H.R., Benbow M.E. (2017) Frozen: thawing and its effect on the postmortem microbiome in two pediatric cases, *Journal of Forensic Sciences*, 62(5), doi: 10.1111/1556-4029.13419.
86. Putman, R.J. (1978) Flow of energy and organic matter from a carcase during decomposition. Decomposition of small mammal carrion in temperate systems 2. *Oikos*, 31(1), pp. 58–68.
87. Quast, C., Pruesse, E., Yilmaz, P., Gerken, J., Schweer, T., Yarza, P., Peplies, J. and Glockner, F.O. (2013) The SILVA ribosomal RNA gene database project: improved data processing and web-based tools, *Nucleic Acids Research*, 41, D590–D596.
88. Quince, C., Lanzen, A., Davenport, R.J. and Turnbaugh, P.J. (2011) Removing noise from pyrosequenced amplicons, *BMC Bioinformatics*, 12, 38.
89. R Development Core Team. (2011). R: A Language and Environment for Statistical Computing. Vienna, Austria: R Foundation for Statistical Computing, http://www.R-project.org (accessed October 28, 2016).
90. Richey, J.E., Perkins, M.A. and Goldman, C.R. (1975) Effects of kokanee salmon (*Oncorhynchus nerka*) decomposition on the ecology of a subalpine stream, *Journal of the Fisheries Research Board of Canada*, 32, 817–820.
91. Rochelle, P.A., Cragg, B.A., Fry, J.C., Parkes, R.J., and Weightman, A.J. (1994) Effect of sample handling on estimation of bacterial diversity in marine-sediments by 16S ribosomal-RNA gene sequence-analysis, *FEMS Microbiology Ecology,* 15(1, 2), pp. 215–225.
92. Roh, C., Villatte, F., Kim, B.G., and Schmid, R.D. (2006) Comparative study of methods for extraction and purification of environmental DNA from soil and sludge samples, *Applied Biochemistry and Biotechnology,* 134(2), pp. 97–112.
93. Salipante, S.J., Kawashima, T., Rosenthal, C., Hoogestraat, D.R., Cummings, L.A., Sengupta, D.J., Harkins, T.T., Cookson, B.T. and Hoffman, N.G. (2014) Performance comparison of Illumina and ion torrent next-generation sequencing platforms for 16S rRNA-based bacterial community profiling, *Applied and Environmental Microbiology*, 80, pp. 7583–7591.
94. Schloss, P.D., Westcott, S.L., Ryabin, T., Hall, J.R., Hartmann, M., Hollister, E.B., Lesniewski, R.A., Oakley, B.B., Parks, D.H., Robinson, C.J., Sahl, J.W., Stres, B., Tallinger, G.G., Van Horn, D.J. and Weber, C.F. (2009) Introducing mothur: open-source, platform- independent, community-supported software for describing and comparing microbial communities, *Applied and Environmental Microbiology*, 75, pp. 7537–7541.
95. Schloss, P.D., Gevers, D. and Westcott, S.L. (2011) Reducing the effects of PCR amplification and sequencing artifacts on 16S rRNA-based studies, *PLoS One*, 6, e27310.
96. Schoch, C.L., Seifert, K.A., Huhndorf, S., Robert, V., Spouge, J.L., Levesque, C.A.,

Chen, W. and Fungal Barcoding Consortium. (2012) Nuclear ribosomal internal transcribed spacer (ITS) region as a universal DNA barcode marker for Fungi, *Proceedings of the National Academy of Sciences of the United States of America*, 109, pp. 6241–6246.

97. Schoenly, K.G., Haskell, N.H., Mills, D.K., Bieme-Ndi, C., Larsen, K. and Lee, Y. (2006) Recreating death's acre in the school yard: using pig carcasses as model corpses, *The American Biology Teacher*, 68(7), pp. 402–410.
98. Singh, B. and Crippen, T.L. (2015) Methodologies in Forensic and Decomposition Microbiology, in Tomberlin, J.K. and Eric Benbow, M.E. (ed.) *Forensic Entomology*, CRC Press, Boca Raton.
99. Singh, B, Crippen, T.L, and Tomberlin, J.K. (2017) An introduction to metagenomics data generation, analysis, visualization, and interpretation, in Carter, D.O., Tomberlin, J.K., Benbow, M.E. and Metcalf, J.L. (ed.) *Forensic Microbiology*, John Wiley and Sons Ltd.
100. Singh, B., Crippen, T., Zheng, L., Fields, A.T., Yu, Z., Ma, Q., Wood, T.K., Dowd, S.E., Flores, M., Tomberlin, J.K. and Tarone, A.M. (2014) A metagenomic assessment of the bacteria associated with Lucilia sericata and Lucilia cuprina (Diptera: Calliphoridae), *Applied Microbiology and Biotechnology*, 99, pp. 1–15.
101. Smith, C.R. and Kukert, H. (1989) Vent fauna on whale remains, *Nature*, 341(6237), pp. 27–28.
102. Smith, C.R., Glover, A.G., Treude, T., Higgs, N.D. and Amon, D.J. (2015) Whale-fall ecosystems: recent insights into ecology, paleoecology, and evolution, *Annual Review of Marine Science*, 7(1), pp. 571–596.
103. Smith, D.P. and Peay, K.G. (2014) Sequence depth, not PCR replication, improves ecological inference from next generation DNA sequencing, *PLoS One*, 9, e90234.
104. Tibbett, M. and Carter, D.O. (2008) *Soil Analysis in Forensic Taphonomy: Chemical and Biological Effects of Buried Human Remains*, CRC Press; Taylor & Francis Group, Boca Raton, FL.
105. Todd, T.C., Powers, T.O. and Mullin, P.G. (2006) Sentinel nematodes of land-use change and restoration, *Journal of Nematology*, 38(1), pp. 20–27.
106. Treude, T., Smith, C.R., Wenzhöfer, F., Carney, E., Bernardino, A.F., Hannides, A.K., Kruger, M and Boetius, A. (2009) Biogeochemistry of a deep-sea whale fall: sulfate reduction, sulfide efflux and methanogenesis, *Marine Ecology Progress Series*, 382, pp. 1–21.
107. Tringe, S.G. and Rubin, E.M. (2005) Metagenomics: DNA sequencing of environmental samples, *Nature Reviews Genetics,* 6(11), pp. 805–14.
108. TWG (2016) NIJ Forensic Science Technology Working Group Operation Requirements. Available at: https://www.nij.gov/topics/forensics/documents/2016-forensic-twg-table.pdf [Accessed March 22, 2018].
109. Vass, A. (2001) Beyond the grave—understanding human decomposition, *Microbiology Today*, 28(28), pp. 190–192.
110. Wagner Mackenzie, B., Waite, D.W. and Taylor, M.W. (2015) Evaluating

variation in human gut microbiota profiles due to DNA extraction method and inter-subject differences, *Frontiers in Microbiology*, **6**, pp. 130.

111. Walters, W., Hyde, E.R., Berg-Lyons, D., Ackermann, G., Humphrey, G., Parada, A., Gilbert, J.A., Jansson, J.K., Caporaso, J.G., Fuhrman, J.A., Apprill, A. and Knight, R. (2016) Improved bacterial 16S rRNA gene (V4 and V4-5) and fungal internal transcribed spacer marker gene primers for microbial community surveys, *mSystems*, 1, e00009–e00015.

112. Wang, Y., Tian, R.M., Gao, Z.M., Bougouffa, S. and Qian, P-Y. (2014) Optimal Eukaryotic 18S and Universal 16S/18S Ribosomal RNA Primers and Their Application in a Study of Symbiosis, *PLoS One,* 9(3), pp. e90053. https://doi.org/10.1371/journal.pone.0090053

113. Weiss, S., Carter, D.O., Metcalf, J.L. and Knight, R. (2015) Carcass mass has little influence on the structure of gravesoil microbial communities, *International Journal of Legal Medicine*, 130, pp. 253–263.

114. Wesolowska-Andersen, A., Bahl, M.I., Carvalho, V., Kristiansen, K., Sicheritz-Ponten, T., Gupta, R. and Licht, T.R. (2014) Choice of bacterial DNA extraction method from fecal material influences community structure as evaluated by metagenomic analysis, *Microbiome*, 2, pp. 19.

115. Wilson, M. (2009) *Bacteriology of Humans: An Ecological Perspective*. Malden, MA: Wiley/Blackwell Publishing.

116. Wold, A.K.F. and Hershey, A.E. (1999) Effects of salmon carcass decomposition on biofilm growth and wood decomposition, *Canadian Journal of Fisheries and Aquatic Sciences*, 56(5), pp. 767–773.

117. Wright, E.S., Yilmaz, L.S., and. Noguera, D.R. (2012) DECIPHER: A search-based approach to chimera identi - cation for 16S rRNA sequences. *Applied and Environmental Microbiology,* (3), pp. 717–725.

118. Yang, B., Wang, Y., and Qian, P-Y. (2016) Sensitivity and correlation of hypervariable regions in 16S rRNA genes in phylogenetic analysis, *BMC Bioinformatics,* 17, pp.135

119. Zheng, L., Crippen, T.L., Singh, B., Tarone, A.M., Dowd, S., Yu, Z., Wood, T.K. and Tomberlin, J.K. (2013) A survey of bacterial diversity from successive life stages of black soldier fly (Diptera: Stratiomyidae) by using 16S rDNA pyrosequencing, *Journal of Medical Entomology*, 50, pp. 647–658.

Chapter 2: Postmortem Submersion Interval (PMSI) Estimation from the Microbiome of *Sus scrofa* Bone in a Freshwater Lake

Abstract

Estimating the postmortem submersion interval (PMSI) is an important step in providing investigative leads for bodies recovered from aquatic environments. While many studies have developed microbial succession-based models for the prediction of postmortem interval (PMI) in terrestrial systems, similar well-replicated long-term decomposition studies are lacking for aquatic systems. Therefore, this study sought to identify temporal changes in bacterial community structure associated with porcine skeletal remains (N=200) for an extended period (5200 Accumulated Degree Days (ADD) / 579 Days) in a fresh water lake. Every ca. 250 ADD, one cage, containing 5 ribs and 5 scapulae, was removed from the lake for a total of nineteen collections. Water was also sampled at each interval. Variable region 4 (V4) of 16S rDNA was amplified and sequenced for all collected samples using Illumina MiSeq FGx Sequencing platform, resulting data was analyzed with the mothur (v1.39.5) and R (v3.6.0). Bacterial communities associated with ribs differed significantly from those associated with scapulae. This difference was mainly attributed to Clostridia, Holophagae and Spirochaete relative abundances. For each bone type, α-diversity increased with ADD; similarly, β-diversity bacterial community structure changed significantly with ADD. Furthermore, β-diversity changes were explained using environmental parameters and inferred functional pathways. Models fit using family-level taxa outperformed those fit with class-level taxa and scapula samples outperformed models fit with rib samples. The models using 24 rib and 34 scapula family-level taxa allowed the prediction of PMSI with root mean square error of 522.97 ADD (~57 days) and 333.8 ADD (~37 days), respectively.

Significance Statement

Post-mortem submersion interval (PMSI) estimation is currently limited, and available methods are primarily applicable to cases of accidental water deaths, where location and date of entry are known and resurfacing time can be predicted from water temperature. Furthermore, the scope of application for these methods has not been tested. The results of this study provide support for PMSI estimation using longitudinal

succession of microbiomes of submerged skeletal remains through 16S rDNA MiSeq sequencing. This will aid investigations by providing information concerning the time interval when the individual likely entered the water as an aid to identifying missing persons, and consequently narrowing suspect pools in the event the death is ruled a homicide.

Introduction

Human remains may be found in, and subsequently recovered from aquatic environments due to natural land erosion (from both modern and archaeological cemeteries on flood plains), accidents (drownings as well as boating and/or ferry disasters), criminal activities (intentional drowning or disposal of remains), suicides or natural disasters (e.g. Hurricane Katrina) (1,2). The aquatic decomposition cycle, which may include periods of floating, submersion, and fluvial transportation, may make the discovery and recovery of remains problematic and prolonged. Similar to terrestrial time since death (e.g., postmortem interval, or PMI), estimating the postmortem submersion interval (PMSI), or time of submersion after death until recovery, is integral to producing investigative leads. Terrestrial and aquatic decomposition differ due to factors inherent to bodies of water (e.g. water temperature, salinity, depth, currents, and scavengers) and methods commonly used for terrestrial time since death estimation (e.g., insect succession pattern, insect developmental data etc.) are not applicable to aquatic systems. Disarticulation and decomposition patterns (3-7), succession of aquatic invertebrates (8) and algal or algal/diatom community composition (9,10) have all been suggested as methods for estimating PMSI; however, these remain largely unvalidated and unstandardized (11).

Because microorganisms are present throughout decomposition, Vass (12) initially proposed that, like insects, their appearance and/or disappearance could be used for PMI estimation. The advancement of next generation sequencing (NGS) and improved bioinformatic pipelines (i.e. Qiime (13), and mothur (14)) have allowed for the comprehensive identification of microbes contributing to community structure and succession. Resulting necromicrobiome-focused studies have successfully identified changes in microbial community structure during terrestrial decomposition using human (15, 16), porcine (17, 18) and murine remains (19). Likewise, initial aquatic decomposition studies using salmon and whale carcasses have suggested microbial shifts in both

freshwater and marine environments (20-22). While these studies provide a proof of concept for the succession of microorganisms in aquatic systems, their applicability to humans is limited by the use of aquatic dwelling model organisms. Therefore, additional studies (23 - 25) have focused on porcine aquatic decomposition in both marine and freshwater systems.

Dickson et al. (23) utilized three swine heads over an 11 day period in autumn and a 21 day period in late winter. Sampling occurred by removing the specimens and swabbing the skin at intervals before replacing them in water. The study reported that bacterial colonization of remains submerged in a marine environment occurred in a successional manner with seasonal variations and identified specific bacteria that could be used to estimate PMSI. For example, early colonizers (i.e. *Fusobacterium* and *Nevskia*) were not present in later periods, while other bacterial genera were found only after a specific period of submersion. A second microbial study submerged three stillborn swine carcasses in a freshwater stream in two separate trials in the summer and late autumn of 2012 (24). As in the previous study, differences in bacterial communities between seasons was observed, as well as differences among sampling days.

While the aforementioned studies provide insight to microbial colonization during aquatic decomposition, they both were performed using small sample sizes ($N \leq 3$), over a short sampling period (11 - 43 days), with repeated sampling and disturbance of the same remains. The studies did not focus on long-term PMSI estimation based on microbial community structure on skeletal remains. This study expands on these limitations, and identifies the extent of microbial community structure, colonization and succession patterns involved in a long-term (5,200 ADD, 579 days, 19 months) aquatic decomposition study, using well-replicated and undisturbed porcine skeletal remains. For remains in aquatic environments the thoracic skeleton remains articulated for the longest time and is most often recovered (3), thus this study focused on the scapulae and ribs. The aims of the study were to determine if bacterial succession occurs in a predictable manner on different bone types during extended decomposition, identify taxa specific to the submersion period, and use those taxa to develop a statistical model for PMSI prediction.

Results

Results associated with environmental parameters, bacterial community structure, and bacterial function are summarized under following subheadings.

Environmental Parameters

While variation in environmental parameters, such as temperature, pH, salinity, specific conductivity, and oxidation reduction potential (ORP), was observed across ADD, ORP was the only environmental parameter that was significantly positively correlated ($p=0.0042$, $rho=0.71$) with ADD (Figure 2.S1 and Table 2.S1). Except pH and ORP, all other environmental parameters increased during spring and summer seasons and decreased in late fall and winter (Figure 2.S1). Time (days) since placement had a significant positive linear relationship ($y=-199 + 9.36x$, $R^2=0.99$, adj. $R^2=0.98$, $p<0.0001$) with ADD (Figure 2.S2, Table 2.S2).

Sequence Characteristics

Out of total 9,078,478 sequence reads generated from 203 samples (on average 44,722 reads/sample), 1,629,022 (~18%) sequence reads were lost during quality control steps (i.e. screening, aligning, filtering, chimera check, etc.), and a total of 7,449,456 sequence reads (on average 36,696 reads/sample) were used for further analysis. Before taxonomic classification and clustering analysis, all samples were subsampled to 6,371 (Figure 2.S3), resulting in the removal of nine samples and all three PCR negative control samples (Figure 2.S4).

Bacterial Community Structure

A mock community sample was included in each sequencing run to detect run-to-run error, and also to determine the impact of sequence pre-processing steps on resulting bacterial community structure. All mock community samples included in this study had very similar bacterial profiles, and matched with manufacturer's suggested profile at the genus level (Figure 2.S5).

For 190 bone and water samples, 1,210,490 total subsampled sequences were classified, into 62 phyla, 178 classes, 333 orders, 520 families, 872 genera and 1,014 species using the Greengenes reference database. At the phyla level, Firmicutes (58%), Proteobacteria (14%), Spirochaetes (9%), Bacteroidetes (8%) and Acidobacteria (5%) were among the most dominant phyla for rib samples (~94%); similarly, Firmicutes (34%), Proteobacteria (17%), Spirochaetes (16%), Acidobacteria (15%) and Bacteroidetes (10%) composed approximately 92% of phylum level taxon for scapulae (Figure 2.S6). Water samples also had high abundances of Proteobacteria (31%) and Bacteroidetes (22%); however, Verrucomicrobia (15%), Actinobacteria (11%) and Cyanobacteria (10%) were recovered in higher abundances from water samples totaling 89% of phyla. The percentage of unclassified sequences increased drastically from class (6%) and family (10-11%) levels to genus level (39-42%) for both bone types (Table 2.S2), and hence the following results are based on class and family level taxonomic data.

A water filter, processed along with experimental samples, shared only two bacterial families (e.g., Chitinophagaceae and Comamonadaceae) with water samples (Figure 2.S7). Both weighted (PERMANOVA, *pseudo*-F= 38.50, R^2=0.30, p=0.0010) and unweighted (PERMANOVA, *pseudo*-F=15.648, R^2=0.14, p = 0.0010) metrics showed significant differences in bacterial community structure among rib, scapula, and water samples. Although many relatively low abundant bacterial families were shared among ribs, scapulae, and water, none of the top 15 bacterial families was shared among all three sample types. Ribs and scapulae shared 12 of the top 15 families, whereas scapula and water samples shared only one of the top 15 families. (Figure 2.S8; Table 2.S3; Figure 2.S9). For both bone types, baseline samples (0 ADD) exhibited class and family level taxa that were very similar to each other, but differed from samples exposed to water (Figure 2.1). After submersion, differences between rib and scapula bacterial community structures were mainly driven by Clostridia (e.g., Clostridiaceae, Ruminococcaceae, Veillonellaceae), Holophagae (e.g., Holophagaeae) and Spirochaetes (e.g., Spirochaetaceae). While Clostridia remained present in high abundances in both bone types, it was relatively more abundant in rib samples. For scapula samples, Holophagae and Spirochaetes were observed in higher abundances. (Figure 2.1).

Bacterial Diversity

The relationship between phylogenetic diversity (PD) and ADD was curvilinear ($y=6.54+0.00484x-5.1(10^{-7})x^2$, $R^2=0.53$) in ribs and linear ($y=7.88+0.00665x$, $R^2=0.73$) in scapulae (Figure 2.2). In general, PD increased with ADD, resulting in the greatest diversity estimates around 5,200 ADD, for both bone types (Figure 2.2). Although baseline (0 ADD) samples had similar PD in both bone types, the same was not true at later time points or ADD (PD in scapulae was almost double of PD in ribs at around 5200 ADD). Phylogenetic diversity also changed with season. It was observed that diversity increased in fall and winter, but plateaued in the spring and summer, with spring demonstrating the highest variability within ADD groupings (Figure 2.S10). Variability in phylogenetic diversity was attributed to ADD (linear model, ANOVA $p<0.0001$) for both ribs and scapula and to temperature (linear model, ANOVA $p=0.0026$) in scapulae.

In both bone types, β-diversity differed significantly between ADD using weighted (PERMANOVA, Rib: *pseudo*-F=20.23, $R^2=0.21$, p=0.001, Scapula: *pseudo*-F=37.67, $R^2=0.31$, p=0.001) and unweighted (PERMANOVA, Rib: *pseudo*-F=11.74, $R^2=0.14$, p=0.0010 ; Scapula: *pseudo*-F=17.04, $R^2=0.17$, p=0.0010) metrics (Figure 2.3; Figure 2.S11). Specifically, communities ordinated chronologically along NMDS1 with greater separation between ADD sampling intervals noted in earlier periods (i.e. 249 and 489 ADD). Vectors of environmental variables were fitted to both weighted and unweighted UniFrac distances, with arrow length and angle indicating strength and direction (Figure 2.3; Figure 2.S11; Table 2.2; Table 2.S4). UniFrac weighted analysis indicated a relationship between some environmental parameters (e.g. ADD, temperature, oxidation reduction potential and pH) and samples collected at different time periods. For both bone types, ADD was significantly and strongly associated with samples from later time periods (Rib: $r^2=0.58$, p=0.0010; Scapula: $r^2=0.71$, p=0.0010) (Table 2.2). Temperature ($r^2=0.15$, p=0.0080) and oxidation reduction potential ($r^2=0.13$, p=0.0170) were statistically significant, but weakly associated with scapula samples collected during mid- to late periods; pH ($r^2=0.13$, p=0.0370) was also statistically significant, but weakly associated with rib samples from earlier ADD periods. Environmental variables, such as season, specific conductivity, salinity and oxidation reduction potential were not significantly correlated with weighted UniFrac distances for either bone type. Except for a few clades, Unweighted Pair Group Method with Arithmetic Mean (UPGMA) trees based on weighted

and unweighted UniFrac distances were mostly congruent for both bone types (cophenetic correlation “spearman”, Rib = 0.79, Scapula = 0.68) (Figure 2.S12).

Bacterial function

To evaluate potential microbial community functional changes across ADD, KEGG pathway profiles were inferred using PICRUSt (26). Resulting level 1 pathways and level 2 metabolic pathways (classified at level 3) were correlated with UniFrac weighted distances for both rib and scapula samples (Figure 2.4). All level 1 pathways, with the exception of rib cellular processes, were significantly associated with the ordination. Of the level 1 pathways, cellular process and signaling pathway (Rib: r^2=0.89, p=0.0010; Scapula: r^2=0.88, p=0.0010) were most strongly correlated with samples from early periods and negatively correlated with metabolism (Table 2.3). Furthermore, the metabolic pathway was highly positively correlated with ADD or samples from later time points (Rib: r^2=0.77, p=0.0010; Scapula: r^2=0.73, p=0.0010). For both bone types, except rib nucleotide metabolism, all metabolic pathways, were significantly associated with weighted UniFrac distances (Figure 2.4,Table 2.4).

Random Forest Model for PMSI Prediction

Using family-level taxa, random forest models were fitted separately for ribs (82 samples, 24 taxa) and for scapulae (89 samples, 34 taxa). Figure 2.5 shows the ten most influential taxa for both bone types, measured by the average percentage increase in mean square error (MSE) when each taxon is excluded from the model. For the model based on rib samples, there is a sharp delineation between Syntrophomonadaceae and the other taxa, indicating its influence in the model. For the scapulae, the differences in between the most influential taxon are not as stark. Figure 2.5 also shows the relative abundance over the entire study period for the 5 most influential taxa in each model. It should be noted that the taxa which are not present at higher abundances can be influential in estimating PMSI, as is the case for several taxa depicted in Figure 2.5.

For ribs, the random forest model explained 89.30% of the variation in ADD, with a root mean square error (RMSE) of 522.97 (~57 days). Figure 2.6 depicts the predicted ADD vs. the actual ADD, with the one-to-one line added for reference. The R-squared value

indicates that 90% of the variability in predicted ADD can be explained through the linear relationship between actual and predicted ADD. The scapulae model was more precise, explaining 95.35% of the variation in ADD, with a RMSE of 333.48 (~37 days). Figure 2.6 depicts the tighter fit of the points around the one-to-one line, with 96% of the variability in predicted ADD explained through the linear relationship between actual and predicted ADD.

Discussion

This study used 16S rDNA MiSeq sequencing techniques to determine if bacterial succession occurred in a predictable manner on submerged bones with time. The observed succession patterns were explained using environmental parameters and inferred functional pathways. Identified predictor taxa were used in random forest statistical modeling to predict PMSI. Significant differences in bacterial community structure were observed among rib, scapula and water samples; notably, this differs from skeletal remains assessed in terrestrial environments, where community profiles have been reported to be similar to surrounding soil communities (27). Furthermore, differences among sample types (i.e., scapula-rib-water) were also observed in bacterial relative abundances at all taxonomic levels, with the number of shared taxa decreasing as classification level increased (i.e., from class to family) This suggests that the surrounding water environment had little impact on bone decomposition, and vice versa; however, future studies should consider sampling sediment, as it may aid in explaining the microbial communities recovered from bone samples.

Bacterial phyla Verrucomicrobia, Actinobacteria, and Cyanobacteria were present in higher abundances in water samples when compared to bone samples. These taxa have been reported to be present in both freshwater and terrestrial (i.e. soil) environments (28-30). In brief, Verrucomicorbia have been reported in lakes, soil, oceans and human feces and as symbionts of eukaryotes (29). Actinobacteria, which actively synthesize DNA and proteins, are present in the bottom waters of freshwater lakes, depending on oxygen and pH levels. Similar to eukaryotic phytoplankton, Cyanobacteria have been reported in a majority of aquatic and terrestrial habitats (30).

The top five phyla identified from all skeletal elements include Firmicutes, Proteobacteria, Spirochaetes, Bacteriodetes and Acidobacteria, which reflect findings from previous studies on porcine remains in aquatic (23, 24) and human remains in terrestrial (27,31) systems. Of these phyla, Proteobacteria, Bacteroidetes and Firmicutes were identified as the majority in a shallow marine New Zealand inlet during autumn and winter (23) and in the Lancaster, Pennsylvania Conestoga River watershed, with the addition of Spirochaetes appearing during the winter trial (24). Firmicutes, a gram positive bacteria commonly reported in soil and aquatic environments, was present in high abundances throughout the study. The increased presence may be due to Firmicutes involvement in organic matter decomposition (32), as the phylum has been reported during terrestrial human decomposition (33). Also associated with aquatic environments, Proteobacteria comprise taxa that have been found during the lipolysis process during adipocere formation and are also associated with the spoilage of meat (24). Proteobacteria decreased after skeletal elements were submerged, whereas Acidobacteria, which is driven by pH and nutrient availability, increased (34). It has been proposed that Proteobacteria and Acidobacteria, which are metabolically similar, have an ecological relationship and can influence the other's position in the community (34, 35). Along with Acidobacteria, Spirochaetes and Bacteroidetes were found in overall lower abundances, yet were also noted to increase in abundance soon after submersion. Bacteroidetes are important in the degradation of complex biopolymers, such as natural fats, amino acids, sugars (29). Spirochaetes have been infrequently recovered from freshwater lake environments, and have been reported in sediments, mud, freshwater (e.g. ponds, lakes and streams), in salt marshes, saline solar lakes, deep-sea hydrothermal vents, and associated with eukaryotic hosts (36).

Differences between skeletal element bacterial community structures were mainly driven by bacteria belonging to Firmicutes (e.g., Clostridia), Acidobacteria (e.g., Holophagae) and Spirochaetes (e.g., Spirochaete). Holophagae and Spirochaetes were observed in higher abundances and at earlier ADD in scapula samples, when compared to ribs. Holophagae and Spirochaetes are both gram-negative bacteria. However, Holophagae are recovered from anoxic environments (37), while Spirochaetes are found in environments ranging from aerobic to facultatively anaerobic and obligately anaerobic (38). Clostridia, an anaerobic genus recovered from soil (terrestrial and marine), freshwater, and feces, remained in high abundances in both skeletal elements across time, but were more

prevalent in rib samples. Clostridiaceae and Clostridium (i.e. Firmicutes, Clostridia) were reported in human terrestrial decomposition by Hyde et al. (15) and proposed to be a key contributor to decomposition, though only Clostridiaceae was reported during mouse (19) and porcine decomposition (17). Clostridiaceae was also reported in high abundances in porcine terrestrial decomposition in Virginia (39); however, its abundance was attributed to adult and larval blowfly activity (40) not applicable to aquatic systems. Therefore, the difference between bone elements was attributed to the persistence of adipocere on rib samples throughout the duration of the experiment. Adipocere (i.e. grave or corpse wax) is the product of lipid saponification in the body by bacteria, which results in a gray-white, waxy, and later crumbly, substance. Studies have related increased adipocere formation to the presence of Clostridium (e.g., Firmicutes, Clostridia, Clostridiaceae) in warm anaerobic environments, due to the production of lecithinase (41, 42). In addition to adipocere formation, dark staining on the bone was observed; however, the discoloration was more prevalent on scapula samples. It has been suggested that black coloration on submerged bone could be attributed to the formation of ferrous sulphide (FeS). Ferrous sulfide is generally formed in an anaerobic environment by both Gram-positive (e.g., Clostridia) and Gram-negative (e.g., Deltaproteobacteria) sulphate-reducing bacteria (43, 44). This study proposes that the differences between bone types can be attributed to the formation of adipocere on the ribs, which created a microenvironment, supporting different abundances and taxa of microorganisms. Therefore, the stage of decomposition, pattern and/or process may impact microbial-based PMSI estimation, as ribs were submerged with slightly more attached tissue than scapulae.

Bacterial phylogenetic (i.e. alpha) diversity (PD) was observed to increase with ADD, which is antithetical to the decreasing alpha diversity noted in short-term terrestrial decomposition of porcine remains where soft tissue was sampled (17). In a long-term decomposition study performed on porcine remains, alpha diversity was reported to be highest after death and decline in early stages of decomposition (e.g. blot and purge) before steadily increasing through active and advanced decay (45, 39). While initially similar in this aquatic study, PD for scapula samples was almost double that of ribs at 5200 ADD and demonstrated greater variation across time. The variability of PD within ADD groupings for scapulae was attributed to temperature and ADD. Bacterial community structure may have been more susceptible to changes in environmental parameters that accompany seasonal changes in scapulae than in ribs, as a result of direct exposure to

the environment (i.e. lack of adipocere encasement). As previously mentioned, bacteria are influenced by environmental factors that impact community structure throughout time. For example, Acidobacteria are driven by pH and nutrient availability; Firmicutes participate in the decomposition of organic compounds; and Proteobacteria are composed of classes with pH, carbon substrate, and seasonal preferences (34, 46).

Significant differences in bacterial community beta diversity between time points were observed for both rib and scapula samples. Differences among later sample groupings for both rib and scapula were explained by ADD, suggesting that cumulative temperature influenced community structure. Meanwhile, earlier collections for ribs were associated with pH, and scapula samples from middle collections were influenced mainly by oxidation reduction potential and temperature. This provides further support that environmental factors directly influence estimates of PMSI, as mentioned by Benbow et al. (24).

Potential bacterial functional changes across ADD were inferred using PICRUSt and also used to explain weighted UniFrac ordinations for both bone types. Of the level 1 predicted KEGG pathway profiles, metabolism demonstrated the strongest association with samples from later collections or time points, suggesting that bacteria performing metabolic functions were driving weighted UniFrac ordination. Within metabolism, lipid, energy and amino acid metabolism, along with metabolism of terpenoids and polyketides, were the most strongly related pathways relative to increased ADD groupings. It is proposed that lipid and energy metabolism may be supported by the presence of adipocere. Since adipocere is formed via hydrolysis of triglycerides into glycerin and free fatty acids (i.e. lipid metabolism), the resulting free fatty acids could then be degraded and used to generate energy (i.e. energy metabolism) (47, 48).

Groupings of ADD or time points were observed in the ordinations and the constructed Unweighted Pair Group Method with Arithmetic Mean (UPGMA) trees. Incongruences between weighted and unweighted UniFrac trees for both bone types are due to the fact that weighted calculations consider both presence or absence of a taxa and their abundances, while unweighted calculations rely only on presence or absence of a taxa. Bacterial community structure association for scapulae was divided roughly into four clades that relate to increasing ADD, which could be due to changing abundances and appearance of taxa as decomposition progressed and temperature accumulated. The

inability to easily group rib sample weighted and unweighted UniFrac trees branches may be attributed to the microenvironment created by adipocere and its effect of abating the decomposition process, which resulted in less predictable changes over time.

Models fit with scapula samples outperformed those fit with rib samples, which may be due to the missing observations in ribs and/or the prolonged duration of adipocere on rib samples. The best model allowed the prediction of PMSI within 522.97 ADD (~57 days) and 333.8 ADD (~37 days) for rib and scapula samples, respectively. Of the 24 taxa used for rib samples, Syntrophomonadaceae, Comamonadaceae, Holophagaceae, Spirochaetaceae and Pseudomonadaceae were identified as the most influential families. Of the 34 taxa used for scapula samples, Pirellulaceae, Campylobacteraceae, Syntrophomonadaceae, Sediment-4, Crenotrichaceae, Comamonadaceae and Spirochaetaceae were identified as the most influential families. Specifically, Comamonadaceae and Campylobacteraceae are gram-negative bacterial families that have been recovered from environmental habitats (e.g. water and soil); however, Campylobacteraceae has also been identified in food animals (i.e. pigs) (49, 50). Both families have been recovered from porcine terrestrial decomposition and utilized in generalized additive models estimating physiological time via random forest results (51). Along with Comamonadaceae, Spirochaetaceae and Syntrophomonadaceae were identified in both bone types. Spirochaetaceae was reported as an indicator family for one year salmon carcasses in epinecrotic communities (52). Meanwhile, Syntrophomonadaceae are gram-positive bacteria that play an important role in fatty acid degredation (53). The remaining prominent bacterial contributors may be unique to aquatic environments. The different indicator bacterial communities observed in terrestrial decomposition studies may be due to the reported presence of insect-associated bacteria (15, 54, 55) related to direct insect colonization, which does not occur in aquatic decomposition.

Conclusion

This study identified changes in bacterial community structure that varied with both skeletal element and accumulated temperature, and these were successfully explained using environmental parameters and inferred functional pathways. Resulting succession patterns provide proof of concept that bone microbial communities may serve as good

qualifiers for predicting the postmortem submersion interval (PMSI). Further research should consider: monitoring the entire decomposition process (e.g. fresh to skeletonization), different types of aquatic ecosystems, such as a fluvial riverain environment or salt water, combining other markers (e.g. 18S rDNA and ITS regions) to improve prediction models, and the applicability of findings to human cases.

Materials and Methods

Henley Lake, a freshwater lake in White Hall, Virginia (38.0863° N, 78.6842° W) was utilized as the field site between November 2016 and June 2018. At the site, nineteen 10'' x 10'' cages, each containing five scapulae and five ribs, were attached to a flotation device, and submerged to a depth of approximately 5 m, allowing the cages to rest on the lake bottom. Haglund (3) discussed the disarticulation sequence of human remains in aquatic environments and noted that the thoracic skeleton remained together as a unit longest, and was hence most often recovered. Thus, this study focused on scapulae and ribs, as, upon recovery, investigators are tasked with determining the origin, identity, cause of death, manner of death, and postmortem interval for individuals recovered from water. Waterproof temperature loggers and a YSI Sonde (Yellow Springs, OH) were also submerged to monitor environmental parameters, including pH, specific conductivity, salinity, temperature, oxidation reduction potential and dissolved oxygen. Upon analysis of dissolved oxygen values, an issue with the probe was identified, resulting in the exclusion of this parameter from the statistical analyses.

Sample Collection

Five ribs and only two scapulae (as a result of sample shortage) were not exposed to water and served as baseline samples for the nineteen experimental collections. After submersion at 5 m, one cage (i.e. five scapula and five ribs) was collected approximately every 250 accumulated degree days (ADD), using a 0 °C threshold for ADD calculation. Water samples (500 mL) from a depth of 5 m were also collected using a Kemmerer bottle (WildCo, Yulee, FL). Bone and water samples were transported on ice to Virginia Commonwealth University, Richmond, VA (37.5485° N, 77.4480° W), where they were stored at -80 °C for bone samples and 4 °C for water samples until processing.

Within six months of collection (56), bone samples were thawed at room temperature and photographed before non-bone tissue, such as adiopocere, was removed. The rib mid-section and the scapular spine were then cut using a Craftsman Cordless Multi-Tool (Craftsman, Chicago, IL). The cut pieces were placed in a mortar filled with liquid nitrogen and ground with a pestle into a fine powder. Bone powder was weighed out to 0.1 g and stored at -20 °C until further processing. Water samples (250 mL) were filtered within a week of collection using a cellulose membrane filtration system and 0.22 µm filters, which were stored at -80 °C.

DNA Extraction and Quantification

DNA extraction was performed using 0.1 g of bone powder or one 0.22 µm filter with the ChargeSwitch® gDNA Plant Kit (Life Technologies – ThermoFisher Scientific, Waltham, MA), according to the Invitrogen CST Protocol for Extracting gDNA from Bone Samples (57) for bone and water samples, respectively. All samples were eluted in 100 µL of the provided elution buffer, quantitated using Qubit 2.0 Fluorometer (ThermoFisher Scientific), according to the Qubit® dsDNA HS Assay Kits User Guide (58), and stored at -20 °C.

16S rDNA Amplification and MiSeq® Sequencing-by-Synthesis

Variable region four (V4) of the 16S rRNA gene was amplified using dual-index primer pairs on the Veriti™ 96-Well Thermal Cycler (Applied Biosystems, USA) following the parameters set forth by Kozich et al. (59) from ZymoBIOMICS™ mock community standard, control filter (e.g., filter not exposed to water), PCR negative controls or no template control, bone powder and filtered water samples. Each reaction (total 20 µL) consisted of template DNA (0 – 10 ng; 6.2 µL maximum), 10 µL Promega PCR master mix (2X), 0.8 µL 25mM $MgCl_2$,and 3 µL of forward/reverse primers (10 µM each). Both forward (V4_515F 5'-AATGATACGGCGACCACCGAGATCTACACXXXXXXXXTATGGTAATTGTGTGYCAGCMGCCGCGGTAA- 3') and reverse primer (806R:5'-CAAGCAGAAGACGGCATACGAGATXXXXXXXXAGTCAGTCAGCCGGACTACNVGGGTWTCTAAT-3') was comprised of an Illumina adapter sequence, 8 nucleotide barcode sequence (XXXXXXXX), and 2 nucleotide linker sequences. DNA extracts that failed to

amplify 16S rDNA, were cleaned (to remove PCR inhibitors) using DNeasy PowerClean Pro Cleanup Kit (Qiagen, MD, USA) according to the manufacturer's protocol (60), and then 16S rDNA was re-amplified from these extracts.

To ensure PCR success, and that amplicons were of expected size, 3 µL of the PCR product in combination with 2 µL of 6X loading dye (New England Biolabs, MA, USA) and 7 µL of 1XTAE buffer were visualized on 1.8% agarose gels. Of the remaining 17 µL of PCR product, 10 µL were purified according to Agencourt® AMPure® PCR Purification kit (Beckman Coulter, Brea, CA) protocol (61). All purified samples, were quantified using the Qubit® 2.0 Fluorometer. A total input DNA of 1 ng from each sample was pooled into a 1.5 mL microcentrifuge tube. The pooled samples were dried down to 1 ng/µL using a Savant DNA120 Speed Vac Concentrator (Fisher Scientific, Waltham, MA). The resulting 16S rDNA library underwent 2x250 paired-end sequencing-by-synthesis on Illumina's MiSeq® FGx system (Illumina, San Diego, CA) using the Illumina MiSeq® v2 Reagent Kit (Illumina).

Sequence Analysis

The resulting raw sequences were analyzed using mothur v 1.39.5 and the MiSeq SOP (14). The *make.contig* command with *trimoverlap* set to "t" (i.e. true) and *insert* set to "20" was first used to create contigs from forward and reverse reads. Resulting contigs with ambiguous bases (*maxambig* of 0) and unusually long and short reads (greater than 275 bp and shorter than 200 bp) were removed from further analysis. Because sequences occur in duplicate, unique sequences were identified before aligning with the entire SILVA bacterial reference (62). Sequences were then screened to cull sequences that failed to meet the specified criteria (i.e. starting at 13862 and ending at 23444) and did not properly align to the SILVA reference dataset. Remaining sequences were pre-clustered (*diffs*= 2) and then all chimeric sequence reads were removed using UCHIME v 4.2 (63) as implemented in mothur v 1.39.5. The aforementioned quality control parameters reduced the number of raw sequences ~18% (9,078,478 to 7,449,456). The remaining sequences were clustered by taxonomy, phylogeny and operational taxonomic units (OTU).

Hierarchical classification was performed using the Naive Bayesian rRNA classifier version 2.2 along with the Greengenes 13_8_99 reference taxonomy (64, 65). Sequences

that had bootstrap support of 80% or greater in naïve Bayesian classifier were considered as classified at that taxonomic level. Any sequences classified as unknown, mitochondria, chloroplast, archaea and eukaryote were removed from further analysis. To minimize bias in diversity estimations because of unequal sequence reads in different samples, sequences were normalized by random subsampling to 6,371 sequence reads/sample. This caused a loss of 9 samples (0.04%) and all three PCR negative controls. Subsampled sequences were reclassified according to the aforementioned parameters. Operational Taxonomic Unit (OTU) and phylogenetic clustering was used to assess α- and β- diversity. OTU's were clustered using average neighbor method at a genetic dissimilarity of 5% (i.e., at hypothetical genus level) (Additional Analyses Figure S13 – S16 and Table S5 – S8). Phylogenetic α-diversity and neighbor-joining (NJ) tree construction were calculated in mothur version 1.39.5 (14), while β-diversity metrics (e.g. Weighted and Unweighted UniFrac distances) were calculated with R version 3.6.0 (66).

Statistical Analyses

All statistical analyses and graphing for site parameters, hierarchical classification and subsequent clustering methods were performed with R (66). The strength and association between field site parameters and ADD were measured using Spearman's rank-order correlation (cor.test) function in stats package version 3.6.0 (66). Furthermore, the relationship between ADD and time since placement was estimated using linear regression (lm; stats package version 3.6.0).

Stacked bar graphs of taxonomic level relative abundance for sample types (i.e., rib, scapula and water) were constructed using ggplot2 package version 3.2.1 (67). Bacterial community composition differences between rib and scapula samples at the class and family level were identified and tested using simper tests in the vegan package version 2.5.5 (68), and kruskal.test in the stats package version 3.6.0, respectively (66). Venn diagrams for presence and absence of bacterial taxa were generated with VennDiagram package version 1.6.20 (69). Relative abundances were also utilized to predict PMSI via random forest modeling, according to the methods outlined by Forger et al. (18).

Temporal phylogenetic α-diversity shifts were assessed via linear modeling (lm) using the stats package (66) and visualized with the ggplot2 package (67). Variations within the dataset were examined by incorporating field site parameters (i.e temperature, pH, etc.)

into the linear model. UniFrac (weighted and unweighted) β- diversity distances were calculated by constructing a phyloseq object (70), which consisted of a meta data file, mothur (14) generated NJ phylogenetic tree, OTU taxonomy and OTU table, that was used with the UniFrac function of the phyloseq version 1.28.0 package (71). Resulting weighted and unweighted UniFrac distances were used to test statistical differences between sample types (i.e. rib, scapula and water) and ADD using permutational multivariate analysis of variance (PERMANOVA) via the adonis function within the vegan package. Relationships between ADD for each bone type were analyzed by the construction of Unweighted Pair Group Method with Arithmetic Mean (UPGMA) trees via the hclust in the stats package (66). The correlation between UPGMA trees based on weighted and unweighted UniFrac distances were further tested with the cor_cophenetic function (method_coef = "spearman") in the dendextend package version 1.12.10 (72). Weighted and unweighted UniFrac distances for each ADD for both rib and scapula were ordinated with non-metric multidimensional scaling (NMDS) (permutations=999). Field site parameters (i.e., temperature, ADD, pH, etc.) were superimposed to both UniFrac and Bray-Curtis distance based ordinations using the envfit function from the vegan package. Plotted vectors ($\alpha < 0.05$) were used to identify the direction in ordination space that changes most rapidly, while maximizing correlations. Resulting squared correlation coefficients (permutations-999) and fitted vectors were used to assess the importance of each parameter.

Kyoto Encyclopedia of Genes and Genomes (KEGG) pathway profiles were inferred based on shared OTU files at 3% genetic distances (i.e., species level) using PICRUSt (phylogenetic investigation of communities by reconstruction of unobserved states) Galaxy web platform (26). While PICRUSt can only predict functional attributes of microbial communities, it has been tested and proven to have high accuracy (>90%) for both metagenomic and 16S rDNA datasets (73). Inferred level one and level two (metabolic only) pathways were superimposed to both OTU (Bray-Curtis) and UniFrac (weighted) ordinations using the envfit function from the vegan package. Plotted vectors ($\alpha < 0.05$) indicate the direction in ordination space that changes most rapidly, while maximizing correlations. Resulting squared correlation coefficients (permutations-999) and fitted vectors were used to assess the importance of each pathway.

Funding

This study was funded in part by the following: B. Singh and T. Simmons start-up grant from College of Humanities and Science of Virginia Commonwealth University (VCU), Richmond, VA; Forensic Science Foundation Lucas Grant 2016; and award 2018-R2-CX-0016 of the National Institute of Justice Graduate Research Fellowship.

References

1. W. Haglund, M. Sorg, “Human Remains in water Environments” in *Advances in Forensic Taphonomy: Method, Theory, and Archaeological Perspectives, Forensics and Criminal Justice*, W. Haglund, M. Sorg, Eds. (CRC Press, 2002), pp. 201-2018.
2. T. Simmons, V. Heaton, “Postmortem Interval: Submerged Bodies” in *Wiley Encyclopedia of Forensic Science*, A. Jamieson, A. Moenssens, Eds. (Wiley, 2013).
3. W. Haglund, Disappearnce of Soft Tissue and the Disarticulation of Human Remains from Aqueous Environments. *Journal of Forensic Sciences* **38**, 806-815 (1993).
4. M.S. Megysei, S.P. Nawrocki, N.H. Haskell, Using Accumulated Degree-Days to Estimate the Postmortem Interval from Decomposed Human Remains. *Journal of Forensic Sciences* **50**, 618-626 (2005).
5. V. Heaton, A. Lagden, C. Moffatt, T. Simmons, Predicting the Postmortem Submersion Interval for Human Remains Recovered from U.K. Waterways. *Journal of Forensic Sciences* **55**, 302-307 (2010).
6. M.K. Humphreys, E. Panacek, G. William, E. Albers, Comparison of Protocols for Measuring and Calculating Postmortem Submersion Intervals for Human Analogs in Fresh Water. *Journal of Forensic Sciences* **58**, 513-517 (2013).
7. A. De Donno ,*et al*., Bodies in sequesterd and non-sequestered aquatic environments: A comparative techonomic study using decompositional scoring system. *Science and Justice* **54**, 439-446 (2014).
8. G.S. Anderson, N.R. Hobischak, Decomposition of carrion in the marine environment in British Columbia, Canada. *International Journal of Legal Medicine* **118**, 206-209 (2002).
9. J.N. Haefner, J.R. Wallace, R.W. Merritt, Pig Decomposition in Lotic Aquatic Systems: The Potential Use of Algal Growth in Establishing a Postmortem Submersion Interval (PMSI). *Journal of Forensic Sciences* **49**, 330-336 (2004).
10. K.A. Zimmerman, J.R. Wallace, The Potential to Determine a Postmortem Submersion Interval Based on Algal/Diatom Diversity on Decomposing Mammalian Carcasses in Brackish Ponds in Delaware. *Journal of Forensic Sciences* **53**, 935-941 (2008).
11. M.A. van Daalen, *et al.*, An Aquatic Decomposition Scoring Method to Potentially Predict the Postmortem Submersion Interval of Bodies Recovered from the North Sea. *Journal of Forensic Sciences* **62**, 369-373 (2017).
12. A.A. Vass, Beyond the Grave – Understanding Human Decomposition. *Microbiology Today* **28**, 190-192 (2001).
13. J. Caporaso, *et al.*, QIIME allows analysis of high-throughput community sequencing data. *Nature Methods* 7, 335-336 (2010).
14. P. Schloss, *et al*., Introducing mothur: Open-source, platform-independent, community-supported software for describing and comparing microbial communities. *Applied and Environmental Microbiology* **75**, 7537-7541 (2009).
15. E.R. Hyde, D.P. Haarmann, J.F. Petrosino, A.M. Lynne, S.R. Bucheli, Initial insights into bacterial succession during human decomposition. *International Journal of Legal Medicine* **129**, 661-671 (2015).
16. J.L. Metcalf, *et al*., Microbial community assembly and metabolic function during mammalian corpse decomposition. *Science* 351, 158-162 (2016).

17. Pechal, *et al.*, The potential use of bacterial community succession in forensics as described by high throughput metagenomic sequencing. *International Journal of Legal Medicine* **128**, 193-205 (2014).
18. L.V. Forger, M.S. Woolf, T.L. Simmons, J.L. Swall, B. Singh, A eukaryotic community succession based method for postmortem interval (PMI) estimation of decomposing porcine remains. *Forensic Science International* **302**, 109838 (2019).
19. J.L. Metcalf, *et al*., A microbial clock provides an accurate estimate of the postmortem interval in a mouse model system. *eLife* **2, (**2013).
20. S.K. Goffredi, R. Wilpiszeski, R. Lee, V.J. Orphan, Temporal evolution of methane cycling and phylogenetic diversity of archaea in sediments from a deep-sea whale-fall in Monterey Canyon, California. *The ISME Journal* **2,** 204-220 (2008).
21. S.K. Goffredi, V.J. Orphan, Bacterial community shifts in taxa and diversity in response to localized organic loading in the deep sea. *Environmental Microbiology* **12**, 344-363 (2010).
22. J.L. Pechal, M.E. Benbow 2016, Microbial ecology of the salmon necromicrobiome: evidence salmon carrion decomposition influences aquatic and terrestrial insect microbiomes. *Environmental Microbiology* **18**, 1511-1522 (2016).
23. G.C. Dickson, R.T.M. Poulter, E.W. Maas, P.K. Probert, J.A. Kieser, Marine bacterial succession as a potential indicator of postmortem submersion interval. *Forensic Science International* **209**, (2011).
24. M.E. Benbow, J.L. Pechal, J.M. Lang, R. Erb, J.R. Wallace, The Potential of High-throughput Metagenomic Sequencing of Aquatic Bacterial Communities to Estimate the Postmortem Submersion Interval. *Journal of Forensic Sciences* **60**, 1500-1510 (2015).
25. J.M. Lang, *et al*., Microbial Biofilm Community Variation in Flowing Habitats: Potential Utility as Bioindicators of Postmortem Submersion Intervals. *Microorganisms* **4**, (2016).
26. M.G.I. Langille, *et al*., Predictive functional profiling of microbial communities using 16S rRNA marker gene sequences. *Nature Biotechnology* **31**, 814-821 (2015).
27. F.E. Damann, D.E. Williams, A.C. Layton, Potential Use of Bacterial Community Succession in Decarying Human Bone for Estimating Postmortem Interval. *Journal of Forensic Sciences* **60**, 844-850 (2015).
28. E. Chiang, *et al*., Verrucomicrobia are prevelant in north-temperate freshwater lakes and display class-level preferences between lake habitats. *PLOSone* **13**, (2018).
29. R.J. Newton, S.E. Jones, A. Eiler, K.D. McMahon, S. Bertilsson, A guide to the Natural History of Freshwater Lake Bacteria. *Microbiology and Molecular Biology Reviews* **75**, 14-49 (2011).
30. M.A. Nienaber, M. Steinitz-Kannan, *A Guide to Cyanobacteria: Identification and Impact* (University Press of Kentucky, 2018).
31. F.E. Damann, “Biomarkers of Human Decomposition Ecology and the Relationship to Postmortem Interval” (National Institute of Justice, 2012)
32. K.S. Baik, *et al*., Diversity of bacterial community in freshwater of Woopo wetland. *Journal of Microbiology* **46**, 647-655 (2008).
33. K.A. Hauther, K.L. Cobaugh, L.M. Jantz, T.E. Sparer, J.M. DeBruyn, Estimating Time Since Death from Postmoretem Human Gut Microbial Communities. *Journal of Forensic Sciences* **60**, 1234-1240 (2015).

34. A,M. Kielak, C.C. Barreto, G.A. Kowalchuk, J.A. van Venn, E.E. Kuramae, The Ecology of Acidobacteria: Moving beyond Genes and Genomes, *f\Frontiers in Microbiology* **7**, (2016).
35. D.B. Meisinger, et al., In situ detection of novel Acidobacteria in microbial mats from a chemolithoautotrophically based cave ecosystem. *Environmental Microbiology* **9**, 1523-1534 (2007).
36. C. Harwood, E. Canale-Parola, Ecology of Spirochetes. *Annual Review of Microbiology* **38**, 161-192 (1984)
37. Y. Fukunaga, N. Ichikawa, "The Class *Holophagaceae*" in *The Prokaryotes*, E. Rosenberg, E.F. DeLong, S. Lory, E. Stackebrandt, F. Thompson, Eds. (Springer, Berlin, Heidelberg, 2014) pp. 683-687.
38. G. Wang, I. Schwartz, "Spirochaetes*"* in eLS, (Wiley, 2006).
39. M.S. Woolf, "Estimation of Long Term Post Mortem Interval (PMI) Based on Bacterial Community Succession on Porcine Remains," Virginia Commonwealth University, Richmond, VA. (2016).
40. J. Wiegel, R. Tanner, F.A. Rainey, "An Introduction to the Family Clostridiaceae" in *The Prokaryotes*, M. Dworkin, S. Falkow, E. Rosenberg, K.H. Schleifer, E. Stackebrandt, Eds. (Springer US, 2006).
41. A. E. Rattenbury, "Chapter 2 – Forensic Taphonomy" in *Forensic Ecogenomics*,T. K. Ralebitso-Senior, Eds. (Academic Press, 2018).
42. M. Tsokos, R.W. Byard, Postmortem Changes: Overview in Encyclopedia of Forensic and Legal Medicine, (Elsevier Inc., 2016).
43. T. Dupras, J. Shultz, "Taphonomic Bone Staining and Color Changes in Forensic Contexts" in *Manual of Forensic Taphonomy*, J. Pokines, S.A. Symes, Eds. (CRC Press, 2013), pp. 315-340.
44. G. Muyzer, A.J.M. Stams, the ecology and biotechnology of sulphate-reducing bacteria, *Nature Reviews Microbiology* **6**, 441-454 (2008).
45. M.S. Woolf, The Six Little Pigs: Estimation of Long-Term Postmortem Interval (PMI) Based on Bacterial Community Succession in Porcine Remains (Proceedings of the American Academy of Forensic Sciences, 2016).
46. C.N. Seong, *et al*., Taxonomic hierarchy of the phylum *Firmicutes* and novel *Firmicutes* species orginated from various enviornments in Korea. *Journal of Microbiology* **56**, 1-10 (2018).
47. S. Fiedler, M. Graw, Decomposition of buried corpses, with special reference to the formation of adipocere. *The Science of Nature* **90**, 291-300 (2003).
48. L. Jimenez-Diaz, A. Caballero, A. Segura, "Pathways for the Degradation of Fatty Acids in Bacteria" in *Aerobic Utilization of Hydrocarbons, Oils and Lipids*, F. Rojo, Eds. (Springer, Cham 2017).
49. A.J. Lastovica, S.L.W. On, Li Zhang, "The Family Campylobacteraceae" in *The Prokaryotes: Deltaproteobacteria and Epsilonproteobacteria*, Rosenberg, E.F. DeLong, S. Lory, E. Stackebrandt, F. Thompson, Eds. (Springer-Verlag Berlin Heidelberg, 2014), pp. 308-335.
50. A. Willems, "The Family Comamonadaceae" in *The Prokaryotes: Alphaproteobacteria and Betaproteobacteria*, Rosenberg, E.F. DeLong, S. Lory, E. Stackebrandt, F. Thompson, Eds. (Springer-Verlag Berlin Heidelberg, 2014), pp. 777-851.
51. J.L Pechal, *et al*., Microbial Community Functional Change during Vertebrate Carrion Decomposition. *PLOSone* **8**, (2013).
52. C.E. Larson, *et al*., Microbial Community Response to a Novel Salmon Resource Subsidy. *Frontiers in Ecology and Evolution* **7**, 505 (2020).

53. B. Schink, R. Munoz, "The Family Syntrophomonadaceae" in *The Prokaryotes: Firmicutes and Tenericutes*, E. Rosenberg, E.F. DeLong, S. Lory, E. Stackebrandt, F. Thompson, Eds. (Springer, 2014), pp. 371-379.
54. B. Singh et al., A metagenomic assessment of the bacteria associated with *Lucillia sericata* and *Lucilia cuprina* (*Diptera: Calliphoridae*). *Applied Microbiology and Biotechnology* **99**, 869-883.
55. D. Wohlfahrt, M. Woolf, B. Singh, A survey of bacteria associated with various life stages of primary colonizers: *Lucilia sericata* and *Phormia regina*. *Science and Justice* **60**, 173-179.
56. I.M. Carroll, T. Ringel-Kulka, J.P. Siddle, T.R. Klaenhammer, Y. Ringel, Characterization of the Fecal Microbiota Using High-Throughput Sequencing Reveals a Stable Microbial Community during Storage. *PLOSone* **7**, e46953 (2012).
57. Invitrogen, CST Protocol for Extracting gDNA from Bone Samples (2009)
58. ThermoFisher Scientific, Qubit® dsDNA HS Assay Kits User Guide (2010)
59. J.J. Kozich, S.L. Westcott, N.T. Baxter, S.K. Highlander, P.D. Schloss, Development of a Dual-Index Sequencing Strategy and Curation Pipeline for Analyzing Amplicon Sequence Data on the MiSeq Illumina Sequencing Platform. *Applied Environmental Microbiology* **79**, 5112-5120 (2013).
60. Qiagen, DNeasy PowerClean Pro Cleanup Kit Protocol (2017)
61. Beckman Coulter, Agencourt AMPure PCR Purification Kit Protocol (2016)
62. C. Quast, *et al*., The SILVA ribosomal RNA gene database project: improved data processing and web-based tools. *Nucleic acid research* **41**, D590-D596 (2013).
63. R.C. Edgar, B.J. Hass, J.C. Clemente, C. Quince, R. Knight, UCHIME improves sensitivity and speed of chimera detection. *Bioinformatics* **27**, 2194-2200 (2011).
64. Q. Wang, G.M. Garrity, J.M. Tiedje, J.R. Cole, Naïve Bayesian classifier for rapid assignment of rRNA sequences into the new bacterial taxonomy. *Applied Environmental Microbiology* **73**, 5261-5267 (2007).
65. T.Z. DeSantis, *et al*., Greengenes, a chimera-checked 16S rRNA gene database and workbench compatible with ARB. *Applied and Environmental Microbiology* **72**, 5069-5072 (2006).
66. R Core Team, R: A Language and Environment for Statistical Computing (2019).
67. H. Wickham, ggplot2: Elegant Graphics for Data Analysis (2016).
68. J. Oksanen, *et al*., vegan: Community Ecology Package (2019).
69. C. Hanbo, VennDiagram: Generate High-Resolution Venn and Euler Plots (2018).
70. K. Dill-McFarland, Microbiota Analysis in R *R Pubs by RStudio* (2017).
71. P.J. McMurdie, S. Holmes, phyloseq: An R package for reproducible interactive analysis and graphics of microbiome census data. *PLOSone* **8**, (2013).
72. T. Galili, dendextend: an R package for visualizing, adjusting, and comparing trees of hierarchical clustering. *Bioinformatics* (2015).
73. G.M. Douglas, R.G. Beiko, M.G.I. Langille, "Predicting the Functional Potential of the Microbiome from Marker Genes Using PICRUSt" in *Microbiome Analysis: Methods and Protocols,* Methods in Molecular Biology, R.G. Beiko, Ed. (Springer Science+Business Media, LLC, 2018), pp. 169-177

Figures and Tables

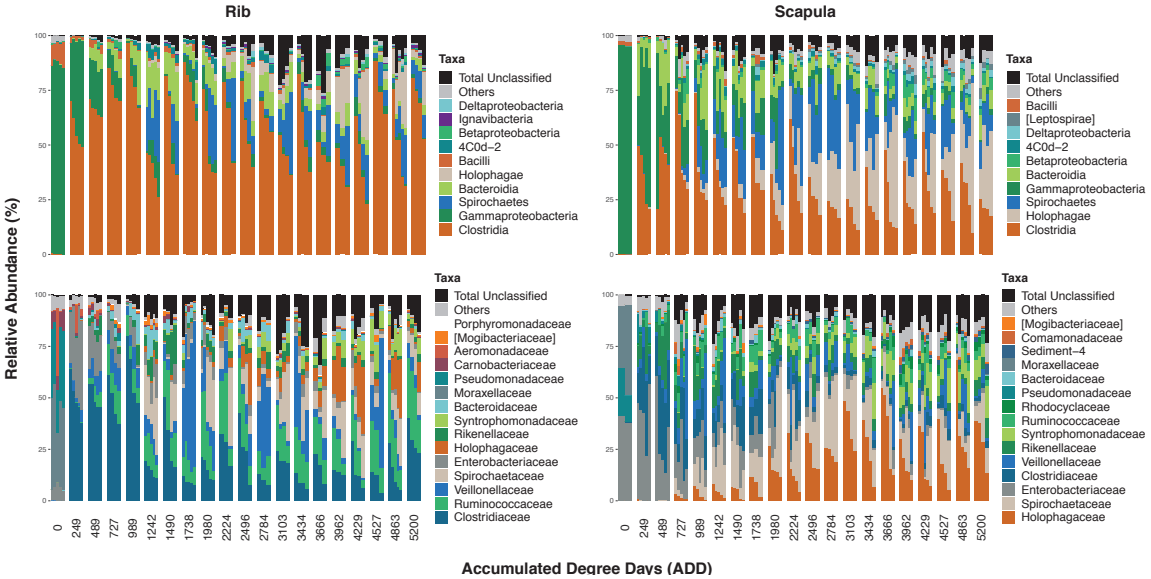

Figure 2.1. Relative abundance of the top ten classes (top panels) and top fifteen families (bottom panels) for rib and scapula samples across ADD. Others and Total Unclassified include remaining classified taxa and unclassified taxa, respectively. Replications are represented by invidiual bars within each ADD.

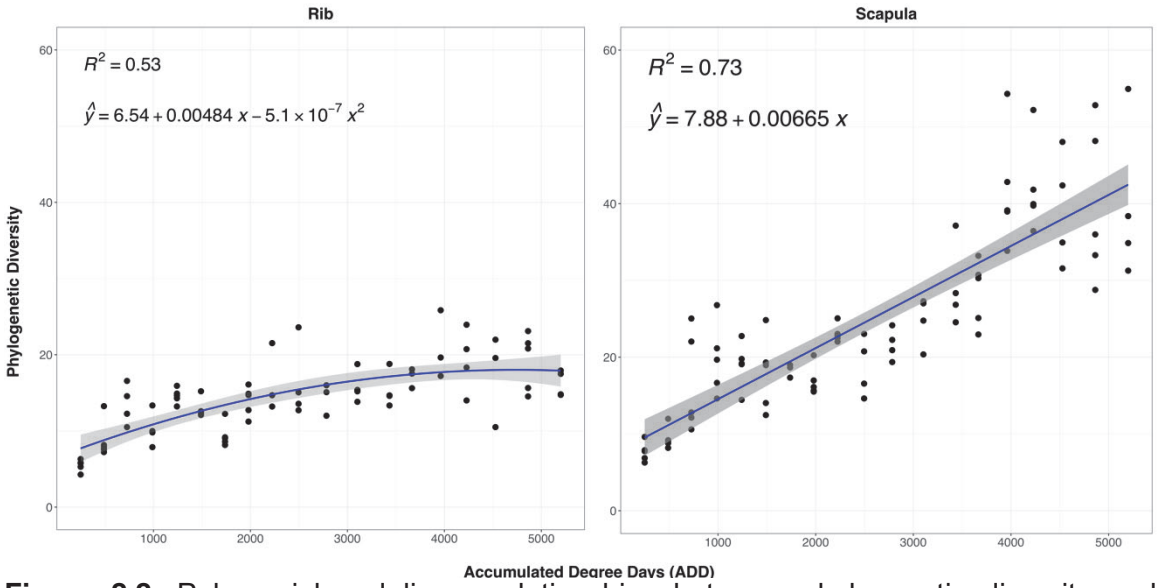

Figure 2.2. Polynomial and linear relationships between phylogenetic diversity and accumulated degree days in rib (left panel) and scapula (right panel) samples. Shaded area demonstrates 95% confidence interval.

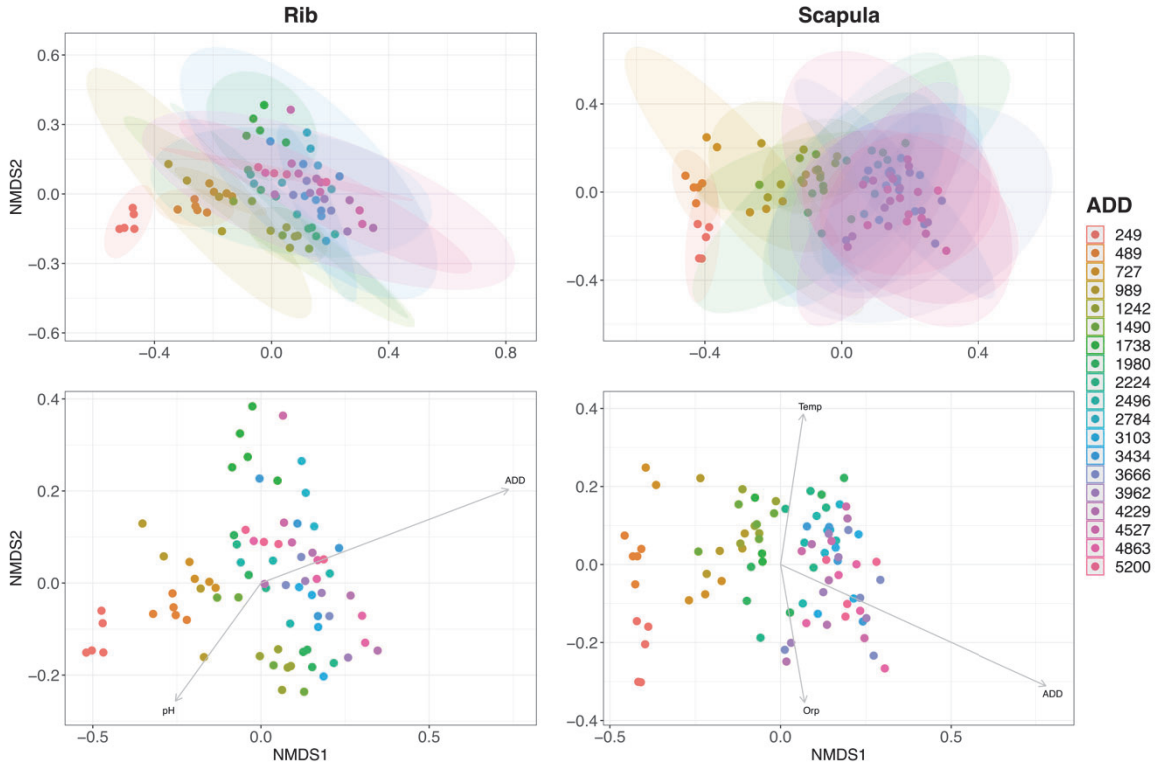

Figure 2.3. Non-metric multidimensional scaling (NMDS) ordination of weighted UniFrac distances across ADD for rib (2D, stress=0.1704) and scapula (2D, stress=0.1467) samples. ADD was found to be significant, according to PERMANOVA (Rib: *pseudo*-F=20.23, R^2=0.21, p=0.001, Scapula: *pseudo*-F=37.67, R^2=0.31, p=0.001). Ellipses represent 95% standard error for the mean or group centroid (top panels). Environmental variables significantly related to ordination (alpha 0.05) are represented by vectors (bottom panels). Significant environmental variables include accumulated degree days (ADD), Temperature (Temp), oxidation reduction potential (ORP) and pH. Lengths and angles of the arrows indicate the strength and direction of the relationship between environmental variables and β-diversity. Positively correlated vectors are those that are close and similar angles, while diverging vectors suggest a negative correlation.

This resource was prepared by the author(s) using Federal funds provided by the U.S. Department of Justice. Opinions or points of view expressed are those of the author(s) and do not necessarily reflect the official position or policies of the U.S. Department of Justice.

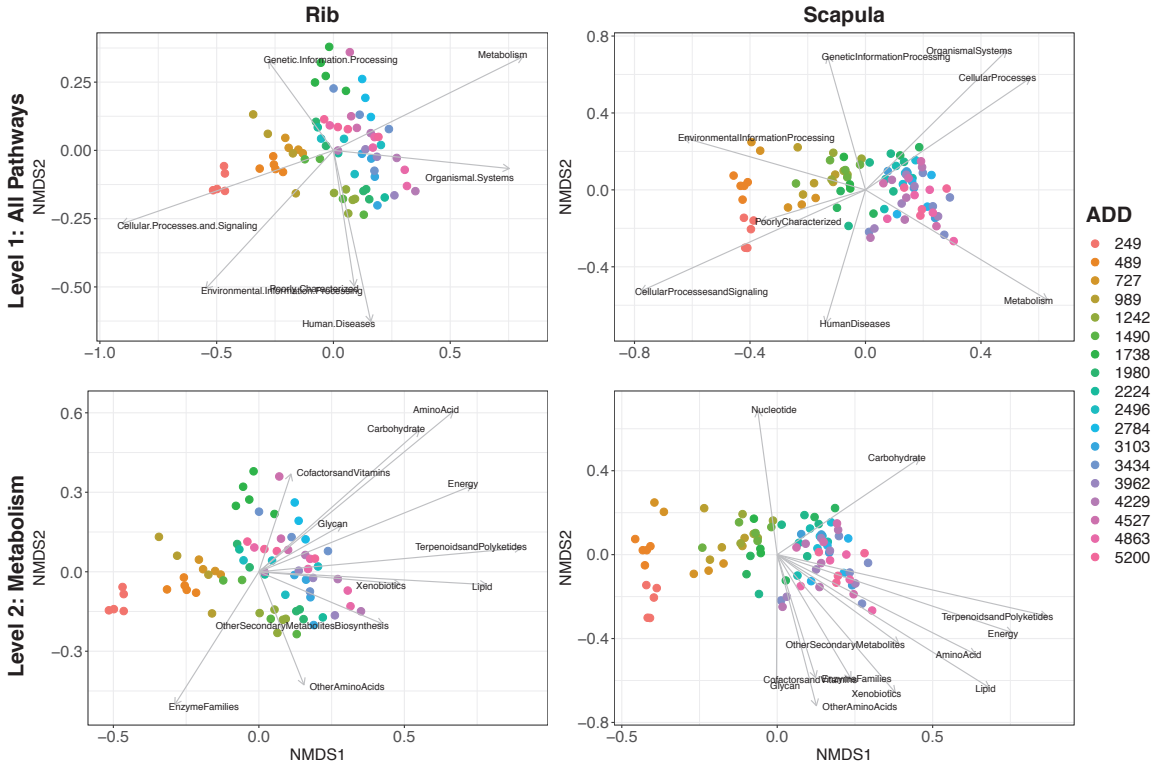

Figure 2.4. PICRUSt predicted functional KEGG Level 1 Pathways and their relationship with β-diversity of bacterial community structure across ADD. Level 1 pathways (top panels) and level 2 metabolism pathways classified at level 3 (bottom panels) that were significantly related to weighted UniFrac distances non-metric multidimensional scaling (NMDS) ordination (alpha 0.05) are represented by vectors. Lengths and angles of the arrows indicate the strength and direction of the relationship between KEGG pathways and β-diversity.

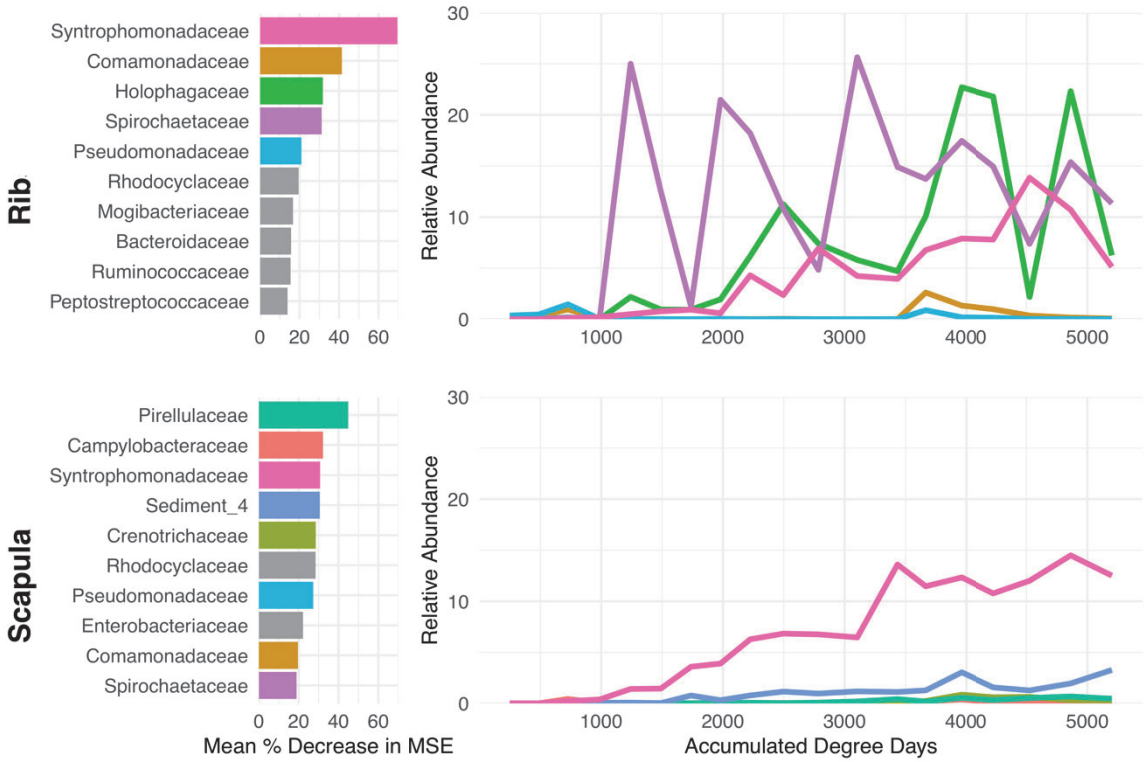

Figure 2.5. List of the top predictor bacteria taxa in decreasing order for rib (top left panel) and scapula (bottom left panel) samples. The changes for the highlighted predictor taxa across accumulated degree days (ADD) are depicted in the top and bottom right panels for rib and scapula, respectively.

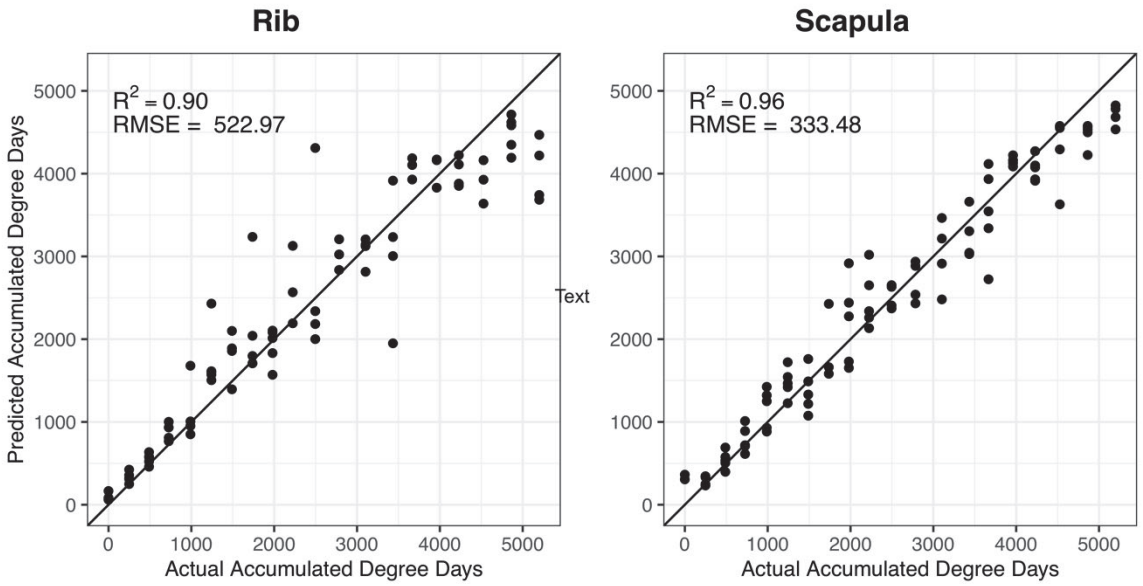

Figure 2.6. Relative abundances of predictor bacterial taxa were used to develop random forest models for each skeletal element. Predicted accumulated degree days (ADD) versus actual ADD for rib (left panel) and scapula (right) samples were plotted with a superimposed one-to-one reference line.

Table 2.1. A comparison of exact accumulated degree days (ADD), time since placement (days), and sample collection numbers.

Accumulated Degree Days (ADD)	Time Since Placement (Days)	Collection
0	0	Baseline
249	23	Collection 1
489	72	Collection 2
727	114	Collection 3
989	150	Collection 4
1242	178	Collection 5
1490	204	Collection 6
1738	227	Collection 7
1980	249	Collection 8
2224	269	Collection 9
2496	291	Collection 10
2784	310	Collection 11
3103	333	Collection 12
3434	353	Collection 13
3666	373	Collection 14
3962	422	Collection 15
4229	477	Collection16
4527	520	Collection 17
4863	556	Collection 18
5200	579	Collection 19

Table 2.2. Summary of the relationship between environmental variables and UniFrac weighted β- diversity NMDS ordination.

Environmental Parameters	**Rib**		**Scapula**	
	r^2	p-value	r^2	p-value
ADD	0.5827	0.001	0.7052	0.001
Season	0.0404	0.316	0.0644	0.13
Temperature	0.0599	0.209	0.153	0.008
Specific Conductivity	0.0003	0.99	0.0755	0.103
Salinity	0.0004	0.989	0.076	0.102
Oxidation Reduction Potential	0.0016	0.969	0.13	0.017
pH	0.1304	0.037	0.0479	0.225

Table 2.3. Summary of the relationship between KEGG level 1 pathway and UniFrac weighted β- diversity NMDS ordination.

KEGG Level 1	Rib		Scapula	
	r^2	p-value	r^2	p-value
Cellular Processes	0.0062	0.8	0.6645	0.001
Cellular Processes and Signaling	0.8911	0.001	0.8814	0.001
Environmental Information Processing	0.5555	0.001	0.4685	0.001
Genetic Information Processing	0.1835	0.001	0.4981	0.001
Human Disease	0.4185	0.001	0.5001	0.001
Metabolism	0.774	0.001	0.7251	0.001
Organismal Systems	0.5719	0.001	0.7625	0.001
Poorly Characterized	0.2547	0.001	0.1585	0.002

Table 2.4. Summary of the relationship between KEGG level 2 pathways and UniFrac weighted β- diversity NMDS ordination.

KEGG Level 2	Rib		Scapula	
	r^2	p-value	r^2	p-value
Metabolism of Terpenoids and Polyketides	0.8202	0.001	0.8393	0.001
Energy Metabolism	0.6453	0.001	0.7094	0.001
Nucleotide Metabolism	0.0383	0.237	0.4768	0.001
Lipid Metabolism	0.615	0.001	0.8693	0.001
Xenobiotics Biodegradation and Metabolism	0.2375	0.001	0.5757	0.001
Carbohydrate Metabolism	0.5907	0.001	0.4218	0.001
Amino Acid Metabolism	0.8122	0.001	0.6323	0.001
Other Amino Acids	0.2062	0.001	0.5345	0.001
Biosynthesis of Other Secondary Metabolites	0.221	0.002	0.332	0.001
Metabolism of Cofactors and Vitamins	0.1484	0.003	0.4053	0.001
Enzyme Families	0.3349	0.001	0.3585	0.001
Glycan Biosynthesis and Metabolism	0.1126	0.011	0.3826	0.001

Supplemental Figures and Tables

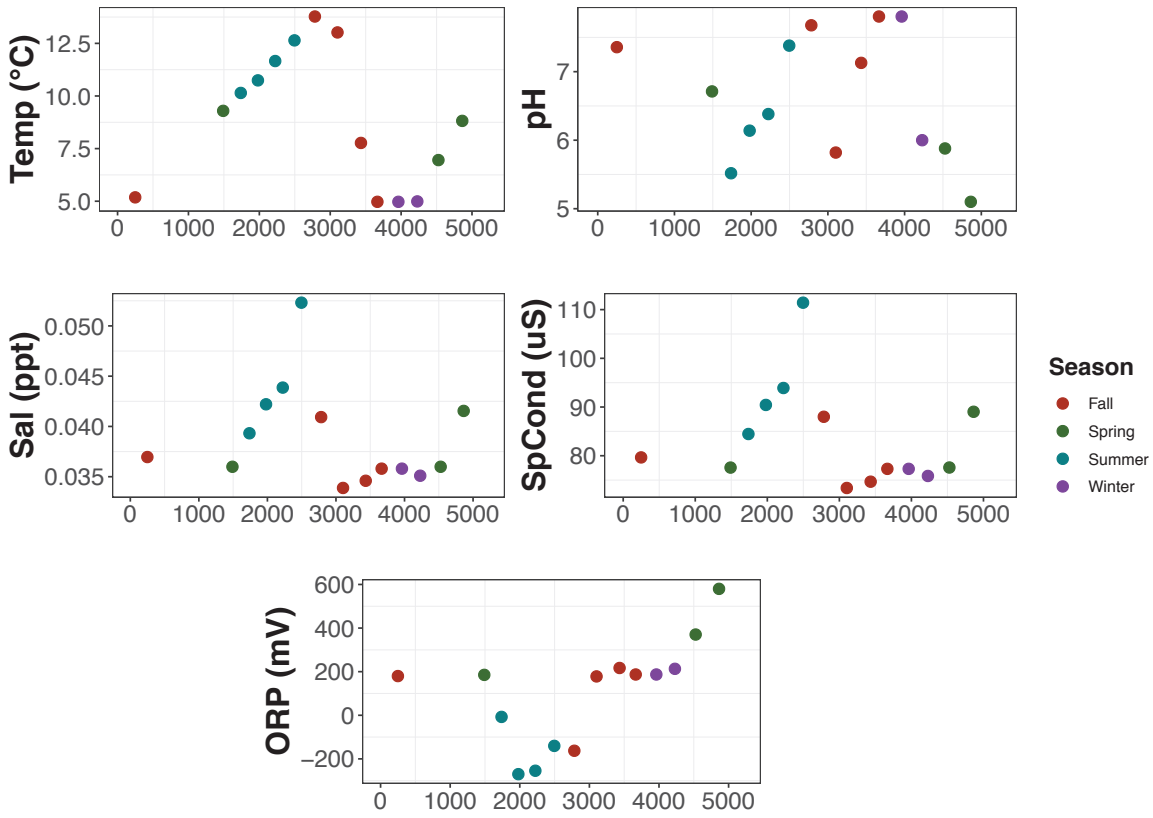

Fig. 2.S1. The relationship between environmental and water quality daily averages for each collection or accumulated degree days (ADD). Fourteen of twenty time points are represented, as a result of difficulties with the Sonde. Abbreviations, such as Temp, Sal and SpCond, represent temperature, salinity and specific conductivity, respectively.

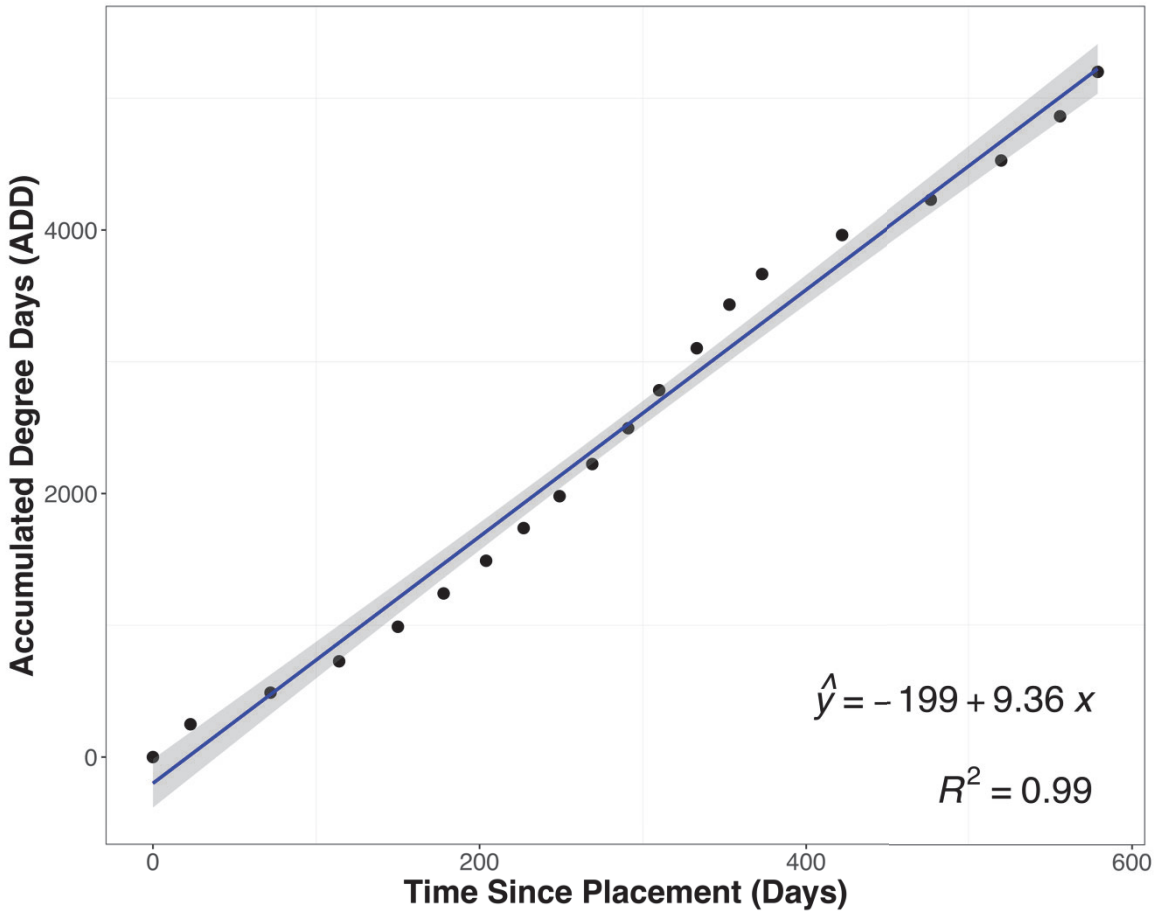

Fig. 2.S2. The linear relationship between accumulated degree days (ADD) and the number of days since the skeletal elements were placed/submerged in Henley Lake. Shaded area demonstrates 95% confidence interval.

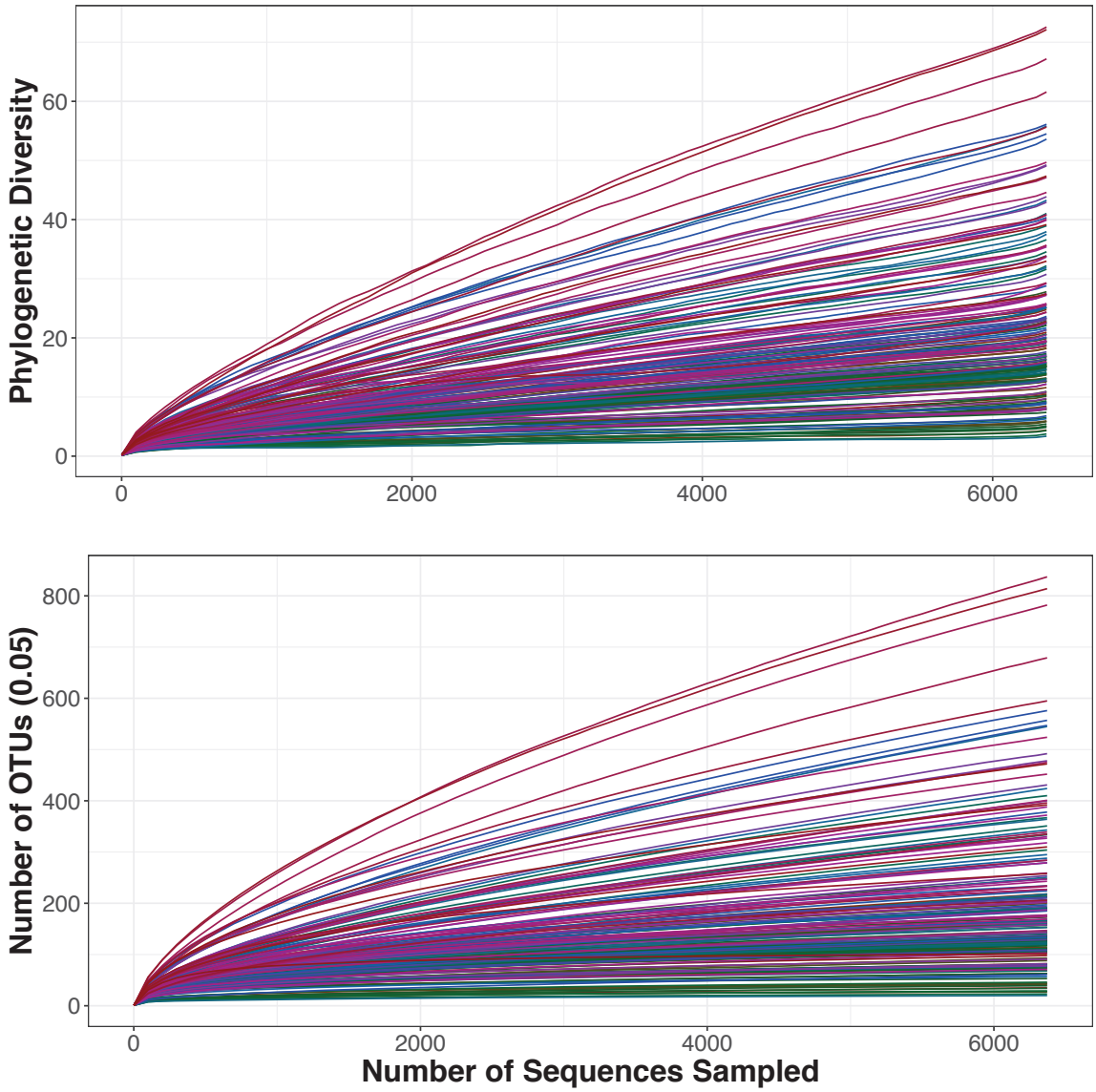

Fig. 2.S3. Rarefaction analysis curves of phylogenetic diversity (top panel) and (b) the number of operational taxonomic units (0.05 or 5%) observed for 6,371 sampled sequences. Most samples have converged and reached a horizontal asymptote, suggesting that sufficient observations were made to get a reasonable estimate of quantity without sacrificing samples.

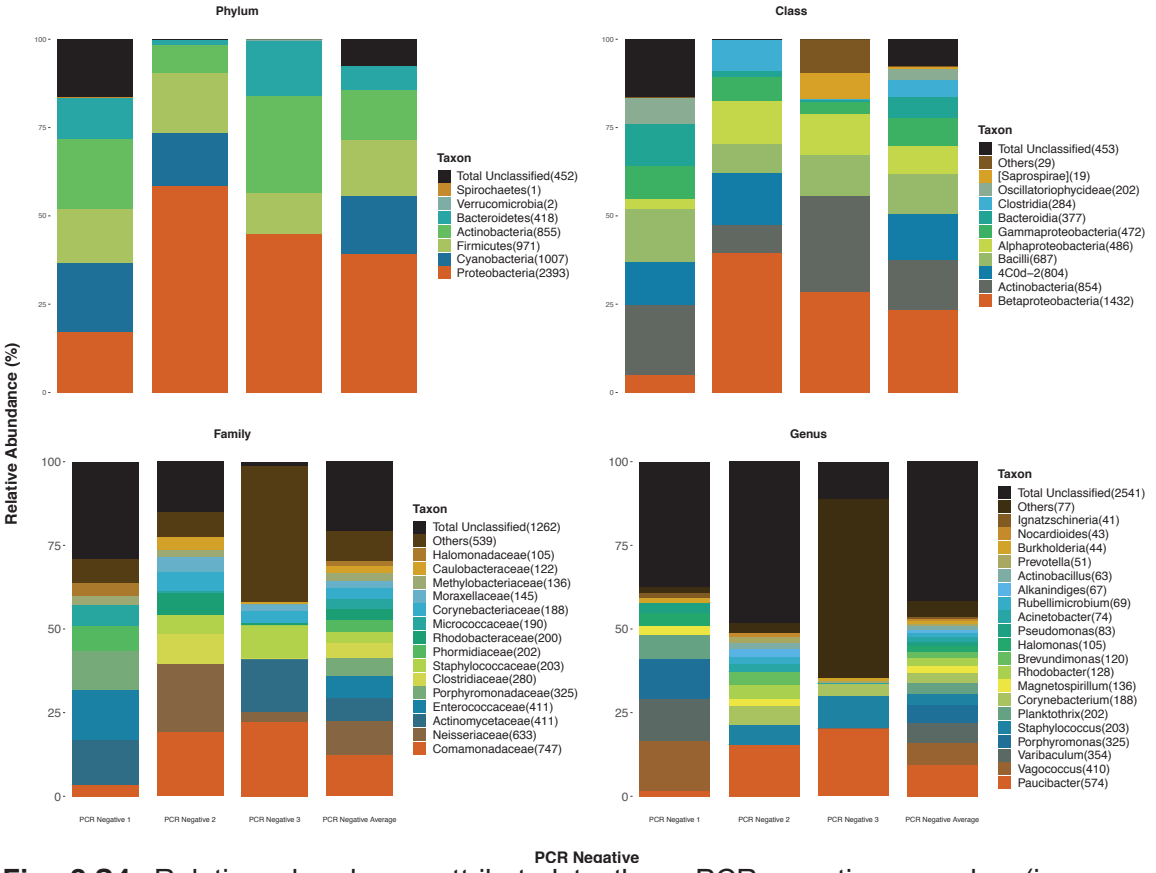

Fig. 2.S4. Relative abundance attributed to three PCR negative samples (i.e., non-template control) and the average number of reads expected from the samples (PCR Negative 1: 2762, PCR Negative 2: 3081, PCR Negative 3: 256, Average: 2033). Unclassified includes remaining unclassified taxa. All negative samples were removed from analysis during subsampling.

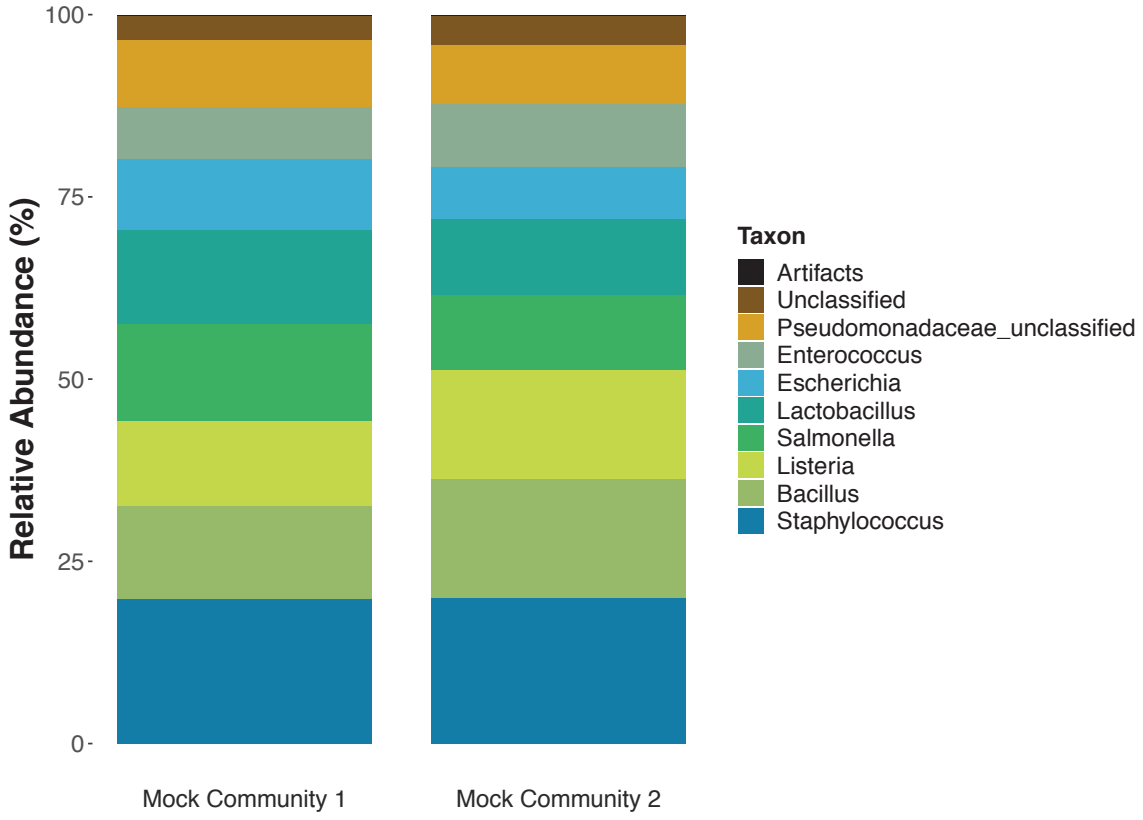

Fig. 2.S5. Relative abundance of ZymoBIOMICS microbial community DNA standard expected eight genera. Unclassified includes remaining unclassified taxa; meanwhile, Artifacts consists of singletons (0.11%) that were excluded from further analyses.

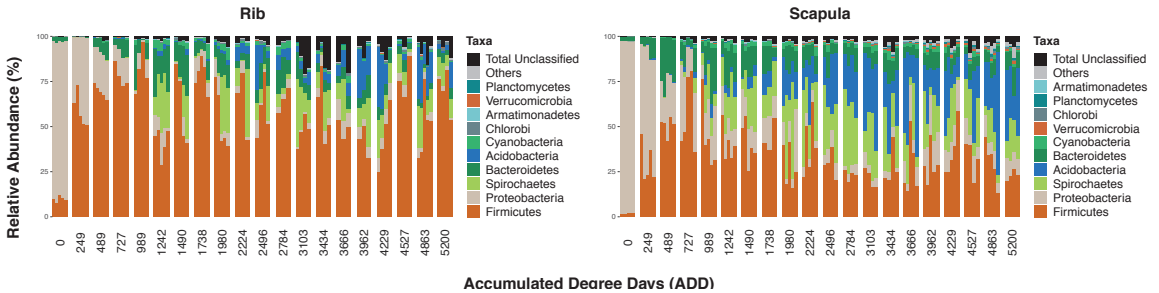

Fig. 2.S6. Relative abundance of the top ten phylum level bacteria for rib (left panel) and scapula (right panel) samples across ADD. Others and Total Unclassified include remaining classified taxa and unclassified taxa, respectively. Invidiual bars within each ADD represent replications.

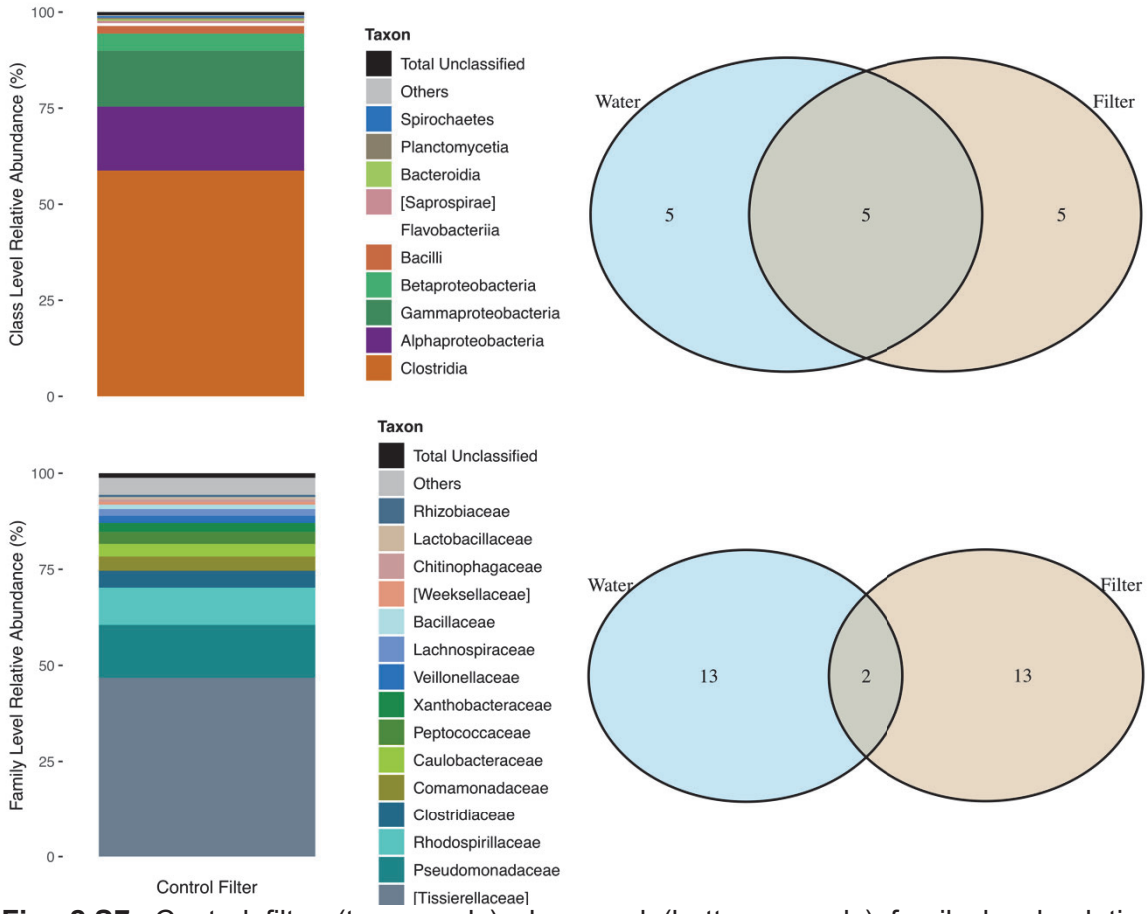

Fig. 2.S7. Control filter (top panels) class and (bottom panels) family level relative abundance and venn diagrams, showing minimal similarities between the most dominant taxa shared between water filters and control filters.

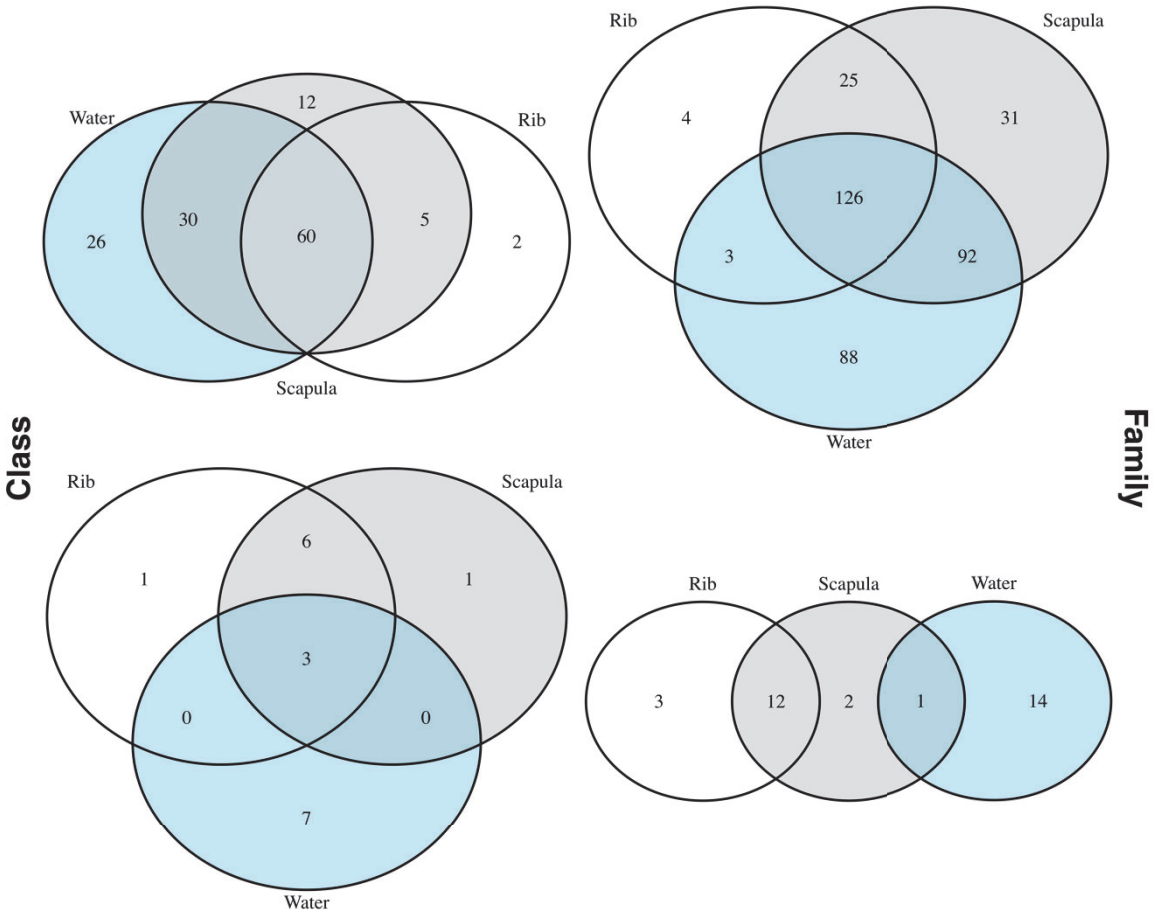

Fig. 2.S8. Presence of class level taxa (left panels), family level taxa (right panels), top ten classes (bottom left panel), and top fifteen families (bottom right panel) recovered from each sample type.

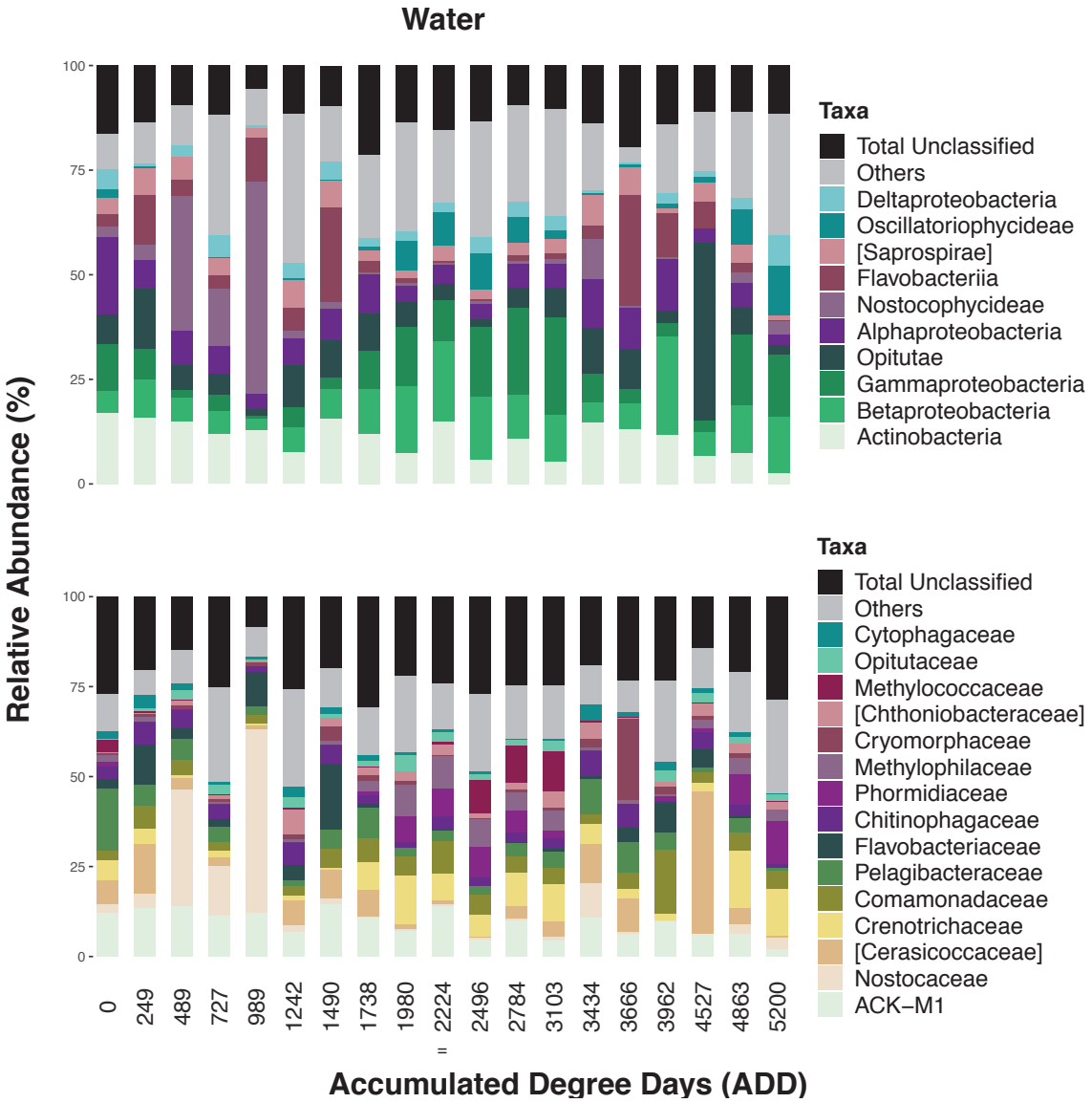

Fig. 2.S9. Relative abundance of the top ten class level (top panel) and top fifteen family level (bottom panel) bacteria for water samples across ADD. Others and Total Unclassified include remaining classified taxa and unclassified taxa, respectively.

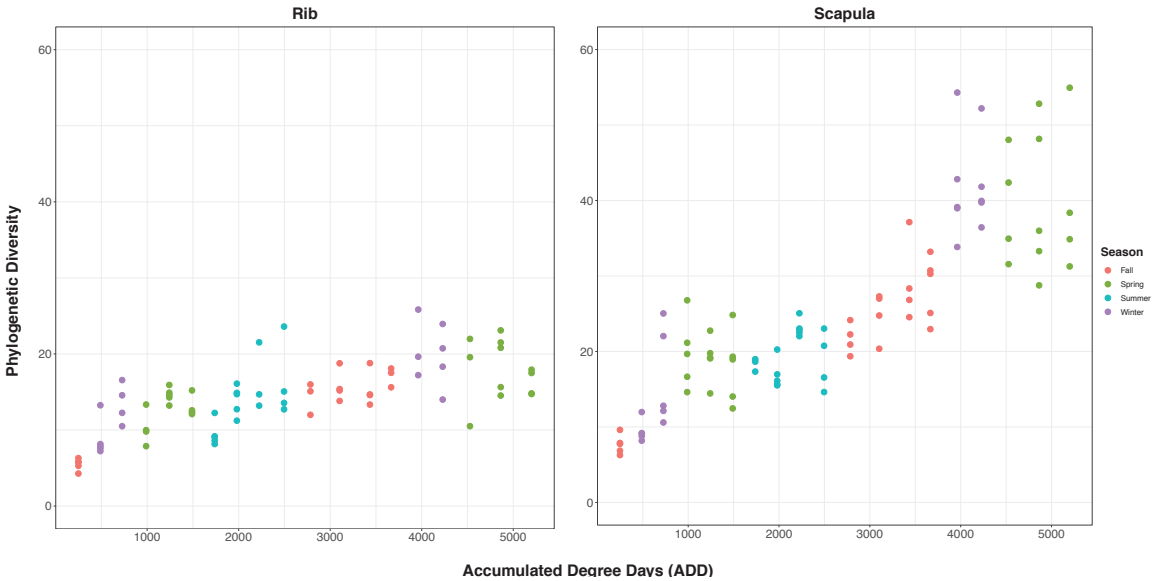

Fig. 2.S10. Relationships between rib (left panel) and scapula (right panel) phylogenetic alpha-diversity and accumulated degree days (ADD) colored by season (Fall, Winter, Spring, Summer).

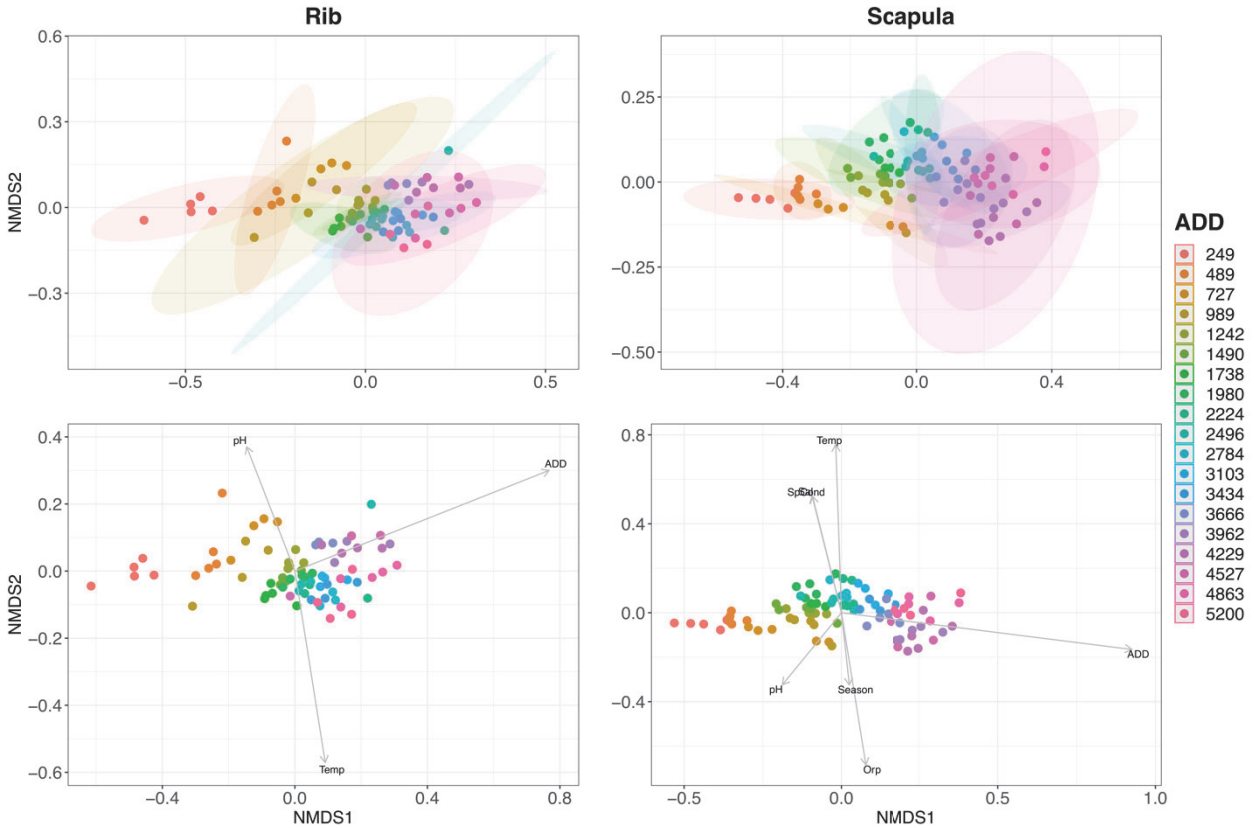

Fig. 2.S11. Microbial non-metric multidimensional scaling (NMDS) ordination of unweighted UniFrac beta-diversity in bacterial community structure across ADD for rib (2D, stress=0.1255) and scapula (2D, stress=0.1066) samples. ADD was found to be significant, according to PERMANOVA (Rib: *pseudo*-F=11.74, R^2=0.14, p=0.001, Scapula: *pseudo*-F=17.04, R^2=0.17, p=0.001). Ellipses represent 95% standard error for the mean or group centroid (top panels). Environmental variables significantly related to ordination (alpha 0.05) are represented by vectors (bottom panels). Significant environmental variables include accumulated degree days (ADD), Temperature (Temp), pH, Oxidation Reduction Potential (ORP), Specific Conductivity (SpCond) and Salinity (Sal). Lengths and angles of the arrows indicate the strength and direction of the relationship between environmental variables and beta-diversity. Positively correlated vectors are those that are close and similar angles (i.e. Sal and SpCond for scapula), while diverging vectors suggest a negative correlation.

This resource was prepared by the author(s) using Federal funds provided by the U.S. Department of Justice. Opinions or points of view expressed are those of the author(s) and do not necessarily reflect the official position or policies of the U.S. Department of Justice.

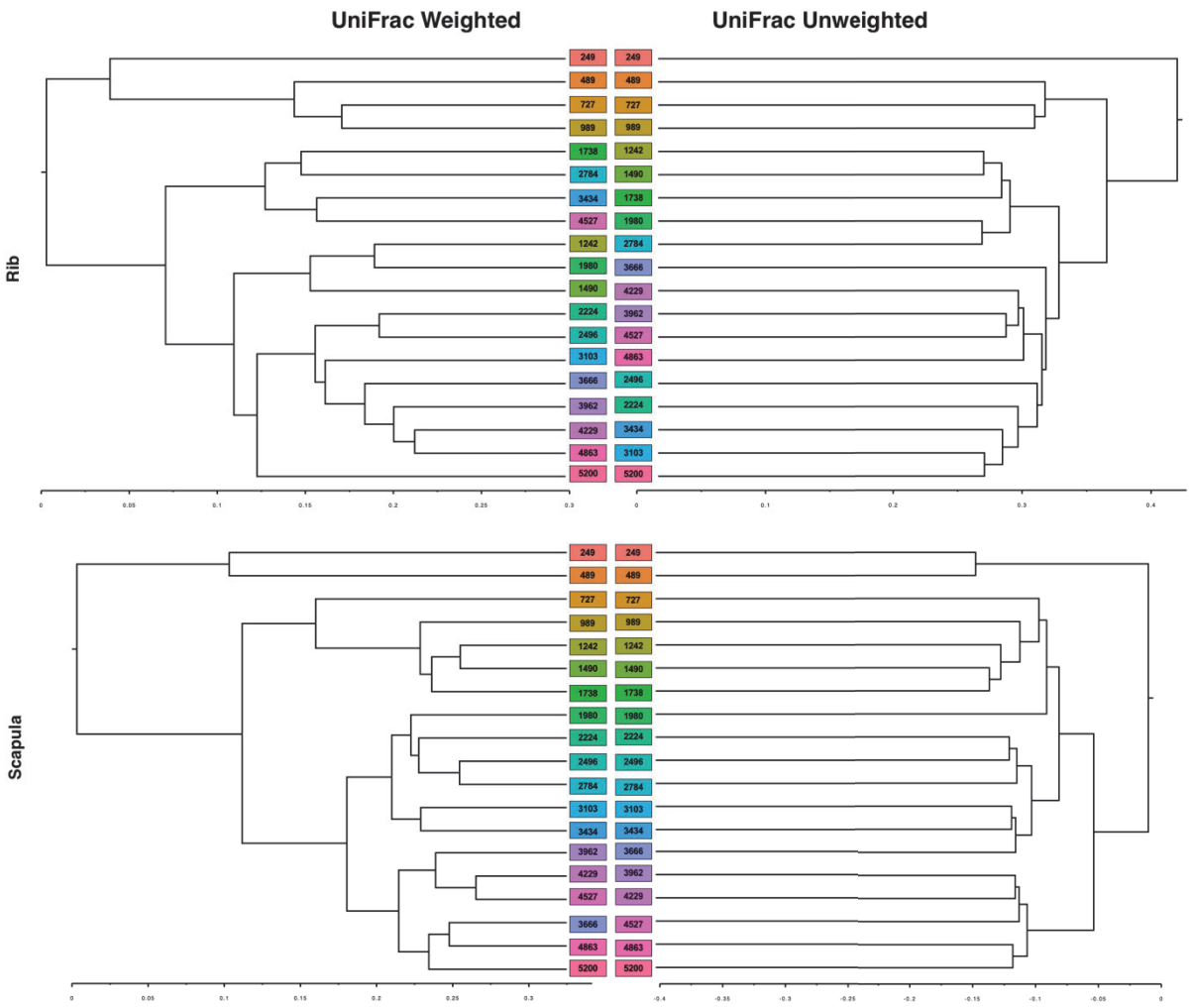

Fig. 2.S12. Unweighted Pair Group Method with Arithmetic Mean (UPGMA) trees grouped by accumulated degree days (ADD) based on weighted (left) and unweighted (right) UniFrac distances. Both rib (top panel) and scapula (bottom panel) had cophenetic correlation values 0.79 and 0.68, suggesting that weighted and unweighted UniFrac trees were highly congruent.

Table 2.S1. The correlation coefficients of environmental and water quality daily averages and their relationship with accumulated degree days (ADD). Oxidation reduction potential was the only parameter significantly and positively associated with ADD.

Environmental Parameters	rho (Spearman's)	p-value
Temperature	-0.38	0.1767
pH	-0.14	0.6311
Salinity	-0.37	0.1991
Specific Conductivity	-0.32	0.2697
Oxidation Reduction Potential	0.71	0.0042

Table 2.S2. The percent of classified and unclassified sequences across all taxonomic levels for the respective bone types.

Taxonomy Number of Sequences				
	Rib		Scapula	
	Classified (%)	Unclassified (%)	Classified (%)	Unclassified (%)
Phylum	96	4	97.61	2.39
Class	94.38	5.62	93.51	6.49
Order	94.06	5.94	92.42	7.58
Family	90.53	9.47	88.94	11.06
Genus	57.52	42.48	61.34	38.66
Species	5.22	94.78	3.06	96.94

Table 2.S3. List of top ten class and top fifteen family level taxa unique to and shared among sample types.

	Rib	Scapula	Water	Rib:Scapula	Rib:Water	Scapula:Water	Rib:Scapula:Water
Top 10 Class Level Taxa	Ignavibacteria	Leptospirae	Actinobacteria Opitutae Alphaproteobacteria Nostocophycideae Flavobacteriia Saprospirae. Oscillatoriophycideae	Clostridia Spirochaetes Bacteroidia Holophagae Bacilli 4C0d-2			Gammaproteobacteria Betaproteobacteria Deltaproteobacteria
Top 15 Family Level Taxa	Carnobacteriaceae Aeromonadaceae Porphyromonadaceae	Rhodocyclaceae Sediment 4	ACK.M1 Nostocaceae Cerasicoccaceae Crenotrichaceae Pelagibacteraceae Flavobacteriaceae Chitinophagaceae Phormidiaceae Methylophilaceae Cryomorphaceae Chthoniobacteraceae Methylococcaceae Opitutaceae Cytophagaceae	Clostridiaceae Ruminococcaceae Veillonellaceae Spirochaetaceae Enterobacteriaceae Holophagaceae Rikenellaceae Syntrophomonadaceae Bacteroidaceae Moraxellaceae Pseudomonadaceae Mogibacteriaceae		Comamonadaceae	

Table 2.S4. Summary of the relationship between environmental variables and UniFrac unweighted beta diversity NMDS ordination.

Environmental Parameters	Rib		Scapula	
	r^2	p-value	r^2	p-value
ADD	0.6817	0.001	0.8843	0.001
Season	0.0648	0.169	0.1061	0.04
Temperature	0.3461	0.001	0.5725	0.001
Specific Conductivity	0.026	0.503	0.2827	0.001
Salinity	0.0263	0.495	0.2852	0.001
Oxidation Reduction Potential	0.1197	0.037	0.4741	0.001
pH	0.1604	0.011	0.1402	0.009

Supplementary Information Text

Additional Analyses. Operational Taxonomic Unit (OTU) clustering via average neighbor occurred at a genetic dissimilarity of 5% (i.e genus level) was used to assess α- and β- diversity. Shannon diversity indices were calculated (iters=1000) using mothur version 1.39.5 (1). Resulting temporal α-diversity changes were assessed via linear modeling (lm) using the stats package (2) and visualized with the ggplot2 package. Variations within the dataset were examined by incorporating environmental parameters (i.e temperature, pH, etc.) into the linear model. OTU β-diversity was explored using a meta data file with mothur (1) generated OTU table and OTU taxonomy in the vegan package (3). Specifically, bacterial community difference calculations utilized Bray-Curtis and Jaccard measures with non-metric multidimensional scaling (NMDS) (permutations=999). Resulting dissimilarity values were tested using permutational multivariate analysis of variance (PERMANOVA) via the adonis function within the vegan and visualized with ggplot2. Field site parameters (i.e temperature, ADD, pH, etc.) were superimposed to both OTU Bray-Curtis ordinations using the envfit function from the vegan package. Plotted vectors ($\alpha < 0.05$) indicate the direction in ordination space that changes most rapidly, while maximizing correlations. Resulting squared correlation coefficients (permutations-999) and fitted vectors were used to assess the importance of each parameter.

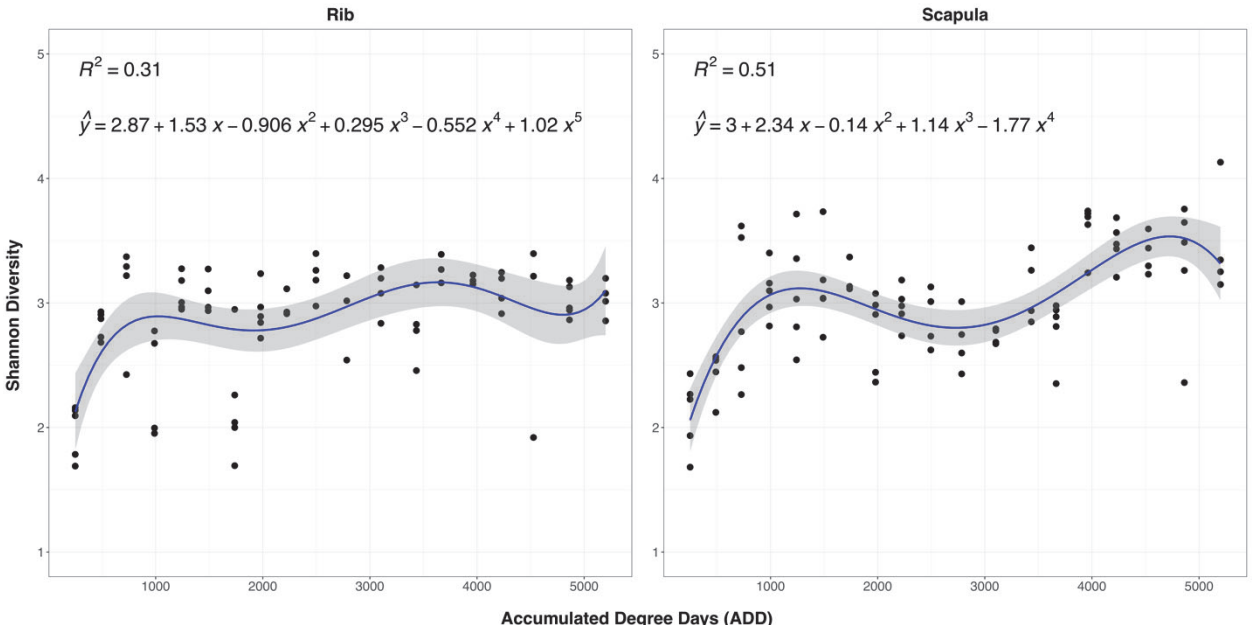

Fig. 2.S13. Polynomial relationships between rib (left panel) and scapula (right panel) OTU (0.05) Shannon alpha-diversity and accumulated degree days (ADD). Shaded area demonstrates 95% standard error.

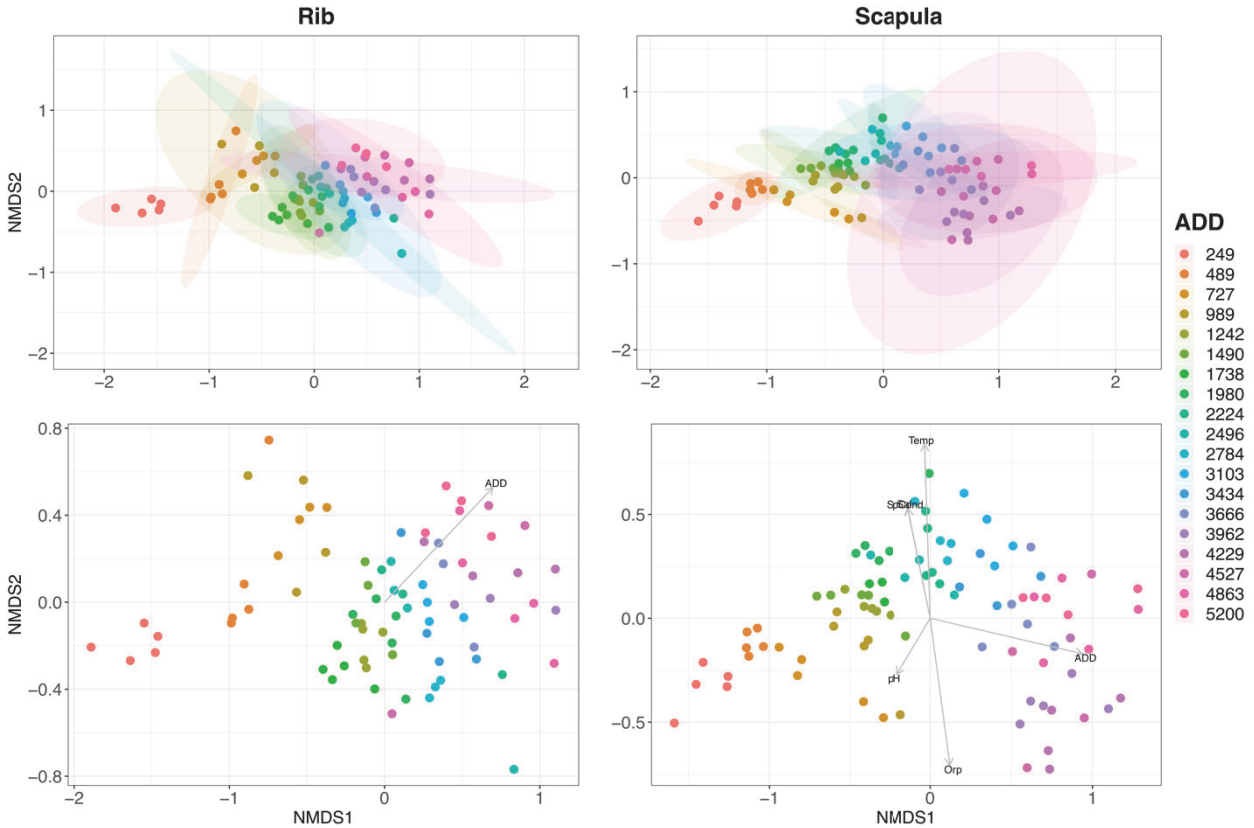

Fig. 2.S14. Microbial OTU (0.05) Bray-Curtis non-metric multidimensional scaling (NMDS) ordination of beta-diversity in bacterial community structure across ADD for rib (2D, stress=0.1404) and scapula (2D, stress=0.1074) samples. ADD was found to be significant, according to PERMANOVA (Rib: *pseudo*-F=20.10, R^2=0.21, p=0.001, Scapula: *pseudo*-F=41.74, R^2=0.33, p=0.001). Ellipses represent 95% confidence standard error for the mean or group centroid (top panels). Environmental variables significantly related to ordination (alpha 0.05) are represented by vectors (bottom panels). Significant environmental variables include accumulated degree days (ADD), Temperature (Temp), pH, Specific Conductivity (SpCond), Salinity (Sal) and Oxidation Reduction Potential (ORP). Lengths and angles of the arrows indicate the strength and direction of the relationship between environmental variables and beta-diversity. Positively correlated vectors are those that are close and similar angles (i.e. Sal and SpCond for scapula), while diverging vectors suggest a negative correlation.

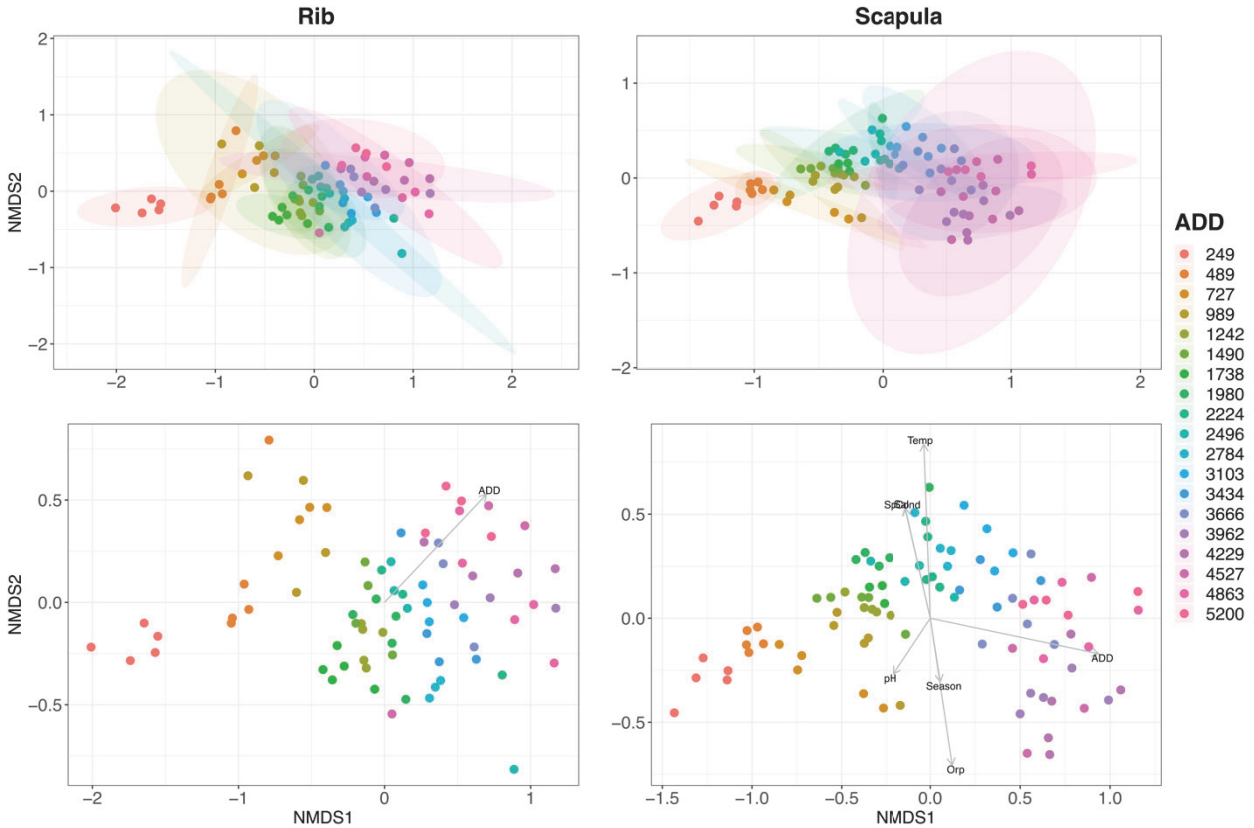

Fig. 2.S15. Microbial OTU (0.05) Jaccard non-metric multidimensional scaling (NMDS) ordination of beta-diversity in bacterial community structure across ADD for rib (2D, stress=0.1414) and scapula (2D, stress=0.1074) samples. ADD was found to be significant, according to PERMANOVA (Rib: *pseudo*-F=20.01, R^2=0.21, p=0.001, Scapula: *pseudo*-F=41.73, R^2=0.33, p=0.001). Ellipses represent 95% confidence standard error for the mean or group centroid (top panels). Environmental variables significantly related to ordination (alpha 0.05) are represented by vectors (bottom panels). Significant environmental variables include accumulated degree days (ADD), Temperature (Temp), pH, Specific Conductivity (SpCond), Salinity (Sal) and Oxidation Reduction Potential (ORP). Lengths and angles of the arrows indicate the strength and direction of the relationship between environmental variables and beta-diversity. Positively correlated vectors are those that are close and similar angles (i.e. Sal and SpCond for scapula), while diverging vectors suggest a negative correlation.

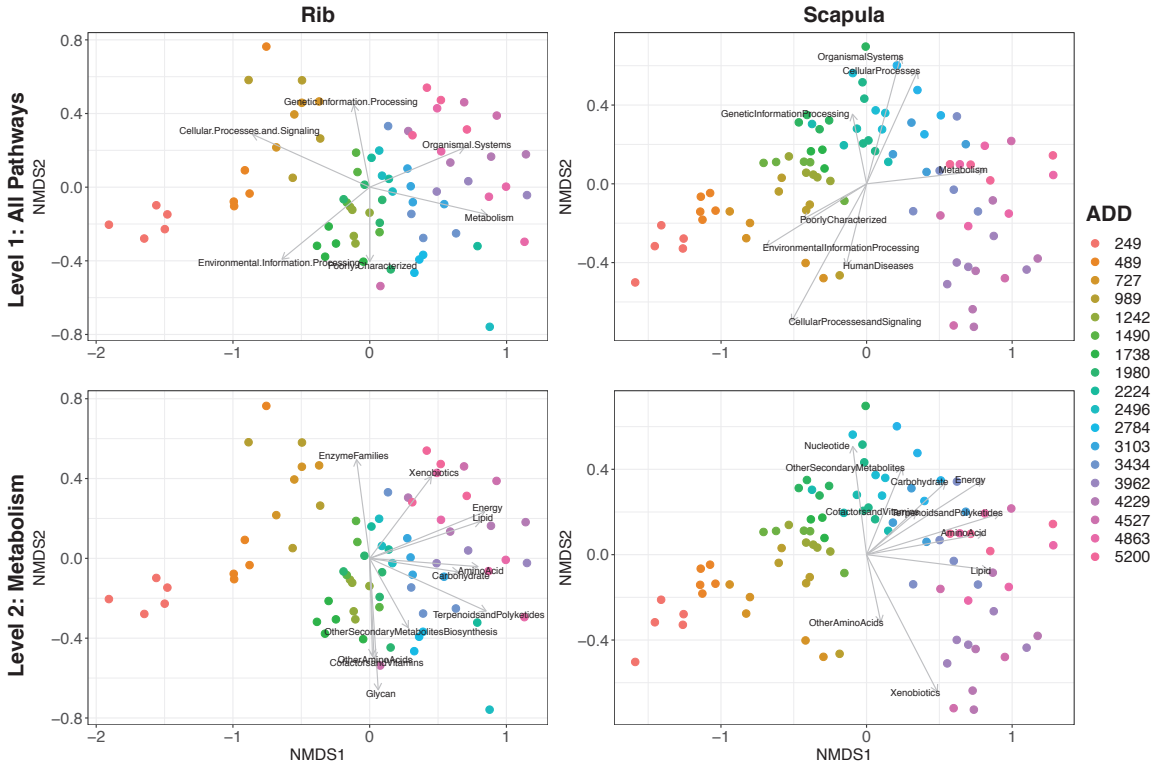

Fig. 2.S16. Microbial community PICRUSt predicted functional KEGG Level 1 Pathways and their relationship with beta-diversity bacterial community structure across ADD. Level 1 pathways (top panels) and level 2 metabolism pathways classified at level 3 (bottom panels) that were significantly related to OTU Bray-Curtis beta-diversity non-metric multidimensional scaling (NMDS) ordination (alpha 0.05) are represented by vectors. Lengths and angles of the arrows indicate the strength and direction of the relationship between environmental variables and beta-diversity.

Table 2.S5. Summary of the relationship between environmental variables and OTU (0.05) Bray-Curtis beta diversity NMDS ordination.

Environmental Parameters	**Rib**		**Scapula**	
	r^2	p-value	r^2	p-value
ADD	0.7657	0.001	0.9081	0.001
Season	0.0235	0.54	0.0972	0.056
Temperature	0.1049	0.056	0.7029	0.001
Specific Conductivity	0.0612	0.202	0.2979	0.002
Salinity	0.0619	0.196	0.3005	0.002
Oxidation Reduction Potential	0.0931	0.081	0.5148	0.001
pH	0.07	0.136	0.1144	0.03

Table 2.S6. Summary of the relationship between environmental variables and OTU (0.05) Jaccard beta diversity NMDS ordination.

Environmental Parameters	Rib		Scapula	
	r^2	p-value	r^2	p-value
ADD	0.7656	0.001	0.9079	0.001
Season	0.0238	0.569	0.0962	0.054
Temperature	0.1062	0.058	0.6993	0.001
Specific Conductivity	0.0616	0.187	0.2971	0.001
Salinity	0.0623	0.186	0.2997	0.001
Oxidation Reduction Potential	0.0935	0.08	0.5139	0.001
pH	0.0694	0.14	0.7766	0.001

Table 2.S7. Summary of the relationship between KEGG level 1 pathway and OTU (0.05) Bray-Curtis β- diversity NMDS ordination.

KEGG Level 1	Rib		Scapula	
	r^2	p-value	r^2	p-value
Cellular Processes	0.0077	0.76	0.4472	0.001
Cellular Processes and Signaling	0.8178	0.001	0.7524	0.001
Environmental Information Processing	0.5647	0.001	0.5814	0.001
Genetic Information Processing	0.2131	0.001	0.1346	0.002
Human Disease	0.0711	0.069	0.1915	0.001
Metabolism	0.7511	0.001	0.6655	0.001
Organismal Systems	0.5218	0.001	0.4724	0.001
Poorly Characterized	0.1627	0.001	0.2224	0.001

Table 2.S8. Summary of the relationship between KEGG level 2 pathways and OTU (0.05) Bray-Curtis β- diversity NMDS ordination.

KEGG Level 2	**Rib**		**Scapula**	
	r^2	p-value	r^2	p-value
Metabolism of Terpenoids and Polyketides	0.7952	0.001	0.8791	0.001
Energy Metabolism	0.7639	0.001	0.7585	0.001
Nucleotide Metabolism	0.0496	0.159	0.2663	0.001
Lipid Metabolism	0.6894	0.001	0.7035	0.001
Xenobiotics Biodegradation and Metabolism	0.3711	0.001	0.6473	0.001
Carbohydrate Metabolism	0.4255	0.001	0.4097	0.001
Amino Acid Metabolism	0.6295	0.001	0.657	0.001
Other Amino Acids	0.2372	0.001	0.1091	0.01
Biosynthesis of Other Secondary Metabolites	0.2001	0.001	0.2248	0.001
Metabolism of Cofactors and Vitamins	0.2538	0.001	0.1572	0.004
Enzyme Families	0.2538	0.001	0.0408	0.184
Glycan Biosynthesis and Metabolism	0.4381	0.001	0.0025	0.889

Supplemental References

1. P. Schloss, *et al*., Introducing mothur: Open-source, platform-independent, community-supported software for describing and comparing microbial communities. *Applied and Environmental Microbiology* **75**, 7537-7541 (2009).
2. R Core Team, R: A Language and Environment for Statistical Computing (2019).
3. J. Oksanen, *et al*., vegan: Community Ecology Package (2019).

Chapter 3: Postmortem Submersion Interval (PMSI) Estimation from the Microbiome of *Sus scrofa* Bone in a Freshwater River

Abstract

Due to inherent differences between terrestrial and aquatic systems, methods for estimating the postmortem interval (PMI) are not directly applicable to remains recovered from water. Recent studies have explored the use of microbial succession for estimating the postmortem submersion interval (PMSI); however, a non-disturbed, highly replicated and long-term aquatic decomposition study in a freshwater river has not been performed. In this study, porcine skeletal remains (N=200) were submerged in a freshwater river from November 2017-2018 (6322 accumulated degree days (ADD)/353 days) to identify changes and successional patterns in bacterial communities. One cage (e.g., 5 ribs and 5 scapulae) was collected approximately every 250 ADD for twenty-four collections; baseline samples never exposed to water acted as controls. Variable region 4 (V4) of 16S rDNA, was amplified and sequenced via the Illumina MiSeq FGx sequencing platform. Resulting sequences were analyzed using mothur (v1.39.5) and R (v3.6.0). The abundances of bacterial communities differed significantly between sample types. These differences in relative abundance were attributed to Clostridia, Holophagae and Gammaproteobacteria. Phylogenetic diversity increased with ADD for each bone type; comparably, β-diversity bacterial community structure ordinated chronologically, which was explained with environmental parameters and inferred functional pathways. Models fit using rib samples provided a tighter prediction interval than scapulae, with a prediction of PMSI with root mean square error of within 472.31 (~27 days) and 498.47 (~29 days), respectively.

Significance Statement

Post-mortem submersion interval (PMSI) estimation methods remain unvalidated, limited and mainly applicable for accidental water deaths. This study provides proof of concept that skeletal element microbial succession can be utilized to estimate long-term PMSI. As a result, this method could be developed and validated to aid investigations by providing law enforcement with a time

interval when the individual likely entered the water (i.e., victim identification), and excluding possible suspects in cases ruled a homicide.

Introduction

Terrestrial decomposition has been studied extensively and methods for estimating time since death, also known as the postmortem interval (PMI), have been established. These methods, which include, but are not limited to, insect succession (1) and total body scoring (TBS) (2,3) are not directly applicable to aquatic systems, due to inherent differences with terrestrial systems (i.e., lack of necrophagous insects). Total body scoring has been adapted for aquatic systems (4,5); however, it has been suggested that this method, while promising, should be used with caution, as it lacks validation studies (6,7). Because several factors have been reported to impact the rate of decomposition (i.e., flora, fauna, microorganisms, water flow, and environmental parameters), other estimation methods have been proposed, such as disarticulation patterns (6,7, 8 - 10), presence of aquatic invertebrates (11), community composition of algal or diatom communities (12,13), and more recently bacterial community structure and succession (14-17).

Specifically, microorganisms both endogenous to remains and the surrounding environment contribute to decomposition, and their patterns of succession over time have been recognized as a potential approach to estimating time since death (i.e., PMI and PMSI) (14-19). While previous aquatic decomposition studies have cited bacterial, fungal and algal activity during various stages of carrion decomposition, there are limited studies exploring microbial succession that utilize recent technologies (i.e., next-generation sequencing and bioinformatic pipelines) and/or model organisms that are comparable to humans (20- 34). Among the first to explore marine bacterial colonization on partial porcine remains, Dickson et al. (18) identified Proteobacteria, Bacteroidetes, Firmicutes, Fusobacteria and Actinobacteria as the dominating phyla. Furthermore, the bacterial communities occurred in a successional manner and differed by season (i.e., autumn and winter). Proteobacteria and Firmicutes were also reported as the dominating phyla in a freshwater stream for both summer and winter (19). In addition to an observed increased in genera, bacterial communities differed significantly between both seasons and days. A third study sought to compare geographic locations by utilizing freshwater streams in Ohio and Pennsylvania. Although succession was observed in both locations, location significantly influenced bacterial community structure (35).

This resource was prepared by the author(s) using Federal funds provided by the U.S. Department of Justice. Opinions or points of view expressed are those of the author(s) and do not necessarily reflect the official position or policies of the U.S. Department of Justice.

The aforementioned studies provided proof that microbial colonization occurs in a successional manner on fresh remains; however, they fail to extend to long-term PMSI estimation, specifically, extended skeletonization, nor have microbial succession studies been repeated in different aquatic environments in the same state. Therefore, this study sought to address these shortcomings by focusing on microbial colonization using well-replicated porcine skeletal elements over an extended period (6322 ADD, 353 days, 12 months) in a Virginia freshwater river. The overall aims were to use scapulae and ribs (as they have been reported to remain articulated for the longest period of time (8), in order to establish whether bacterial succession occurs predictably on bone, to identify taxa indicative to submersion time, and to develop a PMSI prediction method via random forest modeling.

Results

The following subheadings outline results concerning environmental measurements, bacterial community structure and function, and random forest modeling estimations.

Environmental Parameters

Most environmental parameters varied with season (Figure 3.S1 and Table 3.S1); however, salinity ($p= 0.0003$, rho= -0.6767) and dissolved oxygen concentration ($p=0.00003$, rho= -0.6767) were the only measurements that demonstrated a significantly negative correlation with accumulated degree days (ADD). Time (days) since placement demonstrated a significant positive curvilinear relationship ($y=207-7.09x+0.117x^2-0.00013x^3$, $R^2=1$, adj. $R^2=0.1$, $p<0.0001$) with ADD (Figure 3.1, Table 3.1).

Sequence Characteristics

From 273 samples (i.e., control filter and swab, mock communities, mud, water, scapulae and ribs), 11,262,227 total sequence reads were generated (on average 41,254 reads/sample). After quality control steps were processed (i.e., screening, aligning, filtering, chimera check, etc.), 7,930,514 (~70%) sequence reads remained (on average 29,049 reads/sample). Subsampling to 6,371 sequences occurred before taxonomic classification and clustering analysis (Figure 3.S2). Aforementioned methods resulted in the removal of eighteen mud samples, six rib samples, nine

scapula samples, 15 water samples, the control swab and all five PCR negative control samples (Figure 3.S3).

Bacterial Community Structure

To quantify run-to-run errors and evaluate pre-processing steps on subsequent sample bacterial communities, a ZymoBIOMICS mock community DNA standard D6306 sample was incorporated into each sequencing run. Evaluation of these communities at the genus level suggested that the resulting bacterial communities corresponded with the manufacturer's proposed profile (Figure 3.S4).

Along with experimental samples, a water filter, which served as a control, was processed. Results showed that the filter and water samples only shared two bacterial families (e.g Chitinophagaceae and Comamonadaceae) (Figure 3.S5). Significant differences in bacterial community structure for both weighted (PERMANOVA, *pseudo*-F= 16.21, R^2=0.19, p=0.0010) and unweighted (PERMANOVA, *pseudo*-F=6.96, R^2=0.09, p = 0.0010) were identified among rib, scapula, water and mud samples. Because mud samples were significantly different from bone types and represented by a small sample set, they were excluded from further analyses.

Subsampled sequences for 208 bone and water samples totaled to 1,331,539, which were classified using the Grenegenes reference database into 69 phyla, 208 classes, 406 orders, 626 families, 1,109 genera and 1,322. Firmicutes, Proteobacteria, Acidobacteria, Bacteroidetes and Spirochaetes in decreasing ordre were the most dominant phyla for both rib and scapula samples. While Proteobaceria (24%) and Bacteroidetes (12%) were also found in water samples, Cyanobacteria (22%), Verrucomicrobia (15%), Actinobacteria (14%) and Planctomycetes (6%) were present in higher abundances, totaling 92% (Figure 3.S6). Based on the increase of unclassified sequences from class (7-8%) and family (16-21%) to genus levels (39-43%) (Table 3.S2), subsequent results focus on taxa from the class and family levels.

When considering all taxa 90 class-level and 214 family-level taxa were shared among rib, scapula and water. However, when the top fifteen families were considered, only one taxon was shared among sample types; rib and scapula , however, shared 12 taxa (Figure 3.2; Table 3.2; Figure 3.S7). Bacterial community structure and composition differed between baseline and submerged samples (Figure 3.3). Additionally, significant differences between bone types were

driven by Gammaproteobacteria (e.g., Enterobacteriaceae), Clostridia (e.g., Clostridiaceae, Ruminococcaceae) and Holophagae, as well as Others, which consisted of bacteria unclassified and present in low abundances, at the family level. Clostridia was recovered from both bone types and persisted in high abundances, with a gradual decrease over time that was more pronounced in scapula samples. Additionally, as submersion time increased, Gammaproteobacteria decreased, while Holophagae and Spirochaetes became more prevalent (Figure 3.3).

Bacterial Diversity

A curvilinear relationship between phylogenetic diversity (PD) and ADD was observed for both rib ($y=1.3+0.0162x-1.25x^2$, $R^2=0.78$) and ($y=-19+0.135-8.93(10^{-5})x^2+2.69(10^{-8})x^3-3.66(10^{-12})x^4+1.84(10^{-16})x^5$, $R^2=072$) scapula samples (Figure 3.4). The largest PD estimates for both bone types were observed around 6322 ADD; however, the PD in scapulae was slightly higher. While PD increased with ADD, variability also increased within ADD groupings and some seasonal variations were observed (Figure 3.S8). Variability was attributed to ADD (linear model ANOVA, Rib: $p<0.0001$, Scapula: $p<0.0001$) and temperature (linear model ANOVA, Rib: $p<0.0001$, Scapula: $p<0.0001$) in both bone types, while specific conductivity (linear model ANOVA, $p=0.0020$) and chlorophyll-a (linear model ANOVA, $p=0.0397$) contributed to scapula and rib diversity variability, respectively.

For both weighted (PERMANOVA, Rib: *pseudo*-$F=36.04$, $R^2=0.31$, $p=0.001$, Scapula: *pseudo*-$F=50.58$, $R^2=0.32$, $p=0.001$) and unweighted (PERMANOVA, Rib: *pseudo*-$F=13.98$, $R^2=0.15$, $p=0.0010$; Scapula: *pseudo*-$F=13.18$, $R^2=0.11$, $p=0.0010$) metrics, β-diversity differed significantly among ADD groupings (Figure 3.5 and Figure 3.S9). Chronological ordination was observed along NMDS1, with earlier ADD groupings (i.e., 268, 516 and 741 ADD) having greater separation. To explain the ordination, environmental variables were fitted, as vectors, to both the weighted and unweighted UniFrac ordinations (Figure 3.5, Figure 3.S9, Table 3.3 and Table 3.S3). Significant relationships with weighted UniFrac metrics and environmental parameters (e.g., dissolved oxygen concentration, salinity, specific conductivity, pH, chlorophyll-a, temperature, turbidity and ADD) were identified with ADD (Rib: $r^2=0.78$, $p=0.0010$; Scapula: $r^2=0.81$, $p=0.0010$) and temperature (Rib: $r^2=0.70$, $p=0.0010$; Scapula: $r^2=0.53$, $p=0.0010$) were significantly and most strongly associated with samples from later time periods for both bone types (Table 3.3). Weighted and unweighted UniFrac Unweighted Pair Group Method with

Arithmetic Mean (UPGMA) trees were highly congruent for both bone types (cophenetic correlation "spearman", Rib = 0.80, Scapula = 0.66) (Figure 3.S10).

Bacterial Function

KEGG pathway profiles to assess microbial functional changes across ADD were inferred using PICRUSt (36). To further explain the weighted UniFrac groupings for both bone types, level 1 pathways and level 2 metabolic pathways were fit to the ordination (Figure 3.6). For rib and scapula samples, all level 1 pathways were significantly associated with the ordination. Of the level 1 pathways, metabolism (Rib: r^2=0.93, p=0.0010; Scapula: r^2=0.87, p=0.0010) was the most strongly correlated with samples from late periods (Table 3.4). With the exception of scapula enzyme families, all metabolic pathways for both bone types were significantly associated with the weighted UniFrac ordination (Figure 3.6; Table 3.5).

Random Forest Model for PMSI Prediction

Random forest models were fitted for ribs (41 taxa) and for scapulae (55 taxa) separately, using family-level taxa. There is a sharp delineation between Rhodospirillaceae and the other taxa, indicating its influence in the model based on rib samples; differences between scapulae model influential taxa are less noticeable (Figure 3.8). Taxa can be influential in PMSI estimation and not be present in large quantities, as observed in Figure 3.8. The random forest model for rib samples had a root mean square error (RMSE) of 472.3 ADD (~ 28 days). The R-squared value for the predicted ADD versus actual ADD indicates that 94% of the variability in predicted ADD can be explained through the linear relationship between actual and predicted ADD (Figure 3.8). (This is the square of the linear correlation coefficient between actual and predicted ADD.) The scapulae model was less precise, explaining ~93% of the variation in ADD, with a RMSE of 498.5 ADD (~ 29 days). For scapulae, a tighter fit around the one-to-one line was observed, with 94% of the variability in predicted ADD explained through the linear relationship between actual and predicted ADD (Figure 3.9).

Discussion

To identify if bacterial succession could be used to estimate PMSI, this study utilized 16S rDNA MiSeq sequencing and bioinformatic analysis methods. Relative abundances were used to

identify indicator taxa that aided in developing random forest statistical prediction models. Taxa contributing to differences in relative abundances among sample types (i.e., rib-scapula-water) were identified using similarity percentages. Significant differences among sample types (i.e., rib-scapula-water-mud) were also observed in bacterial community diversity metrics. Furthermore, patterns observed in diversity estimates for bone types were explained with environmental measurements and functional pathways that were inferred using PICRUSt. Because sample types were found to be significantly different, it is suggested that the surrounding environment (e.g., water) may impact bone decomposition less than the microbial communities present at the time of submersion. Because a large number of water and mud samples were removed, as a result of sequence analysis quality control steps, future studies should explore new methods of collection and processing to ensure successful sequencing.

Of the top 92% of phyla recovered from water samples Cyanobacteria, Verrucomicrobia, Actinobacteria and Planctomycetes were present in higher abundances when compared to rib and scapula samples. Briefly, Cyanobacteria, a diverse group of photosynthetic prokaryotes that synthesize cholorphyll-a, have been reported in most habitats, such as marine, freshwater, soil, snow, etc. (37, 38). Despite having diverse metabolic abilities and being detected in various aquatic environments, including freshwater rivers, little is known about Verrucomicrobia and their ecology in freshwater systems (39, 40). Commonly recovered in still and flowing freshwater environments, Actinobacteria participate in synthesize DNA and proteins (41, 42). Planctomyetes, which differ phenotypically from most bacteria (i.e., lack peptidoglycan in their cell walls and have intracellular compartmentalization), are fairly ubiquitous, as they have been recovered from fresh water, oceans and soil/sediments. Additionally, anammox, or anaerobic ammonium oxidation planctomycetes found in freshwater, are major contributors to the global nitrogen cycle (43).

For all skeletal elements Firmicutes, Proteobacteria, Acidobacteria, Bacteriodetes and Spirochaetes were the most abundant phyla (93% rib, 87% scapulae). These phyla parallel those reported in previous studies (11-19, 44, 45). In both marine (18) and freshwater stream (19) environments, Proteobacteria and Firmicutes were reported as the dominant phyla exhibiting an inverse relationship with days since placement (i.e., Proteobacteria decreased while Firmicutes increased). Similar patterns were also observed in terrestrial decomposition of porcine remains. Furthermore, Receveur et al. (46) reported Proteobacteria and Firmicutes as indicator taxa via machine learning for decomposition stage of porcine remains in a freshwater stream. In this study, Proteobacteria decreased directly after submersion, but subsequently persisted at higher

abundances in scapulae. Changes in Proteobacteria over time and differences between bone types may be related to the dark staining observed, that was more prevalent on scapulae. Black coloration on waterlogged bones has been credited to ferrous sulphide (FeS), which is formed by sulphate reducing bacteria in anaerobic environments. Gram-positive (e.g., Firmicutes, Clostridia) and gram-negative (e.g., Proteobacteria, Deltaproteobacteria, Desulfobulbaceae) are sulphate-reducing bacteria, which were recovered in this study (47, 48). Proteobacteria, which is associated with the spoilage of meat, has also been linked to adipocere formation, specifically during the process of lipolysis (19). Therefore, the presence and changes of Proteobacteria may be related to the change in black staining, flesh and adipocere. Firmicutes, a phyla comprised of families such as Clostridia (i.e., Clostridiaceae), that have been related to adipocere formation (49, 50), have been reported in soil and aquatic environments (51). Over time, abundances of Firmicutes were higher in rib samples, when compared to scapulae; however, in both sample types abundances generally decreased with increasing ADD, a finding which differs from the aforementioned studies. The higher amounts of Firmicutes observed in ribs at early time points may be due to the presence of adipocere, which decreased as scavenger (i.e., blue crab) activity increased, and black staining.

Present in lower overall abundances, Acidobacteria, Spirochaetes and Bacteroidetes increased after submersion, appearing as soon as 1278, 1278 and 516 ADD, respectively. Acidobacteria's position in the community may have been influenced by Proteobacteria; furthermore, Acidobacteria is largely driven by nutrient availability and pH (52). Spirochaetes, which are associated with eukaryotic hosts, have been identified from sediment, mud and freshwater environments (53). Meanwhile, Bacteroidetes may have contributed to the decomposition process, since they are essential to the degradation of complex biopolymers (i.e., natural fats, amino acids and sugars) (42). Spirochaetes were also recovered in low abundances from a freshwater stream, along with Acidobacteria, which were only present during winter trials (19). Meanwhile, Bacteroidetes were identified in both marine and freshwater stream environments (18, 19).

Bacterial community structure differences between bone types were attributed to Firmicutes (e.g., Clostridia), Acidobacteria (e.g., Holophagae) and Proteobacteria (e.g., Gammaproteobacteria). Overall, differences between bone types were more notable at the family-level. For example, Clostridia was the most abundant class-level taxa in both bone types, but at the family level Clostridiaceae and Ruminococcaceae (e.g., Firmicutes/Clostridia) dominated rib taxa, while

Holophagaceae (e.g., Acidobacteria/Holophagae) dominated scapulae. The adipocere formation observed in early rib collections, corresponds to higher amounts of Clostridia (e.g., Clostridiaceae), which persisted across ADD. Increased adipocere formation in warm anaerobic environments is thought to be related to the presence of Clostridium (e.g., Firmicutes, Clostridia, Clostridiaceae) and the production of lecithinase (49, 50). Proposed as a key contributor to decomposition, the family Clostridiaceae and/or genus Clostridium (e.g., Firmicutes, Clostridia) has also been reported in terrestrial human (16), mouse (15) and porcine decomposition (17, 55). Furthermore, Clostridia, have been recovered from both terrestrial and marine soil, freshwater and feces samples. At the family-level, Enterobacteriaceae were recovered in higher abundances in rib samples, but were observed immediately after submersion and decreased drastically after 1278 ADD in both bone types. Members of the Enterobacteriaceae family are gram-negative facultative anaerobes found in throughout the environment. Characteristics of this family include nitrate reduction and glucose fermentation; additionally, they are pathogenic and have food spoilage characteristics (56, 57). Holophagae, which were found in higher abundances in scapula samples and increased over time, are gram-negative bacteria that are strict anaerobes (53). Overall, differences between bone types may be attributed to the amount of soft tissue present on the partially fleshed skeletal remains when they entered the water.

Phylogenetic diversity (PD) was highest at increased ADD (e.g., after ca. 5000 ADD) for both rib and scapula samples, while overall PD was higher in scapulae. Increasing diversity was also observed in a freshwater stream (19), where taxon richness increased over the first 21 days in the summer (e.g., 21 to 82 genera) and over 42 days in the winter (e.g., 38 to 109 genera). These trends differ from terrestrial decomposition where soft tissue was sampled. In these studies, an inverse relationship was observed between time and alpha diversity during initial stages of decomposition (17, 48). In Virginia, diversity was observed to initially decrease through purge before increasing through advanced decay (48). Variability of PD within ADD grouping was noted at earlier time periods for scapulae than for ribs and attributed to seasonal changes, temperature and ADD in both bone types. Furthermore, specific conductivity also contributed to variability in scapula samples. These environmental factors may have influenced bacterial community structure through time. For example, Proteobacteria consist of classes that have seasonal preferences (58).

For all samples, bacterial community beta diversity ordinated chronologically and differed significantly among collections or time points. ADD significantly influenced samples from

increased ADD in the ordination, suggesting community structure was dependent on cumulative time and temperature. Turbidity, a measure of suspended solids, and temperature were also correlated with samples from later collections for both bone types. Meanwhile, dissolved oxygen concentration, salinity and specific conductivity influenced samples from early collections (268 – 741 ADD). Only pH and chlorophyll a were associated with samples from middle collections (~ 1278 – 2656 ADD). These relationships support the idea that PMSI estimates may be influenced by environmental factors, as proposed by Benbow et al. (19). Beta diversity differences were also explained with PICRUSt inferred functional changes. Bacteria performing metabolic functions were identified as driving the weighted UniFrac ordination, as Metabolism at the level 1 KEGG pathway exhibited the strongest association with samples from later periods. Within the metabolism pathway (e.g., level 2), metabolism of terpenoids and polyketides along with lipid metabolism were most highly correlated to groupings of increased ADD. Therefore, this study proposes that bacterial functions may be as important as environmental parameters when considering factors that might impact PMSI prediction.

Constructed Unweighted Pair Group Method with Arithmetic Mean (UPGMA) trees were also utilized to observe the relationship among ADD groupings. Because weighted UniFrac metrics are based on the abundance of taxa present or absent, while unweighted UniFrac rely solely on taxa present or absent, there were incongruences between trees for both bone types. For both ribs and scapulae, clades grouped roughly according to time of submersion, as bacterial community structure may have been influenced by changing taxa abundance and presence due to accumulated temperature. Relying only on taxa presence or absence, which may be less predictable over time, could have prohibited easy grouping of unweighted UniFrac tree branches.

Rib samples provided the best model predictions, allowing PMSI estimation within 472.31 ADD (~27 days); meanwhile, scapulae estimated PMSI within 498.47 ADD (~29 days). Rhodospirillaceae, Sediment_4, Pirellulaceae, Streptomycetaceae and Xanthobacteraceae were identified as the most influential families of the 41 taxa used for rib samples. Of the 55 taxa used for scapulae, Sediment_4, Dethiosulfobovibrionaceae, Syntrophaceae, Rhodospirillaceae and Rikenellaceae were the most influential families. Between the two sample types, Rhodospirillaceae, Sediment_4, Ruminococcaceae and Syntrophobacteraceae were shared in the top 10 most influential taxa. Briefly, Rhodospirillaceae are purple non-sulfur bacteria that are often recovered from aquatic environments (59). Sediment-4 is a bacterial lineage that has recently been identified, as a result of metagenomic analyses, and possibly belongs to an

undescribed phyla (NCBI). Of the class Clostridia, Ruminococcaceae are short chain fatty acid (SCFA) producers that participate in the degradation of polysaccharides and fibers (60). Members of the family Syntrophobacteraceae are mesophilic or thermophilic sulfate-reducing bacteria, which are found in freshwater or marine habitats (61). These bacteria may have contributed to the black coloration (e.g., ferrous sulphide) observed on both bone types. The aforementioned indicator taxa have not been described in previous aquatic or terrestrial decomposition studies as potential indicators of time since death. Furthermore, the lack of similarity between these results and terrestrial studies is significant, and may well be due to the lack of insects, which have been shown to contribute bacterial signatures (34, 62).

Conclusion

This study successfully developed a model for estimating PMSI within ~27-29 days (472.31 - 498.47 ADD) over a duration of one year's submersion (6322 ADD), using two types of skeletal elements. Bacterial community structure and successional patterns were explained using both environmental factors and PICRUSt inferred functional pathways. Overall, bone microbial communities can be used to estimate long-term PMSI in riverine system. Future studies should take into consideration submerging fresh remains, comparing ecosystems and geographic locations, adding other markers (e.g., ITS, 18S rDNA etc.), standardizing methods for reporting taxa (e.g., family level versus genus level) and validating methods for use in human cases.

Materials and Methods

The Virginia Commonwealth University (VCU) Rice Rivers Center, which is located on the tidal freshwater portion of the James River in Charles City, Virginia (37.3260° N, 77.2056° W), was the field site utilized from November 2017 – 2018. Twenty-four 10'' x 10'' cages, containing five scapulae and five ribs, were attached to the dock and placed on the river bottom (~4 meters). HOBOware (Onset, Bourne, Massachusetts) waterproof dataloggers were submerged with the cages to monitor temperature. Additionally, a multiparameter sonde (YSI, Yellow Springs, OH), which is permanently located at the center, was used to monitor water quality parameters, such as dissolved oxygen concentration, pH, specific conductivity, salinity, temperature, chlorophyll-a and turbidity.

Sample Collection

A baseline sample of five ribs and five scapulae was never exposed to water. Twenty-four submerged cages (i.e., five ribs and five scapulae) were collected every ~250 accumulated degree days (ADD), which was calculated using 0 °C as threshold. In addition, water samples were collected from ~4 m deep using a Kemmerer bottle (WildCo, Yulle, FL) and mud was sampled by swabbing portions of the cages that were not in contact with the bones. After collection, all samples were placed on ice and brought to Virginia Commonwealth University, Richmond, VA (37.5485° N, 77.4480° W) for storage at -80 °C and 4 °C for bone and water samples, respectively, until further processing.

Within six months of collection (63), bone samples were processed, which included thawing at room temperature and photography before removal of non-bone tissue (i.e., adiopocere). Using a Craftsman Cordless Multi-Tool (Craftsman, Chicago, IL), scapular spines and rib mid-sections were cut and placed in a mortar filled with liquid nitrogen and ground into powder using a pestle. A filtration system accompanied with 0.22 µm filters was used to filter water samples (250 mL) within a week of collection. Resulting bone powder and water filters were stored at -20 °C and -80 °C, respectively,

DNA Extraction and Quantification

The resulting bone powder (0.1 g), one 0.22 µm filter and mud swabs were used for DNA extraction via ChargeSwitch® gDNA Plant Kit (Life Technologies – ThermoFisher Scientific, Waltham, MA) and the Invitrogen CST Protocol for Extracting gDNA from Bone Samples (64), with the exception that all samples were eluted in 100 µL of elution buffer. Quantification was performed using the Qubit 2.0 Fluorometer (ThermoFisher Scientific) using the dsDNA HS Assay kit and associated protocol (65). Extracted samples were stored at -20 °C.

16S rDNA Amplification and MiSeq® Sequencing-by-Synthesis

The Kozich et al. (66) dual-index technique was used to amplify variable region four (V4) of the 16S rRNA gene on the Veriti™ 96-Well Thermal Cycler (Applied Biosystems, USA) for control filters/swabs (i.e., filters/swabs processed with samples but never exposed to water/mud),

polymerase chain reaction (PCR) negative controls (i.e., non-template controls), ZymoBIOMICS™ mock community standard, bone powder, mud swabs and filtered water samples. Reactions were performed in 20 µL, which included the following: template DNA (0 – 10 ng; 6.2 µL maximum), 10 µL Promega PCR master mix (2X), 0.8 µL 25mM $MgCl_2$,and 3 µL of forward/reverse primers (10 µM each) (V4_515F 5'-AATGATACGGCGACCACCGAGATCTACACXXXXXXXXTATGGTAATTGTGTGYCAGCMGCCGCGGTAA-3' and 806R:5'-CAAGCAGAAGACGGCATACGAGATXXXXXXXXAGTCAGTCAGCCGGACTACNVGGGTWTCTAAT-3'). Each primer was designed to contain an Illumina adapter sequence, barcode sequence (XXXXXXXX), and linker sequences (2 nucleotides). The DNeasy PowerClean Pro Cleanup Kit (Qiagen, MD, USA) was used to purify (i.e., remove PCR inhibitors) DNA extracts that initially failed amplification before re-amplifying.

Agarose gel electrophoresis (1.8%) was used to verify amplicon size and PCR success by using 2 µL of 6X loading dye (New England Biolabs, MA, USA), 7 µL of 1XTAE buffer and 3 µL of the PCR product. Agencourt® AMPure® PCR Purification kit (Beckman Coulter, Brea, CA), according to the manufacturer's protocol was used to purify 10 µL of the remaining 17 µL PCR product (67). Following purification, the Qubit® 2.0 Fluorometer was used to quantify samples before 1 ng of each sample was pooled. The 1.5 mL microcentrifuge tube, containing the pooled samples, was dried down using a Savant DNA120 Speed Vac Concentrator (Fisher Scientific, Waltham, MA) to 1 ng/µL. Using the Illumina MiSeq® v2 Reagent Kit and Illumina MiSeq® FGx system (Illumina, San Diego, CA), samples underwent 2x250 paired-end sequencing-by-synthesis.

Sequence Analysis

The MiSeq SOP and mothur v 1.39.5 was used to process the raw data obtained from the sequencing run (68). Resulting forward and reverse reads were used to assemble contigs via the *make.contig* command (*trimoverlap*=true and *insert*=20). Quality control steps included removing ambiguous bases (*maxambig*=0), reads greater than 275 bp and shorter than 200 bp and duplicate sequence (i.e., identifying unique sequences) before alignment to the the SILVA bacterial reference occurred (69). If sequences did not properly align or failed to start at 13862 and end at 23444, they were removed. Pre-clustering occurred with *diffs*=2, while chimeric sequences were identified and subsequently removed using the mothur v 1.39.5 implemented UCHIME v 4.2 (70). As a result of pre-processing, ~70% (11,262,227 decreased to 7,930,514) of

the raw sequences were clustered by taxonomy, phylogeny and operation taxonomic unit (OTU) analyses.

The Naive Bayesian rRNA classifier v 2.2 with the Greengenes 13_8_99 reference taxonomy was used to perform hierarchical or taxonomic classification with bootstrap support of 80% or greater (71,72). Only sequences that were classified as bacteria were kept for further analysis (i.e., removal of unknown, mitochondria, chloroplast, archaea and eukaryote). Normalization, through random subsampling to 6,371 sequence reads per sample, minimized bias of unequal sequence reads across samples and resulted in a loss of 48 samples (~18%), the control swab and all five PCR negative control samples. Remaining samples were reclassified as previously outlined. Operational Taxonomic Unit (OTU) based clustering occurred at a dissimilarity of 5% or at the hypothetical genus level using average neighbor method (Additional Analyses Figure S10 – S13 and Table S4 – S7). The main paper focuses on phylogenetic clustering to assess α- and β-diversity. Specifically, mothur v1.39.5 (68) was utilized to evaluate α-diversity and construct neighbor-joining trees (*clearcut*); meanwhile R v3.6.0 (73) was used to estimate both weighted and unweighted UniFrac distances for β-diversity metrics.

Statistical Analyses

Site/environmental parameters, hierarchical classification and phylogenetic clustering methods were statistically analyzed using packages, which are detailed below, in R v3.6.0 (73).

Using spearman's rank-order correlation (*cor.test*, stats package v3.6.0) the association between accumulated degree days (ADD) and environmental measurements (i.e., temperature, salinity, specific conductivity, pH, dissolved oxygen concentration, turbidity and chlorophyll-a) were tested (73). Meanwhile, linear regression (*lm*; stats package version 3.6.0) was used to evaluate the relationship between ADD and time (days) since placement.

Taxonomic relative abundances at the class and family levels were visualized via stacked bar graphs using the ggplot2 package v3.2.1 (74) and differences in sample-type bacterial community composition were identified and tested using simper tests (vegan package v2.5.5) and *kruskal.test* (stats package v3.6.0), respectively (73, 75). Random forest modeling also utilized relative abundances to build a PMSI prediction method as outlined by Forger et al., using the

randomForest package (76, 77). Bacterial taxa that were present and absent in the relative abundance files were examined with the VennDiagram package v1.6.20 (78).

To assess phylogenetic α-diversity shifts and variations, linear modeling (*lm*) and the incorporation of field site parameters (i.e., temperature, pH, etc.) was examined using the stats package (73) and visualized with the ggplot2 package (74). Phyloseq objects (79) that were constructed from a meta data file, NJ phylogenetic tree, OTU taxonomy and OTU table were used to calculate both weighted and unweighted UniFrac β-diversity metrics via the *UniFrac* function (phyloseq package v1.28.0) (80). Furthermore, permutational multivariate analysis of variance (PERMANOVA) was used to identify differences among samples (i.e., rib, scapula, water and mud samples) and ADD in the vegan package (*adonis* function). Distances were also ordinated using non-metric multidimensional scaling (NMDS) (permutations=999). To explore resulting ordinations, site parameters were fit to both weighted and unweighted UniFrac ordinations using *envfit* (vegan package). The fitted vectors and their associated squared correlation coefficients (permutations-999) aided in assessing the significance of each parameter. Unweighted Pair Group Method with Arithmetic Mean (UPGMA) trees were constructed with *hclust* (stats package) to show the relationship between ADD for both weighted and unweighted UniFrac metrics and their correlations were tested with the *cor.cophenetic* function (method.coef="spearman," denextend package v1.12.10) (73, 81).

Funding

This study was funded by the following: B. Singh start-up grant from College of Humanities and Science of Virginia Commonwealth University (VCU), Richmond, VA; VCU Rice Rivers Center Grant and award 2018-R2-CX-0016 of the National Institute of Justice Graduate Research Fellowship.

References

1. J.D. Wells, L.R. Lamotte, “Estimating the Postmortem Interval” in *Forensic Entomology: The Utility of Arthropods in Legal Investigations*, J.H. Byrd, J.L. Castner, Eds. (CRC Press, 2001), pp. 263 – 284.
2. M.S. Megyesi, S.P. Nawrocki, N.H. Haskell, Using accumulated degree-days to estimate the postmortem interval from decomposed human remains, *Journal of Forensic Sciences* **50**, 618 - 626 (2005).
3. C. Moffatt, T. Simmons, J. Lynch-Aird, An Improved Equation for TBS and ADD: Establishing a Reliable Postmortem Interval Framework for Casework and Experimental Studies, *Journal of Forensic Sciences* **61**.
4. V. Heaton, A. Lagden, C. Moffatt, T. Simmons, Predicting the Postmortem Submersion Interval for Human Remains Recovered from U.K. Waterways. *Journal of Forensic Sciences* **55**, 302 – 307 (2010).
5. M.A. van Daalen, *et al.*, An Aquatic Decomposition Scoring Method to Potentially Predict the Postmortem Submersion Interval of Bodies Recovered from the North Sea. *Journal of Forensic Sciences* **62**, 369-373 (2017).
6. M.K. Humphreys, E. Panacek, G. William, E. Albers, Comparison of Protocols for Measuring and Calculating Postmortem Submersion Intervals for Human Analogs in Fresh Water. *Journal of Forensic Sciences* **58**, 513-517 (2013).
7. A. De Donno ,*et al*., Bodies in sequesterd and non-sequestered aquatic environments: A comparative techonomic study using decompositional scoring system. *Science and Justice* **54**, 439-446 (2014).
8. W. Haglund, Disappearnce of Soft Tissue and the Disarticulation of Human Remains from Aqueous Environments. *Journal of Forensic Sciences* **38**, 806-815 (1993).
9. M.S. Megysei, S.P. Nawrocki, N.H. Haskell, Using Accumulated Degree-Days to Estimate the Postmortem Interval from Decomposed Human Remains. *Journal of Forensic Sciences* **50**, 618-626 (2005).
10. V. Heaton, A. Lagden, C. Moffatt, T. Simmons, Predicting the Postmortem Submersion Interval for Human Remains Recovered from U.K. Waterways. *Journal of Forensic Sciences* **55**, 302-307 (2010).
11. G.S. Anderson, N.R. Hobischak, Decomposition of carrion in the marine environment in British Columbia, Canada. *International Journal of Legal Medicine* **118**, 206-209 (2002).
12. J.N. Haefner, J.R. Wallace, R.W. Merritt, Pig Decomposition in Lotic Aquatic Systems: The Potential Use of Algal Growth in Establishing a Postmortem Submersion Interval (PMSI). *Journal of Forensic Sciences* **49**, 330-336 (2004).
13. K.A. Zimmerman, J.R. Wallace, The Potential to Determine a Postmortem Submersion Interval Based on Algal/Diatom Diversity on Decomposing Mammalian Carcasses in Brackish Ponds in Delaware. *Journal of Forensic Sciences* **53**, 935-941 (2008).
14. A.A. Vass, Beyond the Grave – Understanding Human Decomposition. *Microbiology Today* **28**, 190-192 (2001).
15. J.L. Metcalf, *et al*., A microbial clock provides an accurate estimate of the postmortem interval in a mouse model system. *eLife* **2, (**2013).
16. E.R. Hyde, D.P. Haarmann, J.F. Petrosino, A.M. Lynne, S.R. Bucheli, Initial insights into bacterial succession during human decomposition. *International Journal of Legal Medicine* **129**, 661-671 (2015).
17. Pechal, *et al.*, The potential use of bacterial community succession in forensics as described by high throughput metagenomic sequencing. *International Journal of Legal Medicine* **128**, 193-205 (2014).

18. G.C. Dickson, R.T.M. Poulter, E.W. Maas, P.K. Probert, J.A. Kieser, Marine bacterial succession as a potential indicator of postmortem submersion interval. *Forensic Science International* **209**, (2011).
19. M.E. Benbow, J.L. Pechal, J.M. Lang, R. Erb, J.R. Wallace, The Potential of High-throughput Metagenomic Sequencing of Aquatic Bacterial Communities to Estimate the Postmortem Submersion Interval. *Journal of Forensic Sciences* **60**, 1500-1510 (2015).
20. J.B. Keiper, E.G. Chapman, B.A. Foote, Midge Larvae (Diptera: Chironomidae) as indicators of postmortem submersion interval of carcasses in a woodland stream: a preliminary report, *Journal of Forensic Science* **42**, 1074-1079 (1997).
21. N.R. Hobischak, G.S. Anderson, Time of Submergence Using Aquatic Invertebrate Succession and Decompositional Changes, *Journal of Forensic Sciences* **47**, 142-151 (2002).
22. J.E. Richey, M.A. Perkins, C.R. Goldman, Effects of kokanee salmon (*Oncorhynchus nerka*) decomposition on the ecology of a subalpine stream. *Journal of the Fisheries Research Board of Canada* **32**, 817–820 (1975).
23. O.A. Mathisen *et al.* Recycling of marine elements transported into freshwater systems by anadromous salmon. *Verhandlungen des International en Verein Limnologie* **23**, 2249–2258 (1988).
24. R.R. Parmenter, V.A. Lamarra, Nutrient cycling in a freshwater marsh: the decomposition of fish and waterfowl carrion. *Limnology and Oceanography*, **36**, 976 - 987 (1991).
25. D.C. Brickell, J.J. Goering, "Chemical effects of salmon decomposition on aquatic ecosystems" in *Proceedings Symposium on Water Pollution Control in Cold Climates*, R.S. Murphy, Eds. (U.S. Government Printing Office, Washington D.C.,1970).
26. A.G. Durbin, S.W. Nixon, C.A. Oviatt, Effects of the spawning migration of the alewife, *Alosa pseudoharengus* on freshwater ecosystems, *Ecology* **60**, 8-17 (1979).
27. A.K.F. Wold, A.E. Hershey, Effects of salmon carcass decomposition on biofilm growth and wood decomposition, *Canadian Journal of Fisheries and Aquatic Sciences* **56**, 767-773 (1999).
28. N.T. Johnston, E.A. MacIsaac, P.J. Tschaplinski, K.J. Hall, Effects of the abundance of spawning sockeye salmon (Oncorhynchus nerka) on nutrients and algal biomass in forested streams, *Canadian Journal of Fisheries and Aquatic Sciences* **403**, 384–403 (2004).
29. S.K. Goffredi, V.J. Orphan, Bacterial community shifts in taxa and diversity in response to localized organic loading in the deep sea. *Environmental Microbiology* **12**, 344-363 (2010).
30. C.R. Smith, H. Kukert, Vent fauna on whale remains, *Nature* **341**, 27 – 28 (1989).
31. C.R.Smith, A.G. Glover, T. Treude, N.D. Higgs, D.J. Amon, Whale-fall ecosystems: recent insights into ecology, paleoecology, and evolution, *Annual Review of Marine Science* **7**, 571-596 (2015).
32. S.K. Goffredi, R. Wilpiszeski, R. Lee, V.J. Orphan, Temporal evolution of methane cycling and phylogenetic diversity of archaea in sediments from a deep-sea whale-fall in Monterey Canyon, California. *The ISME Journal* **2,** 204-220 (2008).
33. T. Treude *et al*. Biogeochemistry of a deep-sea whale fall: sulfate reduction, sulfide efflux and methanogenesis, *Marine Ecology Progress Series* **382**, 1-21 (2009).
34. J.L. Pechal, M.E. Benbow 2016, Microbial ecology of the salmon necromicrobiome: evidence salmon carrion decomposition influences aquatic and terrestrial insect microbiomes. *Environmental Microbiology* **18**, 1511-1522 (2016).
35. J.M. Lang, *et al*., Microbial Biofilm Community Variation in Flowing Habitats: Potential Utility as Bioindicators of Postmortem Submersion Intervals. *Microorganisms* **4**, (2016).

36. M.G.I. Langille, *et al*., Predictive functional profiling of microbial communities using 16S rRNA marker gene sequences. *Nature Biotechnology* **31**, 814-821 (2015).
37. L. Gaysina, A. Saraf, P. Singh, "Cyanobacteria in Diverse Habiats" in *Cyanobacteria From Basic Science to Applications*, A.K. Mishra, D.N. Tiwari, A.N. Rai, Eds. (Elsevier, 2019).
38. B.A. Whitton, M. Potts, "Introduction to the Cyanobacteria" in *Ecology of Cyanobacteria II: Their Diversity in Space and Time*, B.A. Whitton, Eds. (Springer Science+Business, 2012).
39. E. Chiang, *et al*., Verrucomicrobia are prevelant in north-temperate freshwater lakes and display class-level preferences between lake habitats. *PLOSone* **13**, (2018).
40. He *et al*. Ecophysiology of Freshwater Verrucomicrobia Inferred from Metagenome-Assembled Genomes, *mSphere* **2** (2017).
41. Ghai *et al.* Metagenomics of the water column in the pristine upper course of the Amazon River, *PLoS One* **6**, e97393 (2011).
42. R.J. Newton, S.E. Jones, A. Eiler, K.D. McMahon, S. Bertilsson, A guide to the Natural History of Freshwater Lake Bacteria. *Microbiology and Molecular Biology Reviews* **75**, 14-49 (2011).
43. J. Fuerst, E. Sagulenko, Beyond the bacterium: Plactomycetes challenge our concepts of microbial structure and function, *Nature Reviews Microbiology* **9**, 403-413 (2011).
44. F.E. Damann, D.E. Williams, A.C. Layton, Potential Use of Bacterial Community Succession in Decarying Human Bone for Estimating Postmortem Interval. *Journal of Forensic Sciences* **60**, 844-850 (2015).
45. F.E. Damann, "Biomarkers of Human Decomposition Ecology and the Relationship to Postmortem Interval" (National Institute of Justice, 2012)
46. Receveur *et al*. Aquatic Decomposition of Vertebrate Remains: An Experimental Test for Cold Case Investigation (Proceedings of the American Academy of Forensic sciences, 2020).
47. G. Muyzer, A.J.M. Stams, the ecology and biotechnology of sulphate-reducing bacteria, *Nature Reviews Microbiology* **6**, 441-454 (2008).
48. M.S. Woolf, "Estimation of Long Term Post Mortem Interval (PMI) Based on Bacterial Community Succession on Porcine Remains," Virginia Commonwealth University, Richmond, VA. (2016).
49. M. Tsokos, R.W. Byard, Postmortem Changes: Overview in Encyclopedia of Forensic and Legal Medicine, (Elsevier Inc., 2016).
50. T. Dupras, J. Shultz, "Taphonomic Bone Staining and Color Changes in Forensic Contexts" in *Manual of Forensic Taphonomy*, J. Pokines, S.A. Symes, Eds. (CRC Press, 2013), pp. 315-340.
51. K.S. Baik, *et al*., Diversity of bacterial community in freshwater of Woopo wetland. *Journal of Microbiology* **46**, 647-655 (2008).
52. A,M. Kielak, C.C. Barreto, G.A. Kowalchuk, J.A. van Venn, E.E. Kuramae, The Ecology of Acidobacteria: Moving beyond Genes and Genomes, *f\Frontiers in Microbiology* **7**, (2016).
53. Y. Fukunaga, N. Ichikawa, "The Class *Holophagaceae*" in *The Prokaryotes*, E. Rosenberg, E.F. DeLong, S. Lory, E. Stackebrandt, F. Thompson, Eds. (Springer, Berlin, Heidelberg, 2014) pp. 683-687.
54. J.L. Metcalf, *et al*., A microbial clock provides an accurate estimate of the postmortem interval in a mouse model system. *eLife* **2, (**2013).
55. J. Wiegel, R. Tanner, F.A. Rainey, "An Introduction to the Family Clostridiaceae" in *The Prokaryotes*, M. Dworkin, S. Falkow, E. Rosenberg, K.H. Schleifer, E. Stackebrandt, Eds. (Springer US, 2006).

56. C.L. Baylis, “Enterobacteriaceae” in *Food Spoilage Microorganisms*, C.W. Blackburn, Eds. (Woodhead Publishing, 2006).
57. S. Octavia, R. Lan, “The Family Enterobacteriaceae” in *The Prokaryotes*, E. Rosenberg, E.F. DeLong, S. Lory, F. Thompson, Eds. (Springer, Berlin, Heidelberg, 2014).
58. S. Fiedler, M. Graw, Decomposition of buried corpses, with special reference to the formation of adipocere. *The Science of Nature* **90**, 291-300 (2003).
59. “Bergey’s Manual® of Systematic Bacteriology” in *The Proteobacteria*, G. Garrity, Eds. (Springer US, 2005).
60. Shang *et al*. Dietary fucoidan modulates the gut microbiota in mice by increasing the abundances of *Lactobacillus* and *Ruminococcaceae, Food Function* **7**, 3224-323 (2016).
61. J. Kuever, “The family Syntrophobacteraceae” in *The Prokaryotes: Deltaproteobacteria and Epsilonproteobacteria*, E. Rosenberg, E.F. DeLong, S. Lory, E. Stackebrandt, F. Thompson, Eds. (Springer, Berlin, Heidelberg, 2014).
62. B. Singh et al., A metagenomic assessment of the bacteria associated with *Lucillia sericata* and *Lucilia cuprina* (*Diptera: Calliphoridae*). *Applied Microbiology and Biotechnology* **99**, 869-883 (2015).
63. I.M. Carroll, T. Ringel-Kulka, J.P. Siddle, T.R. Klaenhammer, Y. Ringel, Characterization of the Fecal Microbiota Using High-Throughput Sequencing Reveals a Stable Microbial Community during Storage. *PLOSone* **7**, e46953 (2012).
64. Invitrogen, CST Protocol for Extracting gDNA from Bone Samples (2009)
65. ThermoFisher Scientific, Qubit® dsDNA HS Assay Kits User Guide (2010)
66. J.J. Kozich, S.L. Westcott, N.T. Baxter, S.K. Highlander, P.D. Schloss, Development of a Dual-Index Sequencing Strategy and Curation Pipeline for Analyzing Amplicon Sequence Data on the MiSeq Illumina Sequencing Platform. *Applied Environmental Microbiology* **79**, 5112-5120 (2013).
67. Beckman Coulter, Agencourt AMPure PCR Purification Kit Protocol (2016)
68. P. Schloss, *et al*., Introducing mothur: Open-source, platform-independent, community-supported software for describing and comparing microbial communities. *Applied and Environmental Microbiology* **75**, 7537-7541 (2009).
69. C. Quast, *et al*., The SILVA ribosomal RNA gene database project: improved data processing and web-based tools. *Nucleic acid research* **41**, D590-D596 (2013).
70. R.C. Edgar, B.J. Hass, J.C. Clemente, C. Quince, R. Knight, UCHIME improves sensitivity and speed of chimera detection. *Bioinformatics* **27**, 2194-2200 (2011).
71. Q. Wang, G.M. Garrity, J.M. Tiedje, J.R. Cole, Naïve Bayesian classifier for rapid assignment of rRNA sequences into the new bacterial taxonomy. *Applied Environmental Microbiology* **73**, 5261-5267 (2007).
72. T.Z. DeSantis, *et al*., Greengenes, a chimera-checked 16S rRNA gene database and workbench compatible with ARB. *Applied and Environmental Microbiology* **72**, 5069-5072 (2006).
73. R Core Team, R: A Language and Environment for Statistical Computing (2019).
74. H. Wickham, ggplot2: Elegant Graphics for Data Analysis (2016).
75. J. Oksanen, *et al*., vegan: Community Ecology Package (2019).
76. L.V. Forger, M.S. Woolf, T.L. Simmons, J.L. Swall, B. Singh, A eukaryotic community succession based method for postmortem interval (PMI) estimation of decomposing porcine remains. *Forensic Science International* **302**, 109838 (2019).
77. A. Liaw, M. Wiener. Classification and Regression by randomForest, *R News* **2**, 18-22 (2002).
78. C. Hanbo, VennDiagram: Generate High-Resolution Venn and Euler Plots (2018).
79. P.J. McMurdie, S. Holmes, phyloseq: An R package for reproducible interactive analysis and graphics of microbiome census data. *PLOSone* **8**, (2013).

80. T. Galili, dendextend: an R package for visualizing, adjusting, and comparing trees of hierarchical clustering. *Bioinformatics* (2015).
81. G.M. Douglas, R.G. Beiko, M.G.I. Langille, “Predicting the Functional Potential of the Microbiome from Marker Genes Using PICRUSt” in *Microbiome Analysis: Methods and Protocols,* Methods in Molecular Biology, R.G. Beiko, Ed. (Springer Science+Business Media, LLC, 2018), pp. 169-177

Figures and Tables

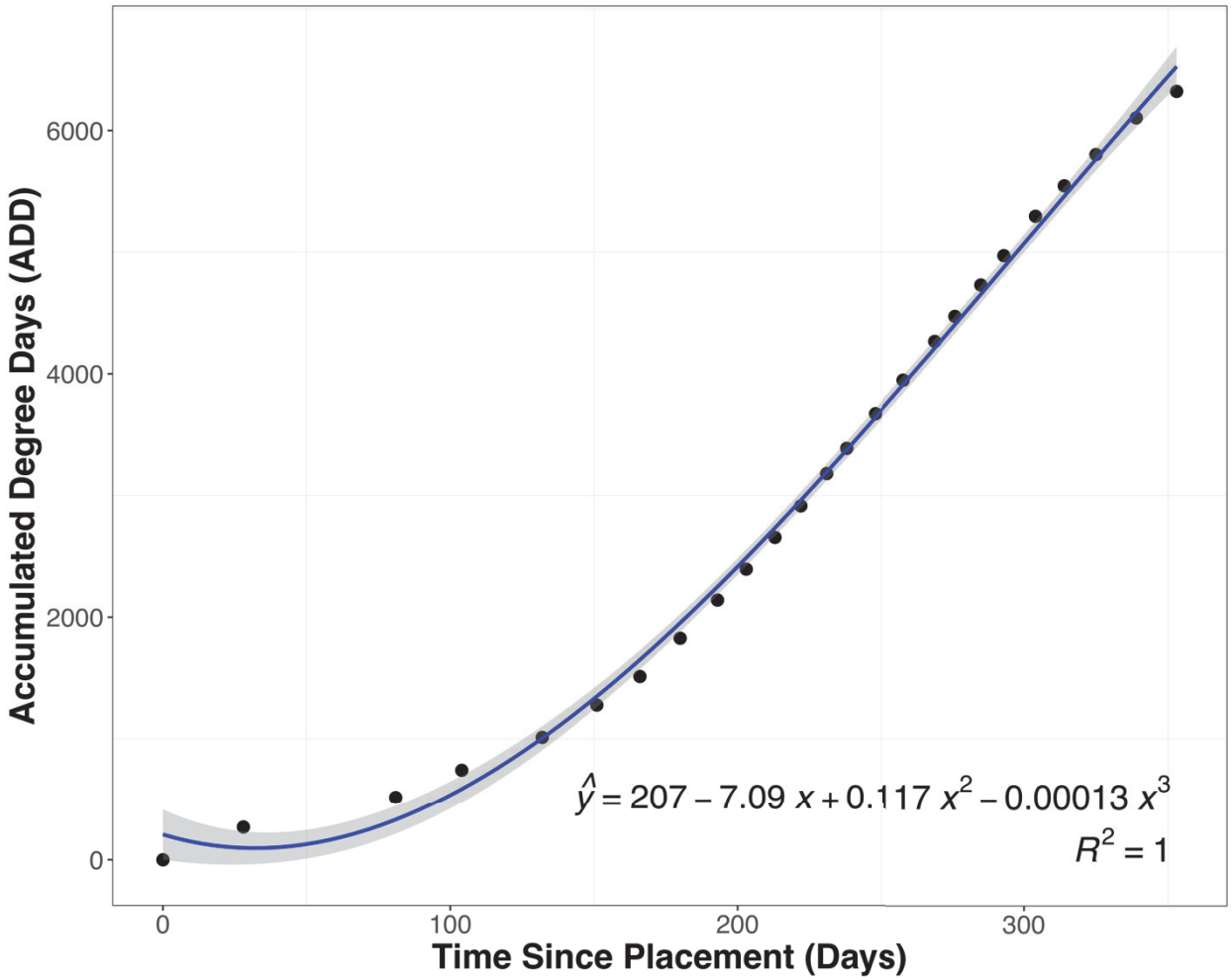

Figure 3.1. The curvilinear relationship between the number of days since submersion/placement and accumulated degree days (ADD) in the James River at the VCU Rice Rivers Center. The shaded area represents the 95% confidence interval.

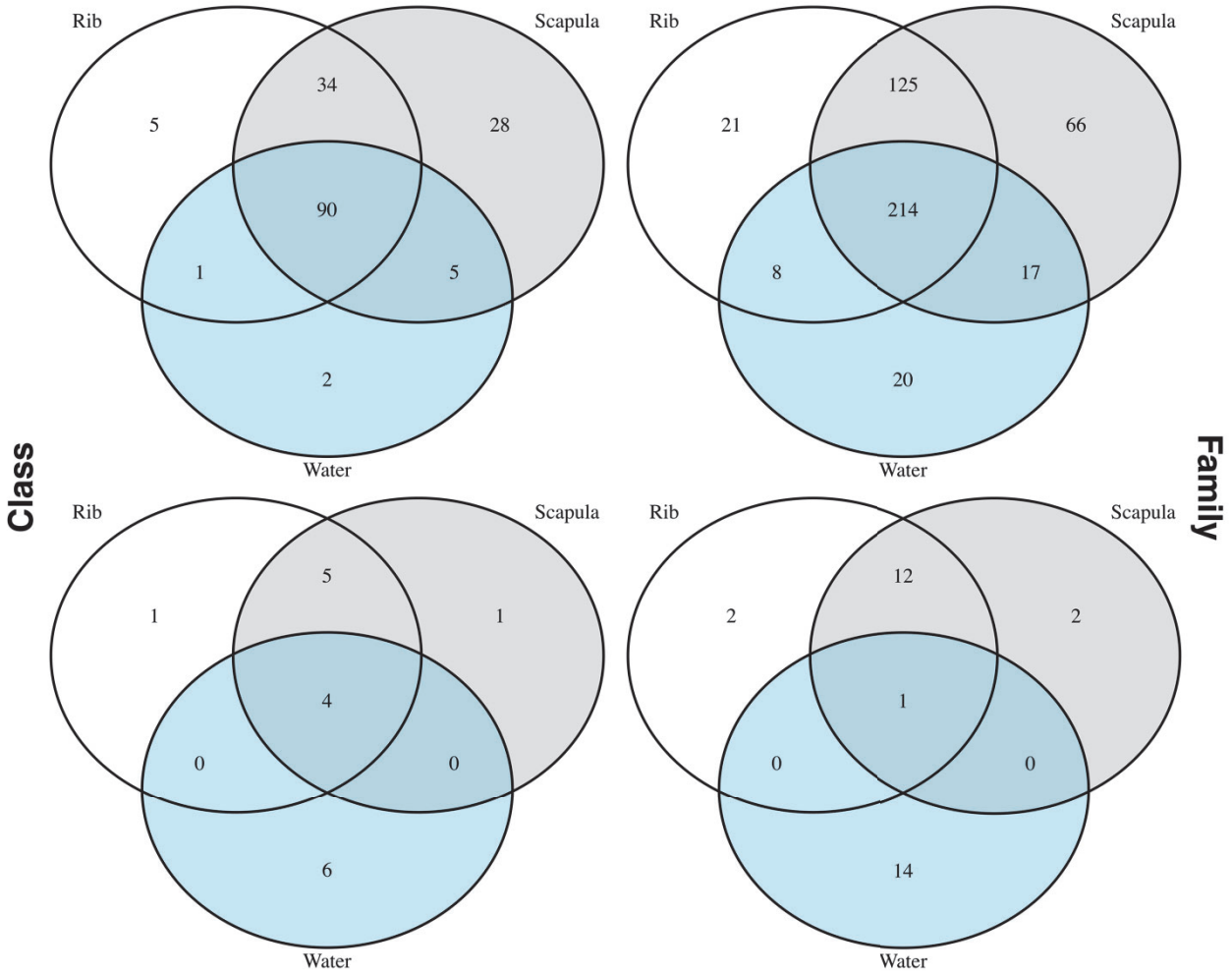

Figure 3.2. Class (left panels) and family (right panels) level taxa presence-absence for water, rib and scapula samples. The top panels include all taxa at the designated level; meanwhile the bottom panels represent the top ten classes and top fifteen families.

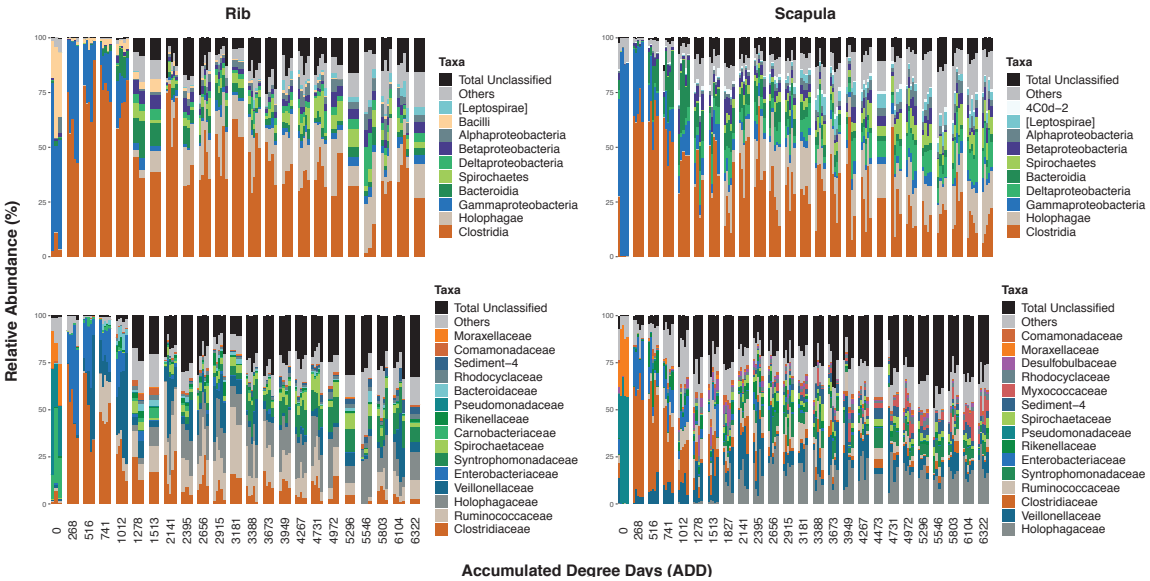

Figure 3.3. The top ten class (top panels) and top fifteen family (bottom panels) relative abundances for rib (left panels) and scapula (right panels) samples across accumulated degree days (ADD). Taxa labeled Others and Total Unclassified are composed of the remaining classified taxa and unclassified taxa, respectively. Replications are represented by invidiual bars within each ADD.

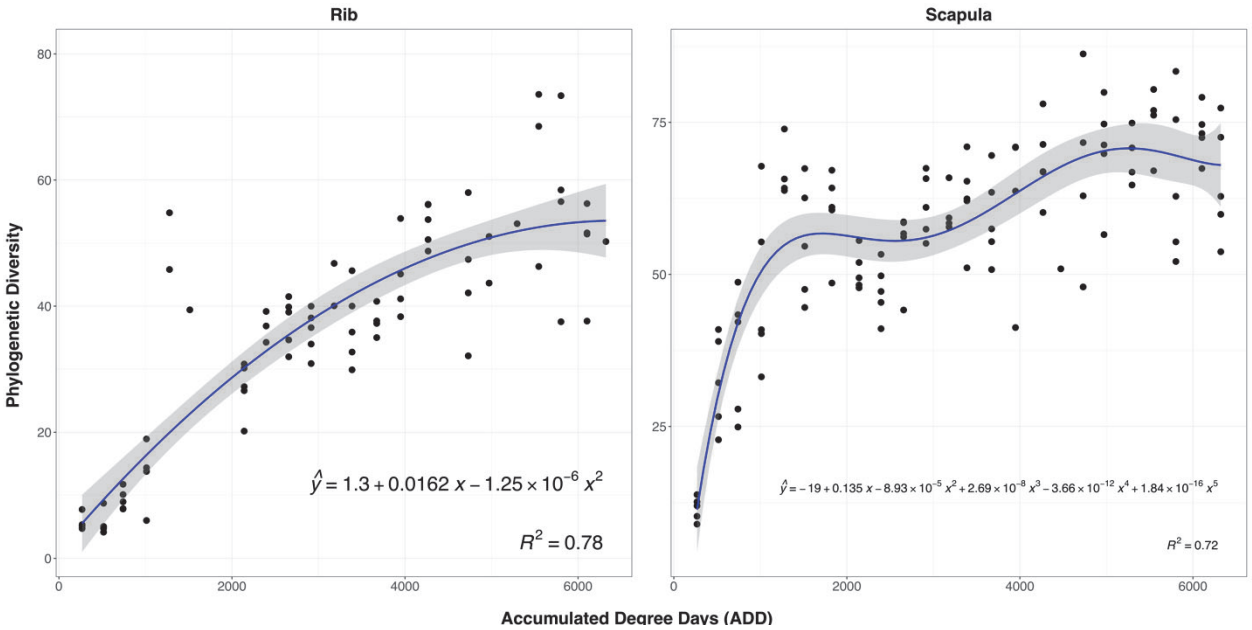

Figure 3.4. Polynomial relationships between accumulated degree days (ADD) and phylogenetic diversity for both rib (left panel) and scapula (right panel) samples. The shaded area represents the 95% confidence interval.

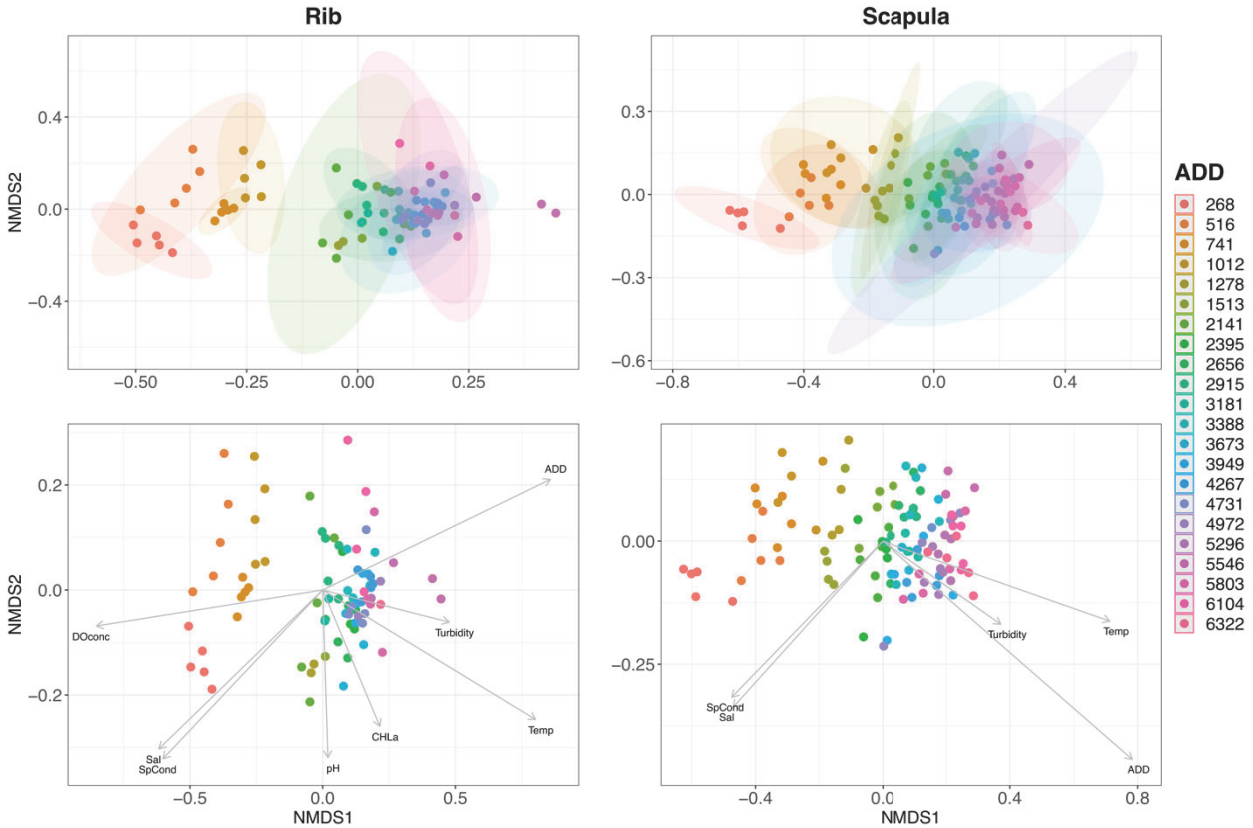

Figure 3.5. Weighted UniFrac distances ordinated via non-metric multidimensional scaling (NMDS) for rib (2D, stress=0.1292) and scapula (2D, stress=0.1144) samples. ADD groupings were indicated to be significant via to PERMANOVA (Rib: *pseudo*-F=36.04, R^2=0.31, p=0.001, Scapula: *pseudo*-F=50.58, R^2=0.32, p=0.001). Ellipses shown in the top panels represent mean or group centroid 95% standard error. Vectors (bottom panels) represent environmental variables significantly related to ordination (alpha 0.05). Significant environmental variables include dissolved oxygen concentration (DOconc), salinity (Sal), specific conductivity (SpCond), pH, chlorophyll-a (CHLa), temperature (Temp), turbidity, and accumulated degree days (ADD). The lengths and angle of the arrows indicates the strength and direction of the relationship between β-diversity and environmental parameters. Vectors that are close and have similar angles are positively correlated, while negative correlations are indicated by diverging vectors.

This resource was prepared by the author(s) using Federal funds provided by the U.S. Department of Justice. Opinions or points of view expressed are those of the author(s) and do not necessarily reflect the official position or policies of the U.S. Department of Justice.

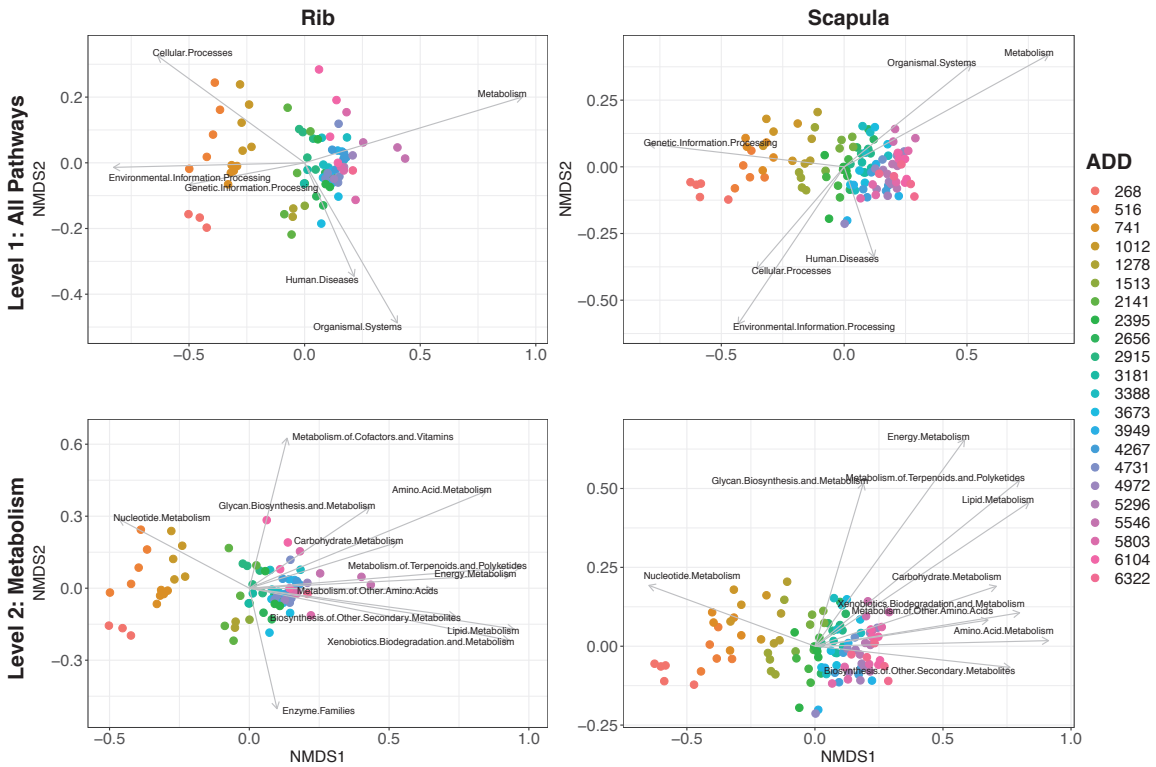

Figure 3.7. Functional KEGG Pathways, predicted via PICRUSt, and their relationship with bacterial community β-diversity. Vectors representing Level 1 (top panels) and level 2 metabolism pathways (bottom panels) were significantly related to weighted UniFrac distances non-metric multidimensional scaling (NMDS) ordination (alpha 0.05). Strength and direction of the relationship between KEGG pathways and β-diversity are indicated by the length and angle of the arrows.

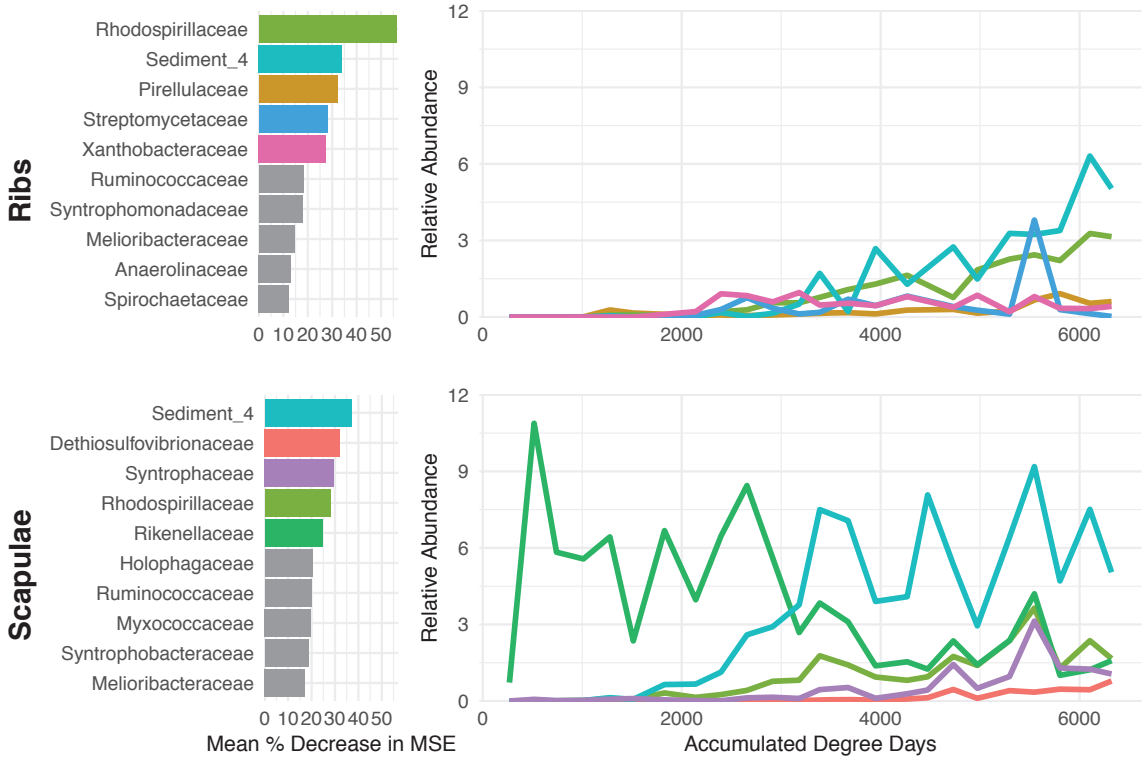

Figure 3.8. The top predictor taxa in decreasing order for rib (top left panel) and scapula (bottom left panel) samples. Changes across accumulated degree days (ADD) for the highlighted predictor taxa across accumulated degree days (ADD) are depicted in right panels for rib (top) and scapula (bottom), respectively.

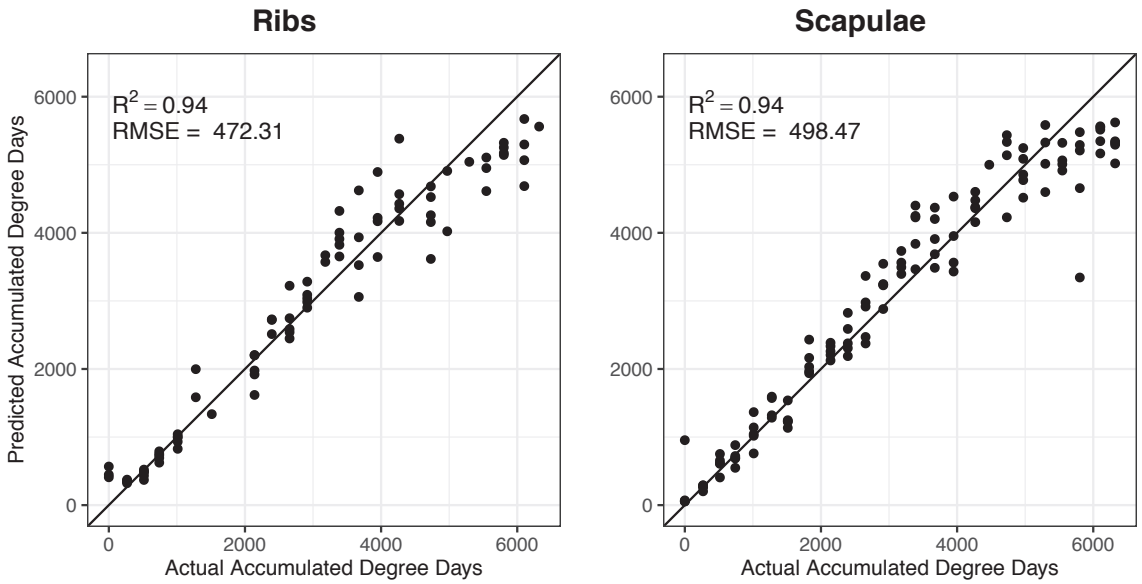

Figure 3.9. Random forest models for each skeletal element were developed using relative abundances of family-level predictor bacterial taxa. A superimposed one-to-one reference line was superimposed on the relationship between predicted accumulated degree days (ADD) versus actual ADD for rib (left panel) and scapula (right) samples.

Table 3.1. A list of calculated accumulated degree days (ADD), time since placement (days), and sample collection numbers.

Accumulated Degree Days (ADD)	Time Since Placement (Days)	Collection
0	0	Baseline
268	28	Collection 1
516	81	Collection 2
741	104	Collection 3
1012	132	Collection 4
1278	151	Collection 5
1513	166	Collection 6
1827	180	Collection 7
2141	193	Collection 8
2395	203	Collection 9
2656	213	Collection 10
2915	222	Collection 11
3181	231	Collection 12
3388	238	Collection 13
3673	248	Collection 14
3949	258	Collection 15
4267	269	Collection16
4473	276	Collection 17
4731	285	Collection 18
4972	293	Collection 19
5296	304	Collection 20
5546	314	Collection 21
5803	325	Collection 22
6104	339	Collection 23
6322	353	Collection 24

Table 3.2. Comparison of the top ten class and top fifteen family-level taxa unique to and shared among water, rib and scapula samples.

	Rib	Scapula	Water	Rib:Scapula	Rib:Water	Scapula:Water	Rib:Scapula:Water
Top 10 Class Level Taxa	Bacilli	4C0d-2	Synechococcophycideae Actinobacteria [Pedosphaerae] Opitutae [Spartobacteria] [Saprospirae]	Clostridia Holophagae Bacteroidia Spirochaetes [Leptospirae]			Gammaproteobacteria Deltaproteobacteria Betaproteobacteria Alphaproteobacteria
Top 15 Family Level Taxa	Carnobacteriaceae Bacteroidaceae	Myxococcaceae Desulfobulbaceae	Synechococcaceae ACK-M1 R4-41B Pelagibacteraceae [Chthoniobacteraceae] Chitinophagaceae [Cerasicoccaceae] Opitutaceae Flavobacteriaceae Oxalobacteraceae Sinobacteraceae Nostocaceae Verrucomicrobiaceae Pseudanabaenaceae	Clostridiaceae Ruminococcaceae Holophagaceae Veillonellaceae Enterobacteriaceae Syntrophomonadaceae Spirochaetaceae Rikenellaceae Pseudomonadaceae Rhodocyclaceae Sediment-4 Moraxellaceae			Comamonadaceae

Table 3.3. Summary of the environmental variables relationship with the UniFrac weighted β-diversity NMDS ordination.

Environmental Parameters	Rib		Scapula	
	r^2	p-value	r^2	p-value
ADD	0.7805	0.001	0.8101	0.001
Temperature	0.7038	0.001	0.5347	0.001
Specific Conductivity	0.4656	0.001	0.3262	0.001
pH	0.1023	0.01	0.0069	0.69
Turbidity	0.2311	0.001	0.1669	0.001
CHLa	0.1138	0.011	0.0486	0.076
Salinity	0.4727	0.001	0.335	0.001
Dissolved Oxygen Concentration	0.7315	0.001	0.6396	0.001

Table 3.4. Summary of the KEGG level 1 pathway and UniFrac weighted β- diversity NMDS ordination relationship.

KEGG Level 1	Rib		Scapula	
	r^2	p-value	r^2	p-value
Cellular Processes	0.5105	0.001	0.2732	0.001
Environmental Information Processing	0.6834	0.001	0.5346	0.001
Genetic Information Processing	0.2526	0.001	0.6408	0.001
Human Diseases	0.1654	0.001	0.1291	0.001
Metabolism	0.9269	0.001	0.8709	0.001
Organismal Systems	0.3987	0.001	0.4154	0.001

Table 3.5. Summary of the KEGG level 2 pathways and UniFrac weighted β- diversity NMDS ordination relationship.

KEGG Level 2	Rib		Scapula	
	r^2	p-value	r^2	p-value
Nucleotide Metabolism	0.2993	0.001	0.4578	0.001
Biosynthesis of Other Secondary Metabolites	0.5569	0.001	0.585	0.001
Metabolism of Other Amino Acids	0.431	0.001	0.4638	0.001
Enzyme Families	0.262	0.001	0.0242	0.265
Glycan Biosynthesis and Metabolism	0.3003	0.001	0.3029	0.001
Energy Metabolism	0.8787	0.001	0.7705	0.001
Metabolism of Cofactors and Vitamins	0.4094	0.001	0.0459	0.093
Lipid Metabolism	0.9241	0.001	0.9082	0.001
Xenobiotics Biodegradation and Metabolism	0.9099	0.001	0.6501	0.001
Metabolism of Terpenoids and Polyketides	0.9551	0.001	0.9165	0.001
Amino Acid Metabolism	0.8828	0.001	0.8326	0.001
Carbohydrate Metabolism	0.3187	0.001	0.5381	0.001

Supplemental Figures and Tables

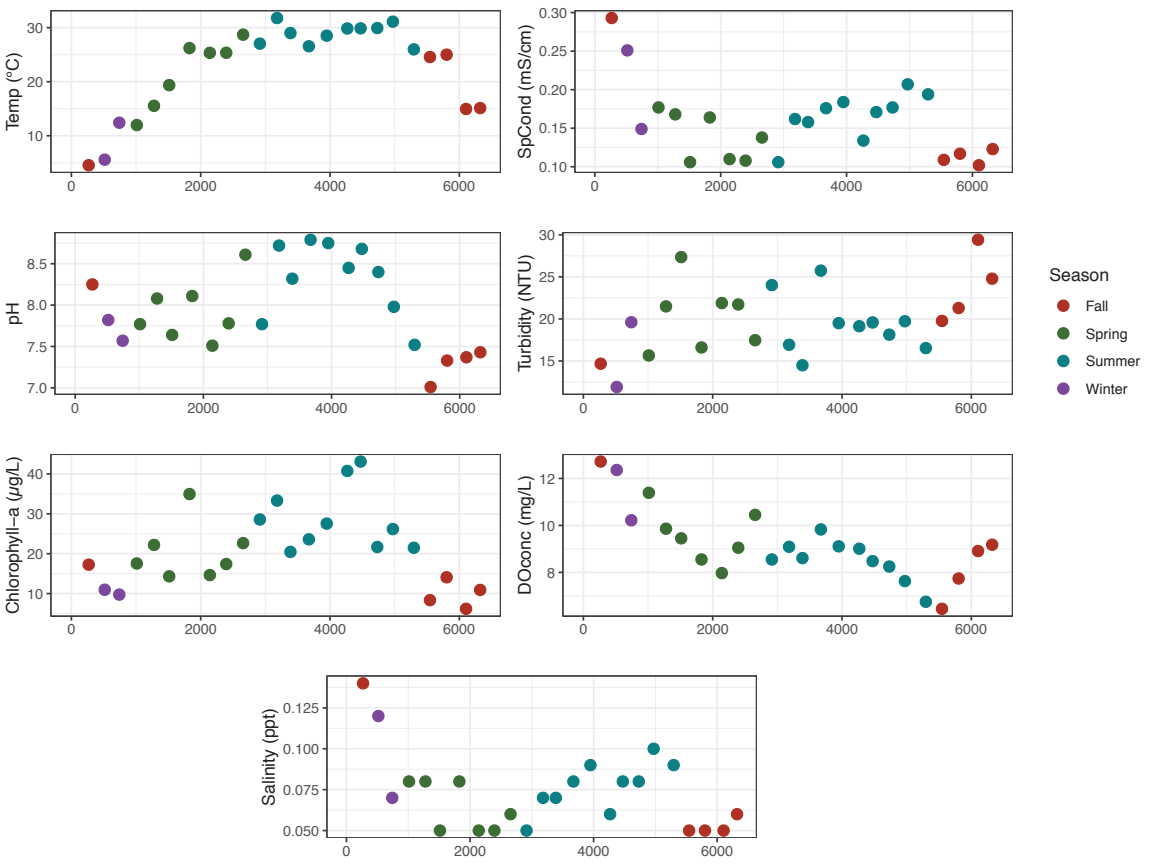

Fig. 3.S1. Environmental and water quality daily averages and their relationship with accumulated degree days (ADD).

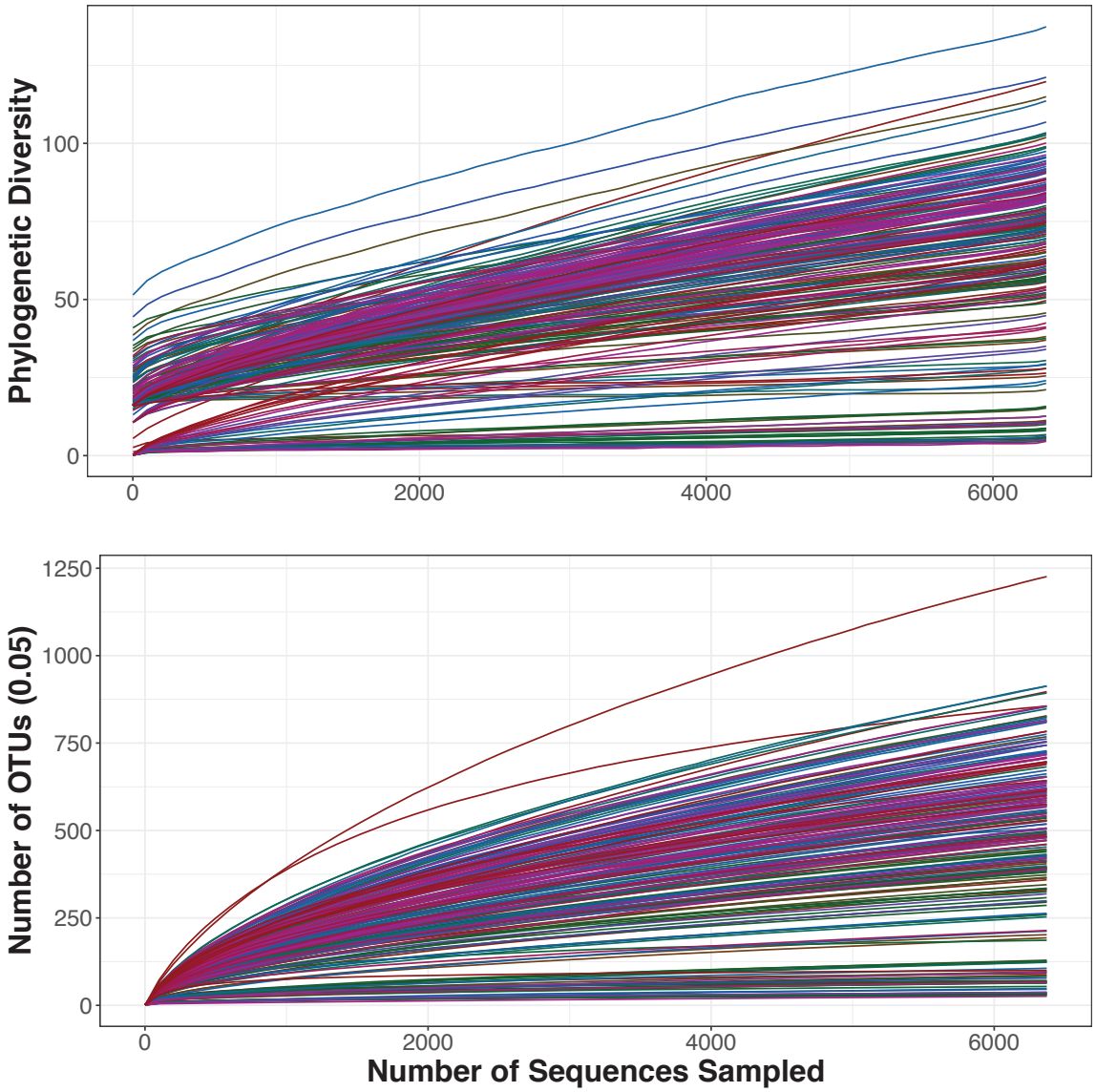

Fig. 3.S2. Phylogenetic diversity (top panel) and the number of operational taxonomic units (0.05 or 5%) (bottom panel) observed for 6,371 sampled sequences for rarefaction analysis curves. A majority of samples converged and reached a horizontal asymptote, which suggests that sufficient observations were made, without sacrificing samples, to get a reasonable estimate of quantity.

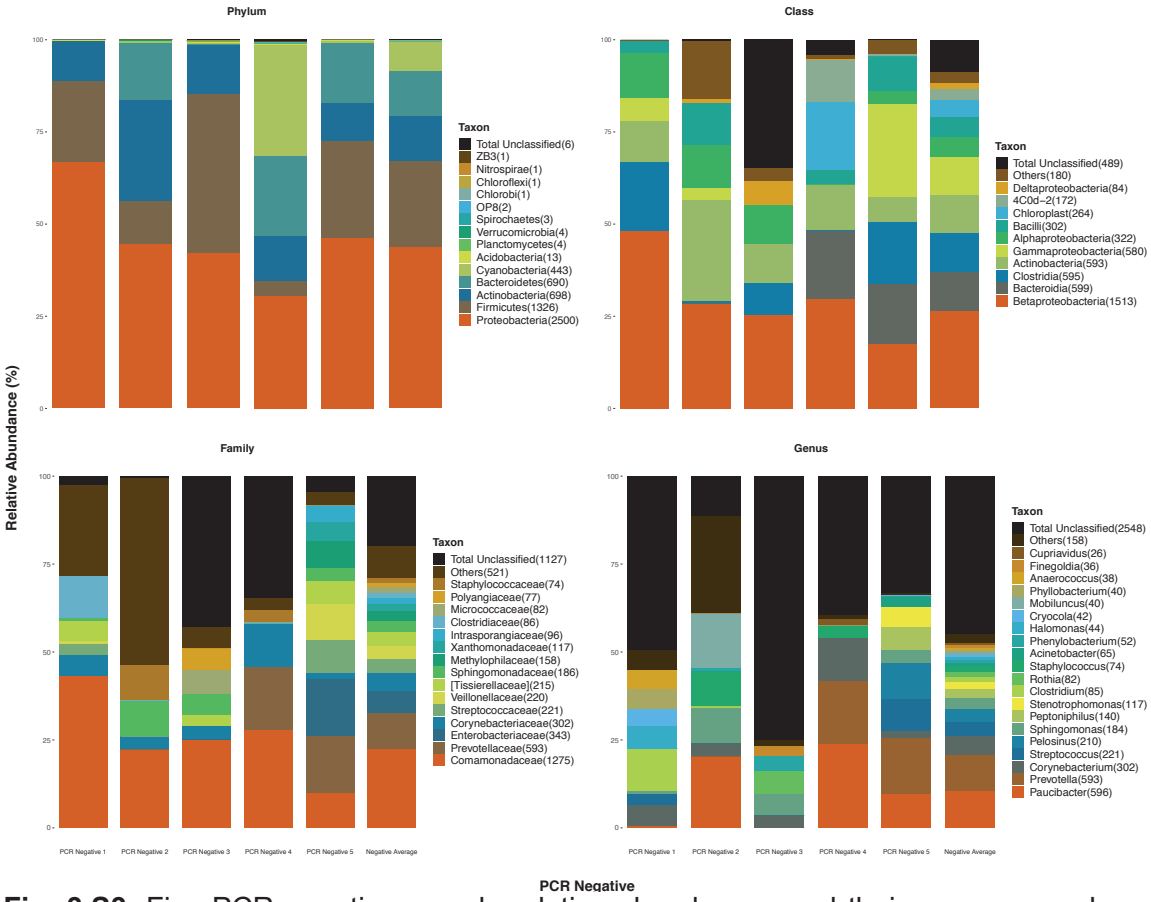

Fig. 3.S3. Five PCR negative sample relative abundances and their average number of reads recovered (PCR Negative 1: 697, PCR Negative 2: 257, PCR Negative 3: 1232, PCR Negative 4: 1418, PCR Negative 5: 2089, Average: 1139). Taxa labeled Unclassified comprise the remaining unclassified taxa. Subsampling resulted in the removal of all negative samples.

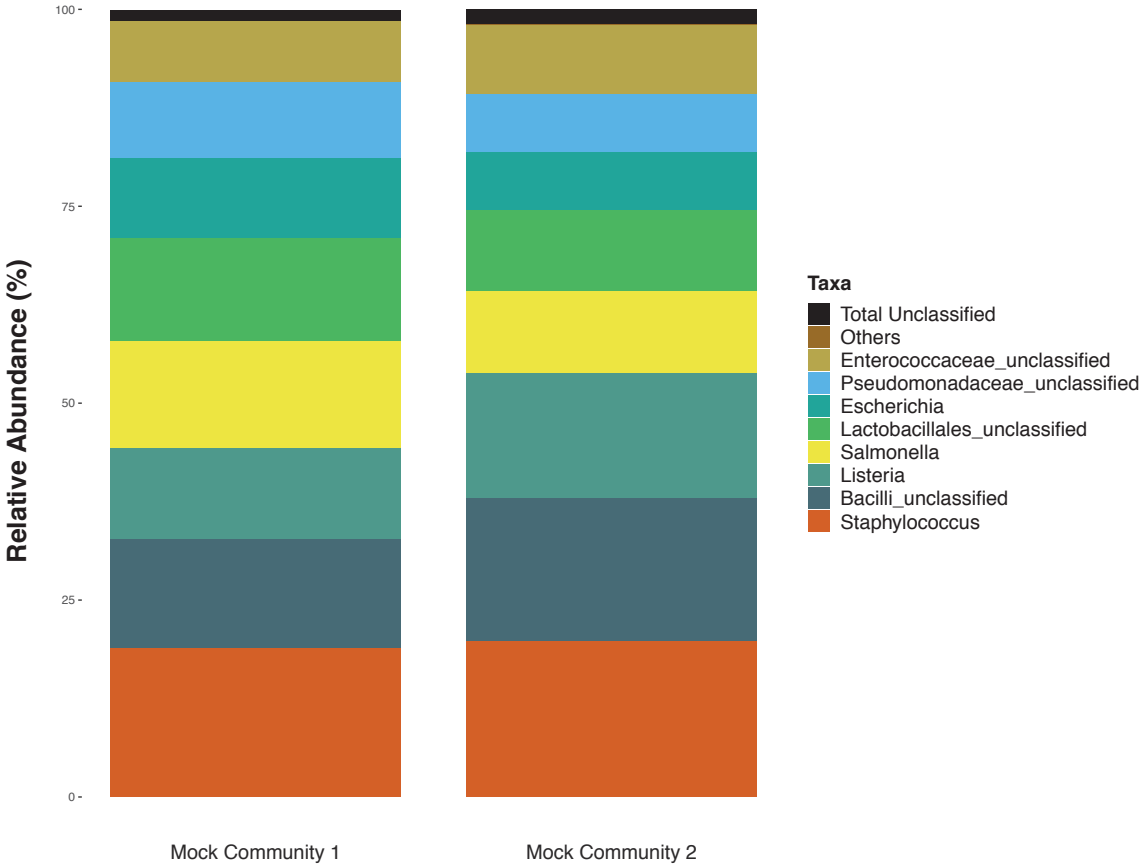

Fig. 3.S4. ZymoBIOMICS microbial community DNA standard expected eight genera and their relative abundances. Taxa labeled Unclassified include the remaining unclassified taxa; meanwhile, Artifacts consists of singletons (0.07%) that were excluded from further analyses.

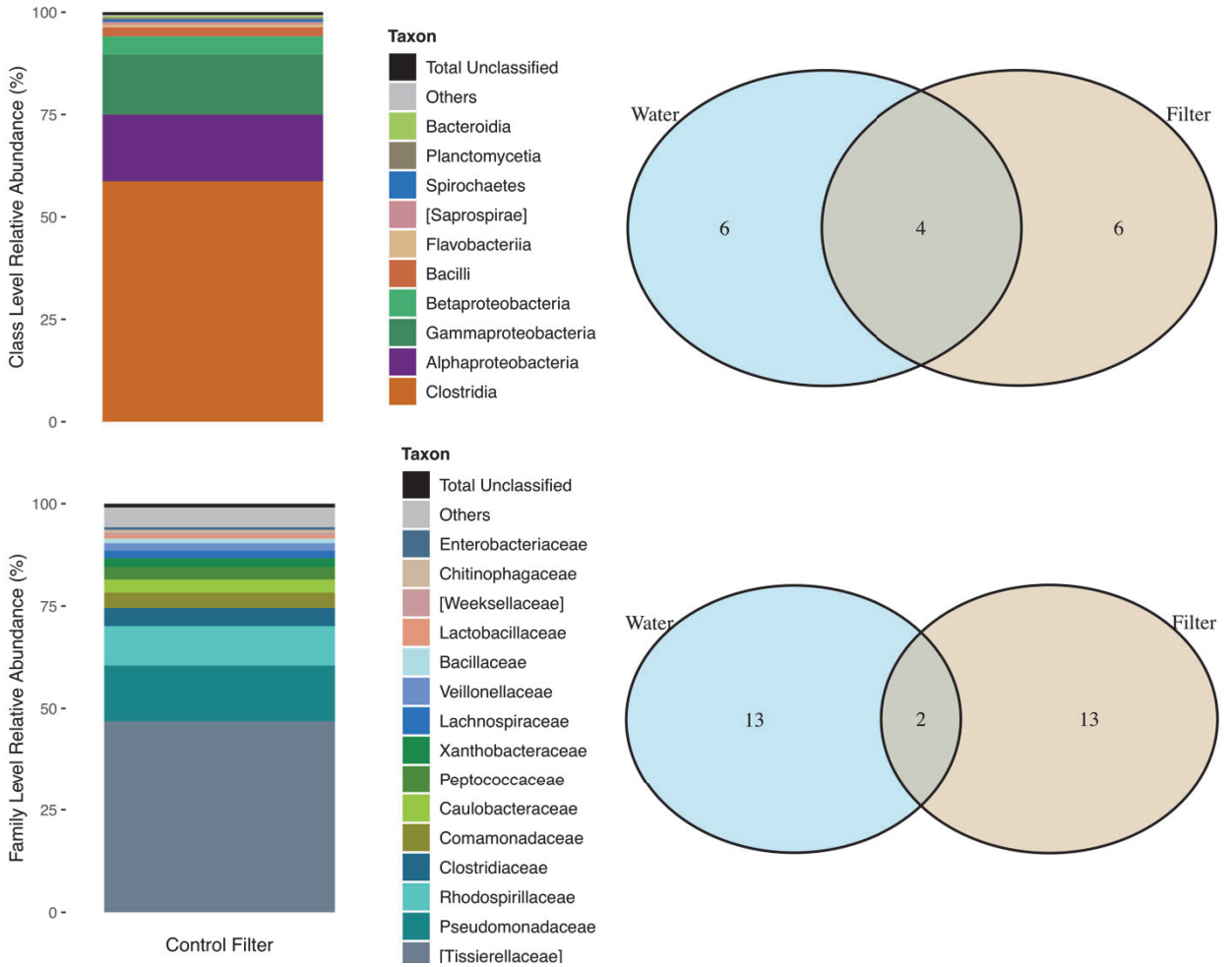

Figure 3.S5. Family level relative abundances at the class (left top) and family (left bottom) levels for the control filter. Venn diagrams (right panels), showing minimal similarities between the most dominant taxa shared between water samples and the control filter.

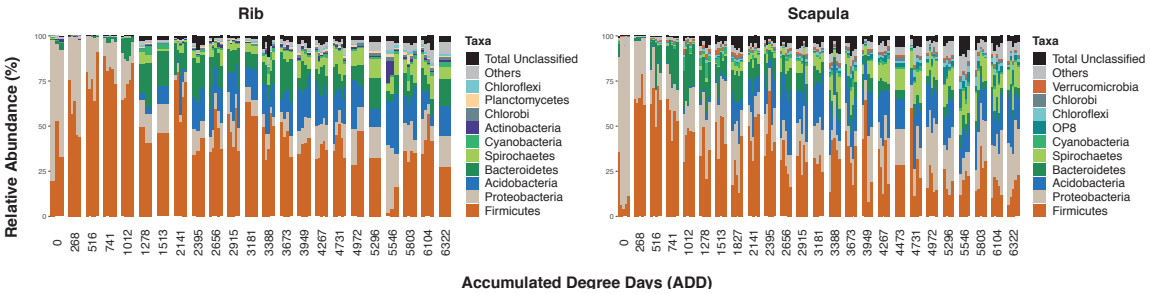

Fig. 3.S6. Top ten phyla relative abundances for rib (left panel) and scapula (right panel) samples across accumulated degree days (ADD). Taxa categorized as Others and Total Unclassified include remaining classified taxa and unclassified taxa, respectively. Within each ADD, bars represent invidividual.

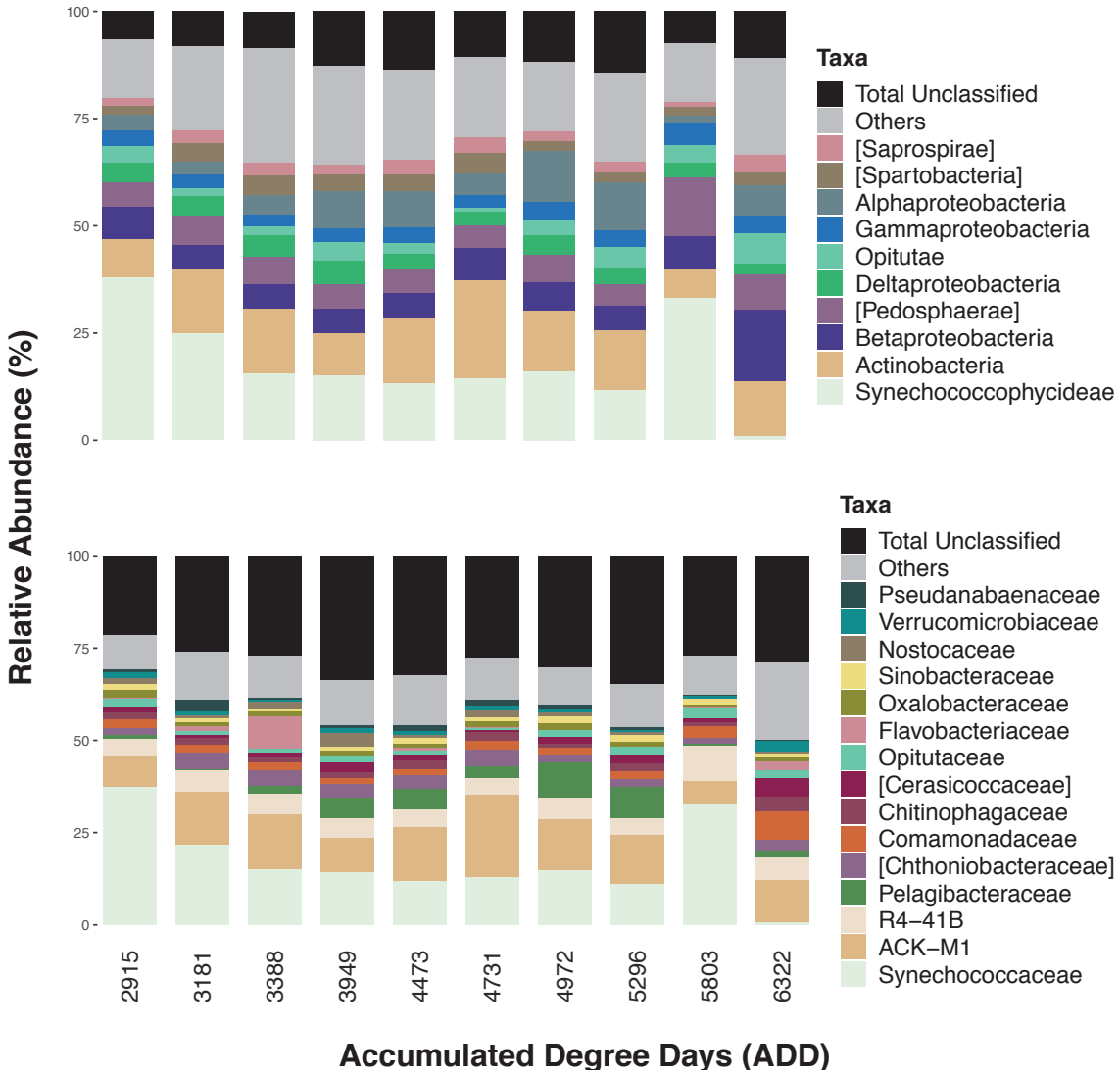

Fig. 3.S7. The top ten class level (top panel) and top fifteen family level (bottom panel) relative abundances for water samples across accumulated degree days (ADD). Taxa grouped as Others and Total Unclassified include the remaining classified taxa and unclassified taxa, respectively.

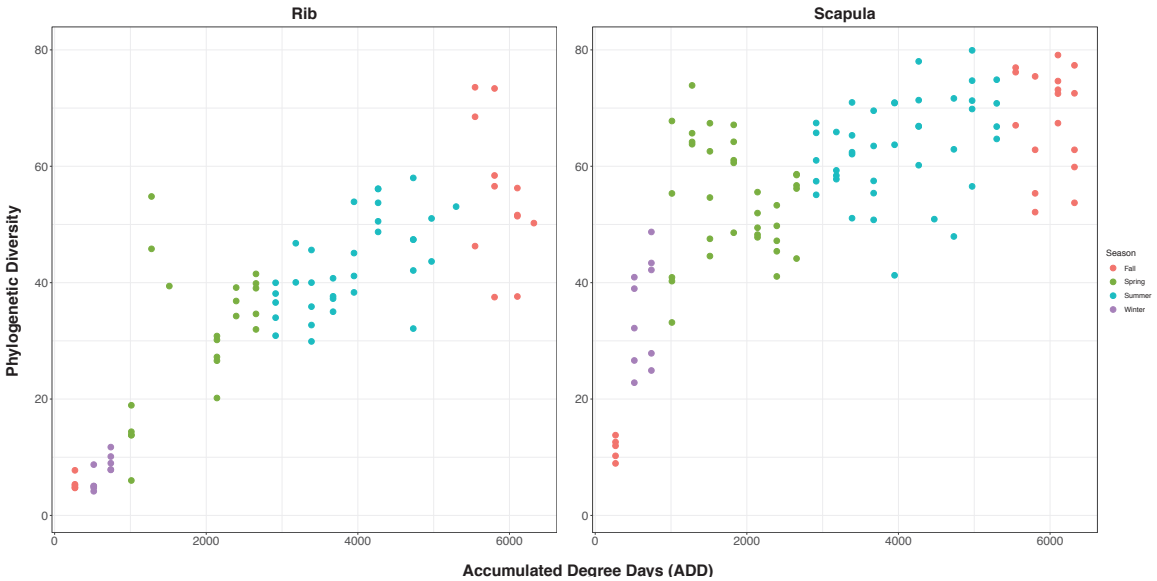

Fig. 3.S8. Phylogenetic diversity and accumulated degree days (ADD) relationships for rib (left panel) and scapula (right panel) samples colored by season (Fall, Winter, Spring, Summer).

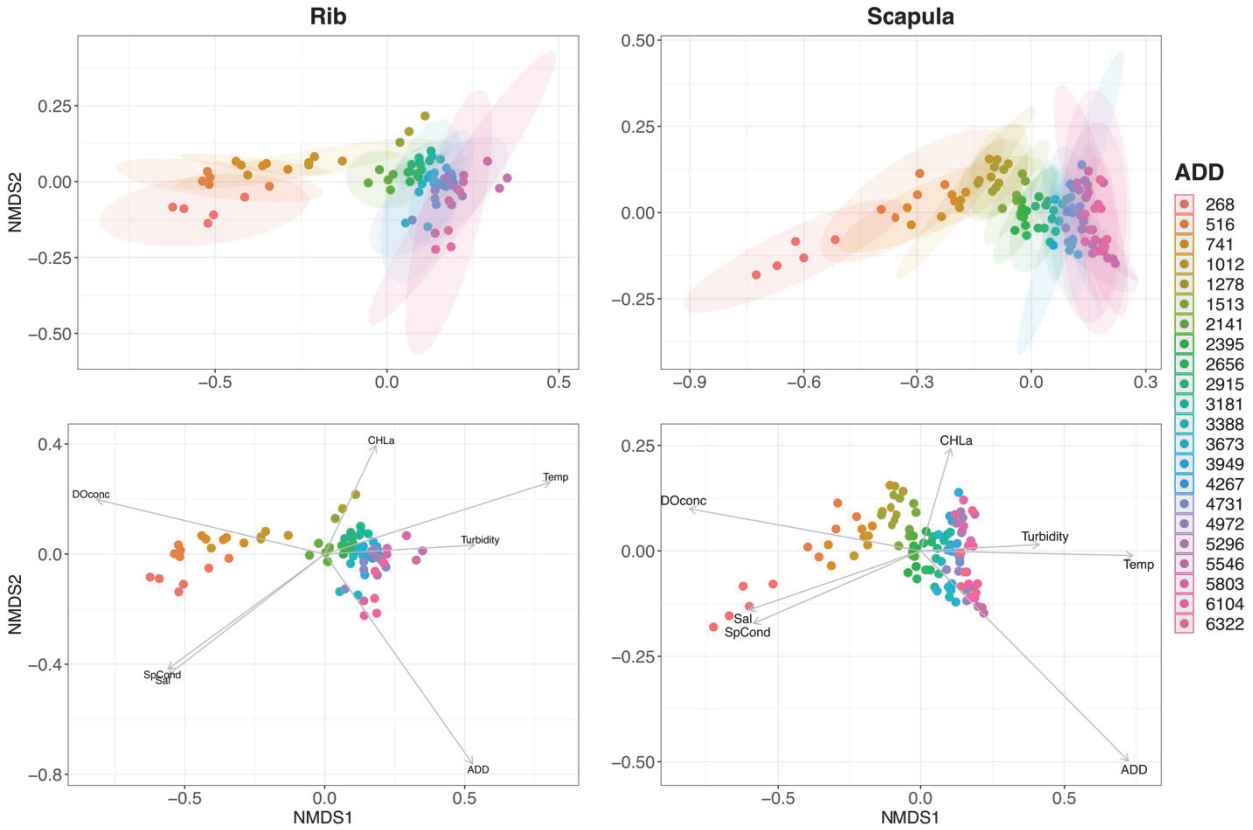

Fig. 3.S9. Unweighted UniFrac distances ordinated via non-metric multidimensional scaling (NMDS) for rib (2D, stress=0.0658) and scapula (2D, stress=0.0978) samples. ADD groupings were indicated to be significant via to PERMANOVA (Rib: *pseudo*-F=13.98, R^2=0.15, p=0.001, Scapula: *pseudo*-F=13.18, R^2=0.11, p=0.001). Ellipses shown in the top panels represent mean or group centroid 95% standard error. Vectors (bottom panels) represent environmental variables significantly related to ordination (alpha 0.05). Significant environmental variables include dissolved oxygen concentration (DOconc), salinity (Sal), specific conductivity (SpCond), chlorophyll-a (CHLa), temperature (Temp), turbidity, and accumulated degree days (ADD). The lengths and angle of the arrows indicates the strength and direction of the relationship between β-diversity and environmental parameters. Vectors that are close and have similar angles are positively correlated, while negative correlations are indicated by diverging vectors.

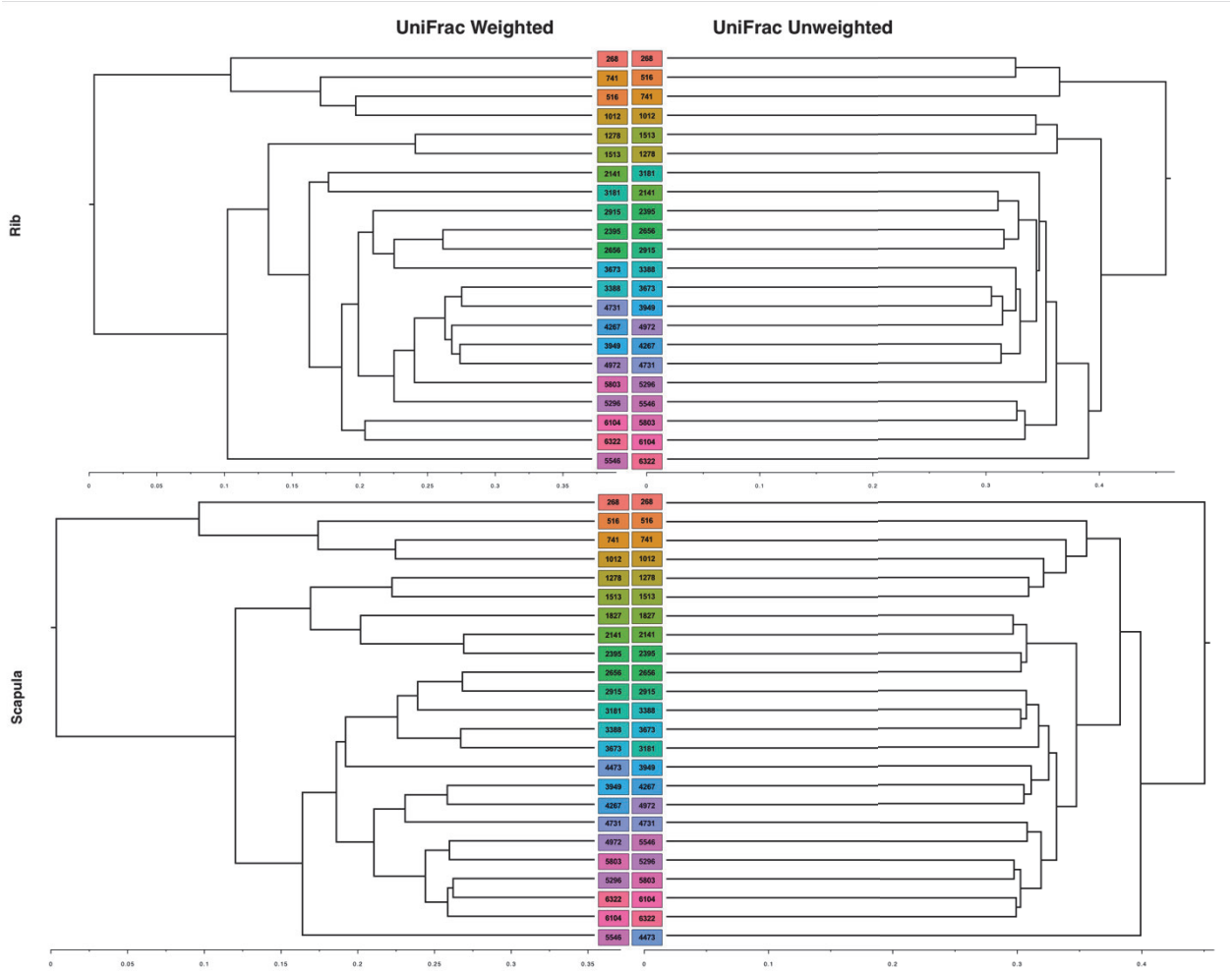

Fig. 3.S10. Weighted (left) and unweighted (right) UniFrac distances grouped by accumulated degree days (ADD) Unweighted Pair Group Method with Arithmetic Mean (UPGMA) trees. Cophenetic correlation values of 0.80 and 0.66 for rip (top panel) and scapula (bottom panel), respectively, suggests that tjeweighted and unweighted UniFrac trees were highly congruent.

Table 3.S1. The relationship between environmental/water quality daily averages and accumulated degree days (ADD) and their correlation coefficients. Salinity and dissolved oxygen concentration were the only parameter significantly and negatively associated with ADD.

Environmental Parameters	rho (Spearman's)	p-value
Temperature	0.39	0.0596
pH	-0.21	0.3349
Chlorophyll-a	-0.02	0.94
Salinity	-0.68	0.0003
Specific Conductivity	-0.23	0.2831
Turbidity	0.34	0.1082
Dissolved Oxygen Concentration	-0.68	0.0003

Table 3.S2. For each bone type, the percent of classified and unclassified sequences at all taxonomic levels.

Taxonomy Number of Sequences				
	Rib		Scapula	
	Classified (%)	Unclassified (%)	Classified (%)	Unclassified (%)
Phylum	98	2	96	3
Class	92	8	93	7
Order	89	11	89	11
Family	84	16	79	21
Genus	61	39	57	43
Species	13	87	14	86

Table 3.S3. Summary of the environmental variables and UniFrac unweighted beta diversity NMDS ordination relationships.

Environmental Parameters	**Rib**		**Scapula**	
	r^2	p-value	r^2	p-value
ADD	0.8595	0.001	0.7698	0.001
Temperature	0.7168	0.001	0.5451	0.001
Specific Conductivity	0.4873	0.001	0.3732	0.001
pH	0.0109	0.666	0.0033	0.851
Turbidity	0.2881	0.001	0.1707	0.001
CHLa	0.1885	0.002	0.0698	0.02
Salinity	0.5027	0.001	0.3824	0.001
Dissolved Oxygen Concentration	0.7025	0.001	0.6654	0.001

Supplementary Information Text

Additional Analyses. At a dissimilarity of 5% (i.e., genus level) Operational Taxonomic Unit (OTU) clustering via average neighbor was used to examine α- and β- diversity. mothur version 1.39.5 (1) was used to calculate shannon diversity indices; linear modeling (lm) using the stats package (2) was used to assess temporal changes in α-diversity. Environmental parameters (i.e temperature, pH, etc.) were incorporated into the linear model to examine variations within the dataset. mothur (1) generated OTU table and OTU taxonomy were used along with a meta data file to explore OTU β-diversity via the vegan package (3). Specifically, Bray-Curtis and Jaccard metrics were ordinated using non-metric multidimensional scaling (NMDS) (permutations=999); additionally, permutational multivariate analysis of variance (PERMANOVA) via the adonis function was used to test significance of accumulated degree days (ADD) on community structure. Site/environmental parameters (i.e temperature, ADD, pH, etc.) were superimposed to both OTU ordinations using the envfit function from the vegan package. While maximizing correlations, the plotted vectors ($\alpha < 0.05$) suggest the direction in ordination space that changes most rapidly. Assessment of the parameters importance was done using squared correlation coefficients (permutations-999) and fitted vectors.

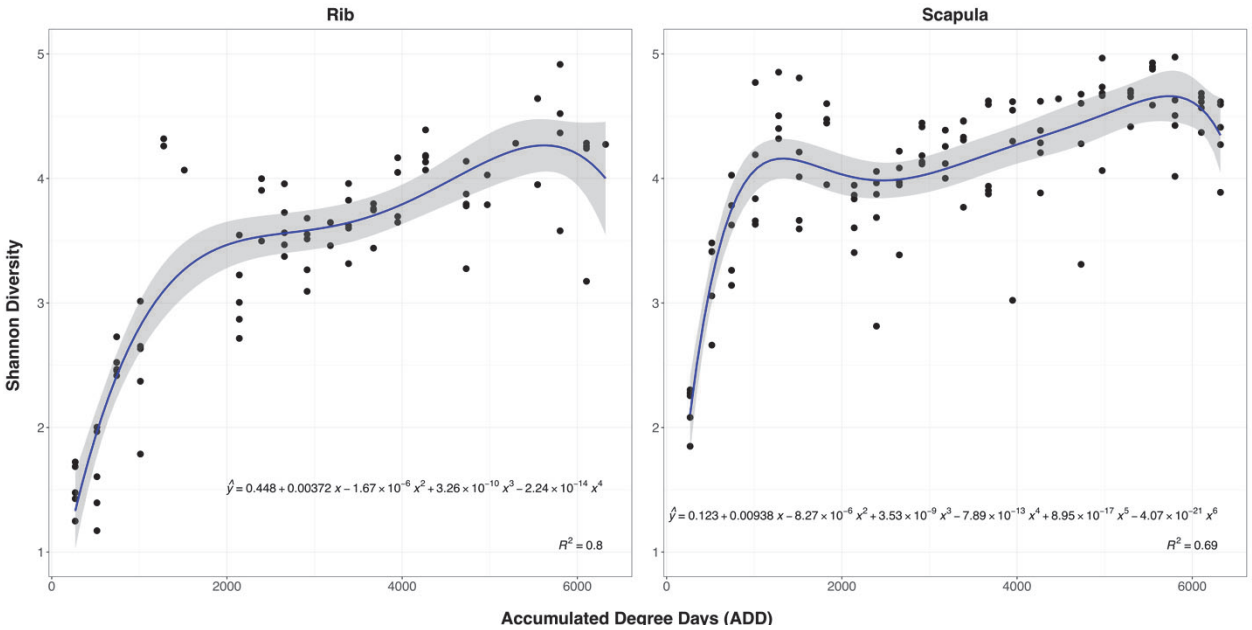

Fig. 3.S11. Polynomial relationships between OTU (0.05) Shannon diversity and accumulated degree days (ADD) for both rib (left panel) and scapula (right panel). The shaded area represent 95% standard error.

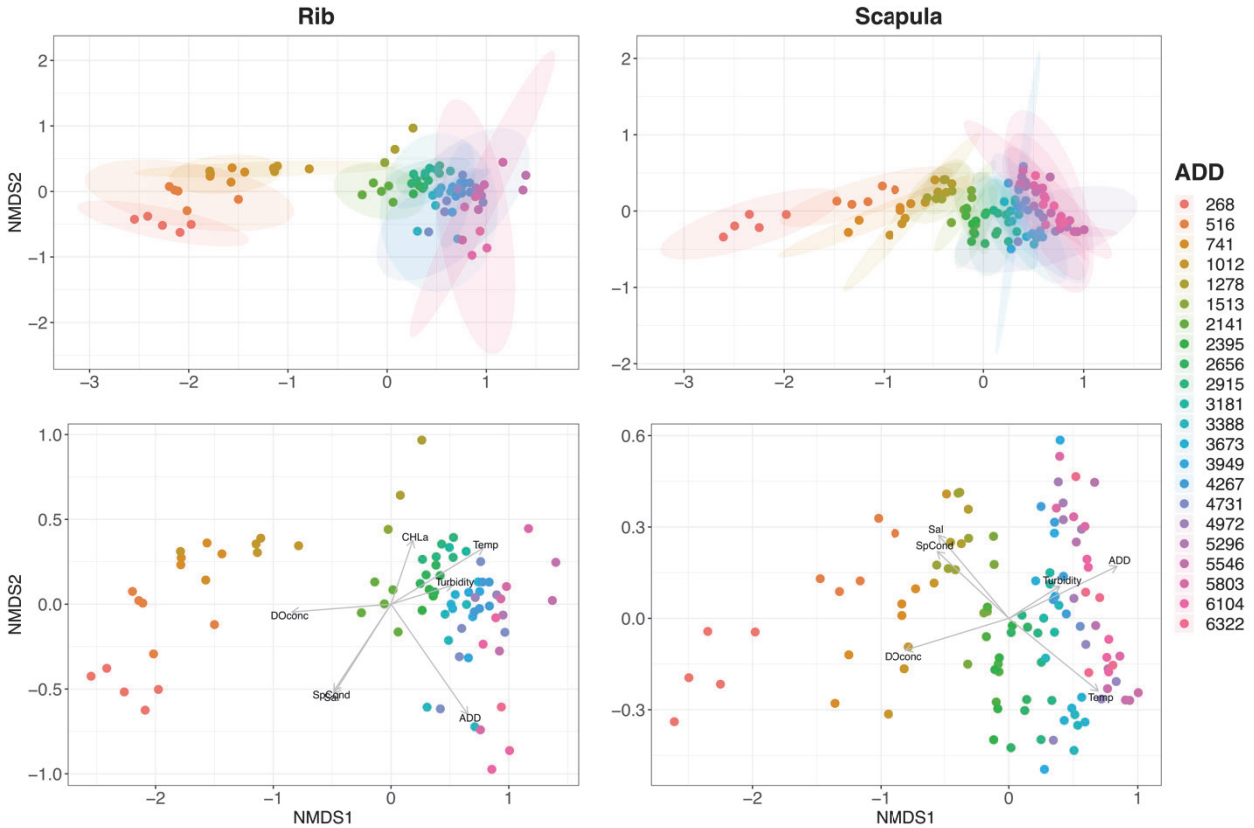

Fig. 3.S12. Non-metric multidimensional scaling (NMDS) ordination of microbial OTU (0.05) Bray-Curtis beta-diversity for rib (2D, stress=0.0812) and scapula (2D, stress=0.1144) samples. ADD was found to be significant via PERMANOVA (Rib: *pseudo*-F=31.27, R^2=0.28, p=0.001, Scapula: *pseudo*-F=42.35, R^2=0.28, p=0.001). The 95% standard error for the mean or group centroid are represented by ellipses in the top panels. Vectors in the bottom panels indicate the relationship between the environmental variables and the ordination (alpha 0.05). Significant environmental variables include dissolved oxygen concentration (DOconc), salinity (Sal), specific conductivity (SpCond), chlorophyll a (CHLa), turbidity, temperature (Temp), and accumulated degree days (ADD). The strength and direction of relationship between beta-diversity and the environmental variables are indicated by the lengths and angle of the arrows. Vectors that are positively correlated are close and have similar angles, while negative correlation is suggested by diverging vectors.

This resource was prepared by the author(s) using Federal funds provided by the U.S. Department of Justice. Opinions or points of view expressed are those of the author(s) and do not necessarily reflect the official position or policies of the U.S. Department of Justice.

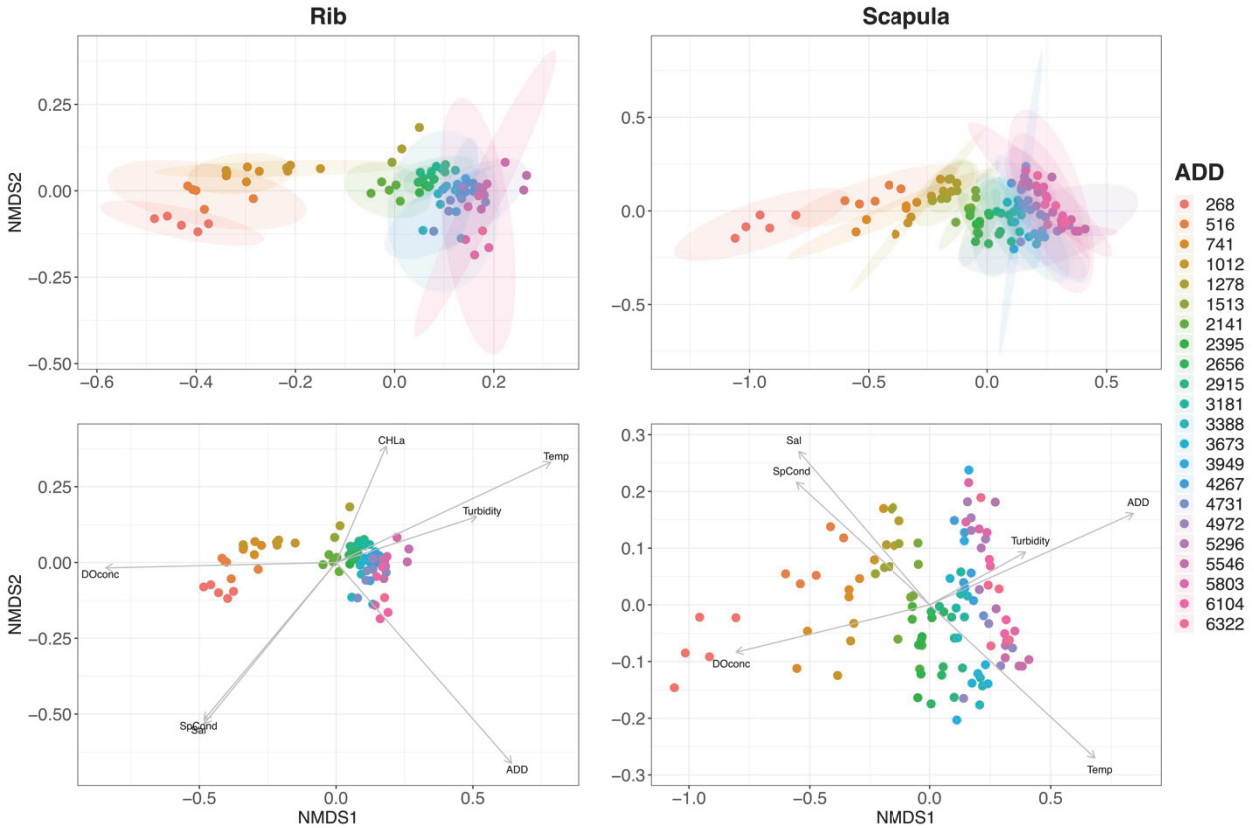

Fig. 3.S13. Non-metric multidimensional scaling (NMDS) ordination of microbial OTU (0.05) Jaccard beta-diversity for rib (2D, stress=0.0814) and scapula (2D, stress=0.1144) samples. ADD was found to be significant via PERMANOVA (Rib: *pseudo*-F=31.27, R^2=0.28, p=0.001, Scapula: *pseudo*-F=42.35, R^2=0.28, p=0.001). The 95% standard error for the mean or group centroid are represented by ellipses in the top panels. Vectors in the bottom panels indicate the relationship between the environmental variables and the ordination (alpha 0.05). Significant environmental variables include dissolved oxygen concentration (DOconc), salinity (Sal), specific conductivity (SpCond), chlorophyll a (CHLa), turbidity, temperature (Temp), and accumulated degree days (ADD). The strength and direction of relationship between beta-diversity and the environmental variables are indicated by the lengths and angle of the arrows. Vectors that are positively correlated are close and have similar angles, while negative correlation is suggested by diverging vectors.

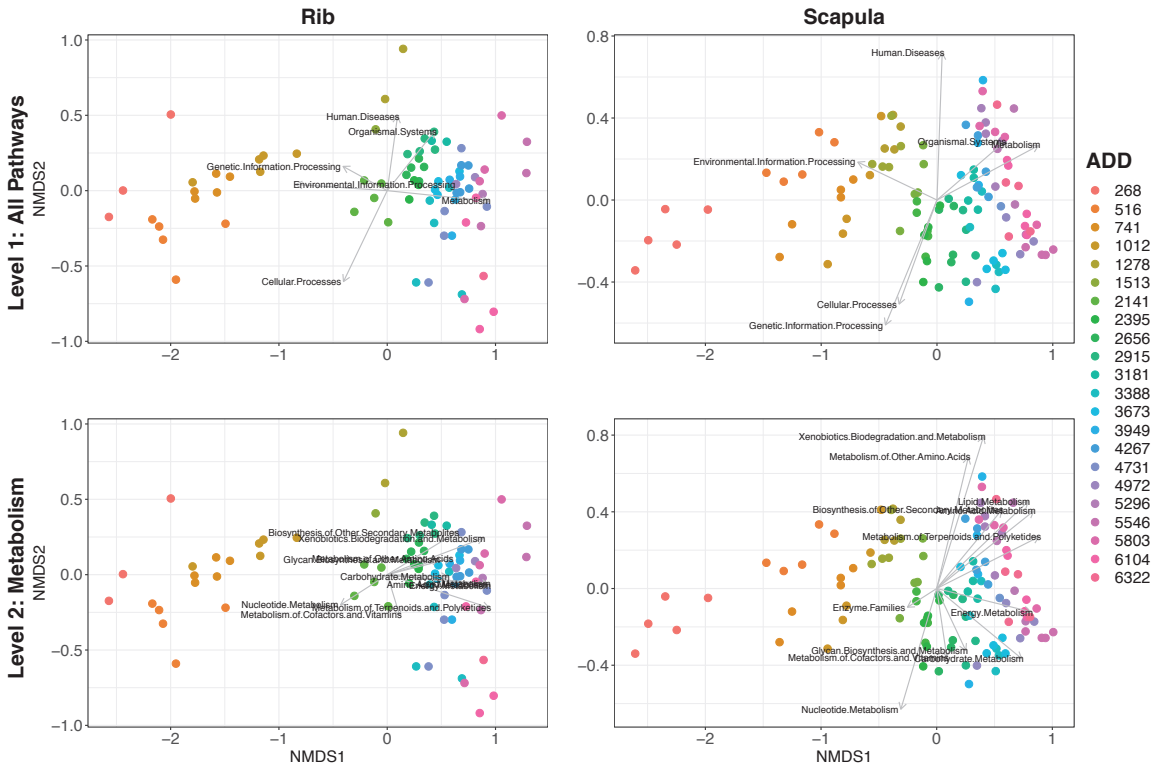

Fig. 3.S14. The relationship between PICRUSt predicted functional KEGG Level 1 Pathways with beta-diversity bacterial community structure. Vectors in the top and bottom panels show Level 1 and level 2 metabolism pathways that were significantly related to OTU Bray-Curtis beta-diversity non-metric multidimensional scaling (NMDS) ordination (alpha 0.05). The arrow length and angle suggest the relationship strength and direction relationship between beta-diversity and environmental variables.

Table 3.S4. Summary of the environmental variables relationship with the OTU (0.05) Bray-Curtis beta diversity NMDS ordination

Environmental Parameters	Rib		Scapula	
	r^2	p-value	r^2	p-value
ADD	0.8461	0.001	0.7342	0.001
Temperature	0.7249	0.001	0.5375	0.001
Specific Conductivity	0.4992	0.001	0.3561	0.001
pH	0.0067	0.762	0.0167	0.399
Turbidity	0.2847	0.001	0.1663	0.001
CHLa	0.1762	0.001	0.0379	0.109
Salinity	0.5137	0.001	0.3716	0.001
Dissolved Oxygen Concentration	0.71	0.001	0.6557	0.001

Table 3.S5. Summary of the environmental variables relationship with OTU (0.05) Jaccard beta diversity NMDS ordination.

Environmental Parameters	Rib		Scapula	
	r^2	p-value	r^2	p-value
ADD	0.8503	0.001	0.7339	0.001
Temperature	0.7254	0.001	0.5389	0.001
Specific Conductivity	0.5019	0.001	0.3552	0.001
pH	0.0067	0.746	0.019	0.378
Turbidity	0.2868	0.001	0.166	0.001
CHLa	0.1808	0.001	0.0362	0.166
Salinity	0.516	0.001	0.3708	0.001
Dissolved Oxygen Concentration	0.7092	0.001	0.6548	0.001

Table 3.S6. Summary of the KEGG level 1 pathways and OTU (0.05) Bray-Curtis β- diversity NMDS ordination relationships.

KEGG Level 1	**Rib**		**Scapula**	
	r^2	p-value	r^2	p-value
Cellular Processes	0.5274	0.001	0.3644	0.001
Environmental Information Processing	0.7162	0.001	0.5021	0.001
Genetic Information Processing	0.1926	0.001	0.5694	0.001
Human Diseases	0.2532	0.001	0.5168	0.001
Metabolism	0.8832	0.001	0.8369	0.001
Organismal Systems	0.3489	0.001	0.4144	0.001

Table 3.S7. Summary of KEGG level 2 pathways relationships with OTU (0.05) Bray-Curtis β-diversity NMDS ordination

KEGG Level 2	Rib		Scapula	
	r^2	p-value	r^2	p-value
Nucleotide Metabolism	0.2253	0.001	0.4924	0.001
Biosynthesis of Other Secondary Metabolites	0.499	0.001	0.4794	0.001
Metabolism of Other Amino Acids	0.3625	0.001	0.543	0.001
Enzyme Families	0.039	0.212	0.0732	0.018
Glycan Biosynthesis and Metabolism	0.2313	0.001	0.1678	0.001
Energy Metabolism	0.8906	0.001	0.6761	0.001
Metabolism of Cofactors and Vitamins	0.0863	0.029	0.1353	0.001
Lipid Metabolism	0.8803	0.001	0.83	0.001
Xenobiotics Biodegradation and Metabolism	0.848	0.001	0.7903	0.001
Metabolism of Terpenoids and Polyketides	0.9315	0.001	0.8552	0.001
Amino Acid Metabolism	0.8134	0.001	0.864	0.001
Carbohydrate Metabolism	0.3132	0.001	0.6734	0.001

Supplemental References

1. P. Schloss, *et al*., Introducing mothur: Open-source, platform-independent, community-supported software for describing and comparing microbial communities. *Applied and Environmental Microbiology* **75**, 7537-7541 (2009).
2. R Core Team, R: A Language and Environment for Statistical Computing (2019).
3. J. Oksanen, *et al*., vegan: Community Ecology Package (2019).

Chapter 4: The Microbiome Associated with *Sus scrofa* Bone from Lacustrine and Riverine Environments in Virginia

Abstract

Microbial communities between lakes and rivers may vary due to physical and chemical differences, such as available nutrients, water source, spatial dimensions, and flow rate. More specifically, benthic bacteria, which are often recovered from lake or stream beds where remains settle, may be important to creating a microbial clock for estimating time since death in aquatic environments, as they participate in the breakdown of organic matter. Previous studies that focused on aquatic microbial decomposition succession have successfully identified indicator taxa and patterns of succession; however, none have compared a freshwater lake and river in the same geographic region. Therefore, this study sought to identify and compare changes in skeletal element bacterial community relative abundances and diversity estimates between Henley Lake and the James River within the state of Virginia. Approximately every 250 accumulated degree days (ADD), five ribs and five scapulae were collected along with a water sample. All samples underwent 16S rDNA variable region 4 (V4) library preparation and Illumina MiSeq sequencing. Site-specific differences among water, rib and scapula samples were identified. While alpha-diversity increased with time, it was higher at the James River site. Furthermore, separation in beta-diversity between sites was also noted and related to different environmental parameters and family-level taxa.

Significance Statement

In 2017, the Office of the Chief Medical Examiner reported 138 deaths by drowning in Virginia alone (1). Unfortunately, methods for estimating the period of submersion, which aids investigators in determining identity as well as cause and manner of death, are limited and not validated. Recent studies have sought to utilize microbial succession to estimate the post-mortem submersion interval (PMSI); however, these studies have not explored the impact of different aquatic environments (e.g., river versus lake) on microbial succession. Therefore, this study

provides proof of concept that skeletal element microbial succession can be utilized to estimate long-term PMSI, regardless of recovery from different freshwater environments.

Introduction

Freshwater environments are generally grouped into lentic or lotic systems, depending on water movement. Lentic systems, such as ponds or lakes, are categorized by standing water; whereas lotic systems are characterized by flowing waters (e.g., rivers and canals) (2). Physically, lakes vary in size, have relatively broad circular perimeters and experience low current velocity with lack of continuous flow in a definite direction (i.e., standing/static waters) (2,3). Water found in lakes is derived from higher order rivers, creeks and streams, and, as a result, individual lake chemistry depends on the inflow of water and entering nutrients, dissolved organic matter, etc. The pelagic zone, the main part of the lake, has minimal light penetration, consists of the vertical water column and is dominated by free-floating bacteria, algae and invertebrates. Weather conditions, which influence physical parameters (e.g., light concentration) and chemical conditions (e.g., nutrient availability), impact the development and growth of these microorganisms. Shallow lakes (i.e., lakes not exceeding a 10 m depth) are potentially low-nutrient bodies of water and develop an expansive autotrophic benthic community. Benthic bacteria often recovered from the lake or stream bed, are important in breaking down organic matter. Rivers fed by lower order streams are typically warmer, narrower, longer, and experience turbulent water disturbance; due to these factors, only attached microorganisms remain in their waters, and competition to colonize exposed surfaces and obtain available nutrients is created. Furthermore, all of these conditions allow benthic organisms to create microhabitats, allowing them to dominate streams and rivers.

Because lentic and lotic systems vary both physically and chemically, their inherent microbial communities may vary. Understanding these differences has significant implications for both microbial ecology and forensic science, as changes in microbial communities and the identification of indicator taxa can aid in the ability to predict temporal succession (e.g., stream health, biofilm formation and time of submersion) (4). Patterns of microbial succession have been observed in terrestrial settings as a method for estimating time since death, or the postmortem interval (PMI) (4-9). As the ability to apply terrestrial-based PMI estimation methods is impacted by inherent differences with terrestrial systems (e.g., lack of necrophagous insect access), studies have focused on identifying microorganisms specific to porcine decomposition in aquatic

environments (10, 11) for the prediction of the postmortem submersion interval (PMSI), or the time of submersion until recovery.

While Dickson et al. (10) identified dominating phyla, such as Proteobacteria, Bacteroidetes, Firmicutes, Fusobacteria and Actinobacteria, and reported bacterial community succession in autumn (N=1) and winter seasons (N=2), their study focused on only submerged porcine heads in a marine environment. A second study, which submerged stillborn porcine remains (N=3) in a freshwater stream during summer and winter trials, also identified Proteobacteria and Firmicutes as dominant phyla (11). In addition, an increase in genera was also observed in summer (e.g., 21 to 82, over 21 days) and winter (e.g., 38 to 109, over 42 days). Lang et al. (4) sought to detect differences between freshwater streams in Ohio and Pennsylvania by submerging both hexagonal unglazed porcelain tiles (epilithic) and stillborn porcine carcasses (epinecrotic). Significant differences were identified between locations and sample types (e.g., epilithic and epinecrotic); however, successional patterns were exhibited in all sample types. While these studies provide proof of concept that microbial community succession occurs in aquatic environments, and may vary between freshwater streams, information is lacking regarding similarities or differences in various freshwater ecosystems (i.e., freshwater river and lake), specifically in the same geographical location.

The objectives of this study were to identify and compare changes in skeletal element bacterial community relative abundances and diversity estimates between a freshwater river and lake in Virginia. To do so, porcine ribs and scapulae were submerged, since they have been reported to remain articulated in the torso for longer periods in aquatic systems (12). To monitor the influence of decomposition on the surrounding environments (and vice versa), water samples from each location were also collected. Regardless of site similarities and differences in both water and bone samples, this study also sought to assess the applicability of a freshwater lake PMSI prediction

model to samples recovered from a freshwater river (and vice versa), or the development of a Virginia-wide freshwater PMSI prediction model.

Results

The following results concerning site differences between environmental measurements, bacterial community structure, and random forest modeling estimations are detailed under each subheading.

Site and Environmental Parameters

The relationship between time since placement (days) and accumulated degree days (ADD) was linear at Henley Lake (y=-199+9.36x, R2=0.99), but curvilinear for the James River (y=123-1.1+0.061x^2, R^2=1) (Figure 4.1). For nineteen collections, the lake accumulated 5,200 degree days over 579 days, averaging 9 ºC/day; meanwhile, the river accumulated 4,972 degree days over 293 days, averaging 17 ºC/day. Overall, the river reached ~5,000 ADD in a shorter period when compared to the lake. Environmental parameters (i.e., temperature, pH, specific conductivity and salinity) differed significantly between sites; whereas, temperature was the only parameter significantly different among seasons. Furthermore, all parameters had higher values in the river (Figure 4.2, Figure 4.S1).

Bacterial Community Structure

Previous site-specific analyses indicated that sample types (i.e., scapula, rib and water) differed significantly, therefore, they were analyzed individually. For water samples, seven of the top ten taxa and nine of the top fifteen taxa from each site were shared at the class and family levels, respectively (Figure 4.3). Taxa contributing to relative abundance differences between water collected from each site were identified through similarity percentages (SIMPER analysis) and include Synechococcophycideae (e.g., Synechococcaceae), Nostocophycideae, Flavobacteria, Pedosphaerae (e.g., R4-41B) and Opitutae (Figure 4.S2). While Actinobacteria were identified as influential taxa at the class level, only ACK-M1 differed significantly between water samples at the family level.

The top six phyla were shared among all sample types and locations, but their ranked abundances varied after Firmicutes and Proteobacteria (Figure 4.S3). Firmicutes remained in high abundances

in rib samples at both locations, while a gradual decrease was noted in scapulae. Similarly, Proteobacteria decreased across ADD in all samples. While Acidobacteria and Spirochaetes increased, Acidobacteria were present in higher abundances at the James River site.

For rib samples, 12 of the top 15 families were shared between sites (Figure 4.3). Significant differences between locations were influenced by Clostridia (e.g., Clostridiaceae), Holophagae (e.g., Holophagaceae) and Spirochaetes (e.g., Spirochaetaceae) (Figure 4.S4, Figure 4.4). Of the top 15 families, 13 taxa were shared between sites for scapulae (Figure 4.3). Fewer taxa influenced the site differences for scapulae, including Clostridia (e.g., Clostridiaceae, Veillonellaceae) and Spirochaetes (e.g., Spirochaetaceae) (Figure 4.S4, Figure 4.4). At the family level, differences in Enterobacteriaceae were also identified as significantly different between sites for both rib and scapula samples.

Furthermore, at the family level Clostridiaceae and Ruminococcaceae were the most abundant taxa in ribs and decreased over time; meanwhile, Holophagaceae was the most abundant taxa in scapulae and increased with ADD. While there were overall site differences, it was noted that bacterial communities recovered from each bone type (e.g., Henley Lake ribs compared to James River ribs) were more similar to each other across sites than between bone types within sites.

Bacterial Diversity

For both bone types and locations, phylogenetic diversity (PD) increased with ADD, as the highest alpha diversity estimates were noted at later collections (Figure 5.5). Henley Lake scapulae were the only samples that demonstrated a linear relationship between PD and ADD ($y=7.88+0.00665x$, $R^2=0.73$); the remaining relationships were curvilinear. Variability in Henley Lake scapulae and ribs was corelated to ADD (linear model ANOVA, $p<0.0001$); furthermore, temperature also influenced scapulae (linear model ANOVA, $p=0.0026$). At the James River, diversity in both sample types was impacted by ADD (linear model ANOVA, $p<0.0001$), temperature (linear model ANOVA, Rib: $p=0.0002$, Scapula: $p<0.0001$) and season (linear model ANOVA, Rib: $p=0.0337$, Scapula: $p<0.0001$). Additionally, pH (linear model ANOVA, $p=0.0010$) was correlated with diversity on ribs, whereas specific conductivity (linear model ANOVA,

p=0.0054) was related to variability in scapulae diversity. Though both sites demonstrated variability across ADD, diversity was generally higher in James River samples.

Using weighted and unweighted UniFrac distances, samples ordinated chronologically along NMDS1 for both bone types and sites (Figure 4.6, Figure 4.S5). While both ordinations demonstrated separation in earlier ADD groupings, separation was greater when abundances were also considered (i.e., weighted UniFrac). Similarly, separation between sites was also observed along NMDS2 (Figure 4.6, Figure 4.S5). Site differences for both weighted (PERMANOVA, Rib: *pseudo*-F=16, R^2=0.10, p=0.001, Scapula: *pseudo*-F=28, R^2=0.14, p=0.001) and unweighted (PERMANOVA, Rib: *pseudo*-F=20, R^2=0.12, p=0.0010 ; Scapula: *pseudo*-F=35, R^2=0.13, p=0.0010) metrics were identified.

To explain separation between sites, the top fifteen families as well as environmental parameters were fitted, as vectors, to the weighted UniFrac ordination (Figure 4.S6, Figure 4.S7, Table 4.S2 and Table 4.S3). Salinity, pH and temperature were correlated with separation of the James River samples along NMDS2, while specific conductivity was related to Henley Lake (Figure 4.S6, Table 4.S2). ADD was the only parameter associated with NMDS1, driving separation in sample collections. In both bone types, Veillonellaceae, Rhodocyclaceae Comamonadaceae, Sediment-4 and Ruminococcaceae contributed to separation of James River samples along NMDS1 (Figure 4.S7, Table 4.S3). Meanwhile, Henley Lake sample ordination along NMDS1 was related with Bacteroidaceae, Mogibacteriaceae, Rikenellaceae and Spirochaetaceae.

Random Forest Model for PMSI Prediction

PMSI estimation models were developed for both Henley Lake and James River samples. For Henley Lake, the scapula model was more precise, explaining ~96% of the variation in predicted ADD, with a root mean square error (RMSE) of 333.48 (~37 days); meanwhile, the rib model outperformed the scapula model at the James River, explaining ~94% of the variation with a RMSE of 472.31 ADD (~ 28 days) (Figure 4.7). Within each bone type, at least 2 of the top 10 most influential taxa were shared between locations (Rib: Spirochataceae and Ruminococcaceae; Scapula: Syntrophomonadaceae and Sediment-4) (Figure 4.8).

Discussion

To determine if predictable bacterial community succession occurred on skeletal elements in different aquatic environments in Virginia over time, this study utilized 16S rDNA MiSeq sequencing techniques. Because previous site-specific analysis suggested that bacterial community structure in rib, water and scapula samples differed significantly, succession patterns that were identified in each sample type were compared between sites (e.g., freshwater river and lake). When comparing locations, some similarities were noted, but significant differences between sites, as well as the bacteria responsible for driving those differences, were identified. Differences between locations, are likely attributable to the environmental parameters. Overall, temperature, pH, salinity and specific conductivity differed significantly between sites and were notably higher at the James River site. Furthermore, temperature differed significantly among seasons, which has previously been reported (13), along with variability in other measurements within locations and seasons.

In water samples, relative abundances of Synechococcophycideae (e.g., Synechococcaceae), Nostocophycideae, Flavobacteria, Pedosphaerae (e.g., R4-41B) and Opitutae contributed to differences between site microbial community structure. Synechococcophycideae and Nostocophycideae were recovered from the James River and Henley Lake, respectively. These families belong to the phylum Cyanobacteria, which have been recovered from most habitats, including freshwater ecosystems (14-16). This phyla, composed of photosynthetic prokaryotes synthesizes chlorophyll-a. As free living organisms, Flavobacteria, which were included in the top ten classes recovered from Henley Lake, are ubiquitous in soil and water environments. While they are not part of animal (or human) flora (17), they have been reported to be responsible for fish diseases (18). Pedosphaerae and Opitutae belong to the phylum Verrucomicrobia, which have been recovered from different freshwater rivers, lakes and as eukaryotic symbionts (19-21); however, little is known about their ecology in freshwater systems. While identified as significantly different only at the family level, ACK-M1 was present in relatively high abundance in both locations. Previous studies have also recovered ACK-M1 from both lake and river freshwater ecosystems (22) and suggested that its presence is related to high-pH lakes (19).

For bone samples at all locations, the same top six phyla were recovered, however, after Firmicutes and Proteobacteria, their ranked abundances varied. At the class and family levels, differences between locations were attributed to Clostridia (e.g., Clostridiaceae), Holophagae

(e.g., Holophagaceae) and Spirochaetes (e.g., Spirochaetaceae) for rib samples; meanwhile, site differences in scapulae were due to Clostridia (e.g., Clostridiaceae, Veillonellaceae) and Spirochaetes (e.g., Spirochaetaceae) relative abundances. For both bone types, relative abundances of Enterobacteriaceae were only significant when family-level taxa were considered. As proposed by previous studies, the increased abundances of Clostridia in rib samples may be related to the greater amounts of adipocere present in the Henley Lake samples (Figure S8). The formation of adipocere, also referred to as grave or corpse wax, results from lipid saponification in wet anaerobic environments (23, 24). The lack of adipocere at the James River site may be related to the presence of scavengers (e.g., blue crabs) and increased water flow, as these factors, along with temperature and water chemistry, are known to alter the rate of decomposition (25). While both sites demonstrated black discoloration of bone samples, the James River scapulae samples demonstrated staining at earlier periods with increased coverage when compared to Henley Lake. Dark staining on bone has been recognized as the formation of ferrous sulphide (FeS), which is also formed in anaerobic environments by sulphate-reducing bacteria, such as gram-positive Clostridia and gram-negative Deltaproteobacteria (Figure S9). Generally, Clostridia abundances were higher in rib samples, which may be related to the presence of both adipocere and black discoloration. Overall, Clostridiaceae and Clostridium (i.e., Firmicutes, Clostridia) have been proposed as a key contributor to the decomposition of various organisms (e.g., murine, porcine and human) in terrestrial environment (6-8, 26).

The highest estimates of phylogenetic diversity (PD) were observed at increased ADD and in James River samples. While increasing diversity contrasts with the decrease observed in early stage terrestrial decomposition (6, 27), it is similar to previously published diversity estimates from aquatic decomposition (11) and in advanced stages of terrestrial decomposition (27). Elevated alpha diversity at the James River site may be related to site-specific environmental factors, as temperature, pH, specific conductivity and salinity were also observed to be higher. Another major difference between the two locations is increased water flow in the James River compared to the more stagnant Henley Lake environment.

Beta-diversity estimates demonstrated chronological ordination along NMDS1 and separation of locations along NMDS2. Site separation was explained by both the top fifteen families recovered from each site and environmental parameters. For ribs and scapulae, Veillonellaceae, Rhodocyclaceae Comamonadaceae, Sediment-4 and Ruminococcaceae contributed to separation of James River samples; meanwhile, Bacteroidaceae, Mogibacteriaceae,

Rikenellaceae and Spirochaetaceae drove separation of samples from Henley Lake. These taxa may have been influenced by environmental parameters. ADD contributed to chronological separation along NMDS1, suggesting that, regardless of location, cumulative temperature influences bacterial community structure; additionally, salinity, pH and temperature was related to the James River site and specific conductivity correlated with the Henley Lake site. Previous studies have also reported that temperature (28), pH (13, 29), salinity (30-32), and specific conductivity (33) have impacted microbial community structure and/or function. As other factors, such as organic matter, phosphates, chlorides, sulphates, nitrates and nitrites, have been reported to influence community structure (13, 34); therefore, future studies might consider measuring these parameters.

Rib-specific PMSI models shared both Spirochataceae and Ruminococcaceae in the top 10 most influential taxa. Spirochaetaceae has been reported as an indicator family for one-year salmon carcasses in epinecrotic communities (35). Ruminococcaceae are short chain fatty acid (SCFA) producers in the class Clostridia that participate in the degradation of polysaccharides (36). Meanwihle, Syntrophomonadaceae and Sediment-4 were the bacterial families shared between locations for scapulae. Syntrophomonadaceae, a family of gram-positive bacteria, are integral in the degredation of fatty acids (37). The remaining prominent bacterial contributors differ from those observed in terrestrial decomposition studies. This difference may be attributed to the presence of insect-associated bacteria (8, 38, 39) related to direct insect colonization, which does not occur in aquatic decomposition. Therefore, when we consider all of the taxa utilized to develop the random forest models (Henley Lake: 24 rib and 34 scapula, James River: 41 rib and 55 scapula), enough similarities may exist to generate a freshwater-specific model. As a result of inherient difficulties with random forest modeling, testing the performance of the Henley lake model with James River samples (and vice versa), as well as the development of a combined (e.g., freshwater specific) model, is currently being explored.

Conclusion

Alpha-diversity increased with time of submersion for both ribs and scapulae; however, diversity estimates were higher at the James River site. Furthermore, separation in beta-diversity was also noted between sites and related to different environmental parameters and family-level taxa. Of the top 10 indictor taxa utilized in the site-specific random forest models, at least two taxa were shared between sites for each bone type. Continuing research evaluates the performance of the

Henley lake model with James River samples (and vice versa), as well as the development of a combined (e.g., freshwater specific) model.

Materials and Methods

Field set up, sample collection, DNA extraction and quantification, 16S rDNA amplification, MiSeq sequencing-by-synthesis, and sequence data pre-processing was previously outlined in *Modeling Postmortem Submersion Interval (PMSI) Estimation From the Microbiome of Sus scrofa Bone in a Freshwater Lake* and *Postmortem Submersion Interval (PMSI) Estimation from the Microbiome of Sus scrofa Bone in a Freshwater River.* Of the original datasets, nineteen collections from each site were utilized in this study, totaling 38 collections plus baseline samples. To combine files for quality control pre-processing in mothur v1.39.5 (40), files for each sample type were merged (*merge.files*), aligned (*align.seqs*) to the SILVA reference database (41), screened (*screen.seqs*, start=13862, end=23444) and filtered (*filter.seqs*) before undergoing phylogenetic and operational taxonomic unit (OTU) clustering.

Statistical Analyses

Statistical analyses and visualization for environmental and water quality measurements, taxonomic classification and diversity metrics were performed with R v3.6.0 (42). The relationship between the number of days since placement and ADD was estimated using linear regression (*lm*; stats package version 3.6.0). Furthermore, seasonal and site differences were measured via analysis of variance using the *aov* function in stats package version 3.6.0 (42) and visualized using both *geom_point* and *geom_boxplot* (43).

Site differences between rib, scapula and water bacterial community relative abundances at the class and family level were identified via similarity of percentage analyses in the vegan package version 2.5.5 (44), and tested using *kruskal.test* in the stats package version 3.6.0, respectively (42). Taxonomic level relative abundances for each sample type (i.e., rib, scapula and water) and location were visualized with stacked bar graphs using ggplot2 package version 3.2.1 (43). Venn diagrams of bacterial taxa present were created with VennDiagram package version 1.6.20 to visualize differences and/or similarities between sites (45). Taxa relative abundances were also utilized to develop PMSI random forest models, as proposed by Forger et al., using the randomForest package (46, 47).

Shifts in phylogenetic α-diversity over time and between sites were assessed with linear modeling (*lm;* stats package) (42) and visualization (*geom_point*; ggplot2 package) (44). β- diversity UniFrac (weighted and unweighted) distances were estimated via phyloseq object assembly (*UniFrac*; phyloseq package version 1.28.0) (48, 49). Resulting distances were ordinated using non-metric multidimensional scaling (NMDS) (permutations=999). Significant differences between sites were tested using permutational multivariate analysis of variance (PERMANOVA) (*adonis*; vegan package) (44). Both water quality estimates or site parameters (i.e., temperature, ADD, pH, salinity, etc.) and the top fifteen families were fit to the UniFrac weighted ordination with the *envfit* function (vegan package) (44). Plotted vectors ($\alpha < 0.05$) and associated squared correlation coefficients (permutations=999) were used to evaluate the importance of each parameter to the ordination.

Funding

Funding from this project was provided by the T. Simmons and B. Singh start-up grants from College of Humanities and Science of Virginia Commonwealth University (VCU), Richmond, VA; Forensic Science Foundation Lucas Grant 2016; VCU Rice Rivers Center Grant and award 2018-R2-CX-0016 of the National Institute of Justice Graduate Research Fellowship.

References

1. K. Hobron, Office of the Chief Medical Examiner Annual Report. Virginia Department of Health. Available at http://www.vdh.virginia.gov/content/uploads/sites/18/2019/04/Annual-Report-2017.pdf
2. D.C. Sigee, "Microbial Diversity and Freshwater Ecosystems" in *Freshwater Microbiology: Biodiversity and Dynamic Interactions of Microorganisms in the Aquatic Environment*, (John Wiley and Sons, Ltd, 2005).
3. M. Reddy *et al.*, Classification, Characterization and Comparison of Aquatic Ecosystems in the Landscape of Adilabad District, Telangana, Deccan Region, India. *OALib* **5**, 1-49 (2018).
4. J.M. Lang, *et al*., Microbial Biofilm Community Variation in Flowing Habitats: Potential Utility as Bioindicators of Postmortem Submersion Intervals. *Microorganisms* **4**, (2016).
5. A.A. Vass, Beyond the Grave – Understanding Human Decomposition. *Microbiology Today* **28**, 190-192 (2001).
6. Pechal, *et al.*, The potential use of bacterial community succession in forensics as described by high throughput metagenomic sequencing. *International Journal of Legal Medicine* **128**, 193-205 (2014).
7. J.L. Metcalf, *et al*., A microbial clock provides an accurate estimate of the postmortem interval in a mouse model system. *eLife* **2, (**2013).
8. E.R. Hyde, D.P. Haarmann, J.F. Petrosino, A.M. Lynne, S.R. Bucheli, Initial insights into bacterial succession during human decomposition. *International Journal of Legal Medicine* **129**, 661-671 (2015).
9. F.E. Damann, D.E. Williams, A.C. Layton, Potential Use of Bacterial Community Succession in Decarying Human Bone for Estimating Postmortem Interval. *Journal of Forensic Sciences* **60**, 844-850 (2015).
10. G.C. Dickson, R.T.M. Poulter, E.W. Maas, P.K. Probert, J.A. Kieser, Marine bacterial succession as a potential indicator of postmortem submersion interval. *Forensic Science International* **209**, (2011).
11. M.E. Benbow, J.L. Pechal, J.M. Lang, R. Erb, J.R. Wallace, The Potential of High-throughput Metagenomic Sequencing of Aquatic Bacterial Communities to Estimate the Postmortem Submersion Interval. *Journal of Forensic Sciences* **60**, 1500-1510 (2015).
12. W. Haglund, Disappearnce of Soft Tissue and the Disarticulation of Human Remains from Aqueous Environments. *Journal of Forensic Sciences* **38**, 806-815 (1993).
13. M. Kaevska, P. Videnska, K. Sedlar, I. Slana, Seasonal changes in microbial community composition in river water studied using 454-pyrosequencing. *Springerplus* **5**, 2043 – 2046 (2016).
14. M.A. Nienaber, M. Steinitz-Kannan, *A Guide to Cyanobacteria: Identification and Impact* (University Press of Kentucky, 2018).
15. L. Gaysina, A. Saraf, P. Singh, "Cyanobacteria in Diverse Habiats" in *Cyanobacteria From Basic Science to Applications*, A.K. Mishra, D.N. Tiwari, A.N. Rai, Eds. (Elsevier, 2019).
16. B.A. Whitton, M. Potts, "Introduction to the Cyanobacteria" in *Ecology of Cyanobacteria II: Their Diversity in Space and Time*, B.A. Whitton, Eds. (Springer Science+Business, 2012).
17. T.J. Inzana, "Miscellaneous Glucose-Nonfermenting Gram-Negative Bacteria" in *Diagnostic Procedure in Veterinary Bacteriology and Mycology*, G.R. Carter, J.R. Cole Jr., Eds. (Academic Press, 1990).
18. T.P. Loch, M. Faisal, Emerging flavobacterial infections in fish: A review. *Journal of Advanced Research* **6**, 283 – 300 (2014).

19. R.J. Newton, S.E. Jones, A. Eiler, K.D. McMahon, S. Bertilsson, A guide to the Natural History of Freshwater Lake Bacteria. *Microbiology and Molecular Biology Reviews* **75**, 14-49 (2011).
20. E. Chiang, *et al*., Verrucomicrobia are prevelant in north-temperate freshwater lakes and display class-level preferences between lake habitats. *PLOSone* **13**, (2018).
21. He *et al*. Ecophysiology of Freshwater Verrucomicrobia Inferred from Metagenome-Assembled Genomes, *mSphere* **2** (2017).
22. G. Zwart, B.C. Crump, M.P. Kamst-van Agterveld, F. Hagen, S. Han, Typical freshwater bacteria: an analysis of available 16S rRNA gene sequences from plankton of lakes and rivers. *Aquatic Microbial Ecology* **28**, 141 – 155 (2002).
23. M. Tsokos, R.W. Byard, Postmortem Changes: Overview in Encyclopedia of Forensic and Legal Medicine, (Elsevier Inc., 2016).
24. T. Dupras, J. Shultz, "Taphonomic Bone Staining and Color Changes in Forensic Contexts" in *Manual of Forensic Taphonomy*, J. Pokines, S.A. Symes, Eds. (CRC Press, 2013), pp. 315-340.
25. B.H. Stuart, M. Ueland, "Decomposition in Aquatic Environments" in *Taphonomy of Human Remains: Forensic Analysis of the Dead and Depositional Environment*, E.M.J. Schotsmans, N. Marquez-Grant, S.L. Forbes, Eds. (John Wiley and Sons Ltd, 2017).
26. J. Wiegel, R. Tanner, F.A. Rainey, "An Introduction to the Family Clostridiaceae" in *The Prokaryotes*, M. Dworkin, S. Falkow, E. Rosenberg, K.H. Schleifer, E. Stackebrandt, Eds. (Springer US, 2006).
27. M.S. Woolf, "Estimation of Long Term Post Mortem Interval (PMI) Based on Bacterial Community Succession on Porcine Remains," Virginia Commonwealth University, Richmond, VA. (2016).
28. S.D. Allison, J.B. Martiny, Resistance, resilience, and redundancy in microbial communities. *PNAS* **105**, 11512-11519 (2008).
29. S. Liu *et al.*, pH levels drive bacterial community structure in sediments of the Qiantang River as determined by 454 pyrosequencing. *Frontiers in Microbiology* **6**, 285 (2015).
30. A.J. Szekely, M. Berga, S. Langenheder, Mechanisms determining the fate of dispersed bacterial communities in new environments. *ISME Journal* **7**, 61-71 (2013).
31. J. Comte, S. Langenheder, M. Berga, E. Lindstrom, Contribution of different dispersal sources to the metabolic response of lake bacterioplankton following a salinity change. *Environmental Microbiology* **19**, 251-260 (2017).
32. R. Logares *et al.* Biogeography of bacterial communities exposed to progressive long-term environmental change. *ISME Journal* **7**, 937 - 948 (2013).
33. L. Liu, J. Yang, X. Yu, G. Chen, Z. Yu, Patterns in the Composition of Microbial Communities from a Subtropical River: Effects of Environmental, Spatial and Temporal Factors. *PLos ONE* **8**, e81232 (2013).
34. H. Dang, C.R. Lovell, Microbial Surface Colonization and Biofilm Development in Marine Environments. *Microbiology and Molecular Biology Reviews* **80**, 91 - 138 (2016).
35. A,M. Kielak, C.C. Barreto, G.A. Kowalchuk, J.A. van Venn, E.E. Kuramae, The Ecology of Acidobacteria: Moving beyond Genes and Genomes, *f\Frontiers in Microbiology* **7**, (2016).
36. Shang *et al*. Dietary fucoidan modulates the gut microbiota in mice by increasing the abundances of *Lactobacillus* and *Ruminococcaceae, Food Function* **7**, 3224-323 (2016).
37. B. Schink, R. Munoz, "The Family Syntrophomonadaceae" in *The Prokaryotes: Firmicutes and Tenericutes*, E. Rosenberg, E.F. DeLong, S. Lory, E. Stackebrandt, F. Thompson, Eds. (Springer, 2014), pp. 371-379.
38. B. Singh et al., A metagenomic assessment of the bacteria associated with *Lucillia sericata* and *Lucilia cuprina* (*Diptera: Calliphoridae*). *Applied Microbiology and Biotechnology* **99**, 869-883.

39. D. Wohlfahrt, M. Woolf, B. Singh, A survey of bacteria associated with various life stages of primary colonizers: *Lucilia sericata* and *Phormia regina*. *Science and Justice* **60**, 173-179.
40. P. Schloss, *et al*., Introducing mothur: Open-source, platform-independent, community-supported software for describing and comparing microbial communities. *Applied and Environmental Microbiology* **75**, 7537-7541 (2009).
41. C. Quast, *et al*., The SILVA ribosomal RNA gene database project: improved data processing and web-based tools. *Nucleic acid research* **41**, D590-D596 (2013).
42. R Core Team, R: A Language and Environment for Statistical Computing (2019).
43. J. Oksanen, *et al*., vegan: Community Ecology Package (2019).
44. H. Wickham, ggplot2: Elegant Graphics for Data Analysis (2016).
45. C. Hanbo, VennDiagram: Generate High-Resolution Venn and Euler Plots (2018).
46. L.V. Forger, M.S. Woolf, T.L. Simmons, J.L. Swall, B. Singh, A eukaryotic community succession based method for postmortem interval (PMI) estimation of decomposing porcine remains. *Forensic Science International* **302**, 109838 (2019).
47. A. Liaw, M. Wiener. Classification and Regression by randomForest, *R News* **2**, 18-22 (2002).
48. K. Dill-McFarland, Microbiota Analysis in R *R Pubs by RStudio* (2017).
49. P.J. McMurdie, S. Holmes, phyloseq: An R package for reproducible interactive analysis and graphics of microbiome census data. *PLOSone* **8**, (2013).

Figures and Tables

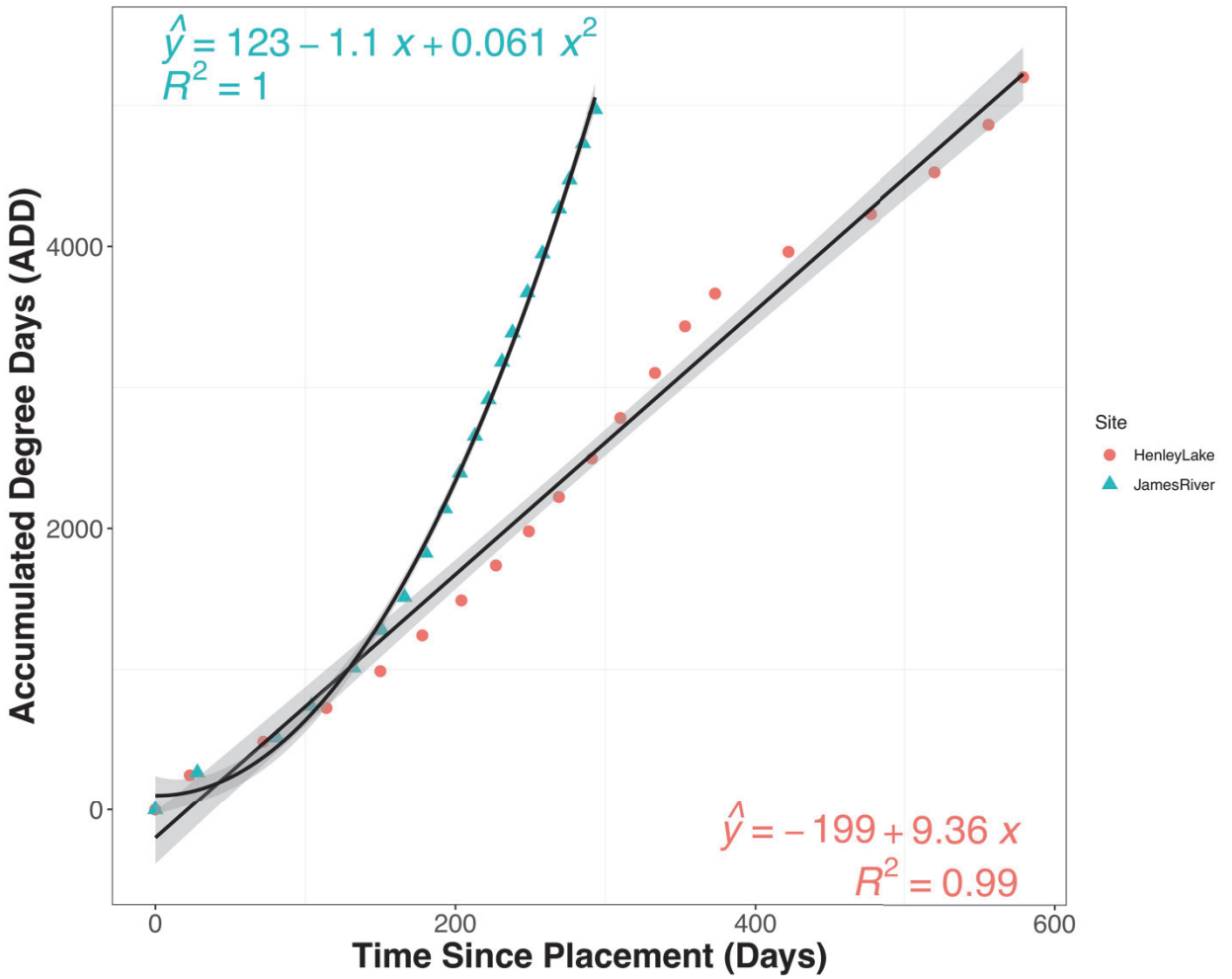

Figure 4.1. The linear and curvilinear relationship between the number of days since placement and accumulated degree days (ADD) at Henley Lake and the VCU Rice Rivers Center, respectively. The 95% confidence interval is represented by the shaded area.

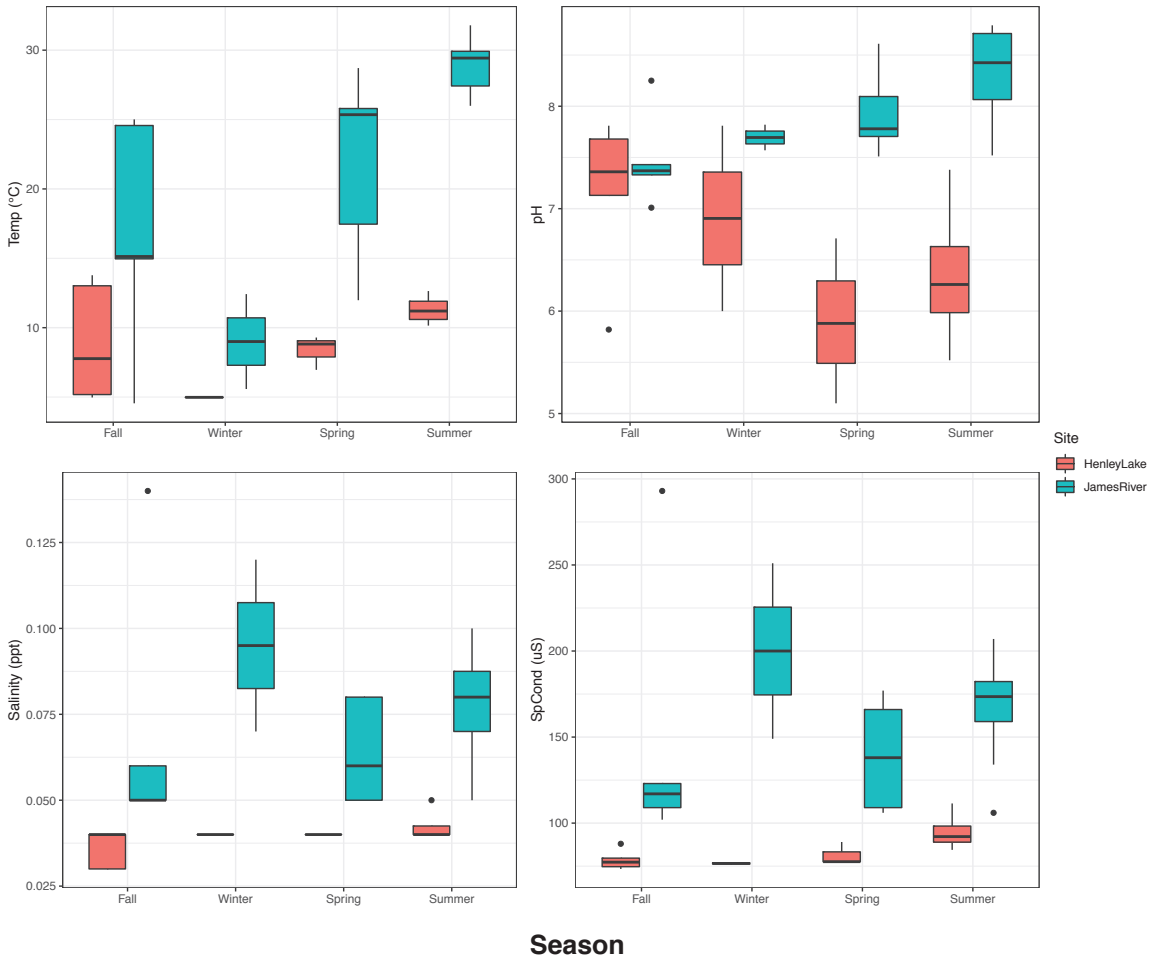

Figure 4.2. The environmental and water quality daily averages shared between sites and their seasonal differences.

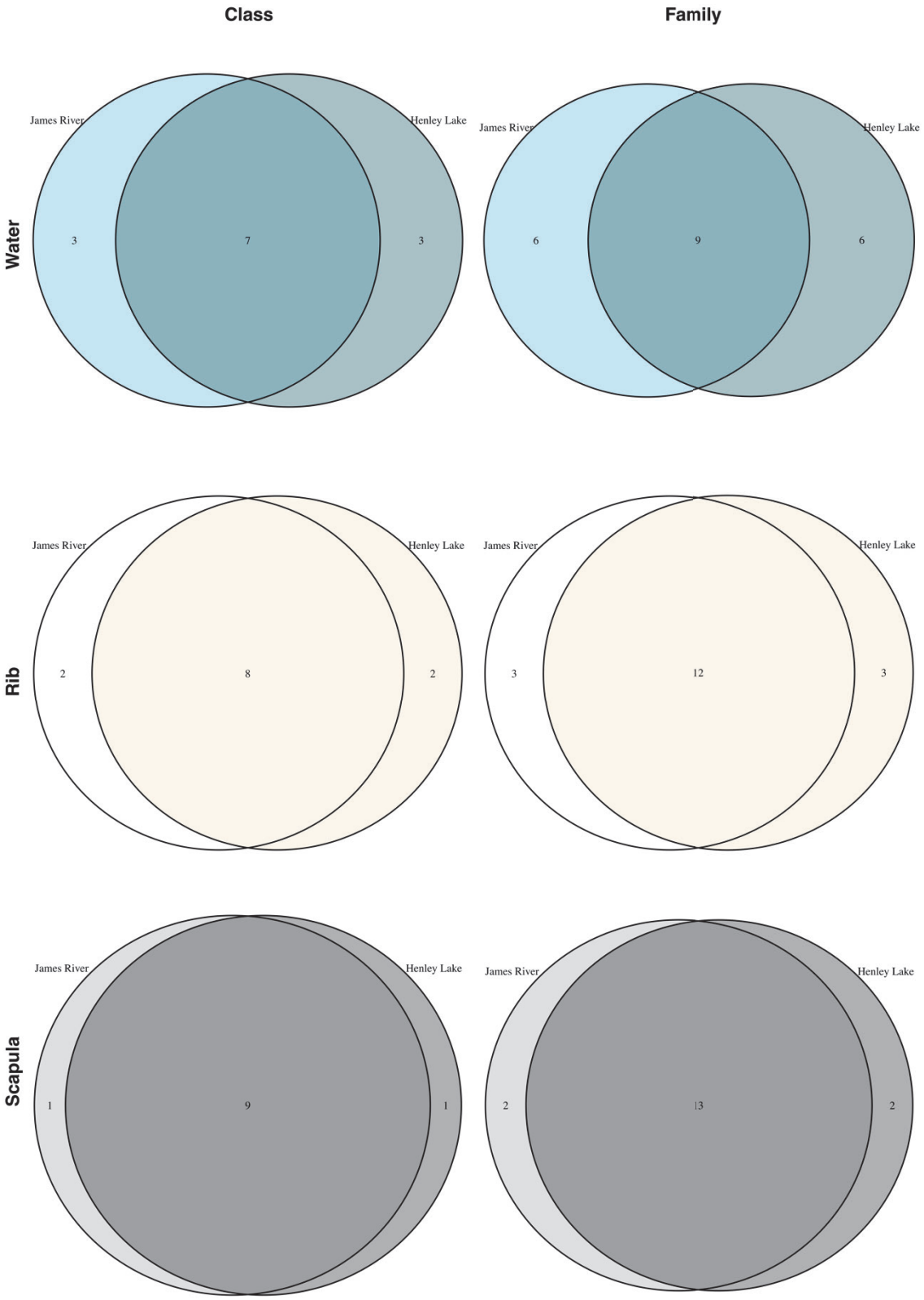

Figure 4.3. The top ten class (left) and fifteen family (right) level taxa presence shared between sites for water, rib and scapula samples.

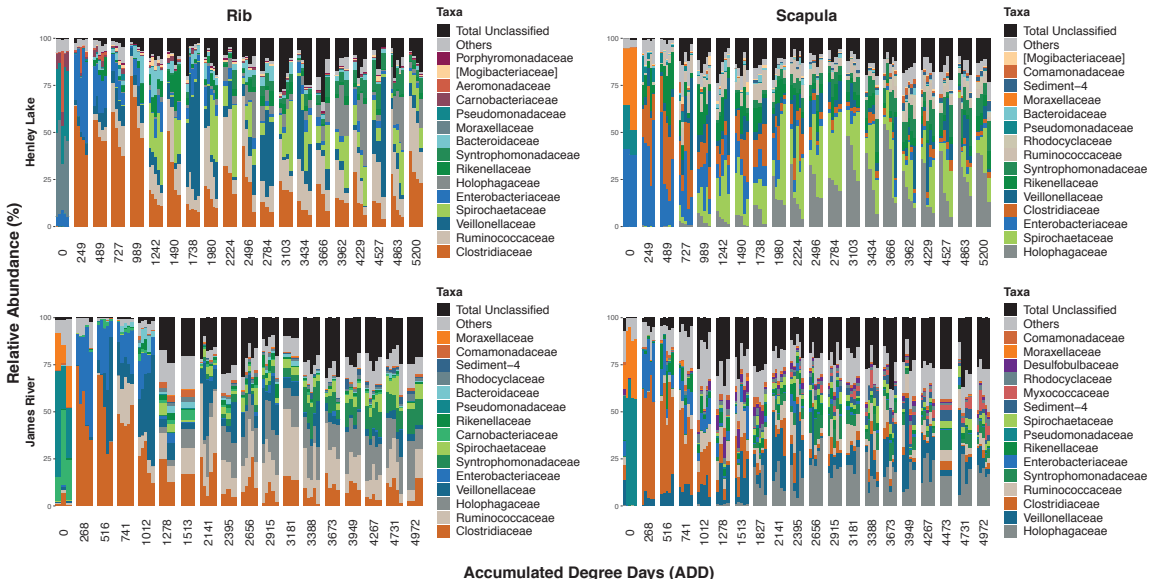

Figure 4.4. The top fifteen family level relative abundance changes for rib (left) and scapula (right) samples recovered from Henley Lake (top) and the James River (bottom) across ADD. Taxa categorized as Others and Total Unclassified comprise the remaining classified taxa and unclassified taxa, respectively. Replications are represented by invidiual bars within each ADD.

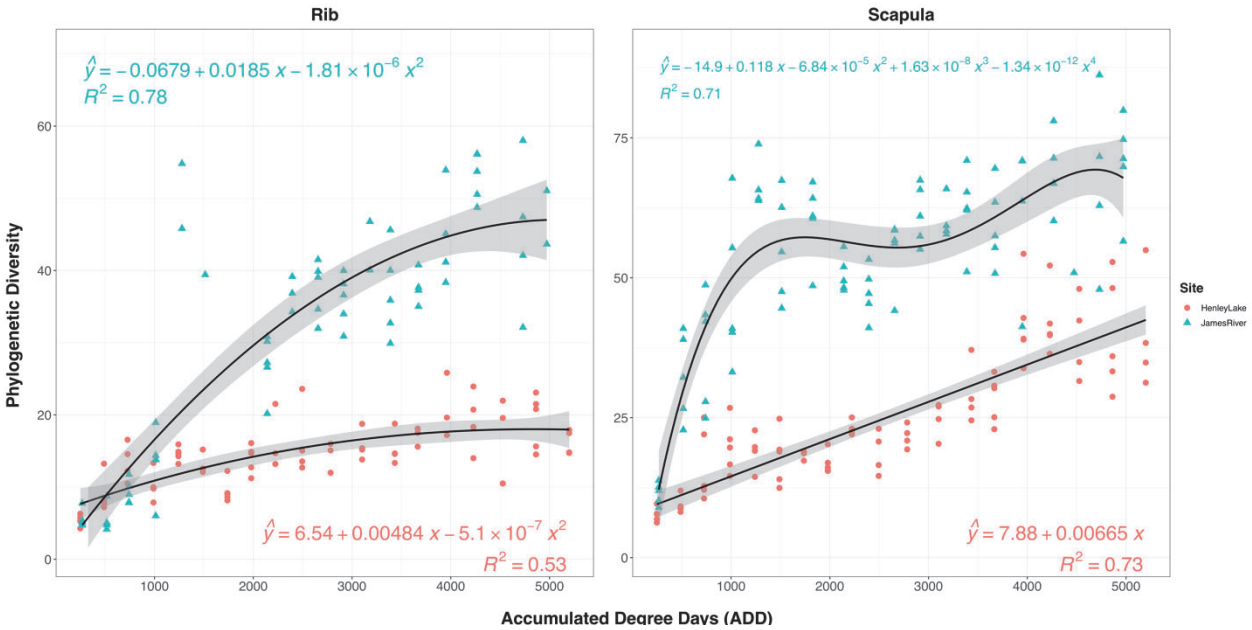

Figure 4.5. The relationships between accumulated degree days (ADD) and phylogenetic diversity for both rib (left) and scapula (right) samples recovered from both sites. The 95% confidence interval are represented by the shaded area.

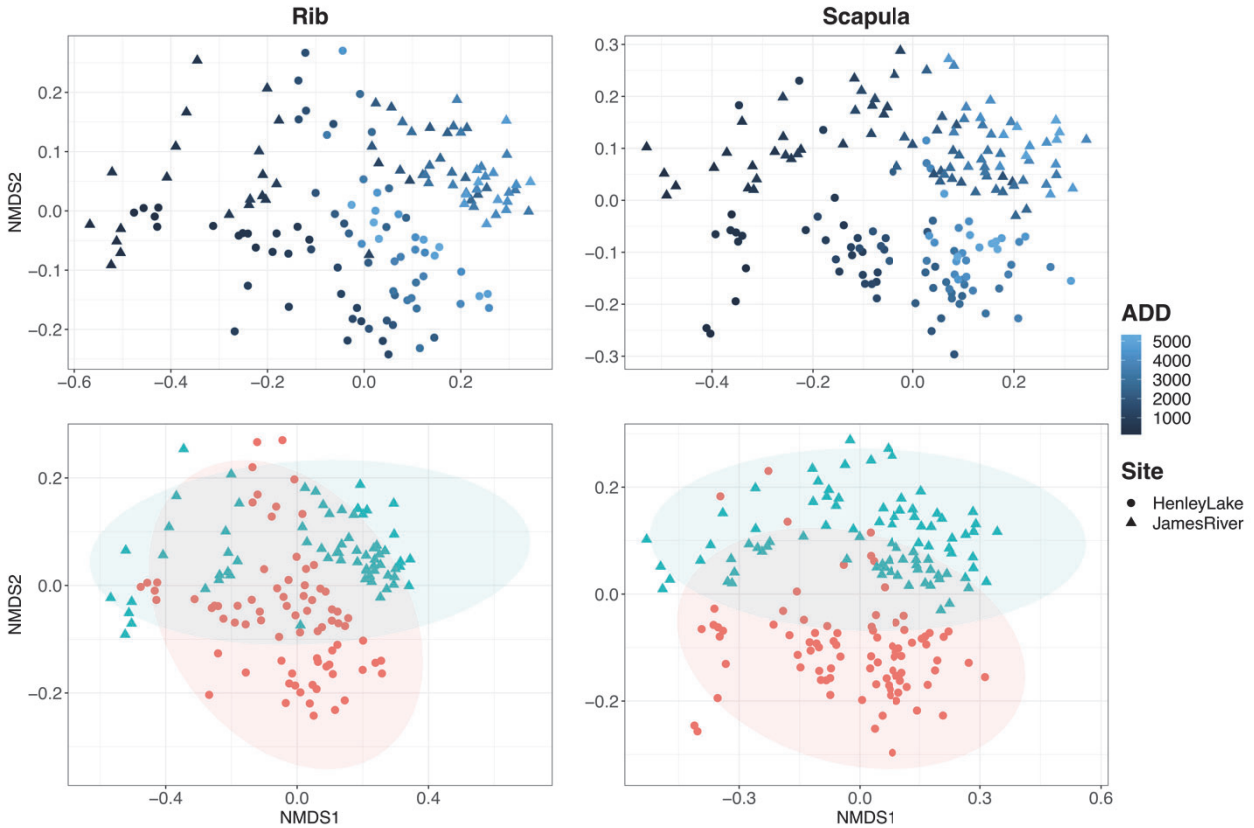

Figure 4.6. Ordination via non-metric multidimensional scaling (NMDS) for rib (2D, stress=0.1595) and scapula (2D, stress=0.1558) weighted UniFrac distances. Samples ordinated chronologically along NMDS1 (top). PERMANOVA indicated significant differences between site groupings. Mean or group centroid 95% standard error are represented by ellipses shown in the bottom panels.

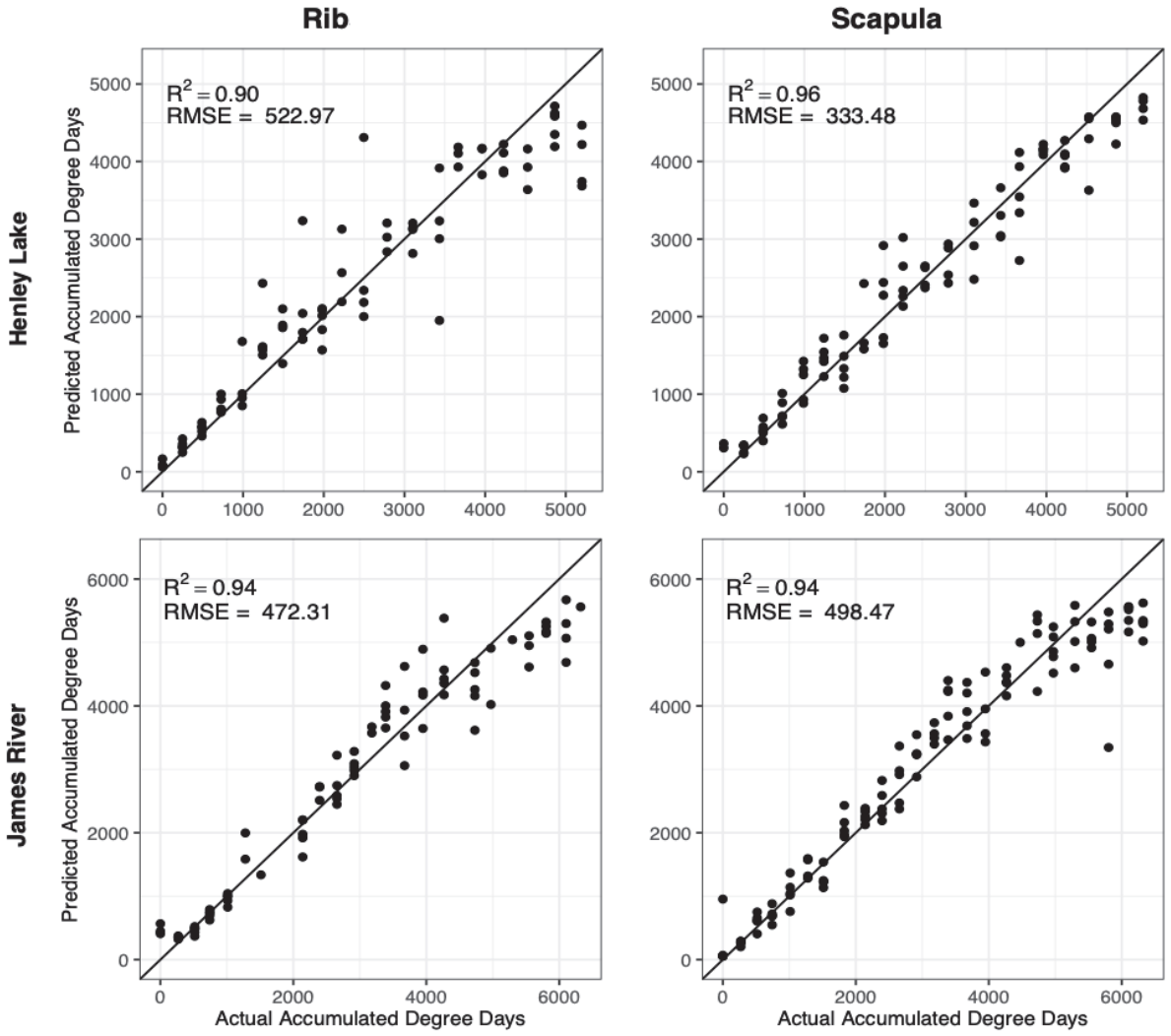

Figure 4.7. Random forest models for each skeletal element and location were developed using relative abundances of predictor bacterial taxa. Predicted accumulated degree days (ADD) versus actual ADD for rib (left panels) and scapula (right panels) samples collected from Henley Lake (top panels) and the James River (bottom panels) were plotted with a superimposed one-to-one reference line.

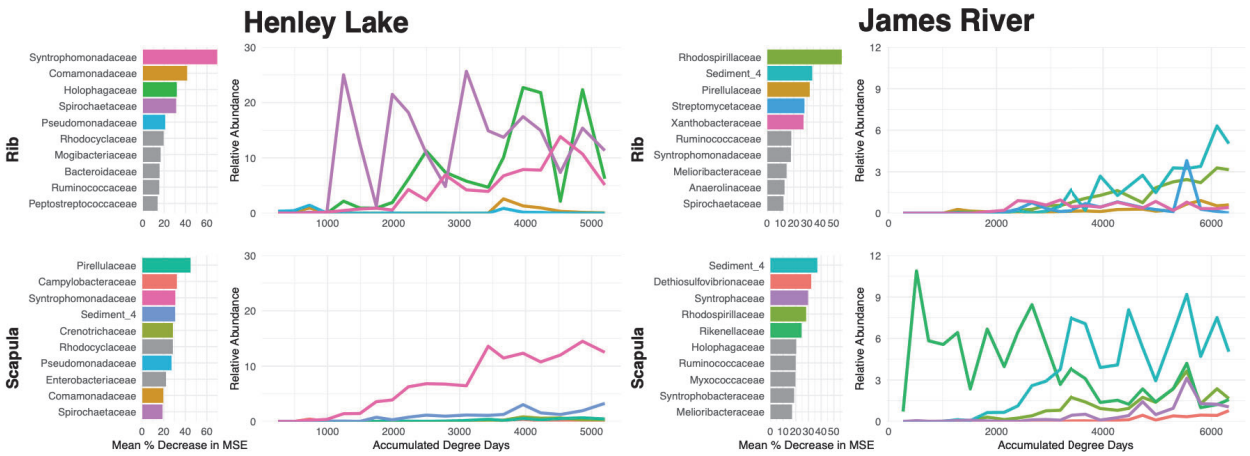

Figure 4.8. List of the top predictor bacteria taxa in decreasing order for rib (top panel) and scapula (bottom panel) samples from Henley Lake (left panel) and the James River (right panel). The changes for the highlighted predictor taxa across accumulated degree days (ADD) are depicted in the top and bottom right panels for rib and scapula, respectively.

Table 4.1. The list of accumulated degree days (ADD) and number of days for each collection at the lake and river.

	Henley Lake		James River	
Collection	**Accumulated Degree Days (ADD)**	**Time Since Placement (Days)**	**Accumulated Degree Days (ADD)**	**Time Since Placement (Days)**
Baseline	0	0	0	0
Collection 1	249	23	268	28
Collection 2	489	72	516	81
Collection 3	727	114	741	104
Collection 4	989	150	1012	132
Collection 5	1242	178	1278	151
Collection 6	1490	204	1513	166
Collection 7	1738	227	1827	180
Collection 8	1980	249	2141	193
Collection 9	2224	269	2395	203
Collection 10	2496	291	2656	213
Collection 11	2784	310	2915	222
Collection 12	3103	333	3181	231
Collection 13	3434	353	3388	238
Collection 14	3666	373	3673	248
Collection 15	3962	422	3949	258
Collection16	4229	477	4267	269
Collection 17	4527	520	4473	276
Collection 18	4863	556	4731	285
Collection 19	5200	579	4972	293

Supplemental Figures and Tables

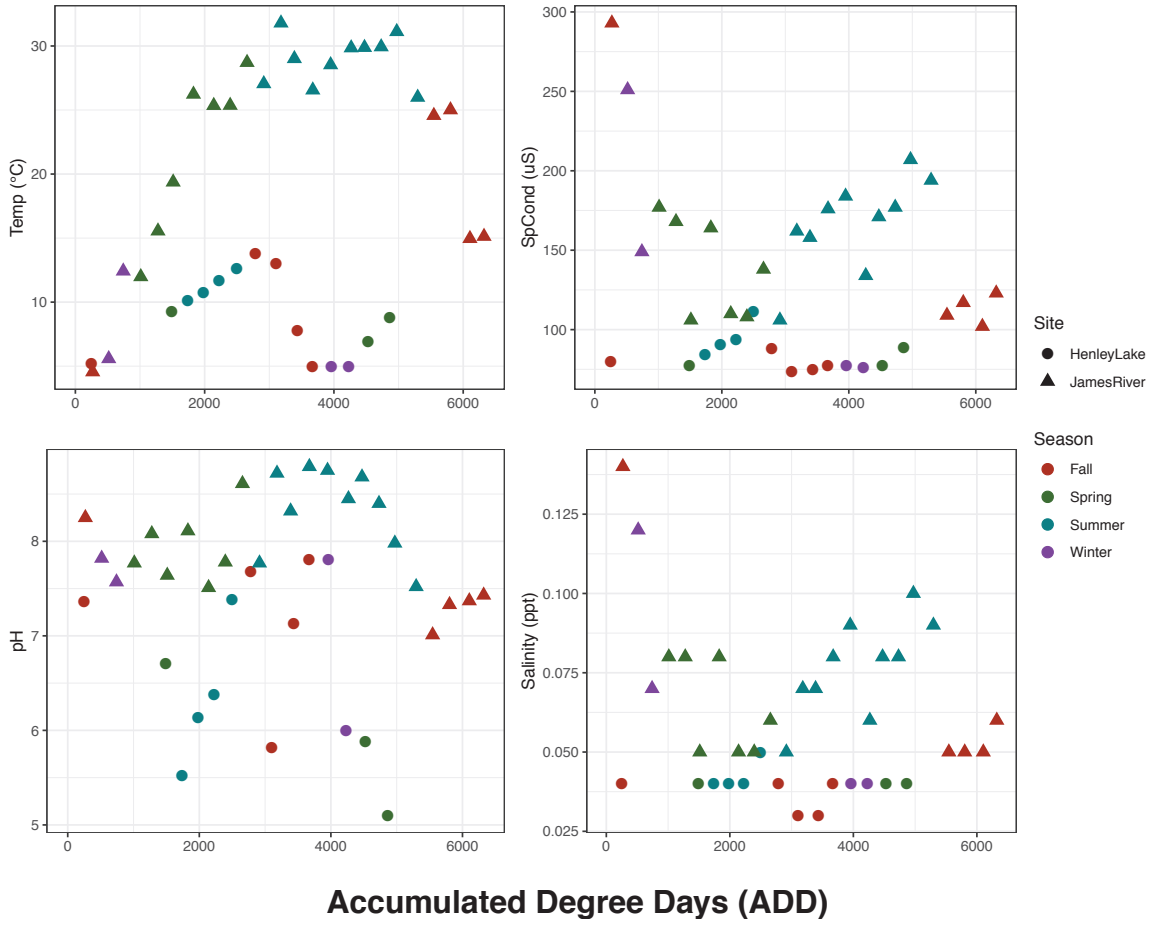

Fig. 4.S1. The changes in environmental and water quality daily averages across accumulated degree days (ADD) for each site.

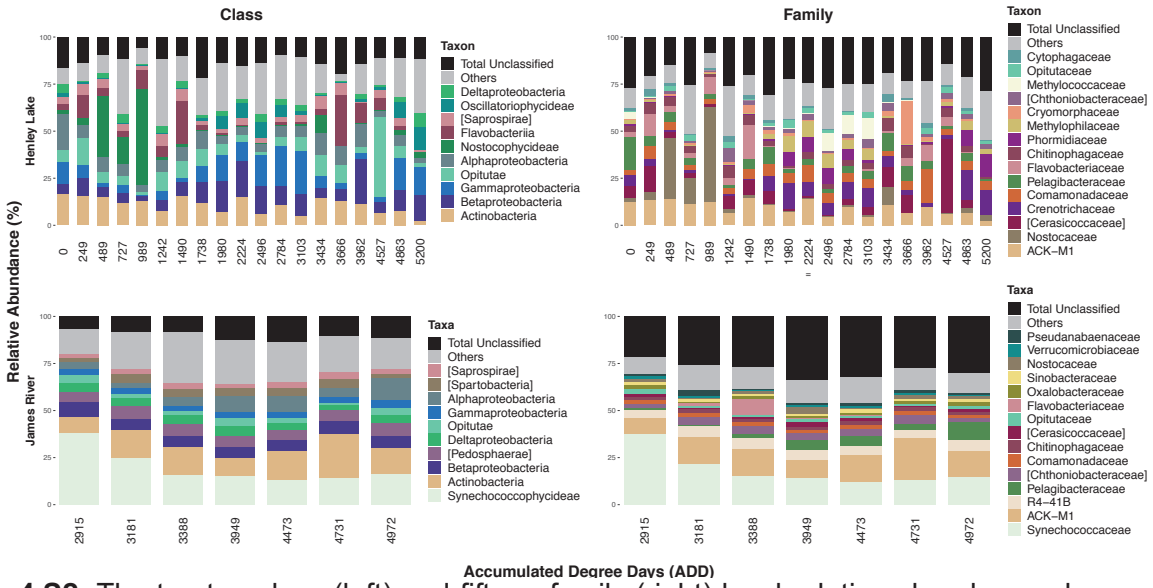

Fig. 4.S2. The top ten class (left) and fifteen family (right) level relative abundance changes for water samples recovered from Henley Lake (top) and the James River (bottom) across ADD. Taxa categorized as Others and Total Unclassified comprise the remaining classified taxa and unclassified taxa, respectively.

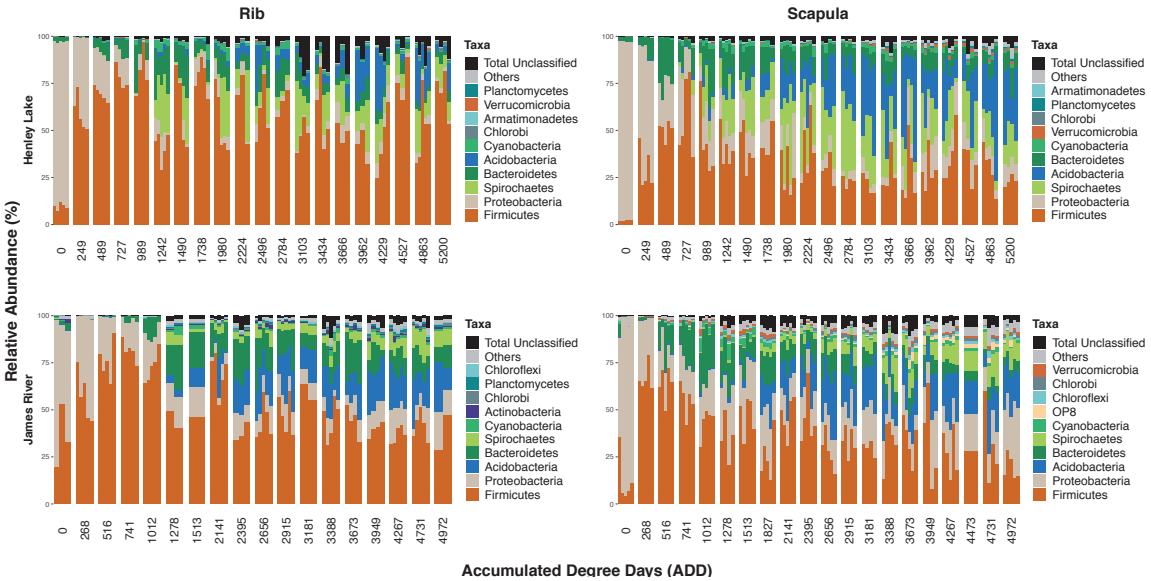

Fig. 4.S3. The top ten phylum level relative abundance changes for rib (left) and scapula (right) samples recovered from Henley Lake (top) and the James River (bottom) across ADD. Taxa categorized as Others and Total Unclassified comprise the remaining classified taxa and unclassified taxa, respectively. Bars, representing each invidiual replication, are located above each ADD.

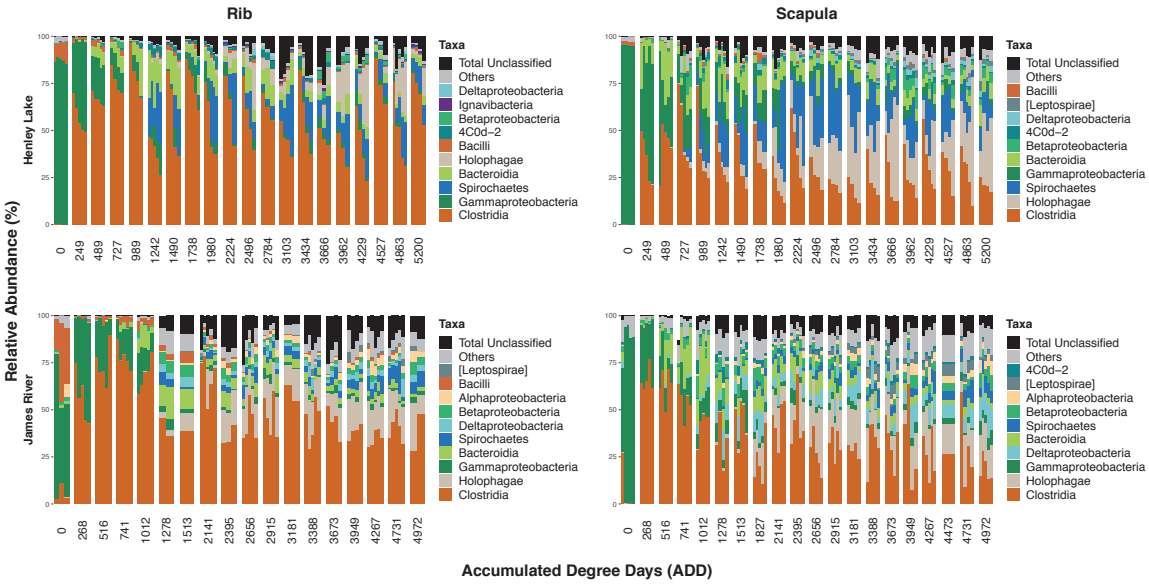

Fig. 4.S4. The top ten class level relative abundance changes for rib (left) and scapula (right) samples recovered from Henley Lake (top) and the James River (bottom) across ADD. Taxa categorized as Others and Total Unclassified comprise the remaining classified taxa and unclassified taxa, respectively. Each ADD contains individual bars, respresenting individual replications.

This resource was prepared by the author(s) using Federal funds provided by the U.S. Department of Justice. Opinions or points of view expressed are those of the author(s) and do not necessarily reflect the official position or policies of the U.S. Department of Justice.

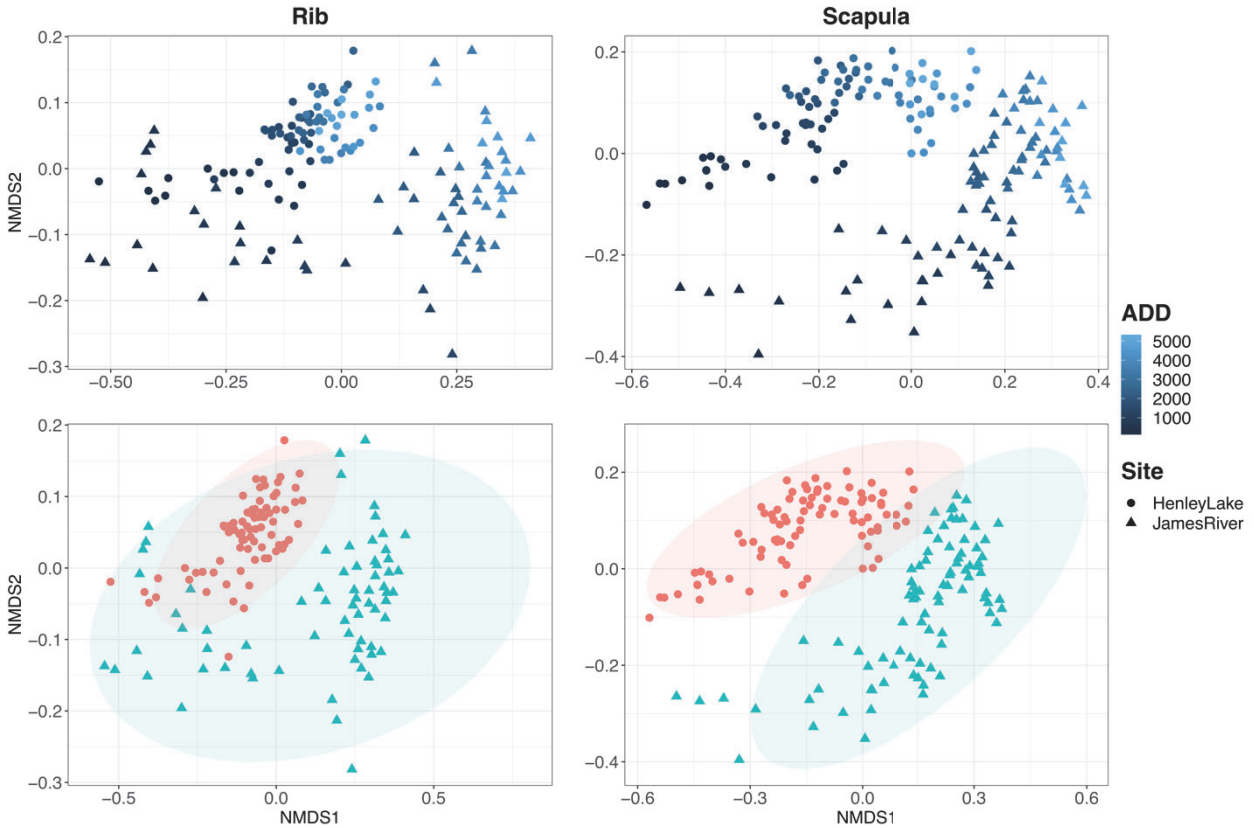

Fig. 4.S5. Ordination via non-metric multidimensional scaling (NMDS) for rib (2D, stress=0.0824) and scapula (2D, stress=0.0889) unweighted UniFrac distances. Samples ordinated chronologically along NMDS1 (top). PERMANOVA indicated significant differences between site groupings. Mean or group centroid 95% standard error are represented by ellipses shown in the bottom panels.

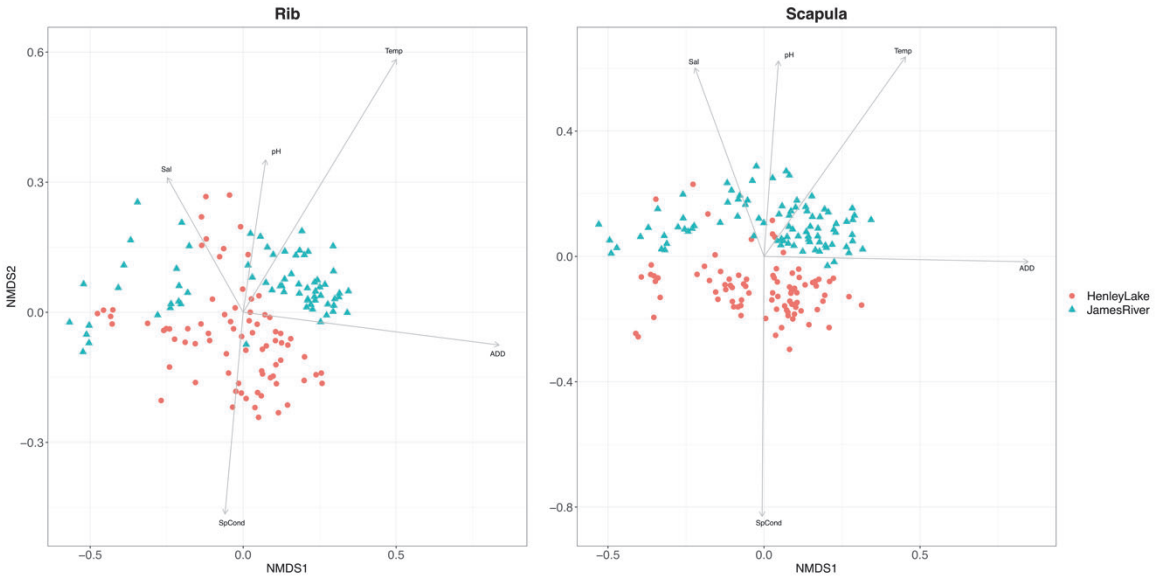

Fig. 4.S6. Vectors representing environmental parameters that were significantly related to weighted UniFrac distances non-metric multidimensional scaling (NMDS) ordination (alpha 0.05) for rib (left) and scapula (right). The strength and direction of the relationship between environmental parameters and β-diversity are indicated by the length and angle of the arrows.

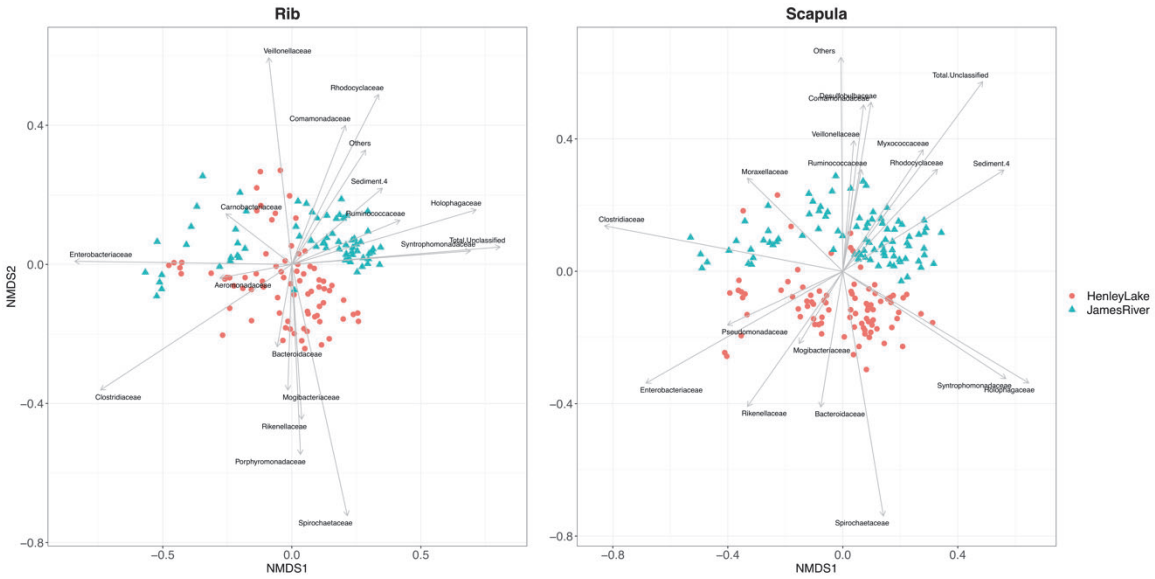

Fig. 4.S7. Vectors representing the top fifteen families for each bone type that were significantly related to weighted UniFrac distances non-metric multidimensional scaling (NMDS) ordination (alpha 0.05). The strength and direction of the relationship between the family and β-diversity are indicated by the length and angle of the arrows.

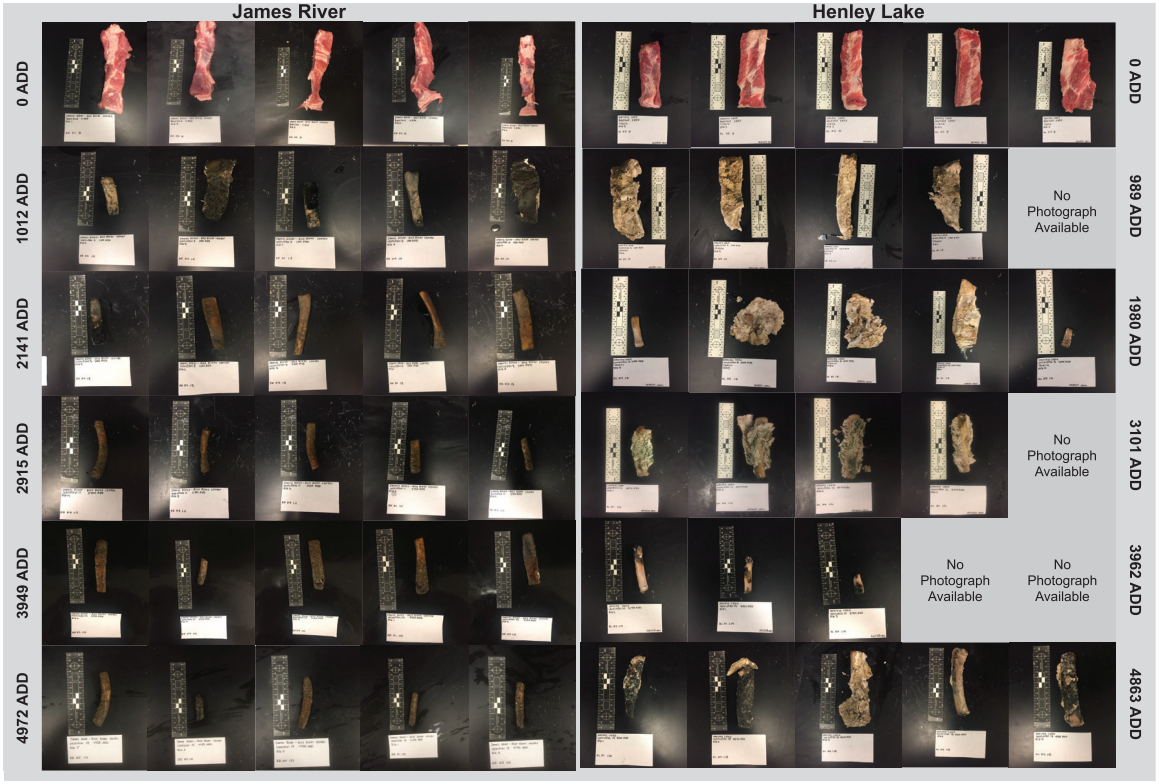

Fig. 4.S8. Observable differences in rib decomposition between sites for approximately every 1000 ADD.

Fig. 4.S9. Observable differences in scapula decomposition between sites for approximately every 1000 ADD.

Table 4.S1. For all taxonomic levels the percent of classified and unclassified sequences for the respective bone types and locations.

Taxonomy	Number of Sequences							
	Henley Lake				James River			
	Rib		Scapula		Rib		Scapula	
	Classified (%)	Unclassified (%)	Classified (%)	Unclassified (%)	Classified (%)	Unclassified (%)	Classified (%)	Unclassified (%)
Phylum	96	4	98	2	98	2	96	3
Class	94	6	94	6	92	8	93	7
Order	94	6	92	8	89	11	89	11
Family	91	9	89	11	84	16	79	21
Genus	58	42	61	39	61	39	57	43

Table 4.S2. The environmental variables relationship with the UniFrac weighted beta diversity NMDS ordination.

Environmental Parameters	**Rib**		**Scapula**	
	r^2	p-value	r^2	p-value
ADD	0.7064	0.001	0.7178	0.001
Temperature	0.5917	0.001	0.6114	0.001
Specific Conductivity	0.2199	0.001	0.6888	0.001
Salinity	0.1578	0.001	0.4112	0.001
pH	0.1289	0.001	0.3914	0.001

Table 4.S3. The relationship between the top fifteen families and the UniFrac weighted beta diversity NMDS ordination

Environmental Parameters	**Rib**			**Scapula**	
	r^2	p-value		r^2	p-value
Aeromonadaceae	0.0796	0.001	Bacteroidaceae	0.1743	0.001
Bacteroidaceae	0.0595	0.014	Clostridiaceae	0.7059	0.001
Carnobacteriaceae	0.0863	0.002	Comamonadaceae	0.2585	0.001
Clostridiaceae	0.6796	0.001	Desulfobulbaceae	0.2708	0.001
Comamonadaceae	0.2028	0.001	Enterobacteriaceae	0.5834	0.001
Enterobacteriaceae	0.7078	0.001	Holophagaceae	0.5327	0.001
Holophagaceae	0.5353	0.001	Mogibacteriaceae	0.0707	0.003
Mogibacteriaceae	0.131	0.001	Moraxellaceae	0.1893	0.001
Moraxellaceae	0.0206	0.242	Myxococcaceae	0.2132	0.001
Porphyromonadaceae	0.3001	0.001	Pseudomonadaceae	0.1872	0.001
Pseudomonadaceae	0.0296	0.121	Rhodocyclaceae	0.2036	0.001
Rhodocyclaceae	0.3519	0.001	Rikenellaceae	0.2768	0.001
Rikenellaceae	0.2	0.001	Ruminococcaceae	0.0988	0.001
Ruminococcaceae	0.1918	0.001	Sediment.4	0.4081	0.001
Sediment.4	0.1713	0.001	Spirochaetaceae	0.567	0.001
Spirochaetaceae	0.5691	0.001	Syntrophomonadaceae	0.4273	0.001
Syntrophomonadaceae	0.4804	0.001	Veillonellaceae	0.1576	0.001
Veillonellaceae	0.3616	0.001	Others	0.4182	0.001
Others	0.1902	0.001	Total Unclassified	0.5655	0.001
Total Unclassified	0.6542	0.001			

Chapter 5: The Impact of Submersion in Aquatic Environments on STR Profile Development from *Sus scrofa* Skeletal Elements

Abstract

Following a temperature-dependent period of time, human identification may rely on DNA analysis of hard tissues, such as bone. While some studies have evaluated DNA recovery from bone, only case reports and pilot studies have investigated the impact of prolonged submersion in freshwater environments on bone DNA short tandem repeat (STR) profile development. In this study, five porcine ribs and scapulae were placed in 10'' x 10'' cages and submerged in either a freshwater lake or river. Every ca. 250 accumulated degree days (ADD), one cage was collected for a total of nineteen collections at the lake (from November 2016 to June 2018) and twenty-four collections at the river (from November 2017 to November 2018). Of these, only three bone samples collected at ca. 1000 ADD intervals from both sites were extracted using both organic phenol-chloroform and ChargeSwitch® gDNA Plant Kit (e.g., silica resin). All extracts (100 µL) were quantified on the ABI 7500 real-time qPCR machine, and STR profiles were generated using the ABI Prism® 3130 genetic analyzer. Resulting electropherograms were analyzed in GeneMapper™ and statistical analyses were performed in R v3.6.0. Findings suggest that peak presence and percent complete profiles were significantly different among ADD and between bone types. In general, profile development success decreased with ADD, as baseline samples produced the highest success rate, followed by 2000, 1000, 3000 and 4000 ADD. Overall results suggest that regardless of extraction method (e.g., solid-phase or organic phenol-chloroform) and location (e.g., lake or river), ribs should be prioritized as they preserve recoverable DNA for longer periods of time and generate more complete STR profile.

Significance Statement

This study addresses critical issues identified by the Forensic Science TWG in 2016 and 2018: "Increase in the success rate of obtaining DNA STR profiles from compromised (damaged) DNA evidence;" "Methods and/or knowledge to inform users about which processes maximize lysis and recovery of DNA at the elution and/or extraction steps, and/or direct amplification, for best downstream DNA analysis results;" and "Best extraction methods for optimal recovery of DNA from different sample types amendable to downstream analysis (e.g., what methods work best with what sample types)" (1,2). These issues were highlighted as pertinent to Forensic

Biology/DNA and as also relevant to Forensic Pathology and Medicolegal Death Investigations. Specifically, knowing the impact of submersion time and different freshwater ecosystems (e.g., lake versus river) on bone decomposition can provide an estimate for DNA quantification and successful STR profile development. Furthermore, the identification of best practices (e.g., extraction methods and bone types) for obtaining DNA from waterlogged bone, may aid in identifying missing persons.

Introduction

Positive identification of victims recovered from natural disasters, terrorist attacks, armed conflicts, accidental deaths and criminal activity is necessary for both legal and emotional reasons (3-6). When traditional methods, such as fingerprinting, dental radiography and biological profile development, are insufficient or unavailable because of decomposition of soft tissues, destruction of skeletal landmarks and/or lack of records, forensic DNA analysis is often utilized (6,7). The physical and chemical components of bone provide protection and stabilization of DNA, making them a commonly sampled hard tissue (8).

Despite the resilience of bone, environmental influences, such as water, may promote degradation and fragmentation of DNA (9). Highly fragmented or compromised recovered DNA can result in mistyped, partial or failed nuclear short tandem repeat (STR) profiles (4, 9-12). Because successful STR amplification largely depends on the recovery of high quality DNA with minimal inhibiting agents (6,11,13), studies have evaluated the impact of preservation, degradation, skeletal element and extraction method on STR profile development (5-8,11,12,14-17). Unfortunately, the majority of these studies are based on skeletal remains from terrestrial settings.

Research regarding the impact of aquatic decomposition on DNA recovery has primarily been limited to case reports and controlled pilot studies (18-22). Therefore, this study sought to supplement current literature on waterlogged skeletal remains by examining the effects of a freshwater lake and river on DNA recovery from skeletal remains in aquatic environments. Porcine

skeletal elements were selected because they allow for large volume experiments, replication and timely receipt of remains, which cannot be currently accomplished with human remains.

This study first sought to determine the best practices for bone DNA recovery by comparing extraction methods and skeletal elements. Previous studies have shown that DNA degradation is impacted by the bone sampled (5,12,23,17). Therefore, both ribs and scapulae were sampled, as they have been shown to remain articulated the longest during aquatic decomposition (24), possibly increasing their likelihood of recovery. Furthermore, ribs are also among the most commonly sampled skeletal elements (5,14,23). Because DNA recovery is further impacted by extraction method, organic phenol-chloroform was compared to ChargeSwitch® gDNA Plant Kit with a protocol adapted for bone samples. Organic phenol-chloroform has served as the traditional method for DNA extraction from compromised or difficult samples and relies on the separation of DNA into a soluble aqueous phase, which utilizes harmful chemicals and several tube transfers. ChargeSwitch® uses silica resin with a pH dependent switchable surface charge to isolate DNA that has the potential to be automatable. This study also aimed to identify variance of DNA recovery in different bodies of water (e.g., freshwater river and lake) and across accumulated degree days (ADD). It has been shown that simulated environmental factors degrade DNA in postmortem tissues (7); however the impact on profile development has not been quantified in a controlled and well-replicated environmental study.

Results

The results for DNA quantity, STR profile development, and peak height values are outlined below.

DNA Quantity

In general, DNA quantity extracted using both methods decreased as decomposition progressed, in both bone types and at both locations. (Figure 5.S1, Table 5.S1, Table 5.S2). Approximately, 28% (n=33) of all samples did not result in quantifiable DNA, but some (n=6) of them did generate

a partial (at least 25% complete) STR profile. On the other hand, no profiles were developed from 15 samples that were successfully quantified.

STR Profile Development

Profile development was assessed using overall success rate (i.e., at least one peak present) for each extraction method, bone type, location and approximate ADD (chi-square test); peak presence or absence in each marker across ADD for ribs and scapulae extracted via ChargeSwitch® gDNA Plant Kit and organic phenol-chloroform (logistic regression); and percent complete profiles across ADD for ribs and scapulae collected from each location and processed with both extraction methods (mixed effects modeling).

The Chi-square test suggested no significant difference in success rate from different extraction methods (i.e., organic versus ChargeSwitch), bone types (i.e., rib versus scapula), and locations (i.e., lake versus river). However, the rate of success did decrese significantly (X_4^2 = 46.47, p < 0.0001) as decomposition progressed (i.e., at different ADD) (Figure 5.1). Baseline samples produced the highest profile development success rate, followed by 2000, 1000, 3000 and 4000 ADD (Table 5.1). While no significant differences were identified, rib samples ($\bar{x}$ = 33), samples extracted via organic phenol-chloroform ($\bar{x}$ = 32), and recovered from the lake ($\bar{x}$ = 29) had higher success rates (Table 5.2).

Peak presence or absence was also analyzed using logistic regression and analysis of variance (ANOVA). Significant interactions resulted in subsetting the data according to location and extraction method. Overall, peak presence differed significantly for bone type, according to each location and extraction method as well as across ADD, suggesting that submersion time impacted the ability to recover peaks. Visual trends indicated that STR peaks were recovered more frequently in ribs than in scapulae (Figure 5.2). Similarly, it was observed that STR peaks were generated more successfully in small fragment target loci (e.g., FH1727 and FH2148) than large fragment larget loci (e.g., S0766), specifically for scapulae. Similarly, bone type ($F_{1,110}$ = 26.64, p < 0.0001) and ADD ($F_{1,116}$ = 43.05, p < 0.0001) were significant when considering the number of peaks present (Figure 5.S2). Specifically, 1012, 2141, 2915, and 3949 ADD differed significantly from baseline samples at the James River; meanwhile, 3103 and 3962 ADD differed significantly from baseline samples at Henley Lake. While the number of peaks recovered was variable across

ADD (Table 5.S3), 1.05 more peaks on average were recovered from ribs compared to scapulae ($\bar{x}$ =0.34) (Table 5.S4).

When examining the percent of complete profiles recovered, the interaction between extraction method and bone type resulted in comparing bone types per extraction method. Both bone type (ChargeSwitch: $F_{1,55}$ = 17.06, p = 0.0001; Organic: $F_{1,55}$ = 5.86, p = 0.0188) and ADD ($F_{1,58}$ = 28;46, p < 0.0001) significantly impacted the percent of complete profiles recovered (Figure 5.3). Specifically, 1012, 2141, 2915 and 3949 ADD differed significantly from James River baseline samples; however, only 3103 ADD differed from baseline at Henley Lake. For samples extracted by both ChargeSwitch ($\bar{x}$ = 0.41) and organic phenol-chloroform ($\bar{x}$ =0.40), ribs ($\bar{x}$ = 0.58) produced more complete profiles than scapulae ($\bar{x}$ = 0.22) (Table 5.3). Furthermore, a decrease from 90% complete profiles from baseline samples to 31% at 3962 ADD was noted in samples from Henley Lake ($\bar{x}$ = 0.45) (Table 5.4). With the exception of 1012 ADD ($\bar{x}$ = 0.19), a similar trend was observed in the James River samples ($\bar{x}$ = 0.37). For both extraction methods, 1012 and 3949 ADD differed significantly from baseline samples at the James River, while 3103 ADD was the only collection to differ significantly from baseline samples in Henley Lake.

Intra- and Inter-locus Balance

Peak height ratio (PHR) was not significantly impacted by bone type, location, extraction method, or ADD (Figure 5.S5). Ribs ($\bar{x}$ = 0.71) and scapulae ($\bar{x}$ = 0.71) had the same mean PHRs, as did both locations (Henley Lake $\bar{x}$ = 0.71; James River $\bar{x}$ = 0.71) and extraction methods (ChargeSwitch $\bar{x}$ = 0.71; Organic $\bar{x}$ =0.70) (Table 5.S5). Likewise, the coefficient of variation for the ratio of locus peak height to total peak height (CV LPH:TPH) did not differ significantly between bone type ($F_{1,25}$ = 0.35, p = 0.5568), extraction method ($F_{1,16}$ = 1.81, p = 0.1967), and location ($F_{1,25}$ = 0.58, p = 0.4547), or among ADD ($F_{1,27}$ = 0.23, p = 0.638) (Figure 5.S4). For rib samples ($\bar{x}$ =0.62), CV TPH:LPH increased until ca. 2000 ADD, whereas scapula samples ($\bar{x}$ = 0.68) increased for ADD periods from which profiles were successfully recovered (Table 5.S6). While PHR and CV LPH:TPH varied somewhat with ADD, no distinct pattern was noted (Table 5.S7, Table 5.S8).

Discussion

This study sought to evaluate how DNA profile development was impacted by bone type, location (i.e., aquatic environment), time of submersion, and extraction method. Overall, peak presence or absence, percent complete profile, and the number of peaks present differed significantly between bone types and among accumulated degree days (ADD). Profile development success rate was significantly impacted by ADD (Table 5).

While the freshwater ecosystem (e.g., lake and river) from which the skeletal elements were recovered did not significantly impact profile development or peak heights, ADD did. This suggested that time/temperature, rather than site, of submersion may be more important. Bone, which is composed of both inorganic calcium phosphate (e.g., hydroxyapatite) and collagen proteins, provides some protection against DNA degradation (9,16,25). Gotherstrom et al. (16) showed that hydroxyapatite calcium ions attract negatively charged DNA, resulting in adsorption and stabilization of DNA. As bone diagenesis occurs, the ratio of inorganic and organic components changes, which impacts the stability of DNA. Once DNA is released from the hydroxyapatite, it is exposed to fragmentation via both enzymatic and non-enzymatic degradation processes (4). Enzymatic degradation of postmortem skeletal DNA is initiated by endogenous nucleases released by host cells.

Another factor that could have contributed to the loss of DNA with ADD of submersion time is the presence of microorganisms (e.g., bacteria and fungi), which produce enzymes that participate in both nucleic acid degradation and the digestion of mineralized collagen (4,6,7,25,26). The colonization of postmortem tissues by microbial communities both exogenous and endogenous to remains is dependent on environmental factors and the availability of nutrients. Studies using the same sample set surveyed and identified microbial organisms associated with skeletal remains throughout long-term skeletal element decomposition. Specifically, bacteria associated with discoloration and adipocere were recovered (Figure 5.S5 and Figure 5.S6) (Chapter 2:*Modeling Postmortem Submersion Interval (PMSI) Estimation From the Microbiome of Sus scrofa Bone in a Freshwater Lake;* Chapter 3: *Postmortem Submersion Interval (PMSI) Estimation from the Microbiome of Sus scrofa Bone in a Freshwater Lake).* Therefore, skeletal elements that are accessible to microorganisms are more likely to undergo DNA degradation.

Non-enzymatic methods of degradation, such as hydrolytic reactions, DNA cross-linkage, oxidative reactions, and radiation, occur at a much slower rate (4). Nevertheless, DNA damage via hydrolytic reactions increases with increasing amounts of water in the decomposition environment because DNA has an affinity for water molecules (9). As water percolates through the bone, dissolution of the inorganic component of bone progresses, contributing to further loss of DNA molecules through dissociation from the hydroxyapatite (as previously discussed).

The aforementioned DNA damage reduces the size of template molecules, contributing to difficulties in recovering analyzable DNA from older tissues (9). As DNA degrades, targets/segments that are larger in size are more likely to be impacted than shorter targets; therefore, preferential amplification of shorter amplicons can occur due to more of them being present. Furthermore, this phenomenon has been reported to occur as a result of degradation impacting longer products during decomposition (4, 27). The difference in amplification efficiency of shorter and larger DNA targets is reflected in STR profiles, as peak heights are inversely proportional to amplicon size. Differences between STR markers in both peak presence or absence and the number of peaks present were impacted by amplicon size, especially in scapulae. Even when other markers were not present, the smallest amplicon (e.g., FH1727) was successfully amplified and observed in STR profiles, suggesting that longer periods of submersion increased fragmentation. Findings from Kaiser et al. (12) also revealed a time-dependent process of DNA degradation due to decomposition. This also suggests that use of degradation index ratio (if available) before STR amplification, can help in determination of whether a successful STR profile will be generated from a particular sample or not.

The objective of the extraction process is to recover the maximum amount of DNA from samples, but extraction method appeared to have no impact on the results in this study, which differs from previous studies (14, 18). Traditionally, organic phenol-chloroform has served as the gold standard for DNA extraction in forensic biology, as it provides a reliable method of recovering DNA from damaged samples (18). However, user friendly solid-phase methods, such as ChargeSwitch® gDNA Plant Kit (e.g., silica resin), that reduce exposure to hazardous chemicals, minimize tube transfers, and are amenable to automation are gaining popularity and preference in the field. Therefore, selection of extraction method for waterlogged bone may rely on ease of use and user preference.

When comparing bone types, ribs produced more complete profiles with peaks present at more loci. When considering flat bones, a previous study that examined remains from the World Trade Center also reported a higher success rate with ribs (60 – 69%) than scapulae (50 – 59%) (5). In this study, the higher success observed with ribs may have been a result of their encasement in adipocere during early time periods at both sites and throughout submersion at Henley Lake. Adipocere may have provided further protection from degradation (Figures S4 and S5), as Mundorff et al. (5) reported higher identification rates from intact elements that were encased in soft tissue and from denser, weight-bearing bones. While research has demonstrated that the most successful DNA profiles have been recovered from teeth and cortical bones, especially of the lower limbs (9), a study using fresh porcine ribs and femora reported greater success across five different extraction methods (14). Similarly, Cartozzo et al. (18) recovered significantly higher quantities of DNA from rib samples submerged in water for six months. Differences in DNA recovery from ribs and humeri were attributed to the DNA-rich cancellous (i.e., spongy) bone in ribs. Previously, DNA yields in spongy tissue were reported to be 10-20 times higher than in compact bone (17). When comparing extraction methods and bone types, Lee et al. (7) also observed that DNA yields from different skeletal elements varied more than the extraction methods utilized.

Although no significant differences were identified upon consideration of PHR and CV LPH:TPH, it is important to note that this method has not been extensively tested and validated. Future studies should evaluate the multiplex procedure and consider utilizing the Platinum Multiplex PCR Master Mix, instead of AmpliTaq Gold® PCR Master Mix, as it has been reported to correct unbalanced peak heights and split peaks. Resulting profiles may have also been impacted by DNA input, as the quantification process and method have been linked to issues with DNA profiles (14, 28).

Conclusions

This study identified that bone type and ADD impacted STR profile development from porcine remains submerged in freshwater ecosystems (e.g., lake and river). Results suggested that regardless of extraction method (e.g., solid-phase or organic phenol-chloroform) ribs, which may be recovered more frequently because they remain articulated for longer periods, should be prioritized in DNA testing. Furthermore, bone encased in tissue performed better as well, so that practitioners should not be discouraged from attempting to extract DNA profiles from bones of

waterlogged fleshed, decomposed, or skeletal remains. Future research should consider sampling shorter periods, including more skeletal elements, expanding the number of STR markers, and validating current methods for porcine DNA quantification, STR amplification, and amplicon separation.

Materials and Methods

Since the goals of the experiment were to examine differences in STR profile development, specifically in various aquatic environments, a freshwater river (the James River, Charles City, VA, 37.3260° N, 77.2056° W) was chosen as a comparison for Henley Lake, a freshwater lake in Crozet, VA (38.0863° N, 78.6842° W). The Henley Lake and James River sites were utilized from November 2016 – June 2018 and November 2017 – 2018, respectively. At each location, 10'' x 10'' cages that contained five ribs and five scapulae were submerged to rest on the lake (5 m) and river (4 m) beds. In addition to baseline samples that were never exposed to water, 19 cages were collected from Henley Lake and 24 cages were collected from the James River. Approximately every 250 accumulated degree days (ADD), one cage was removed, representing one collection. Using a 0° C threshold, ADD calculations were performed using data from waterproof temperature loggers that monitored temperature from the level of the bones. Following each collection, samples were transported on ice to Virginia Commonwealth University, Richmond, VA, where they were stored at -80 °C.

At the time of processing, bone samples were thawed at room temperature, photographed, and underwent non-bone tissue removal. According to the International Commission of Missing Persons (ICMP) standard operating procedure (29), scapulae spines were cut using a Craftsman Cordless Multi-Tool (Craftsman, Chicago, IL). Because the ribs were previously cut, making it difficult to follow ICMP guidelines, the mid-section of the rib was used. The bone pieces were ground into a fine powder using a mortar filled with liquid nitrogen and a pestle. The resulting bone powder was weighed to 0.1 g and stored at -20 °C until DNA extraction.

DNA Extraction Methods

Using 0.1 g of bone powder, DNA extraction was performed using both the ChargeSwitch® gDNA Plant Kit (ChargeSwitch, Life Technologies, Grand Island, NY) and organic phenol-chloroform extraction as outlined by Iyavoo et al. (14). For both methods, the final elution volume was 100 µL and extracts were stored at -20 °C. Only a subsample of 30 ribs and 29 scapulae, which are

comprised of triplicates that represent 1000 ADD intervals, from the original 400 bone sample extracts underwent quantitation and profile development.

DNA Quantitation

To ensure samples were free of inhibitors that could negatively impact real-time quantitative PCR (qPCR), all samples underwent a preliminary 16S rDNA variable region 4 (V4) amplification according to the Kozich et al. (30) duel-indexing system on the Veriti™ 96-Well Thermal Cycler (Applied Biosystems, Foster City, CA) as outlined in Chapter 3: *Modeling Postmortem Submersion Interval (PMSI) Estimation From the Microbiome of Sus scrofa Bone in a Freshwater Lake* and Chapter 4: *Postmortem Submersion Interval (PMSI) Estimation from the Microbiome of Sus scrofa Bone in a Freshwater Lake.* Extracts (50 µL) that failed amplification (38% of samples, 31 scapulae, 14 ribs, 25 ChargeSwitch®, 20 organic, 36 James River and 9 Henley Lake) were purified (i.e., removal of PCR inhibitors) via the DNeasy PowerClean Pro Cleanup Kit and eluted in 50 µL (Qiagen, MD, USA).

Absolute DNA quantification by real-time qPCR via the ABI 7500 (Applied Biosystems) was performed in 12.5 µL reactions, which included 0.25 µL of each 10 µM porcine-specific primer (FH1733 F 5' - AAG CCT CAA ACT CCT CAT CTC A and FH1733 R 5' - ACC AAA GGC ATA CTA GGG CTA A) (31), 2 µL template DNA, 6.25 µL of PerfeCTa SYBR Green SuperMix (2X) (VWR, Radnor, PA, USA), and 3.75 µL of nuclease-free water (31). Thermal cycling parameters followed those outlined by Seashols-Williams et al. (31) with the number of cycles increased to 38.

Short Tandem Repeat (STR) Profile Development

Four porcine STR loci (FH2148, S0766, FH1727 and FH 1733) and a sex marker (Amelogenin), as described by Rebala et al. (32), were amplified on the Veriti™ 96-Well Thermal Cycler (Applied Biosystems). Each reaction (10 µL) consisted of template DNA (0 – 0.125 ng; 5.85 µL maximum), 1 µL 10X PCR Buffer I, 0.1 µL 0.5 U AmpliTaq Gold (ThermoFisher Scientific, Waltham, MA), 0.2 µL 10 mM dNTP Mix (ThermoFisher Scientific), and the following 5' labeled/unlabeled primer pairs: 0.3 µL Amelogenin (5 µM; FAM), 0.2 µL FH2148 (5 µM; FAM), 0.35 µL S0766 (10 µM; FAM), 0.275 µL FH1727 (5 µM; VIC) and 0.3 µL FH1733 (5 µM; NED). Parameters for the multiplex PCR followed the AmpliTaq Gold® DNA Polymerase Protocol (33) with the exceptions of a total of 35 cycles, a 60 °C annealing temperature, and a 60 min final extension step at 72 °C.

Separation on the ABI Prism® 3130 genetic analyzer (Applied Biosystems) was performed according to the Animaltype Pig PCR Amplification Kit run module parameters (run time increased to 2000 s) with 9 µL HiDi-Formamide, 0.5 µL GeneScan™ 500 Rox™ dye size standard (ThermoFisher Scientific, Waltham, MA) and 0.5 µL PCR product (34). Resulting electropherograms for all samples, a PCR negative (non-template control), capillary electrophoresis positive (single-source genomic pig DNA) and capillary electrophoresis negative (non-template control) were analyzed using GeneMapper™ software v3.1 (ThermoFisher Scientific) with a 50 rfu analytical threshold.

Data Analysis

Using only the STR markers, profile development success, coefficient of variation of the locus peak height to total peak height ratio (CV of LPH:TPH), percent complete profile, peak presence and absence, number of peaks present, and peak height ratio (PHR) were analyzed and visualized for each category (e.g., Extraction Method, Bone Type, Site and ADD) in R v3.6.0 (35). Profile development success, using counts, was tested using *chisq.test* function in the stats package v3.6.0 (35). To compare categories for CV of LPH:TPH, percent complete profile, number of peaks present, PHR, as well as interactions at a 0.05 significance level, mixed-effects modeling analysis of variance (ANOVA) with bone as the random variable was performed using the *lme* function in the nlme package v3.1 (36). In cases where significant differences were identified in comparisons of three or more, Tukey's Honest Significant Differences (HSD) was used to compare means and determine where the differences were (*glht*; multcomp package v1.4)(37). Because peak presence or absence had values of 0 or 1, logistic regression was employed using the *glm* function (*link="logit"*) in the stats package (35). Additionally, normality of all resulting residuals was assed using QQplots. Visualization for the aforementioned analyses were performed with ggplot2 package v3.2.1 (38).

Acknowledgments

The authors would like to thank everyone that provided help and support throughout the study, including but not limited to Brittany Hudson, Jordan Cox, Denise Wohlfahrt, Kailey Babcock, Tyler Kennedy, Alaina Albino, Matt Alvarez and Isis Thornton. For providing porcine scapulae, the authors thank Bourgeois Meat Market (Thibodaux, LA); additionally, our gratitude is extended to

the Virginia Commonwealth University (VCU) Rice Rivers Center (Charles City, VA) for providing a location for the field portion of the study.

Funding

This study was funded by the following: B. Singh start-up grant from College of Humanities and Science of Virginia Commonwealth University (VCU), Richmond, VA, Forensic Science Foundation Lucas Grant 2016, VCU Rice Rivers Center Grant and award 2018-R2-CX-0016 of the National Institute of Justice Graduate Research Fellowship.

References

1. TWG, NIJ Forensic Science Technology Working Group Operation Requirements (2016). Available at: https://www.nij.gov/topics/forensics/documents/2016-forensic-twg-table.pdf
2. TWG, NIJ Forensic Science Technology Working Group Operation Requirements (2018). Available at https://nij.ojp.gov/sites/g/files/xyckuh171/files/media/document/2018-2-forensic-twg-table.pdf
3. D. Hartman, O. Drummer, C. Eckhoff, J. Scheffer, P. Stringer, The contribution of DNA to the disaster victim identification (DVI) effort. *Forensic Science International* **205**, 52 – 58 (2011).
4. R. Alaeddini, S. Joseph, A. Abbas, Molecular studies of time- and environment-dependent effects on bone DNA survival. *Australian Journal of Forensic Sciences* **42**, 211 – 220 (2010).
5. A.Z. Mundorff, E. J. Bartelink, E. Mar-Cash, DNA Preservation in Skeletal Elements from the World Trade Center Disaster: Recommendations for Mass Fatality Management. *Journal of Forensic Sciences* **54**, 739 – 745 (2009).
6. J. Davoren *et al.*, Highly effective DNA extraction method for nuclear short tandem repeat testing of skeletal remains from mass graves. *Croatian Medical Journal* **48**, 478 - 485 (2007).
7. D. Rankin, S. Narveson, W. Birkby, J. Lai, Restriction Fragment Length Polymorphism (RFLP) Analysis on DNA from Human Compact Bone. *Journal of Forensic Sciences* **41**, 40 – 46 (1996).
8. J. Samsuwan *et al.*, A method for extracting DNA from hard tissues for use in forensic science identification. *Biomedical reports* **9**, 433 – 438 (2018).
9. K.E. Lantham, M.E. Madonna, “DNA Survivabilty in Skeletal Remains” in *Manual of Forensic Taphonomy*, J. Pokines, S.A. Symes, Eds. (Taylor and Francis Group, 2013).
10. S. Hughes-Stamm, K. Ashton, A. Van Daal, Assessment of DNA degradation and the genotyping success of highly degraded samples. *International Journal of Legal Medicine* **125**, 341 - 348 (2011).
11. M. Putkonen, J. Palo, J. Cano, M. Hedman, A. Sajantila, Factors affecting the STR amplification success in poorly preserved bone samples. *Investigative Genetics* **1** (2010).
12. C. Kaiser *et al.*, Molecular study of time dependent changes in DNA stability in soil buried skeletal residues. *Forensic Science International* **177**, 32 - 36 (2008).
13. V. Prado, A. Castro, C. Oliveira, K. Souza, S. Pena, Extraction of DNA from human skeletal remains: practical applications in forensic sciences. *Genetic Analysis: Biomolecular Engineering* **14**, 41 - 44 (1997).
14. S. Iyavoo, S. Hadi, W. Goodwin, Evaluation of five DNA extraction systems for recovery of DNA from bone. *Forensic Science International: Genetics Supplemental Series* **4**, e174 – e175 (2013).
15. A. Barbaro, P. Cormaci, Validation of DNA typing from skeletal remains using the Invitrogen ChargeSiwtch Forensic DNA Purification Kit. *Forensic Science International: Genetics* **1**, 398 - 400 (2007).
16. A. Gotherstrom, M. Collins, A. Angerbjorn, K. Liden, Bone preservation and DNA amplification. *Archaeometry* **3**, 395 – 404 (2002).
17. H. Lee *et al.*, Genetic Markers in Human Bone: Deoxyribonucleic Acid (DNA) Analysis. *Journal of Forensic Sciences* **36**, 320 - 33 (1991).
18. C. Cartozzo, B. Singh, E. Boone, T. Simmons, Evaluation of DNA Extraction Methods from Waterlogged Bones: A Pilot Study. *Journal of Forensic Sciences* **63**, 1830 – 1835 (2018).

19. A. Mameli, G. Piras, G. Delogu, The Successful Recovery of Low Copy Number and Degraded DNA from Bones Exposed to Seawater Suitable for Generating a DNA STR Profile. *Journal of Forensic Sciences* **59**, 470 – 473 (2014).
20. J. Fredericks, K. Brown, A. Williams, P Bennett, DNA analysis of skeletal tissue recovered from the English Channel. *Journal of Forensic and Legal Medicine* **20**, 757 – 759 (2013).
21. C. Courts, B. Madea, Full STR Profile of a 67-Year-Old Bone Found in a Fresh Water Lake. *Journal of Forensic Sciences* **58**, 172 – 175 (2011).
22. K. Crainic, F. Paraire, M. Leterreaux, M. Durigon, P. de Mazancourt, Skeletal remains presumed submerged in water for three years identified using PCR-STR analysis. *Journal of Forensic Sciences* **47**, 1025 – 1027 (2002).
23. W.L. Perry, W.M. Bass, W.S. Riggsby, K. Sirotkin, The Autodegradation of Deoxyribonucleis Acid (DNA) in Human Rib Bone and Its Relationship to the Time Interval Since Death . *ASTM International* **33**, 144 – 153 (1988).
24. W. Haglund, Disappearnce of Soft Tissue and the Disarticulation of Human Remains from Aqueous Environments. *Journal of Forensic Sciences* **38**, 806-815 (1993).
25. M. Collins *et al*., The survival of organic matter in bone: a review. *Archeometry* **3**, 383 - 394 (2002).
26. M. Thakar, B. Joshi, P. Shirvastava, A. Raina, S. Lalwani, An assessment of preserved DNA in decomposed biological materials by using forensic DNA profiling. *Egyptian Journal of Forensic Sciences* **9**, 1-9 (2019).
27. M. Takahashi, Y. Kato, H. Mukoyama, H. Kanaya, S. Kamiyama, Evaluation of five polymorphic microsatellite markers for typing DNA from decomposed human tissues – Correlation between the size of the alleles and that of the template DNA. *Forensic Science International* **90**, 1-9 (1997).
28. P. Gill, J. Curran, K. Elliot, A graphical simulation model of the entire DNA process associated with the analysis of short tandem repeat loci. *Nucleic acids research* **33**, 632 – 643 (2005).
29. International Commission of Missing Persons (ICMP), Standard Operating Procedure for Sampling Bone and Tooth Specimens from Human Remains for DNA Testing at the ICMP (2015) Available at: https://www.icmp.int/wp-content/uploads/2015/04/icmp-sop-aa-136-2-doc.pdf
30. J.J. Kozich, S.L. Westcott, N.T. Baxter, S.K. Highlander, P.D. Schloss, Development of a Dual-Index Sequencing Strategy and Curation Pipeline for Analyzing Amplicon Sequence Data on the MiSeq Illumina Sequencing Platform. *Applied Environmental Microbiology* **79**, 5112-5120 (2013).
31. S. Seashols-Williams, *et al*. An Accurate bacterial DNA quanitification assay for HTS library preparation of human biological samples. *Electrophoresis* **39**, 2824 – 2832 (2018).
32. Rebala *et al*. STR Profiling for Discrimination between Wil and Domestic Swine Specimens and between Main Breeds of Domestic Pigs Reared in Belarus. *PLoSone* **11**, 1-14 (2016).
33. Life Technologies. AmpliTaqGold® DNA Polymerase Protocol (2014).
34. BioType®. Animaltype Pig PCR Amplification Kit Instructions for Use (2018).
35. R Core Team, R: A Language and Environment for Statistical Computing (2019).
36. J. Pinheiro, D. Bates, S. DebRoy, D. Sarkar, R Core Team, nlme: Linear and Nonlinear Models (2020).
37. T. Hothorn, R. Bretz, P. Westfall, Simultaneous Inference in General Parametric Models. *Biometrical Journal* **50**, 346 – 363 (2008).
38. H. Wickham, ggplot2: Elegant Graphics for Data Analysis (2016).

Figures and Tables

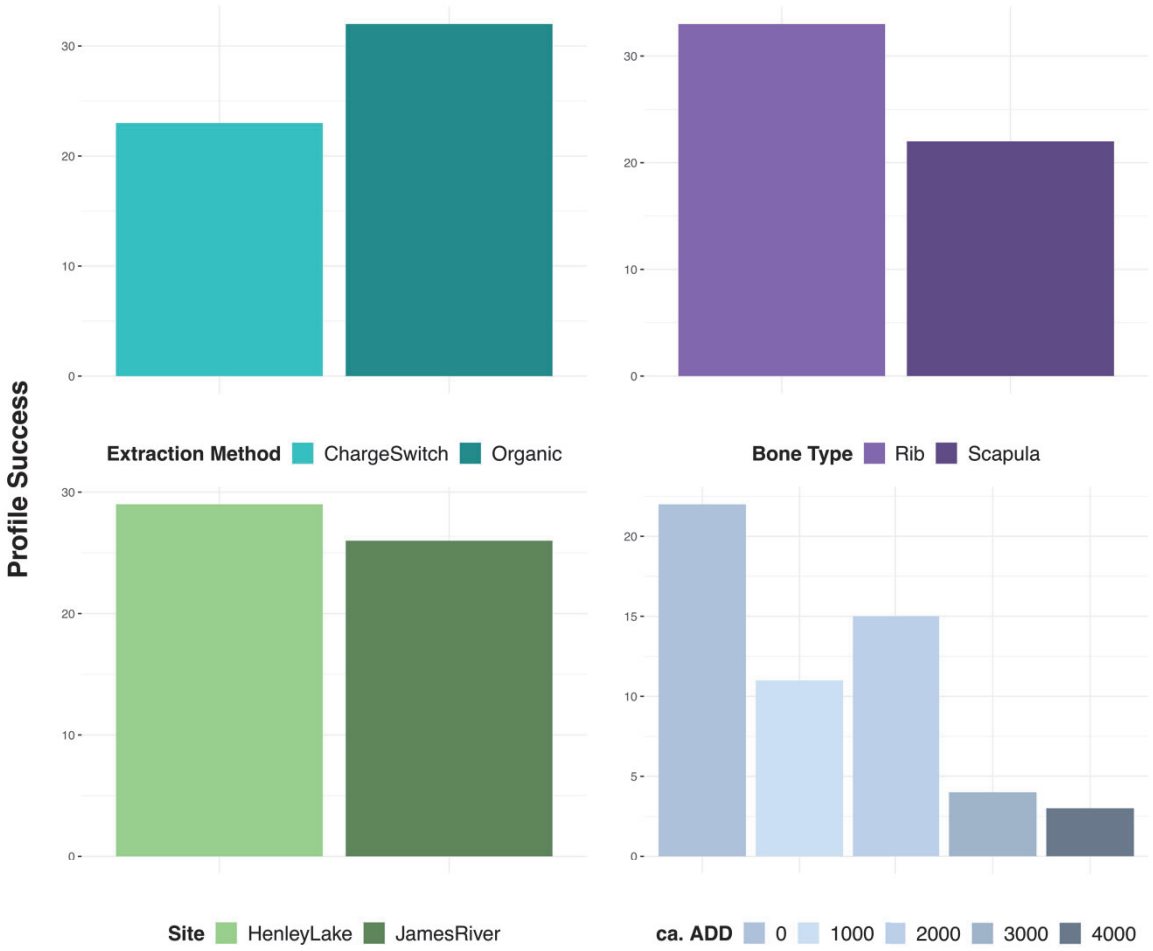

Figure 5.1. The number of successful profiles for each extraction method (top left), bone type (top right), site (bottom left) and approximate accumulated degree day (ADD) (bottom right). Success was considered as profiles having at least one peak present, .

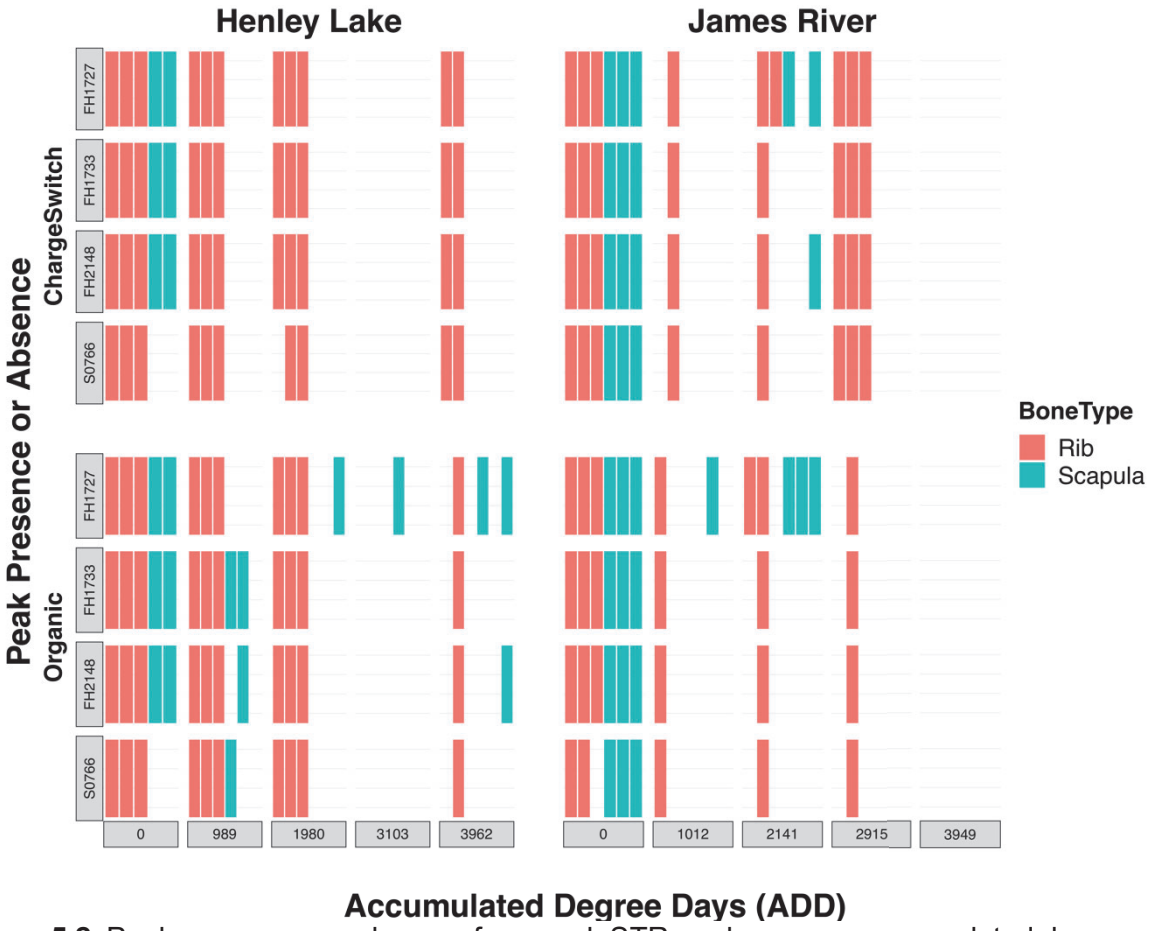

Figure 5.2. Peaks presence or absence from each STR marker across accumulated degree days (ADD) for rib and scapula samples collected from both Henley Lake (left) and the James River (right) and extracted using ChargeSwitch (top) and Organic (bottom) methods

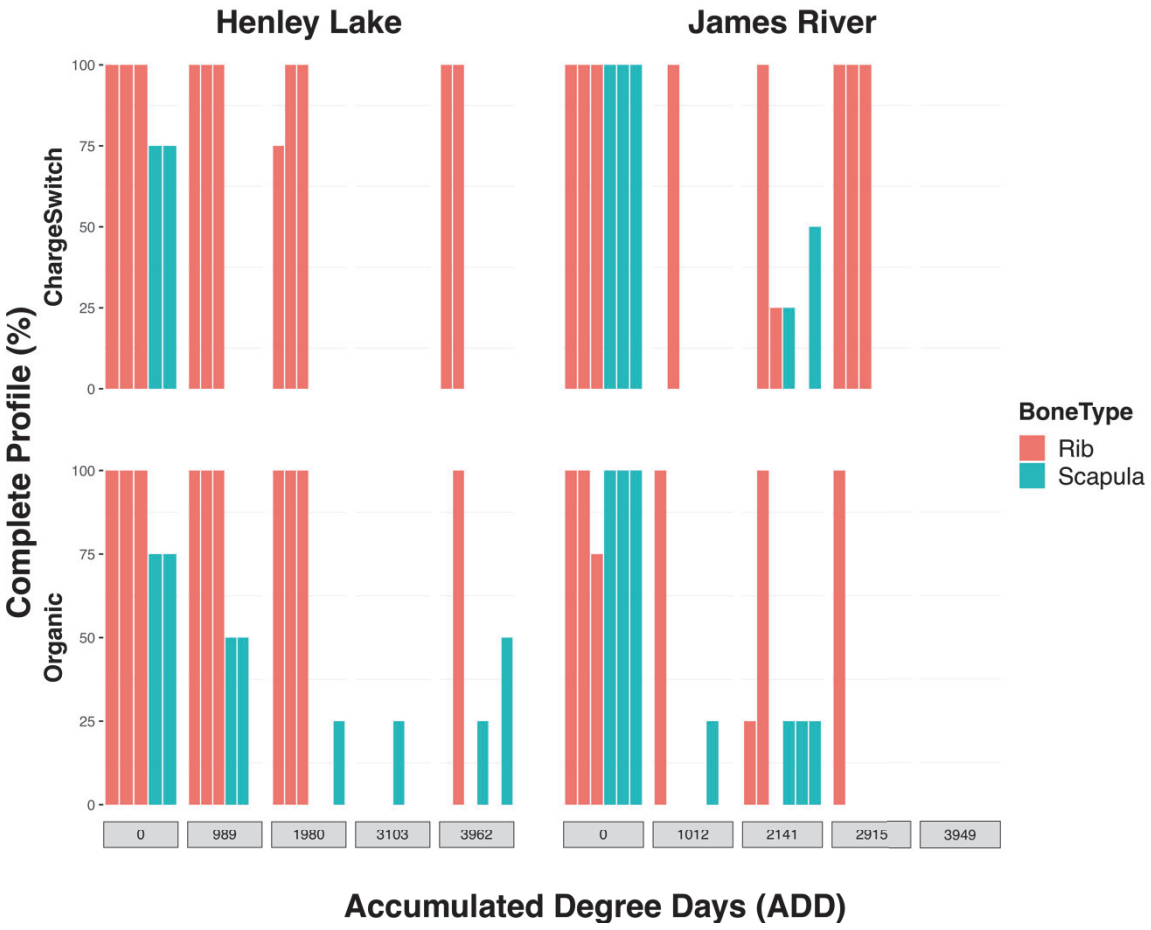

Figure 5.3. The percentage of complete profile recovered across accumulated degree days (ADD) for rib and scapula samples collected from Henley Lake (left), the James River (right), and extraction using ChargeSwitch (top) and Organic (bottom) methods.

Table 5.1. The number of successful profiles recovered from each collection period or accumulated degree days (ADD)

	Profile Success			
Approximate ADD	**Yes**	**No**	**Total**	**Proportion Yes**
0	22	0	22	1.00
1000	11	13	24	0.46
2000	15	8	23	0.65
3000	4	20	24	0.17
4000	3	19	22	0.14

Table 5.2. The number of successful profiles recovered for each extraction method, bone type and location

	Profile Success			
	Yes	**No**	**Total**	**Proportion Yes**
Extraction Method				
ChargeSwitch	23	33	56	0.41
Organic	32	27	59	0.54
Bone Type				
Rib	33	24	57	0.58
Scapula	22	36	58	0.38
Location				
Henley Lake	29	27	56	0.52
James River	26	33	59	0.44

Table 5.3. The percent complete profiles mean values for each extraction method, bone type and location

Mean Percent Complete Profiles	
Extraction Method	
ChargeSwitch	0.41
Organic	0.40
Bone Type	
Rib	0.58
Scapula	0.22
Location	
Henley Lake	0.45
James River	0.37

Table 5.4. The percent complete profile mean values for each accumulated degree days (ADD)

Mean Percent Complete Profiles					
Henley Lake	**0 ADD**	**989 ADD**	**1980 ADD**	**3103 ADD**	**3962 ADD**
	0.90	0.58	0.50	0.33	0.31
James River	**0 ADD**	**1012 ADD**	**2141 ADD**	**2915 ADD**	**3949 ADD**
	0.98	0.19	0.33	0.02	0

Table 5.5. A summary of statistical analyses, demonstrating which categories had the most influence on STR profiles recovered

	Extraction Method	Bone Type	Location	ADD
Profile Development Success (Chi-Square)				X
Peak Present or Absent (Logistic Regression)		X		X
Percent Complete Profile (Mixed-Effects)		X		X
Number of Peaks Present (Mixed-Effects)		X		X
PHR (Mixed-Effects)				
CV Ratio (Mixed-Effects)				

Supplemental Figures and Tables

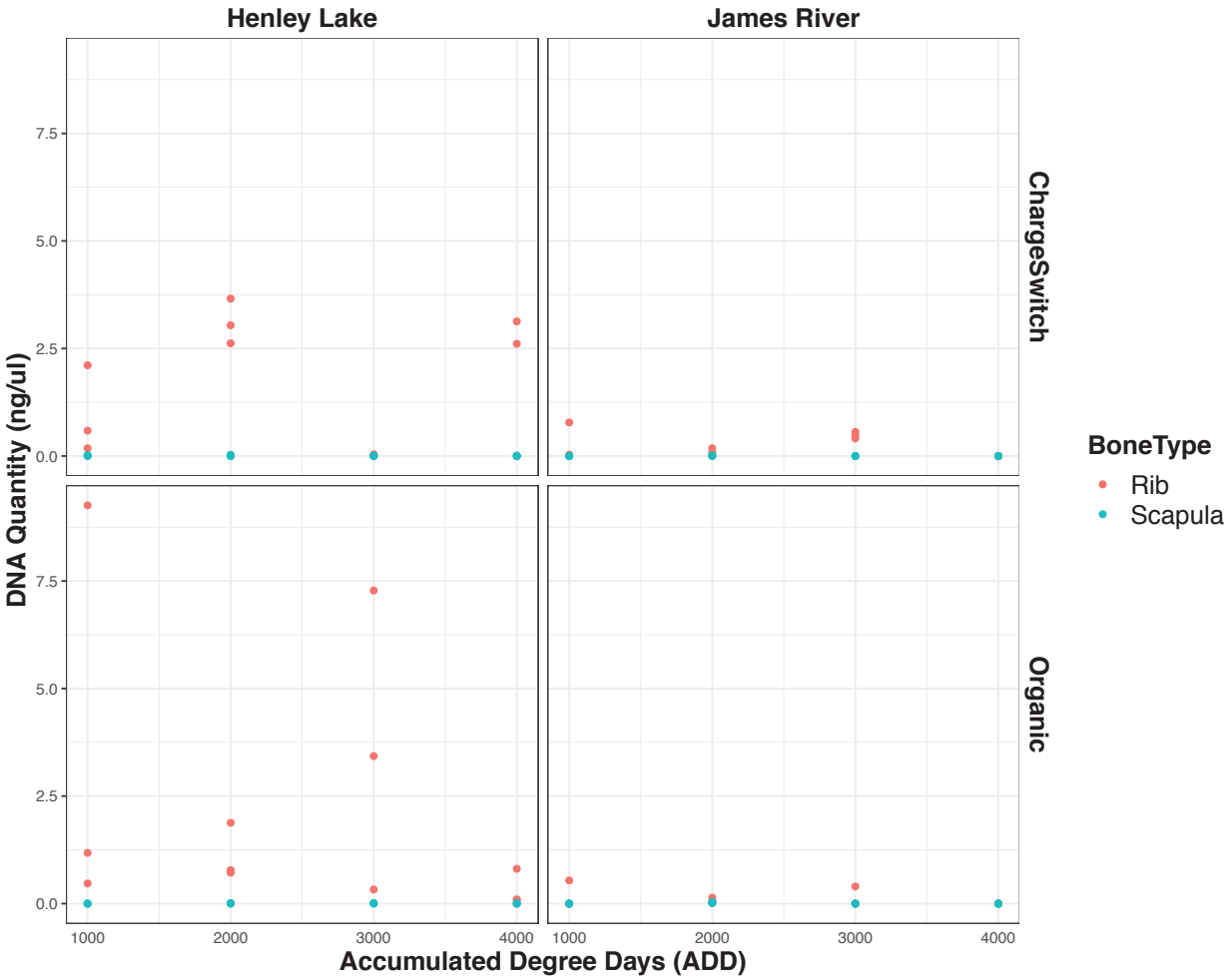

Fig. 5.S1. The quantity of DNA (ng/µl) across accumulated degree days (ADD) for submerged rib and scapula samples collected from Henley Lake (left) and the James River (right) and extracted using ChargeSwitch (top) and Organic (bottom) methods

Fig. 5.S2. The number of peaks present for each STR marker across accumulated degree days (ADD) for rib and scapula samples collected from Henley Lake (left) and the James River (right) and extracted using ChargeSwitch (top) and Organic (bottom) methods

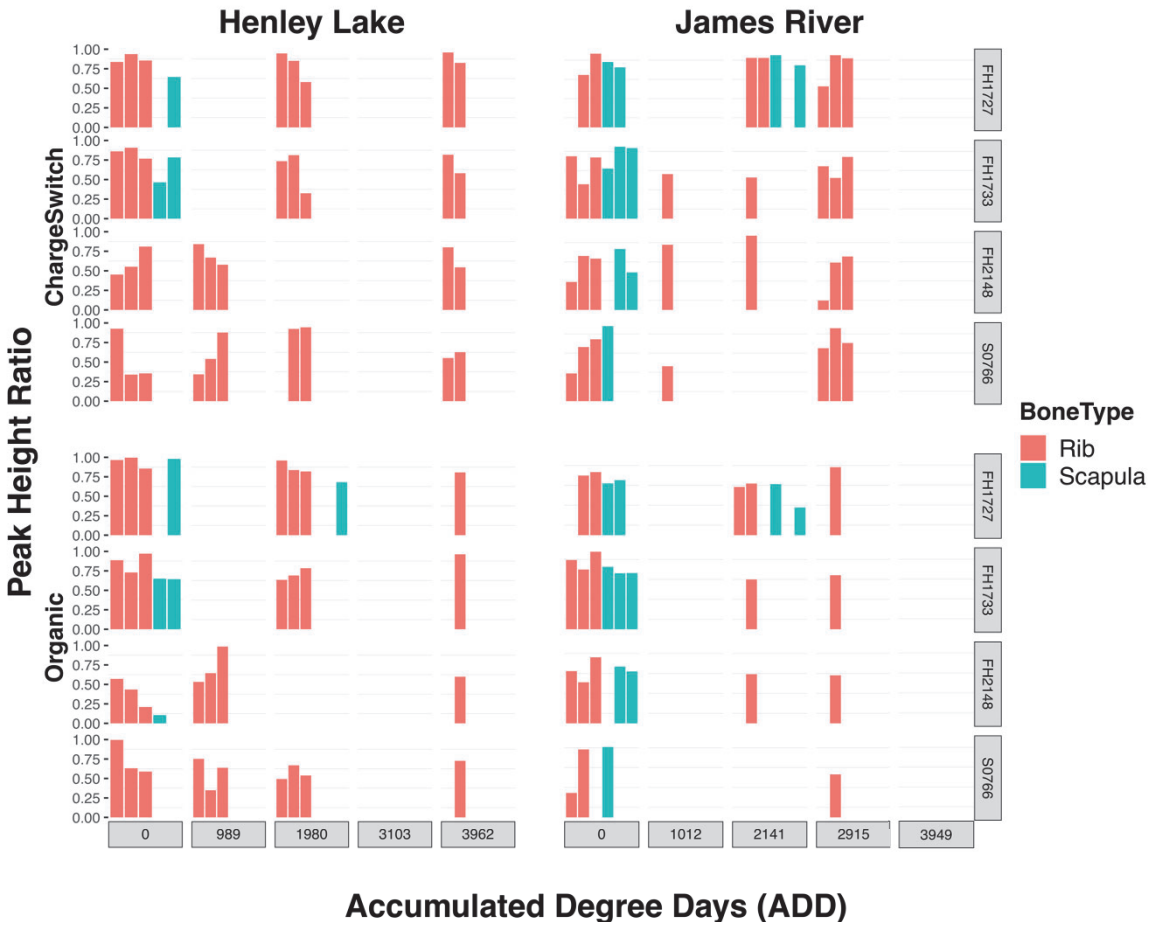

Fig. 5.S3. The peak height ratio (PHR) for each STR marker across accumulated degree days (ADD) for rib and scapula samples collected from Henley Lake (left) and the James River (right) and extracted using ChargeSwitch (top) and Organic (bottom) methods

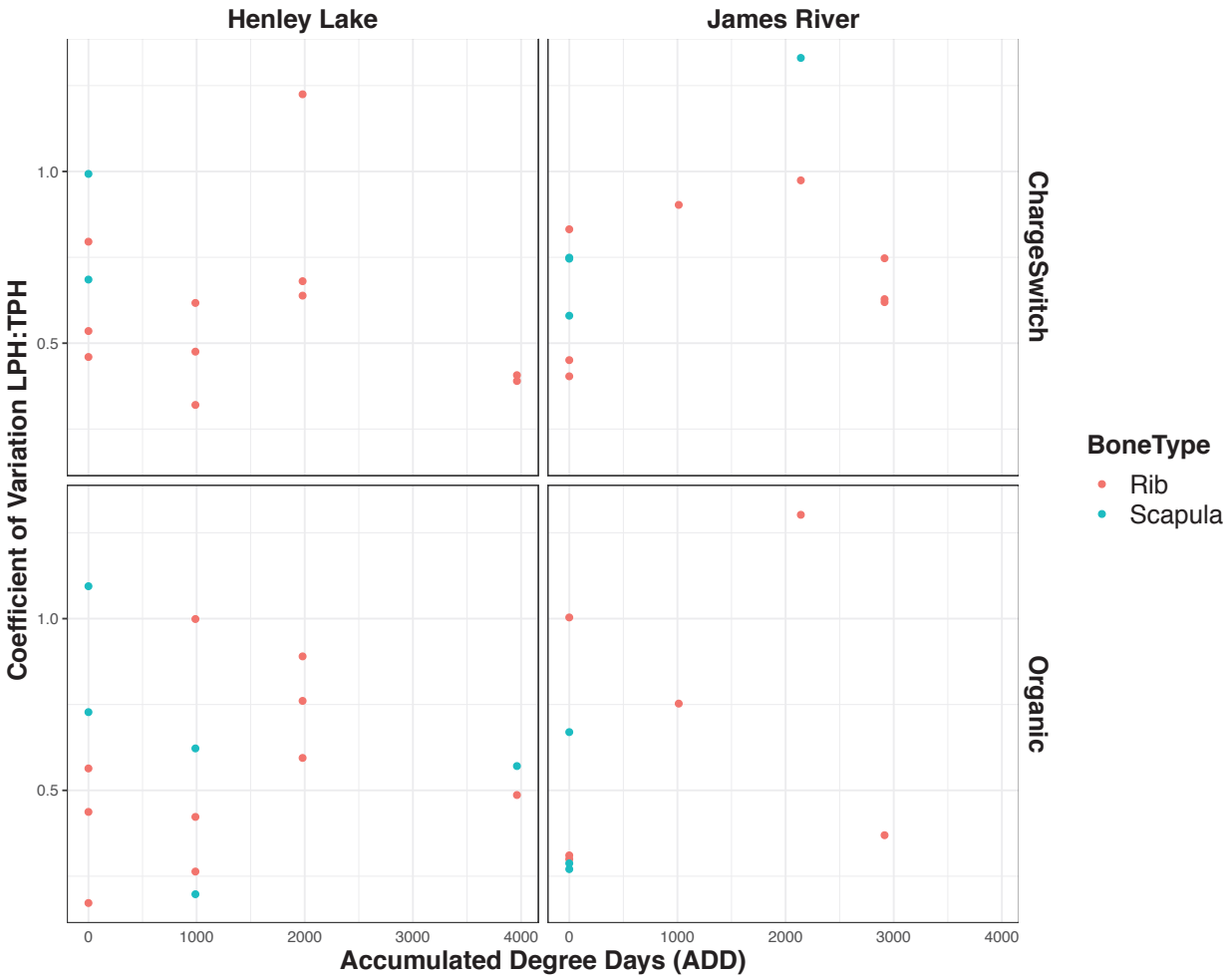

Fig. 5.S4. The coefficient of variation ratio of Locus Peak Height to Total Peak Height (CV LPH:TPH) for each STR marker across accumulated degree days (ADD) for rib and scapula samples collected from Henley Lake (left) and the James River (right) and extracted using ChargeSwitch (top) and Organic (bottom) methods

Fig. 5.S5. Rib samples collected from the James River (left) and Henley Lake (right) every approximate 1000 ADD.

Fig. 5.S6. Scapula samples collected from the James River (left) and Henley Lake (right) every approximate 1000 ADD.

Table 5.S1. The mean DNA quantity for each extraction method, bone type and location after submersion

Mean DNA Quantity	
Extraction Method	
ChargeSwitch	0.91
Organic	1.21
Bone Type	
Rib	1.43
Scapula	0.15
Location	
Henley Lake	1.43
James River	0.37

Table 5.S2. The mean DNA quantity for each accumulated degree day (ADD) after submersion

Mean DNA Quantity				
Henley Lake	**989 ADD**	**1980 ADD**	**3103 ADD**	**3962 ADD**
	1.76	1.51	1.34	1.09
James River	**1012 ADD**	**2141 ADD**	**2915 ADD**	**3949 ADD**
	0.54	0.28	0.47	

Table 5.S3. The mean number of peaks present for each accumulated degree day (ADD)

Mean Coefficient of Variance Ratio					
Henley Lake	**0 ADD**	**989 ADD**	**1980 ADD**	**3103 ADD**	**3962 ADD**
	1.68	0.83	0.88	0.02	0.56
James River	**0 ADD**	**1012 ADD**	**2141 ADD**	**2915 ADD**	**3949 ADD**
	1.76	0.25	0.58	0.67	0

Table 5.S4. The mean number of peaks present for each extraction method, bone type and location

Mean Number of Peaks Present	
Extraction Method	
ChargeSwitch	0.74
Organic	0.67
Bone Type	
Rib	1.05
Scapula	0.34
Location	
Henley Lake	0.76
James River	0.65

Table 5.S5. The peak height ratio (PHR) mean values for each extraction method, bone type and location

Mean Peak Height Ratio (PHR)	
Extraction Method	
ChargeSwitch	0.71
Organic	0.71
Bone Type	
Rib	0.71
Scapula	0.71
Location	
Henley Lake	0.71
James River	0.70

Table 5.S6. The coefficient of variance of locus peak height to total peak height ratio (CV LPH:TPH) mean values for each extraction method, bone type and location

Mean Coefficient of Variance Ratio	
Extraction Method	
ChargeSwitch	0.29
Organic	0.24
Bone Type	
Rib	0.36
Scapula	0.16
Location	
Henley Lake	0.29
James River	0.24

Table 5.7. The peak height ratio (PHR) mean values for each accumulated degree day (ADD)

Mean Coefficient of Variance Ratio					
Henley Lake	**0 ADD**	**989 ADD**	**1980 ADD**	**3103 ADD**	**3962 ADD**
	0.70	0.65	0.73		0.73
James River	**0 ADD**	**1012 ADD**	**2141 ADD**	**2915 ADD**	**3949 ADD**
	0.72	0.63	0.71	0.68	

Table 5.S8. The coefficient of variance of locus peak height to total peak height ratio (CV LPH:TPH) mean values for each accumulated degree day (ADD)

Mean Coefficient of Variance Ratio					
Henley Lake	**0 ADD**	**989 ADD**	**1980 ADD**	**3103 ADD**	**3962 ADD**
	0.65	0.49	0.80		0.46
James River	**0 ADD**	**1012 ADD**	**2141 ADD**	**2915 ADD**	**3949 ADD**
	0.55	0.83	1.20	0.59	

Vita

Claire M. Cartozzo was born to Stephany and James Cartozzo on January 9, 1992. She grew up in Thibodaux, Louisiana with her younger brother, Samuel Cartozzo. After graduating from Edward Douglas White Catholic High School, she attended Louisiana State University and graduated summa cum laude in 2014 with a major in biological sciences, as a first generation college student. During her undergraduate studies, Claire interned at the Baton Rouge Louisiana State Police Crime Lab, which lead her to pursue a Master of Science in forensic science at Virginia Commonwealth University. Her master's research served as a preliminary study for her PhD dissertation in the VCU Integrative Life Sciences program. To fund her research, she secured two Forensic Science Foundation Lucas Grants (2016 and 2019), a Rice Rivers Center Research Award (2018) and a National Institute of Justice Graduate Research Fellowship in STEM (2018). Furthermore, she was the recipient of a Forensic Science Foundation Travel Grant (2016) and Forensic Science Foundation Scholarship Award (2018), which provided travel to and registration for professional conferences. Since 2017, she has co-authored eight poster presentations and three oral presentations of which she was the first and presenting author for two oral and six poster presentations. In addition to research, Claire has taught both lab and lecture courses (BIOZ 151 and ANTH 102), leading her to complete the VCU Preparing Future Faculty Program. Her teaching extended to students in the VCU FRSC Singh Lab, as she has mentored both undergraduate and graduate students.